Investigating grape berry cell wall deconstruction by hydrolytic enzymes

by

(Anscha) Johanna Jacoba Zietsman

Dissertation presented for the degree of
Doctor of Philosophy (Agricultural Sciences)

at
Stellenbosch University
Institute for Wine Biotechnology, Faculty of AgriSciences

Supervisor: Prof Melané A Vivier
Co-supervisor: Dr John P Moore

March 2015

Declaration

By submitting this dissertation electronically, I declare that the entirety of the work contained therein is my own, original work, that I am the sole author thereof (save to the extent explicitly otherwise stated) that reproduction and publication thereof by Stellenbosch University will not infringe any third party rights and that I have not previously in its entirety or in part submitted it for obtaining any qualification.

Date: 15 December 2014

Summary

Maceration enzymes for the wine industry are preparations containing mainly pectinases, cellulases and hemicellulases, used during wine making to degrade the berry cell walls and release polyphenolic and aroma molecules to increase wine quality. These types of enzymes are also used for the harvesting of revenue-generating molecules from pomace (skins, pulp and seeds from grape processing waste), or as processing aids when used in the production of bioethanol.

Grape berry cell walls are recalcitrant towards degradation, therefore knowledge about their structures and compositions, as well as *how* the application of enzymes modify these structures is essential in order to optimise these processes. The aim of this study was to extend current knowledge by using a mixture of existing and novel methodologies to study grape berry cell walls by focusing on the profiles of polymers present in the walls.

Cell wall profiling techniques used in this study include the Comprehensive Microarray Polymer Profiling (CoMPP) method that employs monoclonal antibodies and Carbohydrate Binding Modules (CBM) which specifically recognise the polymers in the plant cell wall. With this method we measured the abundance of specific polymers and traced the fluctuation in their levels of abundance as influenced by external factors such as enzyme hydrolysis. The CoMPP method was coupled with monosaccharide profile analysis by GC-MS to determine the building blocks of the cell wall polymers, as well as with Infrared Spectroscopy to monitor the changes in the bulk chemistry profile. Data sets generated by the cell wall profiling methods were analysed with uni- and multivariate statistical methods to detect the major patterns in the data.

This study highlighted the cell wall differences on the polymer level, in the berry skin cells of Pinotage grapes at different ripeness levels and how it changes during a standard wine fermentation, leading to the release of homogalacturonans and the exposing of arabinogalactan proteins. When maceration enzymes were added, further depectination was evident and the enzymes unravelled the cell wall of the ripe grapes. In overripe grapes no additional degradation could be observed due to maceration enzyme actions, presumably indicating that the endogenous grape enzymes already caused extensive degradation.

When purified enzymes were incubated under buffered conditions with isolated skin cell walls from Pinotage grapes or with Chardonnay grape pomace, different levels of enzymatic hydrolysis were observed and defined. The sequence in which cell wall polymers were extracted, and the influence of specific enzymes in facilitating the extraction process, provided important information on the accessibility of specific cell wall polymers. Synergistic action between, for example an endo-polygalacturonase (EPG) and an endo-glucanase (EG) was demonstrated with CoMPP.

This EPG and EG synergism was also demonstrated with a yeast strain (a *Saccharomyces paradoxus* x *S. cerevisiae* hybrid) fermented in a buffered pomace suspension. This yeast strain has a native EPG and was engineered to also express a recombinant EG from a genome integrated cassette. The cell walls isolated from the pomace after fermentation were unravelled and depectination took place, as evident from CoMPP data.

The cell wall profiling techniques used in this study were proven to be fast and sensitive. It provided insights into the structure of grape cell walls and was used to evaluate the changes due to ripening, fermentation, enzymatic hydrolysis and a heat pre-processing treatment. In addition to the knowledge gained, we also demonstrated that these techniques can be used to evaluate different enzymes and enzyme combinations as well as the potential of microorganisms to degrade grape tissue.

Opsomming

Maserasie ensieme vir die wynindustrie is ensiem mengsels wat hoofsaaklik pektinases, sellulases en hemisellulases bevat en word tydens wynbereiding gebruik om die druifkorrel se selwand af te breek, die polifenole en aroma molekules vry te stel en sodoende die wyn kwaliteit te verbeter. Hierdie soort ensieme word ook gebruik om inkomste-genererende molekules vanuit druiweprosesserings afval (doppe, pulp en pitte) te isoleer, en ook as prosesserings hulpmiddels in die produksie van bioetanol.

Druifkorrel selwande is weerstandig teen ensiem afbraak en daarom is kennis oor die struktuur en samestelling van die selwand, asook *hoe* die selwand strukture deur die toediening van ensieme verander word noodsaaklik om sodoende hierdie prosesse te optimaliseer. Die doel van hierdie studie was om die huidige kennis uit te brei deur bestaande asook nuwe metodes te gebruik om die druifkorrel selwand te bestudeer met die fokus op die polimeerprofiel van die selwande.

Selwand karakteriserings tegnieke wat in hierdie studie gebruik is sluit in die *Comprehensive Microarray Polymer Profiling* (CoMPP) metode wat monoklonale teenliggaampies en koolhidraat bindende modules (*Carbohydrate binding modules, CBMs*) wat spesifiek die selwandpolimere van die plant selwand herken, gebruik. Met hierdie metode het ons die vlakke van spesifieke polimere gemeet asook die skommeling in hulle vlakke soos dit beïnvloed is deur eksterne faktore soos ensiem hidroliese. Die CoMPP metode is tesame met monosakkaried profiel analise, met behulp van GC-MS, wat die boublokke van die selwand polimere bepaal, asook infrarooi spektroskopie om die veranderinge in die oorhoofse chemiese profiel te bepaal, gebruik. Datastelle wat met die selwand karakteriserings tegnieke gegenereer is, is ontleed met een- en multiveranderlike statistiese metodes om die hoof tendense in die data op te spoor.

Hierdie studie het die selwand verskille, op die polimeervlak, van Pinotage druiwe uitgelig. Verskillende rypheidsgrade asook hoe dit verander tydens ‘n standaard wynfermentasie is gevolg. Laasgenoemde het die vrystelling van homogalakturonaan en die ontbloting van arabinogalaktoproteïene tot gevolg gehad. Met die byvoeging van maserasie ensieme was dit duidelik dat addisionele pektienverwydering plaasgevind het en dat die ensieme die selwand van die ryp druiwe ontrafel het. In oorryp druiwe was daar geen addisionele selwand afbreking sigbaar as gevolg van die aksie van maserasie ensieme nie, wat moontlik aandui dat die inherente druif ensieme reeds uitgebreide selwand afbraak versoorsaak het.

Wanneer gesuiwerde ensieme met geïsoleerde selwande van Pinotage druiwedoppe en met Chardonnay druiweprosesserings afval geïnkubeer is onder gebufferde kondisies, is verskillende vlakke van ensiematiese hidroliese waargeneem en geklassifiseer. Die volgorde waarin die selwand polimere geëkstraheer is, asook die invloed van spesifieke ensieme in die bevordering van die ekstraksie proses, het belangrike inligting verskaf oor die toeganglikheid van spesifieke selwand polimere. Sinergistiese aksie tussen, byvoorbeeld ‘n endo-poligalakturonase (EPG) en ‘n endo-glukanase (EG) is geidentifiseer met behulp van die CoMPP data.

Hierdie EPG en EG sinergisme is ook geïllustreer met ‘n gisras (‘n *Saccharomyces paradoxus* x *S. cerevisiae* hibried) wat in ‘n gebufferde druifprosesserings afval suspensie gefermenteer het. Hierdie gisras het ‘n endogene EPG en is ontwerp om ook ‘n rekombinante EG uit te druk vanaf ‘n genoom geïntegreerde kasset. Die selwande van die

druiweprosesserings afval wat na die fermentasie geïsoleer is, was ontrafel en pektienverwydering het plaasgevind, soos bevestig met CoMPP data.

In hierdie studie is bewys dat die selwand karakteriserings tegnieke vinnig en sensitief is. Dit het insigte verskaf oor die struktuur van die druifselwand en is gebruik om die veranderinge as gevolg van rypheidsverskille, wynfermentasie, ensiem hidroliese en hitte prosessering te evalueer. Buiten die bydraes tot kennis oor hierdie onderwerpe, is die bruikbaarheid van hierdie tegnieke ook aangetoon, veral in die evaluasie van verskillende ensieme en ensiemkombinasies, asook mikroörganismes vir die afbraak van druifweefsel.

This dissertation is dedicated to
my parents

Biographical sketch

Anscha Zietsman (nee Visser) was born in Stellenbosch on 26 August 1972. She matriculated in 1990 at High School Stellenbosch and enrolled for a BSc(Agric) in Food Science in 1991 at Stellenbosch University. Her BSc(Agric) Food Science degree was completed in 1994 and she received her HonsBScAgric degree in Microbiology in 1995. She enrolled for a MSc (Agric) degree in Microbiology in 1996 and this degree was obtained in 1999. She worked at the Department of Microbiology, Stellenbosch University for 5 years and is currently employed at the Institute for Wine Biotechnology at the same university.

Acknowledgements

I wish to express my sincere gratitude and appreciation to the following persons and institutions:

- Wine industry network of expertise and technology (Winetech)
- Technology and Human Resources for Industry Programme (THRIP)
- Institute for Wine Biotechnology (IWBT), Stellenbosch University
- National Research Fund (NRF).
- My supervisor Prof Melané Vivier and co-supervisor Dr John Moore
- Karin Vergeer
- My friends and colleagues at IWBT
- My friends and family
- My best friend and husband, Hans-Jurie

Preface

This dissertation is presented as a compilation of six chapters. Chapter 3 was accepted for publication in the Journal of Agricultural and Food Chemistry and Chapter 4 will be submitted to Carbohydrate Polymers. Chapter 5 was written according to the style of the journal Applied and Environmental Microbiology.

Chapter 1 **General Introduction and project aims**

Chapter 2 **Literature review**
Investigating grape berry cell wall deconstruction by hydrolytic enzymes

Chapter 3 **Research results**
Following the compositional changes of fresh grape skin cell walls during the fermentation process in the presence and absence of maceration enzymes

Chapter 4 **Research results**
Unravelling grape skin and pomace cell walls with enzymes and heat pretreatment

Chapter 5 **Research results**
Commercial wine yeast strains expressing a polygalacturonase and glucanase unravel the cell walls of Chardonnay grape pomace

Chapter 6 **General discussion and conclusion**

Table of Contents

Chapter 1

Introduction and project aims

1. General introduction and project aims

Grapes are commercially important fruits that are used in the international wine, table and dried grape industries. In addition to the direct uses of grapes as products, the grape berry and in particular the grape berry skin is also a valuable source of vitamins, minerals, carbohydrates, fibers and polyphenolic compounds (1, 2). Berry development progresses through a double sigmoidal growth pattern from fruit set until ripeness (3). The accumulation and degradation of sugars and organic acids, polyphenolic substances, such as anthocyanins, as well as volatile aroma compounds, such as monoterpenes, follow specific developmental patterns, that can also be influenced by environmental conditions (4–8). These compounds contribute to the aroma, flavour, colour, bitterness and astringency of wine (8). Per grape berry we find 50 – 60% [w/w] of the aroma compounds and 20-30% [w/w] of the phenolics in the grape berry skin cells while the seeds contain 60% of the [w/w] phenolics (1, 9). During the fermentation of wine the organic acids, ethanol and sulfur present in the must can all contribute to the extraction of aroma and polyphenolic compounds (10–12) from the berry cells. In red wine fermentations, skin contact is important to promote the extraction of these compounds into the wine, thus improving the overall quality of the wine (8). In white wine production the grapes are usually pressed and removed before fermentation resulting in limited skin contact and less extraction of skin compounds.

The main waste product of the wine industry is the pomace (pressed red and white grape skins and seeds). Since polyphenolic compounds also exhibit many biological activities and health promoting properties, they are extracted from grapes or grape pomace to be used in the food, pharmaceutical and skin care industries (2). Grape pomace also has the potential to serve as a source of fermentable sugars in the production of second generation bioethanol (13).

The grape berry cell wall forms the natural barrier preventing the polyphenols from being extracted during wine fermentation or pomace valorisation (14). The cell walls of skins are thicker than that of the pulp cells and the polysaccharide composition was estimated to be (in mol%) 57-62 homogalacturonan, 6-14 cellulose, 10-11 xyloglucan, 4.5-5 rhamnogalacturonan-I, 3.5-4 rhamnogalacturonan-II, 3 arabinogalactan and 0.5-1 mannans (15). The cell walls also contain cell wall proteins.

Enzymes are used in both wine preparation and grape pomace valorisation to enhance the extraction of the compounds of interest (phenolic and aroma compounds), or the degradation of the cell wall polysaccharides into fermentable sugars for the production of bio-ethanol (16, 17). Based on what is known about berry cell walls, pectinase, cellulase and hemicellulose enzymes are typically used to unravel the cell walls.

In order to optimize the enzymatic hydrolysis of grape tissue many studies are investigating grape cell wall composition and how this vary between grape cultivars in terms of recalcitrance towards degradation (18, 19). Other topics of study involve the type and composition of the enzyme preparations and how well the enzyme activities match the grape cell wall components as well as determining the optimal enzyme-substrate ratio and other conditions such as pH, temperature and duration of the contact time (20). Treatment processes, used either during wine fermentation (e.g. punching down, grape freezing) or prior to grape pomace valorisation (e.g. milling or heat pretreatment) can alter the grape cell wall structure and can be advantages to the enzymatic hydrolysis process (10, 21, 22). The berry ripeness level has an influence on the cell wall composition and the cell wall pectin and hemicellulose polymers are degraded by endogenous grape enzymes during ripening. The ripeness level thus, also determines the ease of polyphenol extractability (23–25).

All these previous studies judged the extent of enzymatic degradation by measuring the properties of the end product (e.g. colour of the wine) or the compounds released from the grape tissue (26–29). Some studies investigated the cell wall residue after enzymatic hydrolysis by measuring the monosaccharide composition (30). They are then able to infer the levels of the polysaccharides that were present and the changes that happened during a specific treatment (15). None of these studies measured the changes on a polymer level.

1.1 Specific aims and objectives of the study

This study focuses on the analysis of the berry cell wall and particularly evaluates the impact of enzymatic hydrolysis on this matrix by profiling and quantifying the cell wall polymers pre-and post-hydrolysis. Cell wall profiling methods that include Comprehensive Microarray Polymer Profiling (CoMPP) (31), monosaccharide compositional analysis (32) and Infrared spectroscopy (FT-IR) (33) will be used to study cell walls and their hydrolysis on a polymer level. These methods have been tested, optimized and successfully applied on grape matrices in our laboratory (34, 35).

Ripe berry skins and freshly pressed grape pomace will be used as matrices. The berry skins will be analysed to understand the compositional and structural barriers presented by the skin cell wall during red wine fermentations on grape skins, and how enzymes will act on it. The pomace will be used to simulate the unraveling of this matrix by enzymes. The following experiments were planned:

1.1.1 Cell wall analysis of the skin of ripe Pinotage berries, before and after enzyme treatments.

Vitis vinifera cv. Pinotage is a locally bred cultivar with Pinot noir and Cinsaut as parents and has a tough, thick skin (36) with a high polyphenolic content. The skin cell wall composition of this cultivar will be studied at two different ripeness levels to see if the cell wall modifications during ripening are similar to other grape cultivars. Information on the modifications that happen in the skin cell wall polymers during a standard red wine fermentation with and without the presence of commercial maceration enzymes will be provided by this study and we will discuss the influence of the grape ripeness level on the results. In order to compare how hydrolytic enzymes targeting cell wall polymers will perform under ideal conditions we will incubate isolated cell walls from Pinotage skin with different purified enzymes in buffered conditions at temperatures close to optimum for the enzymes. Under these circumstances we want to investigate to what extent the degradation will proceed and how a specific enzyme or combinations of enzymes change the cell wall polymer profile.

1.1.2 The effect of heat and enzyme treatment on the cell walls of Chardonnay pomace

This study will furthermore focus on the grape pomace cell wall structure of just-pressed Chardonnay grapes and determine the polymer and monosaccharide profile of this matrix. Processing techniques used in pomace valorisation will be investigated to determine how it modifies the cell wall composition. Towards this goal we will subject the pomace to a heat pretreatment step and investigate cell wall composition before and after the treatment. The pretreated pomace will then be used as substrate for enzymatic hydrolysis by commercial enzyme preparations to measure the cell wall modifications caused by different enzyme combinations and incubation conditions. These results will be compare to the changes caused by purified enzymes with the goal to link specific enzyme activities with specific cell wall modifications.

1.1.3 Cell wall analysis of Chardonnay pomace fermented with a hydrolytic enzyme producing yeast

In a final experiment we aim to determine if CoMPP cell wall analysis can be used as a tool to determine the potential of enzyme producing yeast strains to degrade the grape cell wall. Towards this goal we will modify a commercial wine strain that produces a native endo-polygalacturonase by introducing a genome integrated expression cassette coding for an endo-glucanase. This engineered strain as well as the appropriate control strains will be tested for the production of the recombinant enzyme and will also be used in fermentations with Chardonnay pomace as substrate. The pomace suspension will be buffered to provide optimum

pH conditions for both enzymes and the cell walls of the pomace will be analysed after the fermentation.

The cell wall profiling methods that will be used generate large and complex sets of data. To facilitate the extraction of meaningful information from the data sets it require the use of multivariate projection methods such as principle component analysis (PCA) to show the main patterns and correlations within the data. With the CoMPP method we should be able to directly measure the abundance of cell wall polymers and determine the influence of the different enzymatic treatment. This will be the first study that will use CoMPP to determine the level of cell wall degradation in grape tissue.

1.3 References

1. **Gomez E, Martinez A, Laencina J**. 1994. Localization of free and bound aromatic compounds among skin , juice and pulp fractions of some grape varieties. Vitis **4**:1–4.

2. **Xia E-Q, Deng G-F, Guo Y-J, Li H-B**. 2010. Biological activities of polyphenols from grapes. Int. J. Mol. Sci. **11**:622–46.

3. **Coombe BG, McCarthy MG**. 2000. Dynamics of grape berry growth and physiology of ripening. Aust. J. Grape Wine Res. **6**:131–135.

4. **González-Barreiro C, Rial-Otero R, Cancho-Grande B, Simal-Gándara J**. 2015. Wine aroma compounds in grapes: a critical review. Crit. Rev. Food Sci. Nutr. **55**:202–18.

5. **Adams DO**. 2006. Phenolics and ripening in grape berries. Am. J. Enol. Vitic. **57**:249–256.

6. **Fournand D, Vicens A, Sidhoum L, Souquet J-M, Moutounet M, Cheynier V**. 2006. Accumulation and extractability of grape skin tannins and anthocyanins at different advanced physiological stages. J. Agric. Food Chem. **54**:7331–8.

7. **Kennedy J**. 2008. Grape and wine phenolics: Observations and recent findings. Cienc. e Investig. Agrar. **35**:107–120.

8. **Garrido J, Borges F**. 2013. Wine and grape polyphenols — A chemical perspective. Food Res. Int. **54**:1844–1858.

9. **Teixeira A, Eiras-Dias J, Castellarin SD, Gerós H**. 2013. Berry phenolics of grapevine under challenging environments. Int. J. Mol. Sci. **14**:18711–39.

10. **Sacchi KL, Bisson LF, Adams DO**. 2005. A review of the effect of winemaking techniques on phenolic extraction in red wines. Am. J. Enol. Vitic. **56**:197–206.

11. **González-Neves G, Gil G, Ferrer M, Charamelo D, Balado J, Bochicchio R, Gatto G, Tessore A**. 2010. Prediction of the colour and polyphenolic composition of the young red wines from the phenolic potential of the grapes. Int. J. Food Sci. Technol. **45**:1843–1851.

12. **Jarvis MC**. 2011. Plant cell walls: Supramolecular assemblies. Food Hydrocoll. **25**:257–262.

13. **Rodríguez LA, Toro ME, Vazquez F, Correa-Daneri ML, Gouiric SC, Vallejo MD**. 2010. Bioethanol production from grape and sugar beet pomaces by solid-state fermentation. Int. J. Hydrogen Energy **35**:5914–5917.

14. **Bautista-Ortin AB, Martinez-Cutillas A, Ros-Garcia JM, Lopez-Roca JM, Gomez-Plaza E**. 2005. Improving colour extraction and stability in red wines: the use of maceration enzymes and enological tannins. Int. J. Food Sci. Technol. **40**:867–878.

15. **Arnous A, Meyer AS**. 2009. Quantitative prediction of cell wall polysaccharide composition in grape (*Vitis vinifera L*.) and apple (*Malus domestica*) skins from acid hydrolysis monosaccharide profiles. J. Agric. Food Chem. **57**:3611–9.

16. **Van Rensburg P, Pretorius IS**. 2000. Enzymes in winemaking : harnessing natural catalysts for efficient biotransformations - A review. South African J. Enol. Vitic. **21**:52–73.

17. **Arnous A**. 2009. P.hD. thesis. Technical University of Denmark, Lynby, Denmark. Enzymatic release of phenolics from fruit skins – with grape as the main model.

18. **Ortega-Regules A, Romero-Cascales I, Ros-García JM, López-Roca JM, Gómez-Plaza E**. 2006. A first approach towards the relationship between grape skin cell-wall composition and anthocyanin extractability. Anal. Chim. Acta **563**:26–32.

19. **Hernández-Hierro JM, Quijada-Morín N, Martínez-Lapuente L, Guadalupe Z, Ayestarán B, Rivas-Gonzalo JC, Escribano-Bailón MT**. 2014. Relationship between skin cell wall composition and anthocyanin extractability of *Vitis vinifera L*. cv. Tempranillo at different grape ripeness degree. Food Chem. **146**:41–7.

20. **Kammerer D, Claus A, Scieber A, Carle R**. 2005. A novel process for the recovery of polyphenols from grape (*Vitis vinifera L .*) pomace. Food Chem. Toxicol. **70**:157–163.

21. **Maier T, Göppert A, Kammerer DR, Schieber A, Carle R**. 2007. Optimization of a process for enzyme-assisted pigment extraction from grape (*Vitis vinifera L.*) pomace. Eur. Food Res. Technol. **227**:267–275.

22. **Rio-Segade S, Torchio F, Giacosa S, Aimonino DR, Gay P, Lambri M, Dordoni R, Gerbi V, Rolle L**. 2014. Impact of several pre-treatments on the extraction of phenolic compounds in winegrape varieties with different anthocyanin profiles and skin mechanical properties. J. Agric. Food Chem. **62**:8437–8451.

23. **Bindon KA, Bacic A, Kennedy JA**. 2012. Tissue-specific and developmental modifications of grape cell walls influence the adsorption of proanthocyanidins. J. Agric. Food Chem. **60**:9249–9260.

24. **Gil M, Kontoudakis N, González E, Esteruelas M, Fort F, Canals JM, Zamora F**. 2012. Influence of grape maturity and maceration length on color, polyphenolic composition, and polysaccharide content of Cabernet Sauvignon and Tempranillo wines. J. Agric. Food Chem. **60**:7988–8001.

25. **Río Segade S, Soto Vázquez E, Díaz Losada E**. 2008. Influence of ripeness grade on accumulation and extractability of grape skin anthocyanins in different cultivars. J. Food Compos. Anal. **21**:599–607.

26. **Ortega-Heras M, Pérez-Magariño S, González-Sanjosé ML**. 2012. Comparative study of the use of maceration enzymes and cold pre-fermentative maceration on phenolic and anthocyanic composition and colour of a Mencía red wine. LWT - Food Sci. Technol. **48**:1–8.

27. **Doco T, Williams P, Cheynier V**. 2007. Effect of flash release and pectinolytic enzyme treatments on wine polysaccharide composition. J. Agric. Food Chem. **55**:6643–9.

28. **Ortega-Regules A, Ros-García JM, Bautista-Ortín AB, López-Roca JM, Gómez-Plaza E**. 2008. Differences in morphology and composition of skin and pulp cell walls from grapes (*Vitis vinifera L.*): technological implications. Eur. Food Res. Technol. **227**:223–231.

29. **Chamorro S, Viveros A, Alvarez I, Vega E, Brenes A**. 2012. Changes in polyphenol and polysaccharide content of grape seed extract and grape pomace after enzymatic treatment. Food Chem. **133**:308–314.

30. **Romero-Cascales I, Ros-García JM, López-Roca JM, Gómez-Plaza E**. 2012. The effect of a commercial pectolytic enzyme on grape skin cell wall degradation and colour evolution during the maceration process. Food Chem. **130**:626–631.

31. **Moller I, Sørensen I, Bernal AJ, Blaukopf C, Lee K, Øbro J, Pettolino F, Roberts A, Mikkelsen JD, Knox JP, Bacic A, Willats WGT**. 2007. High-throughput mapping of cell-wall polymers within and between plants using novel microarrays. Plant J. **50**:1118–28.

32. **York WS, Darvill AG, L MM, Stevenson TT, Albersheim P**. 1985. Isolation and characterization of plant cell walls and cell wall components. Methods Enzymol. **2**:3–40.

33. **Kacurakova M, Capek P, Sasinkova V, Wellner N, Ebringerova A, Kac M**. 2000. FT-IR study of plant cell wall model compounds : pectic polysaccharides and hemicelluloses. Carbohydr. Polym. **43**:195–203.

34. **Moore JP, Fangel JU, Willats WGT, Vivier MA**. 2014. Pectic-β(1,4)-galactan, extensin and arabinogalactan-protein epitopes differentiate ripening stages in wine and table grape cell walls. Ann. Bot. **114**:1279–1294.

35. **Nguema-Ona E, Moore JP, Fagerström A, Fangel JU, Willats WGT, Hugo A, Vivier MA**. 2012. Profiling the main cell wall polysaccharides of tobacco leaves using high-throughput and fractionation techniques. Carbohydr. Polym. **88**:939–949.

36. **Goussard PG**. 2008. Grape cultivars for wine production in South Africa. Cheviot Publishing, Cape Town.

Chapter 2

Literature review

Investigating grape berry cell wall deconstruction by hydrolytic enzymes

Investigating grape berry cell wall deconstruction by hydrolytic enzymes

Enzyme assisted grape maceration and valorisation of pomace waste

Wine maceration is the process where the grapes are soaked in the juice (steeping liquid) to make it softer or penetrable with the consequential leaching of aroma precursors and molecules collectively known as polyphenols from the vacuoles of the skin and the pulp cells of the grape berry into the must (1). These aroma as well as the polyphenol compounds are valuable because of their contribution towards wine flavour, colour, health properties and overall quality (2). Thus, it follows that by disrupting the cell wall and releasing the contents of the cells, it will lead to an increase in juice yield and a higher concentrations of aroma precursors and polyphenols in the final product. The disruption of the grape berry cell wall structure can be achieved by the application of heat, chemicals, physical methods (e.g. crushing) and cell wall disrupting enzymes (3).

Grape pomace valorisation is similar to maceration because both processes involve the disruption of the cell walls in the grape berry. Valorisation of grape pomace can entail the release of valuable compounds (mostly polyphenols) located in the cell vacuole or bound to the cell wall, or it can be the complete hydrolysis of the cell wall in order to liberate the monosaccharides (4). These monosaccharides then serve as a fermentable carbon source in bioethanol production. As with maceration, the pomace valorisation process can be enhanced by mechanical methods or with enzymes. Pretreatment with for example steam, acid or alkali selectively removes different components from the tissue and makes the residue more accessible for enzymes (5, 6). The enzymes unravel the cell wall polysaccharides and this may enhance the extraction of polyphenols. For the complete reduction of the cell walls to monosaccharides, both acid and enzymatic hydrolysis can be used.

2.1 Maceration

Maceration of white grape cultivars falls outside the scope of this thesis and will not be discussed. Maceration with red wine production usually takes 3 to 5 days to allow for the extraction of enough aroma and colour compounds (anthocyanins) as well as tannins from the skins. Longer maceration periods can lead to the extraction of the harsher seed tannins as well as some off flavours (2). Factors that increase the permeability of the cells and membranes of the grape are the alcohol content, sulfur dioxide as well as the heat generated in the

fermentation (3). To ensure good contact between skins and juice during maceration the skin cap that forms on top of the must is punched down several times per day or the juice/must is pumped over the skin cap. Some cultivars are recalcitrant towards releasing sufficient amounts of polyphenols during maceration and techniques were developed to improve their maceration success. One of these, cold maceration, is a pre-fermentative technique often used with cultivars such as Pinot Noir (7) . With cold maceration, the crushed grapes are left to macerate for 3 to 4 days at temperatures between 4 and 15°C. This process enhances colour density and flavor complexity and differential aroma profiles can be obtained depending on the chosen maceration temperature (8). However, the colour enhancement is not always permanent and after a relatively short storage period, the cold maceration wines sometimes have the same colour density values as the wines prepared with standard methods (3, 9, 10). Maceration conducted at elevated temperatures will increase the extractability of phenolics as the permeability of the grape berry membranes would be increased (11). This principle is applied in a process called thermovinification, but it can lead to the formation of volatile acids or oxidized off-flavours (12). As a non-thermal option, pulsed electric field treatment, has been studied in recent years as a way to enhance phenolic extraction (13, 14). With optimized pulsed electric field parameters, it is possible to modify the organization of the berry skin cell wall polymers, which increases the extraction rate of anthocyanins and other phenols and enhance the sensory attributes of the wine.

Sacchi et al. (3) reviewed a number of specialized maceration techniques and concluded that higher fermentation temperatures, thermovinification, must freezing (ice particles rupture cell walls and membranes), *saigneé* (decreasing the juice to skins ratio by removing some of the juice early on), the use of pectolytic enzymes and an extended maceration period will all increase the phenolic concentration of finished wines. An increase in sulfur dioxide levels (higher levels than what is normally used) and cold maceration prior to inoculation do not increase phenolic concentration although there is sometimes a non-permanent effect. Finally, techniques and operational methods such as carbonic maceration (whole bunch fermentation of uncrushed grapes under CO_2), the employment of specific wine yeast strains and the use of different skin and juice mixing practices produced variable results, which are dependent on the grape variety that was used.

2.1.1 The use of maceration enzymes in wine production

Enzymes can enhance and accelerate the maceration process by breaking down the cell walls and membranes in the berry, weakening or destroying the boundary that is retaining the aroma and phenolic molecules from the must (15–17). These enzymes can originate from the grape tissue or from the microorganisms present on the grapes, in the vineyard or the cellar equipment (18). However, the extent of the hydrolysis performed by these endogenous

microbial or grape derived enzymes are not usually sufficient to make an impact on the properties of the resulting wine since the must conditions are not optimal for their activity. In the must the enzymes can be inhibited by the high sugar concentration, the low pH and low fermenting temperatures, and it can be inhibited by ethanol, sulfur dioxide, tannins and bentonite. Thus, enzymes, which are not adversely affected by the conditions prevalent in fermenting must are added to enhance the extraction of aroma, colour and other phenolic compounds during maceration (19, 20). Commercial maceration enzymes are extracts from *Aspergillus niger* and *Trichoderma* species grown under specific conditions in order to produce specific enzymes. The Organisation International de la Vigne et du Vin (OIV) stipulates that only these species may be used for isolation of wine enzymes due to their GRAS (generally regarded as safe) status. Pectin degrading enzymes have been used since the 1970s in wine fermentations (19). Although maceration enzyme mixes consist primarily of pectinases there are always a wide variety of other additional enzymes present such as cellulases, hemicellulases, esterases, β-glucosidases etc. (21, 22). These additional activities can have a positive or negative effect as discussed in section 2.1.1.3. Studies (21, 23, 24) showed that by combining pectinases with cellulases, the synergistic effect of these enzymes ensures a more complete breakdown of cell walls from both grape and apple tissues. An overview of the enzymes that are used in the wine industry is shown in Table 1 [adapted from (25)].

Table 1: Enzyme families and enzymes commonly used in the wine industry (25)

Enzyme family	Enzymes	Commercial wine enzyme examples
β-Glucanases	exo-β-1,3-glucanase, endo-1,3-1,4-glucanase, endo-β-1,4-glucananse	Lallzyme MMX™ (Lallemand), Depectil Elevage (Martin Vialatte), Glucanex® 200 G (Lamothe-Abiet)
Pectinases	Pectate lyase, endo-Polygalacturonase,	Lallzyme C™ (Lallemand), Rapidase® CB (DSM), Rapidase® Vinosuper (DSM), Rapidase® X-Press L (DSM), Depectil Clarification (Martin Vialatte), Ultrazym® Premium (Lamothe-Abiet)
	Pectin lyase, Pectin methyl esterase, Galactanase, Rhamnosidase, Rhamnogalacturonase	Rapidase® X-Press L (DSM) Rapidase® Vinosuper (DSM) Lallzyme EX™ (Lallemand) Lallzyme BETA™ (Lallemand) Rapidase® Expression (DSM) Rapidase® X-Press L (DSM)
Hemicellulases	Arabinase Arabinofuranosidase	Rapidase® Expression (DSM) Rapidase® X-Press L (DSM)

2.1.1.1 Enzyme effect on wine colour and polyphenolic composition

In general enzyme treated wines result in a higher amount of total phenolic compounds (16, 26) being extracted which can improve overall wine quality (27). The polyphenols are important components of wine. Anthocyanins are the colour pigments of red wine and hydroxycinnamic acids, flavonols and tannins are colour enhancing and stabilizing factors. Catechins and tannins contribute to the complexity, astringency and mouth feel of the wine. The phenolics may also have health promoting qualities (28). The grape skin contains 20 – 30% (w/w) and the seed 60 % (w/w) (29) of the phenolic compounds of the grape berry (Fig. 1). However, skin phenolics are favoured by winemakers because they result in wines that are less bitter and astringent (30). This is linked to the type and mean degree of polymerization of the proanthocyanidins that are found in the seeds and skins (31).

Wine made from riper grapes generally contains more skin than seed proanthocyanidins (32) because the extraction of seed tannins happens more regularly in the period before the seeds reach phenolic ripeness, before the outer layer of the seed dehydrates and becomes hard (33). Enzymes can unfortunately also modify the tannin composition and there is more than one study showing that enzymes can increase the tannin extraction from specifically the seeds (34–36). Tannin extraction from seeds will be enhanced even further in the presence of ethanol since ethanol helps to solubilize the cell wall components of seeds (37).

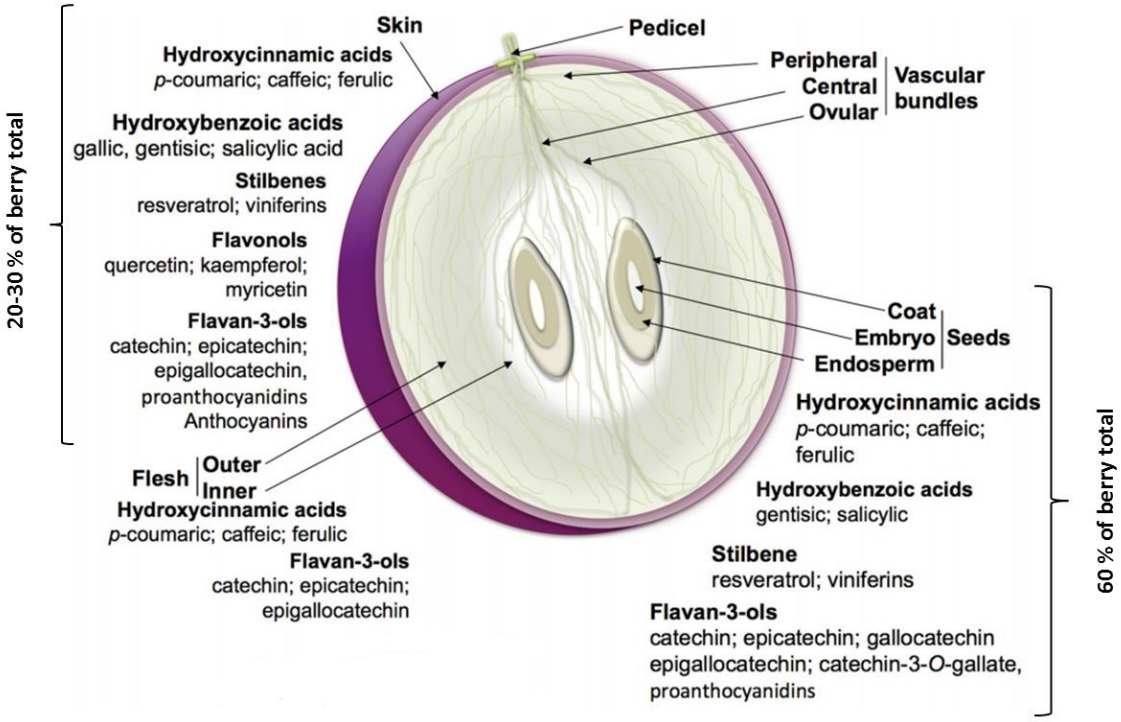

Figure 1: The structure of the grape berry and the distribution of the phenolic compounds (29, 38).

However, if maceration enzymes extract predominantly skin phenolic compounds it can result in a wine with improved mouth feel (30). Furthermore, free and glycosidically bound flavour compounds of wine made from Bobal grapes (from the Utiel-Requena region of Spain) were increased by using a yeast that expressed an endo-glucanase and an endo-xylanase enzyme during the maceration period (39). A similar result was seen by a *Saccharomyces cerevisiae* x *S. paradoxus* hybrid yeast strain that produces an endo-polygalacturonase (40). Finally, Salinas et al. (41) observed an increase in ester content and stabilization in the evolution of terpenols such as linalool, geraniol and nerolidol, when using enzymes for phenolic and aroma extraction in Rosé wine preparation.

2.1.1.2 Enzyme effect on the polysaccharide composition of wine.

Wine polysaccharides play important roles during wine production as they can prevent haze formation (42), stabilize flavour (43), colour and foam in effervescent wines, but they can also cause filtration problems (44). Vidal et al. (45) showed that polysaccharides, similar to polyphenols, contribute towards the body, mouth feel, bitterness and astringency of wine. They isolated a neutral polysaccharide fraction from wine consisting of type II arabinogalactan-proteins (AGPs), originating from grape cell walls, and mannoproteins originating from yeast cell walls and demonstrated that this fraction contributes to the 'fullness' sensation of wine. The second acidic fraction, containing rhamnogalacturonan-II (RG-II), significantly decreased the astringency of wine. Rhamnogalacturonan-I (RG-I) was also detected, but constituted only 4 % off all the polysaccharides found in wine (46) and was associated with xyloglucan-like polysaccharides. This contributed to early evidence suggesting cross-links between pectic polymers and xyloglucans. Ayestarán et al. (47) used size exclusion chromatography and monosaccharide analysis (GC-MS) and followed the wine polysaccharide profile throughout the wine making process. The early stages of fermentation are characterized by the release of low molecular weight AGPs followed by RG-II from the grape tissue into the fermenting wine. The RG-II are mostly dimers but some RG-I monomers and small quantities of homogalacturonan (HG) were also detected. In the later stages of the fermentation, there was an increase in larger AGP molecules as well as yeast mannoproteins released from the yeast cell walls. At the end of alcoholic fermentation and during malolactic fermentation, the larger AGPs as well as some mannoproteins precipitated but the levels of the latter stayed constant because it was presumably replenished from the yeast cell walls in the lees. Furthermore, the levels of the wine polysaccharides stayed relatively stable during oak and bottle aging. Apolinar-Valiente et al. (48) showed that terroir might have an influence on the RG-II concentration of wine which might be linked to the availability of micronutrients such as Boron in the different soils.

A few studies investigated how the use of maceration enzymes alters the polysaccharides and oligosaccharides found in wine. Ayestarán et al. (47) showed that the use of commercial

enzymes increased the arabinogalactan, AGPs and RG-II levels in wine from Tempranillo grapes in comparison to the control wines, but it had no effect on yeast mannoproteins. In contrast Ducasse et al. (49) showed a decrease in the amount of AGPs and arabinans in Merlot wine that was treated with enzymes. They also saw and increase in RG-II and lower molecular weight products. The latter can be the degradation products from the AGP and arabinans and might indicate that more extensive enzyme hydrolysis took place than in the first study. In another study Ducasse et al. (50) compared the oligosaccharides of Merlot wines that were prepared with and without the addition of commercial enzyme preparations and found that the enzymes demethylated and hydrolysed HG and cleaved the RG-I backbone, releasing RG-I with neutral side chains attached. Doco et al. (51) showed that pectinolytic enzyme treatment are responsible for the removal of the terminal arabinose unit from AGPs.

2.1.1.3 Inconsistent results and side effects ascribed to the use of maceration enzyme preparations

Numerous studies on how maceration enzymes change wine properties have been done over the last 40 years (15–17, 26, 49, 52). The reason for the continued interest in the topic from a commercial and scientific point of view is that the results achieved by using enzymes for wine preparation are not consistent. Several studies have shown that the enzymes had no observable/detectable effect (15, 16, 52) or improved some but not all of the wine properties and sometimes the effects were not long lasting (9, 10).

The inconsistencies have traditionally been attributed to impurities or side-activities present in the enzyme preparations. The OIV recommends that detrimental side activities should be absent in commercial enzyme preparations and all enzymatic activities and their activity levels should be declared on the label (Resolution OIV/OENO 365 (2009), International Oenological Codex) (www.oiv.int). Studies investigating the specific enzymatic activities present in maceration enzyme preparations (21, 22) revealed that most of the preparations have the same types of activities present, but the levels of specific activities varies between different preparations and preparations that are marketed for specific applications do not always have the optimal enzymatic profile. Additionally all the preparations included unwanted activities or side activities such as β-glucosidases, cinnamoyl esterase (only a problem in white wine) and esterases, although at different concentrations. Few of these so-called side activities were sufficiently characterized and described on the product labels as required by the OIV.

The presence of β-glucosidases in enzyme preparations is problematic because it can remove the glycosyl moiety from anthocyanins rendering a colourless molecule and can thus result in a red wine with a low colour intensity (53). In white wine it can liberate non-volatile flavour compounds from their glycosides and improve the sensory profile (54). Esterases can hydrolyse

both the wine esters responsible for the fruity and floral like aromas but they also hydrolyse ethyl acetate and long-chain fatty acid esters, which have solvent and soap-like aromas (55). Thus, whether the presence of esterases in a maceration enzyme preparation is positive or negative depends on the specificity of those enzymes. Proteases are regarded as a side or secondary activity but protease action may contribute positively towards wine fermentations by reducing filtration and clarification problems (56) and enriching the assimilable nitrogen content of must, benefitting the fermentation microbes (57). Proteases can degrade the proteins from the grape cell membrane and the vacuole membrane to facilitate the release of phenolic compounds but protease activity was not found in any of the maceration enzyme preparations tested by Romero-Cascales et al. (21). In contrast, Fia et al. (22) found proteases in all 21 maceration enzyme preparations tested on bovine serum albumin but under winemaking conditions, the protease activities were 10 to 20% reduced.

Besides side activities, many other factors that might be the cause for inconsistent successes with enzymes have been investigated. All factors that can influence the composition of the berry cell wall can have an influence on the success of the enzymatic hydrolysis. These factors include the skin thickness [some cultivars are known to have thick skins e.g. Pinotage and Monastrell (58)], cell wall porosity as well as the relative abundance of the different components (pectins, celluloses and hemicelluloses) and how that matches up with the activity profile of the maceration enzyme preparation (pectinases:cellulases:hemicellulases). The composition of the cell wall is dependent on the tissue type (skin or pulp), cultivar (59), the ripeness stage (60), the vintage (which depend largely on the climatic properties) (9, 34) and the vineyard practices that was followed and the geographical orientation of the vineyard. Other factors that may influence the enzyme success are inhibiting substances that may be present in the must (high tannin or alcohol concentrations), the residual activity of the enzymes at winemaking conditions or the enzyme to substrate ratio (16, 61).

A side effect associated with the use of maceration enzymes is the production of methanol. Pectinmethylesterase is responsible for the de-esterification of pectin to pectate with the release of methanol (62). During maceration, we thus see the formation of methanol because of the action of this enzyme whether is it the endogenous grape enzyme or a part of a commercial preparation. The high activity of the commercial enzyme preparations results in higher levels of methanol being produced in wines treated with pectinolytic enzymes (63). Methanol is toxic to humans with the oral lethal dose at 340 mg/kg body weight and the limit for methanol is set at 150 mg/l in white and rosé wines and 300 mg/l for red wines (64). Gnekow and Ough (62) reported white wine methanol levels between 20 to 32 mg/l and red wines between 48 and 135 mg/l when there was no addition of pectinolytic enzymes. When enzymes were added, the levels increased to a maximum of 73 mg/l in white wines and 140 mg/l in red wines. Most

studies show that when pectinolytic enzymes are added at the recommended dosages the final methanol concentration is still far from the maximum allowable concentration, but there are exceptions. For example, one of the enzymes tested by Romero-Cascales et al**.** (21) increased the methanol concentration from 152 mg/l to 338 mg/l.

We have summarized the use of maceration enzymes, and how they affect the properties of the wine. In the next section we will focus on one of the waste products of the wine making process, the grape pomace. Pomace is the grape skins, stalks and seeds that remain after both the red and white wine making process. The global wine industry is moving towards using more sustainable practices and therefore the development of methods to extract value from waste is an area of great importance. Enzymes are one of the central tools used in the upcycling of this waste product.

2.2 Grape pomace valorisation

The different types of waste originating from the wine production process include wastewater, pomace (skins and seeds), filter cakes, lees and wine (65). Recycling the waste generated by the wine industry and harvesting from it substances of value is a common practice in most major wine producing countries. Traditionally most skins, seeds and stalks were used as animal fodder and as composting material (66). However, because of the low pH of pomace (3.5 – 3.8) the composting rate is slow if not supplemented with lime or other feed stocks. This supplementation increases the pH to create a suitable environment for compost microbes, which prefer a pH of 6.2. Furthermore the high lignin present in the seeds and stalks (17 to 35%) can limit decomposition and wet piles (>60% moisture) may continue to ferment and produce acetic acid resulting in poor quality compost. As fodder, pomace on its own is not considered to be of high value although the animals find it extremely palatable once the tartaric acid has been removed. The high amounts of tannin found in specifically red grape pomace, results in protein binding and indigestibility in bovines (67).

Large quantities of pomace are generated each year: In 2012, the production of wine in South African resulted in 213 000 tonnes of pomace (according to SAWIS [http://www.sawis.co.za/info/download/Book_2013_eng_web.pdf] and worldwide the number was 5.3 million tonnes. It is clear that if all of this ends up as landfill it will have dire environmental consequences. Fortunately, pomace (and some of the other winery waste products) can be processed and valorized (4). In South Africa, the company Brenn-O-Kem processes 35 000 tonnes of pomace and wine lees annually into products such as grape spirits, grape seed extract and cream of tartar (68). Grape seed oil pressed or chemically removed from the grape seeds (65) has a burn point at 216°C, is used for food preparation and is rich in

omega-6 fatty acids (linoleic acid) and other polyunsaturated fats. Because of its high antioxidant concentration the oil is also incorporated into skin therapy products.

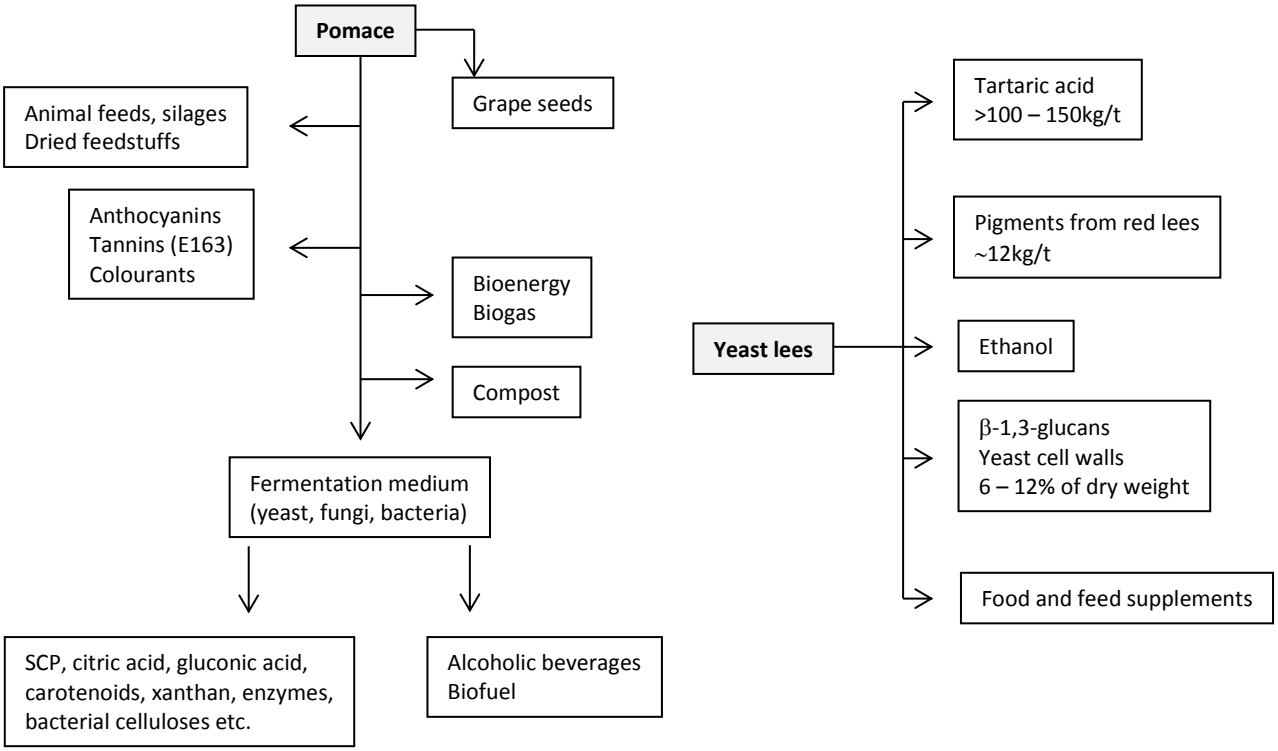

Figure 2: Products derived from grape pomace and yeast lees. (SCP, single cell protein). Adapted from (65).

The residue that remains after the oil extraction is the so-called press cake, a source of antioxidants, antimicrobials and phytochemicals that can be incorporated into pesticides, food additives, antibacterial ointments and serves as UV protectant in sunscreens. Grappa is a distilled spirits that can be produced from grape pomace (skins, seeds and stalks) and originated in Italy (2). Furthermore, tartaric acid can be isolated from the pomace (50 – 75kg/t) as well as the lees (100 – 150kg/t) (65). Valuable polyphenols and triterpenic acids can be extracted from grape skins and these molecules are used in the pharmaceutical, cosmetic and nutritional industries (69). Other products that can be isolated from the lees and the pomace are shown in Figure 2. After extraction of the molecules from the grape pomace, the remaining fibrous material, (i.e. the cell walls of the cells in the grape pulp and skin), can be used in a biomass power plant to produce electric or thermal energy or it can be saccharified with enzymes and fermented to bioethanol.

2.2.1 The use of enzymes in pomace valorisation

The following paragraphs will focus on the role that enzymes play in the extraction of valuable molecules from the pomace as well as the enzymatic hydrolysis of grape cell wall polysaccharides as preparation for bioethanol fermentations.

The phenolic composition of grapes and thus pomace is dependent on many factors e.g. the soil, geographical characteristics, weather conditions, maturity at harvest and the grape variety (27, 70). Furthermore, the phenolic concentration (content/composition) depends on the types of tissues included (skins, seeds and stalks) and whether the pomace were collected before or after alcoholic fermentation (70–72). The phenolic compounds are bound to the polysaccharides of the cell walls, either with hydrophobic interactions or hydrogen or covalent bonds and they can be found within cell vacuoles (73). Acidified alcohol, sulfited water or organic solvents are commonly used for the extraction of polyphenols from pomace (28, 74) but the sulfite can be seen as an allergen risk in the downstream products and the use of large amounts of organic solvents is environmentally unfriendly. In an effort to reduce or eliminate the use of organic solvents and SO_2 other methods using microwaves, ultrasound or cell wall degrading enzymes have been developed (28). The advantages of hydrolytic enzymes are that they deliver a more stable bioactive product at lower temperatures and pressure and with a lower impact on the environment. Furthermore, some studies showed that enzymes decrease the molecular weight of phenolics which can improve the ease of absorption (bioavailability) of these molecules in the human gut (75, 76).

Enzymes are also invaluable for the production of monosaccharides from plant material that serves as a fermentable carbohydrate source for yeast in bioethanol production. Established bioethanol production processes using lignocellulosic biomass as starter material usually consist of five steps: (i) Pretreatment to enhance the enzyme accessibility to cellulose during hydrolysis, (ii) enzymatic hydrolysis of cell wall polysaccharides (iii) fermentation of sugars to ethanol (iv) separation of lignin residue and (v) recovery and purification of ethanol (6). The use of grape pomace waste in the production of bioethanol has been investigated (65, 69, 77) but the seasonal availability of pomace, makes it less economically attractive. However, a recent study (78) showed how fresh and fermented pomace can be preserved and enhanced for digestibility via the process of ensilage (lactic acid fermentation) which would make pomace available to use as biomass throughout the year.

2.2.2 Factors that influence the effectiveness of enzymatic hydrolysis of pomace

As was briefly mentioned in the previous paragraph, pomace (when it includes stalks, skins, some flesh and seeds) as bioethanol biomass, would have to be pretreated to ensure effective enzymatic hydrolysis (6). The pretreatment is largely necessary to remove and convert the lignin

and hemicellulose matrix that surrounds the cellulose and to decrease the crystallinity of cellulose. The presence and amount of lignin present in grape skins is a topic with divergent opinions (see section 2.3.1.4) but it is known that the grape stalks contain 17% (w/w) lignin (79) which was confirmed by solid state ^{13}C NMR spectroscopy. Grape seeds contain 41% (w %, dry basis) lignin (80). Besides lignin, cutin might also hinder enzymatic hydrolysis of cell wall polysaccharides since (81) found a major part of the structural polysaccharides from *Touriga Nacional* grape skins embedded in an acid-insoluble cuticular residue.

The different pretreatment processes that are commonly used in the bioethanol industry include biological (white and soft-rot fungi), physical (milling and extrusion), chemical (alkali, acid, organic solvents) and physico-chemical (steam explosion, liquid hot water, microwave, ultrasound) pretreatments which are discussed in detail in (6) and (5). When pomace is used for the extraction of polyphenols the pre-treatment step usually only involves hot water extraction (61, 82). In this literature review, we will briefly look at milling and steam pretreatment since these are the two processes used for enzyme substrate preparation in Chapter 4 and 5 of this study.

Meyer et al. (23) showed that when the size of the pomace particles are reduced (for example, with milling) the surface area and enzyme accessibility increase, enhancing the enzymatic hydrolysis of the pomace cell walls which results in a tenfold increase in the extraction of polyphenols. During steam treatment of wheat straw part of the hemicelluloses hydrolyse to form acids which catalyse further hemicellulose hydrolysis (5). This leads to pore formation, which gives the enzymes better access to the cellulose. Information on the effect of steam treatment on grape pomace cell walls, which have a much higher pectin content, is not available. The natural pore size of the grape cell wall is between 4 and 10 kDa (83). This is too small for most hydrolytic enzymes to enter (84, 85) and emphasizes the importance of pretreatment processes.

Other factors that can affect the enzyme hydrolysis success in polyphenol extracting processes are the type of enzyme selected, the enzyme-substrate ratio and the time and temperature of the reaction. These parameters were all investigated in studies by (23, 61, 75, 82, 86) and in general a better extraction was observed if a combination of enzymes (for example, pectinolytic with celluloytic enzymes) were used. Most studies achieved extraction levels and rates similar to what was achieved with sulfite extraction.

Enzymes are an integral part of the processes discussed above but a major obstacle in the future development of bioconversion processes of waste is the low efficiency and high cost of enzymes (87). The high chemical and structural complexity of plant cell wall biomass

contributes to this inefficiency and it has become imperative to determine the limitations of enzymatic deconstruction and in parallel gain knowledge on the architecture of the plant cell wall. This is also true for the use of maceration enzymes in the production of red wine and thus the next section is a short summary of the available knowledge on the plant (dicotyledon) cell wall followed by the grape berry cell wall. We will also focus on the location of the polyphenols in the grape berry and the factors that influence the extractability of these compounds. Finally, we will summarize findings from previous studies that investigated how the grape cell wall was changed by hydrolytic enzymes.

2.3. Investigating the grape berry cell wall structure

2.3.1 An introduction to plant cell walls

The obvious structural functions of plant cell walls includes being a vital component of the hydrostatic skeleton of plant tissues and organs; resisting mechanical stress by producing secondary cell wall layers (e.g. wood in trees) and acting as a physical barrier against biotic and environmental stresses (88). Apart from these classical roles it has become increasingly apparent that the cell wall plays a number of dynamic biological roles; including recognition, signaling and responding (via the cell wall components) to pathogen invasion and environmental stresses; as well as being an active component in plant growth and development processes (89, 90). *Vitis vinifera* is a dicotyledonous angiosperm and therefore further discussion will be limited to the structure and properties of the cell walls of dicots. Most of the research in plant cell walls has been performed on *Arabidopsis*, rice (*Oryza sativa L*.) and poplar (*Populus*).

Three inter-dependent networks form the structure of plant cell walls; these being the cellulose-hemicellulose (xyloglucan); pectin and protein (glycoprotein and proteoglycan) matrices (91). Traditionally it has been common practice to consider these as separate components; mainly due to the classical fractionation methods employed to analyse cell walls from various sources. However, it has become increasingly appreciated that such separations are rather artificial and arbitrary, and that in order to fully appreciate the complexity of plant cell walls a more nuanced understanding of the higher order structure and architecture using more recently developed techniques is needed.

2.3.1.1 Cellulose-hemicellulose network

Cellulose consist of neutral, unbranched β-1,4-D-glucan chains. Primary cell walls (surrounding growing and dividing plant cells) contain on average between 20 and 30% cellulose while secondary cell walls (deposited once the cell has ceased to grow) contain up to 50% (88). Investigations into the nature of the parenchyma cell wall surface of maize, by using atomic force microscopy (AFM) and immuno-transmission electron microscopy (TEM), showed that 36

β-D-glucan chains assemble into a cellulose microfibril with hydrogen bonds and van der Waals forces holding it together (92, 93). Microfibrils made of glucan chains, containing as many as 14 000 glucose units, corresponds to a microfibril length of 7μm (94) with a 3 nm diameter (84) and these microfibrils are arranged 10-20 nm apart. Cellulose has a crystalline core surrounded by a paracrystalline layer of cellulose and then hemicelluloses. Callose is a β-1,3-D-glucan (with occasional β-1,6- linked branches) found in plant cell walls and is usually formed in response to stress conditions such as wounding or pathogen attack. Callose also accumulates around the plasmodesmata opening and might regulate the aperture of this intercellular channel (95).

Hemicelluloses are polysaccharides with backbones of β-1,4-linked glucose (Glc), mannose (Man) or xylose (Xyl) with an equatorial configuration (96). Hemicelluloses include xylans (such as arabinoxylans and glucuronoarabinoxylans), xyloglucans (composed of mainly Glc, Xyl, galactose (Gal) and fucose (Fuc)), and β-1,3/1,4-D-glucans (not present in dicotyledons).The typical distribution of the different hemicelluloses between the primary and secondary cell wall of dicots are shown in Table 2. Mannans are structurally important but they also serve as storage polysaccharides (96). Xyloglucans cross-links cellulose microfibrils thus strengthens cell walls and xyloglucan derived oligosaccharides have diverse functions in the plant cell wall since they can act as physiological signals (97) and are sometimes implicated in cell adhesion (98).

Table 2: Typical distribution of hemicelluloses in primary and secondary cell walls of dicots (96).

% Hemicellulose polysaccharide in dicot walls (%w/w)		
Polysaccharide	**Primary**	**Secondary**
Xyloglucan	20-25	Minor
Glucuronoxylan	Absent or minor	20-30
Glucuronoarabinoxylan	5	Absent or minor
Glucomannan	3-5	2-5
Galactoglucomannan	Absent or minor	0-3

2.3.1.2 Pectin network

Pectins are galacturonate-rich acidic polysaccharides and represent up to 30% of the cell walls of dicots (99). The different structural classes of pectic polysaccharides found in plant cells are homogalacturonan (HG), xylogalacturonan (XGA), apiogalacturonan (AGA) (not found in dicots), RG-II and RG-I. HG is galacturonic acid (GalA) residues linked together with a α-1,4-bond and they can be methyl-esterified at the C-6 carboxyl and/or acetylated at the O-2 or O-3. HG with a high degree of methyl esterification is called 'pectin' and HG with low or no methyl esterification is termed 'pectic acid' (100). The degree of methyl esterification can differ significantly between plant species and tissue type from which the cell wall was harvested (99). Unmethylated C-6 residues carry a negative charge and if there is a stretch of more than 10 unmethylated C-6

residues present, two HG molecules can form a double helix with Ca^{2+} forming a bridge between the molecules. This is referred to as the egg-box model or Ca^{2+}-induced gelling (101). In contrast, HG with a very high degree of methyl esterification can form a calcium independent gel. This type of gel forms in water limiting environments with the aid of hydrogen bonds and hydrophobic interactions (88). The formation of a gel by HG can affect all the polysaccharide interactions in the cell wall and therefore also the physical and functional properties of the cell wall. Non-esterified HG is mostly found in the middle lamella and in cell corners while esterified HG is found throughout the cell wall surrounding the cellulose-hemicellulose network (84). HG isolated from apples, beet (*Beta vulgaris)* and citrus showed that HG molecules contained approximately 72 – 100 galacturonic acid residues (99). The backbone of HG is covalently linked to RG-I, RG-II and presumably covalently cross-linked to xyloglucan (XyG) (105). HG substituted with D-xylose residues at C-3 is known as Xylogalacturonan (XGA). RG-II is the most complex polysaccharide found in the plant cell wall and the complexity of RG-II makes it resistant to microbial attack (103). RG-II exists in the primary wall as a monomer or a dimer with a single borate diester cross-link. The dimer contains heavy metals such as Pb^{2+}, Ba^{2+} and St^{2+} and it is a major component of wines (up to 100mg/ in red wine) and fruit juices. A stretch of approximately eight 1,4-linked α-D-Gal*p*A (Galacturonosyluronic acid) residues that is substituted with up to five side chains (A – E) and comprising 12 different monosaccharides makes up a typical RG-II monomer (104). There is some variability in the structure across plant species and recently variation within an individual plant, involving monosaccharide substitution, chain A methylation and variation in the length of chain B was demonstrated (105). Natural diversity as well as modifications (dearabinosylation and deacetylation) due to acid treatment were observed in RG-II that was isolated from wine (106). And finally; RG-I is a family of structurally similar molecules and has a backbone of repeating units of $[\rightarrow\alpha$-D-Gal*p*A-1,2-α-L-Rha*p*-1,4$\rightarrow]_n$. RG-I has as many as 40 structurally different branches attached to about half of the rhamnose residues at the C-4 position. These branches contain mainly arabinosyl and galactosyl residues but fucosyl, glycosyluronic acid and 4-O-methyl glycosyluronic acid residues can be present in low amounts (88) depending on the source of RG-I .

Concerning the function of the pectic polysaccharides in the cell wall, it has been established that calcium crosslinking brings together blocks of unmethylesterified HG and this contributes to the rigidity of the cell wall (99). RG-II borate dimers are also important for cell wall integrity and is specifically required in the elongation of the pollen tube of *Arabidopsis* (107). Furthermore, the HG-calcium complexes and the RG-I side chains mediate cellular adhesion in plant tissues and plays a central role in the functioning of stomata (108). Pectic oligosaccharides produced by the action of hydrolytic enzymes secreted by plant pathogens, acts as elicitors that induce the defense response pathways (109) in plants. The pectin network is extensively modified

during fruit ripening/softening (110) and modifications include solubilization, depolymerization, loss of neutral side chains and reduction in length of individual pectin chains.

2.3.1.3 The proteins of the cell wall

The plant cell wall contains structural and functional proteins (88). The structural proteins include the hydroxyproline-rich glycoproteins, the glycine-rich proteins and the proline-rich proteins. A definitive characteristic of the structural proteins are their repeated sequence motifs of between 2-16 amino acids, which acts as putative functional domains. These domains in conjunction with each other can create certain geometrical conformations (helical domains, β-strands and –sheets) or form segments with specific characteristics (hydrophobic, or –phylic, charged or stiff domains). The hydroxyproline-rich glycoproteins, also known as extensins, have a basic polypeptide backbone substituted with mono- to tetra-saccharide side-chains of arabinose (Ara) and Gal (111). Extensins are amphiphilic and can form cross-links in the cell wall with other proteins. Extensins can also function as intra- and intermolecular cross-linking or -binding sites and glycosylation domains. In fact, extensins are believed to form a fibrillar network independent from the cellulosic network and thus, contribute significantly towards cell wall strength, toughness, flexibility, pore size and hydration (112).

Another family of proteins found in the cell wall is the arabinogalactans (AGP). The polysaccharide portion of these proteoglycans accounts for more than 90% of the molecule and it is rich in Gal and Ara (113). The protein portion is rich in hydroxyproline, alanine and serine. The AGPs have diverse biological roles (114) and have been implicated in many plant growth and development processes such somatic embryogenesis, root growth and development, hormone responses, xylem differentiation, signaling, salt tolerance, cell expansion etc. Recently (115) a very important link was made between AGPs and Ca^{2+} signaling and the existence of an AGP-Ca^{2+} oscillator was proposed which would explain the involvement of AGPs in plant morphogenesis.

The enzymes located in the cell wall are those that are involved in the cell wall metabolism such as the endo- and exoglycanases, methyl- and acetyl esterases and the trans-glycosylases (100). Additionally the cell wall contains enzymes such as peroxidases, that can generate cross-links between wall polymers (116). Functional but non-enzymatic proteins located in the cell wall are the lipid transporters, pathogen protectors (such as thionins, glucosidases, chitinases, polygalacturonase-inhibitors) and expansins, which presumably break hydrogen bonds between xyloglucan and cellulose, regulating wall expansion in the process (88).

2.3.1.4 Cutin and lignin

The cuticle is the final interface between the plant and the environment and is a non-cellular, protective layer that consists of cutin bi-polymers with waxes (soluble lipids) embedded in or deposited on the cutin matrix (117). Cutin is a biopolyester of saturated C_{16} ω-hydroxy and unsaturated C_{18} hydroxy-epoxy fatty acid monomers and the cutin layer can contain small amounts of phenolic acids such as ferulic acid. The imbedded cuticular waxes serves as waterproofing filler in the cutin matrix while those deposited onto the surface form complex three-dimensional crystalline structures such as platelets, rod lets and tubules. They consist of long-chain aliphatic compounds, such as very long chain fatty acids (C_{20} to C_{34}), aldehydes, primary and secondary alcohols, ketones, alkanes and alkyl esters.

Lignin is a phenolic polymer mainly found in secondary cell walls of plants. Lignin provides the mechanical strength in plant cell walls that enables trees to grow tall, it is the hydrophobic water-impermeable surface of xylem cells and it protects the plant against pathogens because of its high resistance towards microbial decay (88). According to Brummel (118) the cell walls in the fruit flesh of most species do not have secondary cell walls and have very low levels of lignin. On the other hand and according to some authors, fruit skins do contain lignin (Table 3). The amount of lignin in grape skins has been a topic of debate for some time. Some authors recorded lignin values between 2 and 56% for grape pulp and skin (Table 3). In contrast others belief that the presence of true lignin in grape skin (or pulp) is highly unlikely (83, 119) or speculate that the acid insoluble fraction that are traditionally classified as lignin might rather be cellulose embedded in cuticular waxy material (69). Thus, the high variability in the lignin concentration recorded in Table 3 is probably due to the variation in analysis methods that were used and in how the lignin fraction is defined.

Table 3: Lignin content of different fruit skins as percentage of skin weight

Fruit	% dry weight of skin	Reference
Citrus fruit skins	1.3 – 2.2	(120)
Banana skins	6 -16	(121) (122)
Apple skin	34 - 39	(123)
Grape skin	*40 - 45*	(123)
Grape skin	*24-56*	(124)
Grape skin *Grape pulp*	*10* *2*	(125)

2.3.1.5 Models of the primary cell walls of plants

Several models have been proposed over the years in an effort to explain how the cellulose, hemicellulose, pectin and cell wall proteins fit together in a three dimensional structure while allowing for plant growth and differentiation (90). Examples of these are the Keegstra (126) model based on sycamore cell walls. The tethered network model by Fry (127) and Hayashi (128) cited in Cosgrove (116) (FIG 3 A) with xyloglucan chains that span the gap between cellulose microfibrils was the standard model with many others proposing variations on this model. Examples are the multicoat model of (129) (cellulose is coated with successively looser layers of matrix polysaccharides) and the stratified model (130) (strata of pectic polysaccharides separate cellulose-xyloglucan layers). Carpita and Gibeaut (131) developed a general model for flowering plants and for *Poaceae* and illustrated how these models would accommodate cell expansion. Somerville (94) published an illustration of a model (Fig. 3 B) based on Vincken (132) and although this model is not widely accepted (133) it was a good attempt to show the complexity of the cell wall. In 2012 (98) the tethered network model where xyloglucan is seen as a gap-spanning, taunt, load bearing feature between cellulose microfibrils, was challenged. An alternative model proposed regions of xyloglucan-mediated, close contact between cellulose microfibrils and these regions would then be critical in the regulation of cell wall loosening during growth. The importance of the cellulose microfibril-xyloglucan network in regulating expansive growth were confirmed by Yi and Puri (134) using a computational cell wall model and they suggested that the pectic matrix might also contribute to load-bearing in the plant cell wall. Tan et al. (135) suggested a new model in which AGPs serve as a cross-linker that connects pectin and hemicellulose polysaccharides after identifying covalent links between an arabinoxylan-pectin-AGP complex isolated from *Arabidopsis* tissue culture.

These models were largely build on evidence of interactions between the different cell wall polymers. Some of the earlier examples are the interaction between pectins and structural cell wall proteins (126). This was found when a cell wall fraction isolated after treatment with endo-polygalacturonase, endo-glucanase and alkali rendered pectic polymers only after protease hydrolysis. Each individual polysaccharide and glycoprotein of the cell wall is water-soluble (except cellulose) but when forming part of the cell wall matrix the molecules are cross-linked into a structure that holds together in an aqueous environment (136). The links can be non-covalent and thus weak but ensuring strength because of their abundance. Examples are the hydrogen bonds between hemicelluloses and cellulose, the Ca^{2+} bridges crosslinking HG and basic glycoproteins ionically linked to acidic polysaccharides. Covalent links, which are individually strong but few in numbers, are for example the borate diester cross-links between RG-II molecules. The interaction between xyloglucan and cellulose has been extensively studied and the binding capacity depends on the surface area of the cellulose, the degree of fucosylation of xyloglucan (137) and the source of the xyloglucan (138). It has been proposed

that mannans also cross-link cellulose (139) and it is shielded by HG (140). We have already mentioned that the backbone of HG is covalently linked and continuous to the backbone of RG-I and –II (102), and the pectin network can thus be envisioned as a macromolecular structure with different domains. There are many reports in literature that suggest a stable covalent link between xyloglucan and HG and/or RG-I (97, 133, 141–143)

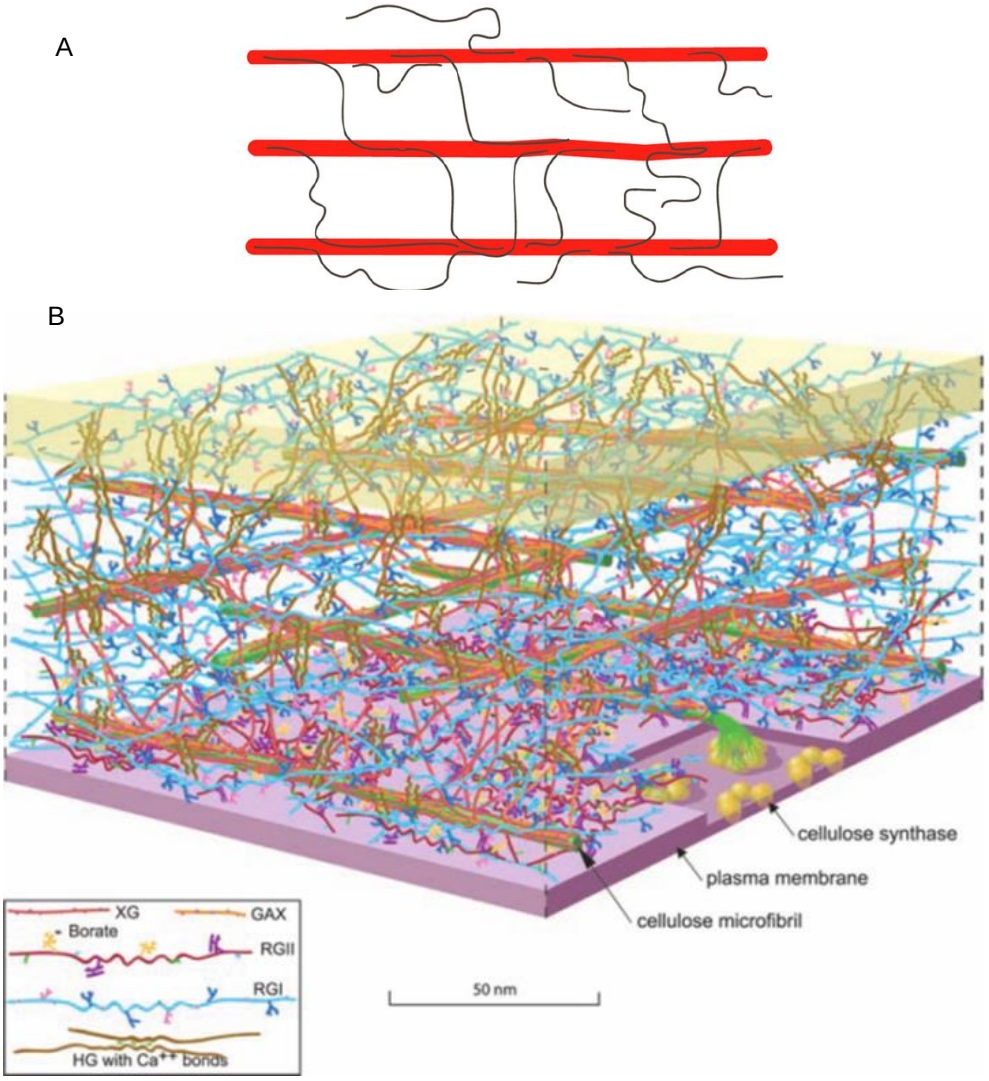

Figure 3: (A)The tethered network plant cell wall model proposed by Fry (127) and Hayashi (128) cited in (116) [figure adapted from (98)]. The figure only shows the cellulose microfibrils cross-linked with xyloglucan. The space in between is filled up by pectin and structural proteins. (B) Scale cell wall model by (94) of the *Arabidopsis* leave with the amount of cellulose reduced to provide more clarity.

The galactan and arabinan side chains of RG-I binds to cellulose but this association is not of the same strength as between cellulose and xyloglucan (141, 144). Where the xyloglucan-cellulose association has been described as an ‘entrapment’ the cellulose-arabinan or -galactan

association is limited to the surface of cellulose. Pectin polymers, in particular β-1,4-D-galactan, α-1,5-L-arabinan and arabinogalactan are cross-linked to phenolic compounds (99, 100). Finally, new evidence of interaction between AGPs and cell wall polymers such as the previously mentioned arabinoxylan-pectin-AGP complex (135) as well as the AGP31 interaction with galactan branches of RG-I (145) are showing how these cell wall proteins form part of the cell wall structure. It was proposed that AGP31 participates in supra-molecular scaffolds that play a role in cell wall strengthening, specifically in plant organs displaying rapid growth (145).

2.3.2 The grape berry cell wall

2.3.2.1 The cell wall of the mesocarp (pulp)

The cell walls of mesocarp cells of mature grape berries are a maximum of 100 nm thick and the composition is approximately 90% polysaccharides and 10% proteins (146). The major polysaccharides are cellulose and galacturonans and there is a definite, observable difference between firmer and softer grape cultivars. The firmer cultivars have more cellulose, xyloglucans and hydroxyproline-rich proteins while the softer varieties have cell walls enriched by polygalacturonans, thus a more extensive pectic matrix (146). Ortega-Regules et al. (147) determined the sugar composition of the cell walls of both the skin and the pulp cells (of four different wine grape cultivars) and found that the pulp cell walls had slightly higher fucose (Fuc), rhamnose (Rha), Xyl and cellulose but lower Ara, Gal, Man and hemicellulosic glucose (Glc) than the skin cell walls. The uronic acid was about the same in the different tissues but the degree of methylesterification was lower in the pulp cell walls.

2.3.2.2 The pericarp (skin) and the cell wall of the skin cells

The grape skin constitutes for 5 – 10% of the total dry weight of the grape berry and three layers can be differentiated (148). On the outside is the cuticle (1 – 4 µm thick) consisting of hydroxylated fatty acids (cutin) and this is covered by hydrophobic waxes. The cuticle protects the fruit from fungal infection, dehydration, UV light and physical damage (149). Underneath the cuticle is the epidermis that consists of one or two layers of cells with moderately thick cell walls (Fig. 4). Following this is the hypodermis that can have a variable number of cell layers and forms the border between the pulp and the skin. The number of cell layers in the grape berry skin and the size of the cells are cultivar-specific (150) as well as the cell wall composition (147). However, on average the cell wall of the skin cells consist of 30% neutral polysaccharides (cellulose, xyloglucan, arabinan, galactan, xylan and mannan) and 20% of acidic pectin components (62% methyl esterified). The remainder consists of approximately 15% insoluble proanthocyanidins and less than 5% structural proteins (148). Working with the values that they determined for monosaccharides, Arnous and Meyer (123) used an iterative calculation method to infer the polysaccharides present in the skin cell walls. With this method they estimated the polysaccharides to be 57-62 mol % HG, 6-14 mol % cellulose, 10-11 mol % xyloglucan, 7 mol %

arabinan, 4.5-5 mol % RG-I, 3.5 – 4 mol % RG-II, 3 mol % arabinogalactan and 0.5 – 10 mol % mannans.

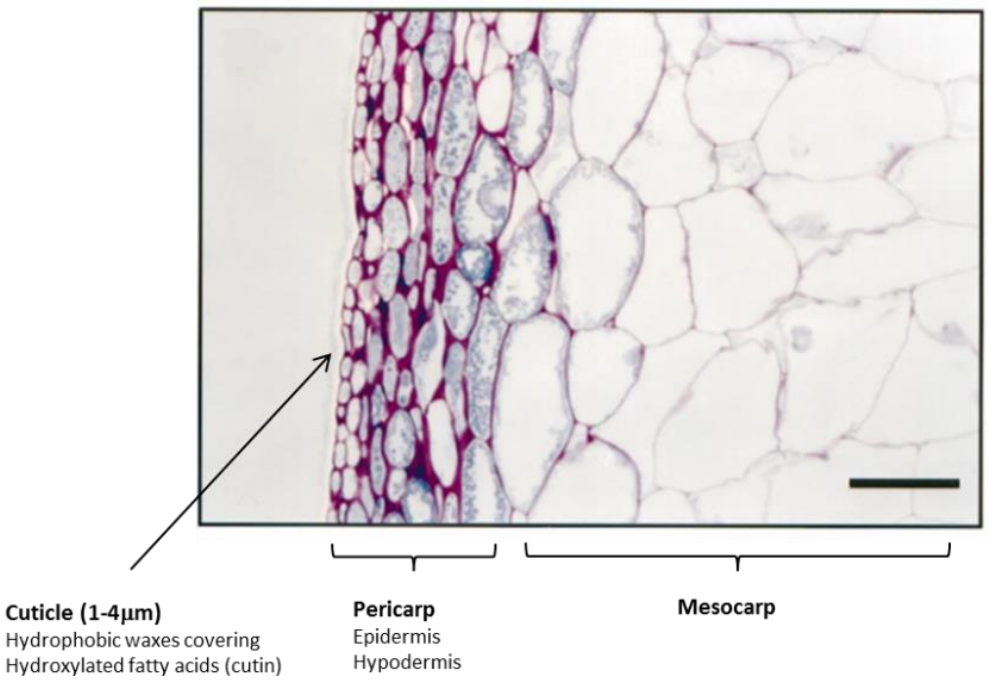

Figure 4: The cell layers of the grape berry (151). The bar is 100μm.

2.3.2.3 The cutin layer of the grape berry

The grape berry cuticle plays a crucial role in protecting against *Botrytis cinerea* infection by being a hydrophobic and chemical barrier (152). However, it is still possible for *B. cinerea* to enter through undamaged cuticle presumably by secreting a lipase that hydrolyses long chain fatty acids. Comménil et al. (153) investigated the development of the cuticle from flowering to maturity. They reported that the composition of the cuticular waxes changed (the percentage primary alcohols decreased and the hydrocarbons increased) and that there was an increase in waxy deposits but a decrease in the cutin content per berry surface unit. The wax surface morphology at maturity showed cracks, which could be a penetration point for the *B. cinerea* conidia. Grape berry wax contains 50-80% (total weight of wax extract) oleanolic acid, which is a triterpenoid (154). Other triterpenoids present are oleanolic aldehyde, erythrodiol and phytosterols such as β-sitosterol, campesterol, stigmasterol and lanosterol. The high abundance of these triterpenoids in grape berry waxes can contribute to the health benefits associated with grape consumption because pharmacological properties such as anticancer, anti-inflammatory, antidiabetogenic, antimicrobial, cardio protective, anti-HIV and anti-multiple sclerosis effects has been attributed to tripterpenoids (154). The levels of phytosterols present

in the berry cuticle wax exhibited a fluctuation with ripening by increasing at peak berry maturity and then decreasing in the last stage of ripening.

2.3.3 The changes in the cell wall of the grape berry during ripening

The development of the grape berry consists of a cell division phase followed by a cell expansion phase (155). The onset of this second phase, known as veraison, signifies the initiation of events such as sugar accumulation, a decrease in organic acids, colour development, berry expansion and softening. Information regarding fruit ripening or softening is commercially important because it goes hand in hand with the development of flavour and colour of the fruit and can indicate the point of optimum ripeness (156). In addition, by preventing excessive ripening/softening the fruit is protected from mechanical damage that will set it vulnerable for microbial attack. The textural change that takes place during ripening is partially explained by the changes happening in the cell wall polysaccharides (157). With the development of the berry, the size and morphology changes are accommodated by a series of coordinated biochemical reactions. These reactions encompass both the biosynthesis and the degradation of cell wall components and numerous plant enzymes are involved. Several reviews (97, 136, 157) discuss in detail the processes and the enzymes responsible but for the purpose of this literature review we will only focus on the degradation effect that these enzymes are believed to have on the cell wall components.

In literature, most of the studies investigating the changes during ripening focus on the cell walls of the mesocarp cells. Nunan et al**.** (151) studied these cell walls during the different developmental stages using fluorescent and light microscopy and could not detect a measurable change in the cell wall thickness. Compositional analysis showed a major decrease in Gal and galactan content during ripening of the berry, especially the (1,4)-linked galactopyranose residues of type I arabinogalactan. This could be the result of the grape β-galactosidase activity that was detected (158) throughout all the ripening stages of the berry. Furthermore, the mRNA for this enzyme was accumulating from pre-veraison until early post-veraison berries. During ripening there was also a major increase in the solubility of the pectic polysaccharides (151) which was ascribed by the authors to the detected activity (158) of α-galactosidase, β-galactosidase and/or pectin methylesterase. The solubilisation can also be a result of the action of polygalacturonases and/or pectate lyases but they could not observe these activities although the genes were actively expressed after veraison. In contrast with other fruits, grapes showed only a slight decrease (from 58 to 48%) in the degree of methylesterification in the mesocarp cell wall during ripening. The levels of cell wall-associated proteins, in particular the hydroxyproline rich proteins, increase during ripening (inferred from changes in the amino acid profile) while cellulose and xyloglucan levels remained the same with

no increase in solubility. However, Yakushiji and co-workers (159) studied the mesocarp cell walls of *Vitis vinifera* L. x *V. labrusca* L. during veraison and found, in contrast to Nunan (151), that the cellulose content decreased. They also noted a depolymerization of xyloglucan and pectic polysaccharides and a general decrease in hemicellulose. Furthermore, Guillaumie et al. (160) correlated the expression profile of four xyloglucan endotransglycosylases/hydrolyses from Chardonnay berries with fruit ripening and Moore et al. (60) showed the decrease in epitope abundance for mAb LM15 (that binds to xyloglucan) as ripening progresses.

Ortega-Regules and co-workers (59) investigated the skin cell from veraison up to technological maturity (related to the sugar concentration, titratable acidity and pH of the grape juice) . In contrast with the observations recorded for the pulp cells (151) the Ortega-Regules study showed with transmission microscopy how the cell walls became thinner as the grapes ripen. This correlated with the decrease in cell wall material per gram of skin that they were able to isolate as time progressed through the ripening process. Chemical changes included a decrease in Gal (similar to the mesocarp cell wall) and a decrease in the degree of pectin methylation and acetylation. This was true for the cultivars Mourvèdre (Monastrell J), Merlot and Cabernet Sauvignon while the pectin methylation in Shiraz remained constant. In contrast, a study by Vicens et al. (161) focusing on the grape skin of Shiraz, measured a decrease in methylesterification of uronic acid and an increase in the water-soluble fraction. According to Huang et al. (162), the degradation and consequential loss of polysaccharides in the cell wall are accompanied by cell wall acidification and the loss of pectin bound calcium.

2.3.4 The factors affecting the extractability of polyphenols from the grape skin

In order to understand every aspect involved in the enzyme assisted maceration step we not only need to know the composition of the barrier (cell wall) between the phenolic compounds and the wine must, but we also need to understand how these polyphenols are bound to cell structures and the factors that influence the ease of extractability of these compounds from the grape tissue to the must.

The phenolic compounds of grapes that contributes to wine quality are mainly the hydroxycinnamic acid, anthocyanins and tannins (163). Most of the phenolic compounds of the grape berry are located (Figure 1) in the hypodermal and epidermal cells of the skin (20 – 30% w/w) and in the epidermal seed coat (60% w/w) (33, 83, 164). Within these cells, the anthocyanins are mostly found in the vacuole but some are bound to the cell nucleus or to the cell wall polymers (73). The vacuole, which can occupy more than 90% of the space in the cell (164) is surrounded by a tonoplast (vacuolar membrane). Tannins can be free in the vacuole, bound to the proteins on the inside of the tonoplast, or bound to the cell wall polymers by

glycosidic bonds (165). Flavonols and hydroxybenzoic acids are believed to interact with the cell wall polysaccharides via hydrophobic interactions or hydrogen bonds (23, 73) and hydroxycinnamic acids might be esterified to the Ara and Gal molecules of β-1,4-D-galactan and α-1,5-L-arabinan side chains of RG-I (166).

Grape proanthocyanidins can bind to a variety of molecules because of the availability of both a hydrophobic aromatic ring and a hydrophilic hydroxyl group (83). In grape skins, they interact with proteins via hydrogen bonding as well as hydrophobic interactions and in the same way, they interact with the hydroxyl groups and glycosidic oxygen atoms of the cell wall polysaccharides (167). Proanthocyanidins shows a hierarchy of affinity for polysaccharides and would preferentially bind to pectin, then xyloglucan and lastly to cellulose (168). However, this hierarchy is also dependent on the accessibility of the polysaccharide-binding site within the cell wall structure. In apple tissue, the degree of pectin methylation shows a positive correlation with proanthocyanidin binding while protein content has no influence (169).

The phenolic content of grapes is a factor of the cultivar, the climatic conditions during the growing season, the terroir, vineyard practices that were followed and the degree of maturation of the grapes (27). The levels of most phenolic compounds in grape tissue increase during ripening followed by a slight decline close to, what can be considered as, the overripe stage (170). The decline is due to their degradation, their bioconversion into other products or their covalent association with other cellular components. Similarly, anthocyanin synthesis that starts during veraison, accumulate in the skin cells during ripening and show a slight decrease in concentration in overripe grape skins (163, 171, 172). Grapes with high levels of polyphenols do not always deliver wines with high colour intensity or polyphenol content. Even with extended maceration only a fraction of the total polyphenols present in the grapes, will be extracted (163). The extraction of polyphenols from the grape berry to the wine is in essence a diffusion process. Therefore, the extraction depends on the molecular size and the type of polyphenol, the time and temperature of the extraction process, the concentration gradient, cell permeability, the composition of the extraction medium (for example ethanol concentration) and the surface area over the concentration gradient (163). In general, anthocyanins from the skin are extracted early in the maceration while the tannins are extracted later (173). This is also linked to the solubility characteristics since anthocyanins can dissolve in aqueous solutions but tannins need a certain level of ethanol in which to dissolve (15, 174).

The ease of extractability of polyphenols from berry skin differs between cultivars (172, 175) and according to an extractability index developed by Saint-Criq et al. (1998). A cultivar that is known to have a high extractability index (not easy to extract) is Monastrell (also known as Mourvèdre) (147, 175, 176) while cultivars such as Merlot, Shiraz and Cabernet Sauvignon have a lower extractability index. The berry of Monastrell has a thick and tough skin and the

same description is true for the Pinotage cultivar (58) that was used in Chapter 3 and 4 of this thesis. In contrast, Chardonnay that was also used in Chapter 4 and 5, has a thin (0.14 mm) (177) but tough skin (58). The divergence in the extractability indexes was studied by investigating the properties of the skin and the skin cell walls of a number of cultivars in conjunction with the maturity level of the grapes. Ortega-Regules and co-workers (176) found that a low extraction index (easy to extract) was linked to a low concentration of Gal in the cell wall as well as a low degree of pectin methylation and acetylation. Although these are all typical characteristics of a cell wall of ripe or mature berries (see ripening section 2.3), they could not form a direct link between extractability index and ripeness (measured in °Brix). This is an unexpected result because we know (147) that the skin cell wall becomes thinner with ripening and that thinner skin are associated with a greater release of red pigments (178). However, other authors (171) showed with Shiraz and with Mencía grapes (178) that the percentage of free anthocyanins and the tannins that could be extracted from skin remained the same irrespective of the sugar content of the berry pulp. According to Fournand (171) it is rather the mean degree of polymerization of the tannins, and to a lesser degree, the galloylation percentage, which are the determining factors concerning extractability. It is only in the past three years that researchers started to show a positive link between extractability and ripeness. For example Hernández-Hierro et al. (179) showed how the extractability is strongly linked to the ripeness level and went on to confirm this in the cultivar Tempranillo (180). Gil et al. (30) worked on Cabernet Sauvignon and Tempranillo and investigated both grape ripeness and maceration length. They found a positive correlation between colour extractability, phenolic compounds, polysaccharide concentrations in the wine and ripeness. Furthermore, mature grapes released more proanthocyanidins from skins than from seeds, which contributed positively towards the sensory attributes of the wine (lower astringency and bitterness). They observed that with an extended maceration the color and anthocyanin concentration decreased but polysaccharide and proanthocyanidin concentration still increased along with an increase in the galloylation percentage, indicating proanthocyanidin extraction from seeds.

In studies done by Bindon et al. (125, 181, 182) it was shown that overripe berries have a higher cell wall porosity (probably due to pectin degradation) and this corresponded with enhanced adsorption of high molecular mass tannins and anthocyanins. This led to the hypothesis that these polyphenols are encapsulated within the pores, where they bind to the cell wall components and it result in a reduction in the extractability of these tannins during vinification.

2.4 Investigating the cell wall degradation by enzymes

2.4.1 Investigating the cell wall degradation by maceration enzymes in wine

Evaluating the extent of the cell wall degradation done by hydrolytic enzymes by measuring polyphenol release (section 2.1.1.1) is an indirect measure and does not tell us how the enzymes changed the structure of the cell wall. A more direct method is to determine the cell wall components that are released during enzyme incubation. Arnous and Meyer (183) measured the monosaccharides released from grape skins treated with a cellulolytic and two pectinolytic maceration enzymes. Overall, higher levels of monosaccharides were liberated by the pectinolytic than the cellulolytic enzyme preparations and more monosaccharides were liberated from Cabernet Sauvignon skins than from Merlot skins. This might be a reflection of the differences in cell wall composition between cultivars and/or the ease of accessibility (e.g. pore size) for maceration enzymes to the polysaccharides in the cell wall. Enzymatic monosaccharide release were 2.8 times lower than what were obtained when hydrolyzing the cell walls with trifluoroacetic acid which indicated that the cell wall polysaccharides were not completely degraded during prolonged enzymatic treatment. With this study, they could also correlate the release of specific polyphenols with specific monosaccharides that gave an indication of the location and bonding of the polyphenols in the cell walls.

Alternatively, methods that isolate and compare cell walls of grape tissue before and after maceration enzyme treatment were developed. Romero-Cascales et al. (26) isolated cell wall material from the pomace of enzyme (pectinase) treated fermentations and determined that enzymatic hydrolysis renders more cell wall material per gram of tissue. They speculated that since the cell wall has been partially degraded more of the cell content was extracted during the fermentation, thus at the end of alcoholic fermentation the ratio of cell wall to tissue is larger for enzyme treated skins. They also showed that the Ara, Gal, uronic acids and total sugar content of cell wall was lower for enzyme treated samples. These are typical changes seen during fruit ripening (146, 151) and indicate the degradation of the pectic polysaccharides of the cell wall. As a consequence of the reduction in pectin polysaccharides (26) they saw an proportional increase in Man and Glc content indicating that the hemicellulose remained in the cell wall.

2.4.2 Investigating the changes in the pomace cell wall due to enzyme treatment

Chamorro et al. (75) investigated the monosaccharides released from grape pomace after treatment with different enzyme preparations as an indication of cell wall degradation but they did not analyze the actual residual matter. None of the other studies that used enzymes on grape pomace for either polyphenol extraction of bioethanol production studied the cell wall residues or the changes that happened to the composition of the cell wall during all the steps involved. A study by DeMartini et al. (184) investigated the sequence of structural changes that happened in *Populus* biomass during hydrothermal pretreatment using Immunolabeling. The

steam treatment disrupted the lignin-polysaccharide interactions, pectins and arabinogalactans were lost, and this was followed by removal of xylans and xyloglucans. And finally a review by Paës (87) discussed the use of fluorescent probes to study the deconstruction of biomass but these technique has not yet been used with grape pomace as subject matter.

2.5 Concluding remarks

Enzymes are essential tools for the processing of grapes and it is important to optimize their use in order to improve the effectiveness and economic viability of these applications for future use (87). Many factors are thought to determine the success of enzymatic degradation of the grape berry cell wall. These factors can be connected to the properties of the enzyme, such as enzyme type, the enzyme-substrate ratio and hydrolysis conditions (pH, time, temperature). The studies investigating this are in essence all optimizing experiments because for each enzyme and enzyme combination and for every type of grape tissue substrate as well as the scale of the experiment the ideal conditions will be different.

Other factors that can determine the enzyme effectiveness has to do with the grape skin and the composition of the cell wall of the skin and pulp cells. Many things can influence the composition of the cell walls and those that are being studied are for example the morphological differences in the skin and the compositional differences in the cell walls of different cultivars. There are the so-called recalcitrant cultivars (such as Monastrell) that have a tough, thick skin and many studies focus on the skin properties of these cultivar as well as the effect that enzymes have on extracting compounds from the Monastrell skin (6, 48, 175, 176, 185). However, another important South African grape cultivar, Pinotage, is also known for its tough and thick skin (58, 186), but there is very little information available on the skin or cell wall properties of this grape.

For the extraction of molecules from recalcitrant grape cultivars pretreatment steps can be employed (8, 61, 82, 187, 188). Different pretreatments are being evaluated by measuring the levels of molecules yielded but very little, if any information is available on how these pretreatment steps change the grape cell wall. Another factor that has a large influence on the cell wall properties are the level of maturity/ripeness of the grapes (59, 180, 181). There are subtle differences detectable in how the composition of the cell wall polymers change during ripening, between cultivars (59). There is no information available on how the cell wall properties of Pinotage change during ripening. This grape can sometimes deliver a bitter tasting wine and it has been speculated that it can be linked to the bitterness in the unripe skin (186). Thus, it is important to gain more information on this topic. Furthermore, there is also no

information on how the maturity level of grapes, in general, affects the success of maceration enzymes.

A general theme of all previous investigations looking into enzymatic hydrolysis of grape cell walls is the measuring of indirect and associated molecules or characteristics, for example measuring red wine colour, polyphenols or typical cell wall monosaccharides released or determining the monosaccharide composition in the residual cell wall fragments after enzymatic hydrolysis. From all these studies, it was only possible to infer the actual polymer changes that took place in the cell walls due to enzymatic hydrolysis. Therefore, in order to understand what happens at the cell wall during enzyme assisted wine maceration or the use of hydrolytic enzymes in the valorisation of grape pomace, a detailed investigation on the grape cell wall structure is needed at the polymer level.

2.6 References

1. **Ribéreau-Gayon P, Dubourdieu D, Doneche B, Lonvaud A**. 2006. Handbook of enology, 2nd ed. John Wiley and Sons, Chichester.

2. **Jackson RS**. 2008. Wine science: Principles and applications, 3rd ed. Academic Press, Inc., San Diego.

3. **Sacchi KL, Bisson LF, Adams DO**. 2005. A review of the effect of winemaking techniques on phenolic extraction in red wines. Am. J. Enol. Vitic. **56**:197–206.

4. **Naziri E, Nenadis N, Mantzouridou FT, Tsimidou MZ**. 2014. Valorization of the major agrifood industrial by-products and waste from Central Macedonia (Greece) for the recovery of compounds for food applications. Food Res. Int. **65**:350–358.

5. **Hendriks ATWM, Zeeman G**. 2009. Pretreatments to enhance the digestibility of lignocellulosic biomass. Bioresour. Technol. **100**:10–8.

6. **Alvira P, Tomás-Pejó E, Ballesteros M, Negro MJ**. 2010. Pretreatment technologies for an efficient bioethanol production process based on enzymatic hydrolysis: A review. Bioresour. Technol. **101**:4851–61.

7. **Dambergs R, Sparrow A, Carew A, Scrimgeour N, Wilkes E, Godden P, Herderich M, Johnson D**. 2012. Quality in a cool climate – maceration techniques in Pinot Noir production. Wine Vitic. J. **3**:18–26.

8. **De Beer D, Joubert E, Marais J, Manley M**. 2006. Maceration before and during fermentation : Effect on Pinotage wine phenolic composition , total antioxidant capacity and objective colour parameters. South African J. Enol. Vitic. **27**:137–150.

9. **Ortega-Heras M, Pérez-Magariño S, González-Sanjosé ML**. 2012. Comparative study of the use of maceration enzymes and cold pre-fermentative maceration on phenolic and anthocyanic composition and colour of a Mencía red wine. LWT - Food Sci. Technol. **48**:1–8.

10. **Parley A, Vanhanen L, Heatherbell D**. 2001. Effects of pre-fermentation enzyme maceration on extraction and colour stability in Pinot Noir wine. Aust. J. Grape Wine Res. **7**:146–152.

11. **Koyama K, Goto-Yamamoto N, Hashizume K**. 2007. Influence of maceration temperature in red wine vinification on extraction of phenolics from berry skins and seeds of grape (*Vitis vinifera*). Biosci. Biotechnol. Biochem. **71**:958–65.

12. **Carranza-Concha J, Del Mar Camacho M, Martinez-Navarrete N**. 2012. Effects of blanching on grapes (*Vitis Vinifera*) and changes during storage in syrup. J. Food Process. Preserv. **36**:11–20.

13. **Delsart C, Ghidossi R, Poupot C, Cholet C, Grimi N, Vorobiev E, Milisic V, Mietton Peuchot M**. 2012. Enhanced extraction of phenolic compounds from Merlot grapes by pulsed electric field treatment. Am. J. Enol. Vitic. **63**:205–211.

14. **Cholet C, Delsart C, Petrel M, Gontier E, Grimi N, L'Hyvernay A, Ghidossi R, Vorobiev E, Mietton-Peuchot M, Gény L**. 2014. Structural and biochemical changes induced by pulsed electric field treatments on Cabernet Sauvignon grape berry skins: impact on cell wall total tannins and polysaccharides. J. Agric. Food Chem. **62**:2925–34.

15. **Bautista-Ortin AB, Martinez-Cutillas A, Ros-Garcia JM, Lopez-Roca JM, Gomez-Plaza E**. 2005. Improving colour extraction and stability in red wines: the use of maceration enzymes and enological tannins. Int. J. Food Sci. Technol. **40**:867–878.

16. **Revilla I, González-Sanjosé ML**. 2002. Multivariate evaluation of changes induced in Red Wine characteristics by the use of extracting agents. J. Agric. Food Chem. **50**:4525–4530.

17. **Ough CS, Crowell EA**. 1979. Pectin-enzyme treatment of white grapes: temperature, variety and skin-contact time factors. Am. J. Enol. Vitic. **30**:22–27.

18. **Van Rensburg P, Pretorius IS**. 2000. Enzymes in winemaking : harnessing natural catalysts for efficient biotransformations - A review. South African J. Enol. Vitic. **21**:52–73.

19. **Mojsov K**. 2013. Use of enzymes in wine making: a review. Int. J. Mark. Technol. **3**:112–127.

20. **Sieiro C, García-Fraga B, López-Seijas J, Da Silva AF, Villa TG**. 2010. Microbial pectic enzymes in the food and wine industry, p. 201–218. *In* Valdez, B (ed.), Food industrial processes - Methods and Equipment. InTech, Rijeka.

21. **Romero-Cascales I, Fernández-Fernández JI, Ros-García JM, López-Roca JM, Gómez-Plaza E**. 2008. Characterisation of the main enzymatic activities present in six commercial macerating enzymes and their effects on extracting colour during winemaking of Monastrell grapes. Int. J. Food Sci. Technol. **43**:1295–1305.

22. **Fia G, Canuti V, Rosi I**. 2014. Evaluation of potential side activities of commercial enzyme preparations used in winemaking. Int. J. Food Sci. Technol. **49**:1902–1911.

23. **Meyer AS, Jepsen SM, Sørensen NS**. 1998. Enzymatic release of antioxidants for human low-density lipoprotein from grape pomace. J. Agric. Food Chem. **46**:2439–2446.

24. **Mehrländer K, Dietrich H, Sembries S, Dongowski G, Will F**. 2002. Structural characterization of oligosaccharides and polysaccharides from apple juices produced by enzymatic pomace liquefaction. J. Agric. Food Chem. **50**:1230–6.

25. **Moore JP, Divol B**. 2010. Tracking the carreers of grape and wine polymers using biotechnology and systems biology, p. 387–404. *In* Bagchi, D, Lau, FC, Ghosh, DK (eds.), Biotechnology in Functional Foods and Nutraceuticals. CRC Press, Boca Raton.

26. **Romero-Cascales I, Ros-García JM, López-Roca JM, Gómez-Plaza E**. 2012. The effect of a commercial pectolytic enzyme on grape skin cell wall degradation and colour evolution during the maceration process. Food Chem. **130**:626–631.

27. **Garrido J, Borges F**. 2013. Wine and grape polyphenols — A chemical perspective. Food Res. Int. **54**:1844–1858.

28. **Xia E-Q, Deng G-F, Guo Y-J, Li H-B**. 2010. Biological activities of polyphenols from grapes. Int. J. Mol. Sci. **11**:622–46.

29. **Gomez E, Martinez A, Laencina J**. 1994. Localization of free and bound aromatic compounds among skin , juice and pulp fractions of some grape varieties. Vitis **4**:1–4.

30. **Gil M, Kontoudakis N, González E, Esteruelas M, Fort F, Canals JM, Zamora F**. 2012. Influence of grape maturity and maceration length on color, polyphenolic composition, and polysaccharide content of Cabernet Sauvignon and Tempranillo wines. J. Agric. Food Chem. **60**:7988–8001.

31. **González-Manzano S, Rivas-Gonzalo JC, Santos-Buelga C**. 2004. Extraction of flavan-3-ols from grape seed and skin into wine using simulated maceration. Anal. Chim. Acta **513**:283–289.

32. **Kontoudakis N, Esteruelas M, Fort F, Canals JM, De Freitas V, Zamora F**. 2011. Influence of the heterogeneity of grape phenolic maturity on wine composition and quality. Food Chem. **124**:767–774.

33. **Cadot Y, Miñana-Castelló MT, Chevalier M**. 2006. Anatomical, histological, and histochemical changes in grape seeds from *Vitis vinifera L*. cv Cabernet franc during fruit development. J. Agric. Food Chem. **54**:9206–15.

34. **Ducasse M-A, Canal-Llauberes R-M, de Lumley M, Williams P, Souquet J-M, Fulcrand H, Doco T, Cheynier V**. 2010. Effect of macerating enzyme treatment on the polyphenol and polysaccharide composition of red wines. Food Chem. **118**:369–376.

35. **Busse-Valverde N, Gómez-Plaza E, López-Roca JM, Gil-Muñoz R, Bautista-Ortín AB**. 2011. The extraction of anthocyanins and proanthocyanidins from grapes to wine during fermentative maceration is affected by the enological technique. J. Agric. Food Chem. **59**:5450–5.

36. **Bautista-Ortín AB, Jiménez-Pascual E, Busse-Valverde N, López-Roca JM, Ros-García JM, Gómez-Plaza E**. 2012. Effect of wine maceration enzymes on the extraction of grape seed proanthocyanidins. Food Bioprocess Technol. **6**:2207–2212.

37. **Sun-Waterhouse D, Luberriaga C, Jin D, Wibisono R, Wadhwa SS, Waterhouse GIN**. 2011. Juices, fibres and skin waste extracts from white, pink or red-fleshed apple genotypes as potential food ingredients. Food Bioprocess Technol. **6**:377–390.

38. **Teixeira A, Eiras-Dias J, Castellarin SD, Gerós H**. 2013. Berry phenolics of grapevine under challenging environments. Int. J. Mol. Sci. **14**:18711–39.

39. **Gil J V, Vallés S**. 2001. Effect of macerating enzymes on red wine aroma at laboratory scale: exogenous addition or expression by transgenic wine yeasts. J. Agric. Food Chem. **49**:5515–23.

40. **Mocke B**. 2005. M.Sc thesis.*The breeding of yeast strains for novel oenological outcomes.* Stellenbosch University. Stellenbosch, South Africa.

41. **Salinas MR, Garijo J, Pardo F, Zalacain A, Alonso GL**. 2003. Color , polyphenol , and aroma compounds in Rosé wines after prefermentative maceration and enzymatic treatments. Am. J. Enol. Vitic. **54**:195–202.

42. **Waters EJ, Wallace W, Tate ME, Williams PJ**. 1993. Isolation and partial characterization of a natural haze protective factor from wine. J. Agric. Food Chem. **41**:724–730.

43. **Chalier P, Angot B, Delteil D, Doco T, Gunata Z**. 2007. Interactions between aroma compounds and whole mannoprotein isolated from *Saccharomyces cerevisiae* strains. Food Chem. **100**:22–30.

44. **Vernhet A, Pellerin P, Belleville M-P, Planque J, Moutounet M**. 1999. Relative impact of major wine polysaccharides on the performances of an organic microfiltration membrane. Am. J. Enol. Vitic. **50**:51–56.

45. **Vidal S, Francis L, Williams P, Kwiatkowski M, Gawel R, Cheynier V, Waters E**. 2004. The mouth-feel properties of polysaccharides and anthocyanins in a wine like medium. Food Chem. **85**:519–525.

46. **Vidal S, Williams P, Doco T, Moutounet M, Pellerin P**. 2003. The polysaccharides of red wine: total fractionation and characterization. Carbohydr. Polym. **54**:439–447.

47. **Ayestarán B, Guadalupe Z, León D**. 2004. Quantification of major grape polysaccharides (Tempranillo v.) released by maceration enzymes during the fermentation process. Anal. Chim. Acta **513**:29–39.

48. **Apolinar-Valiente R, Williams P, Romero-Cascales I, Gómez-Plaza E, López-Roca JM, Ros-García JM, Doco T**. 2013. Polysaccharide composition of Monastrell red wines from four different Spanish terroirs: effect of wine-making techniques. J. Agric. Food Chem. **61**:2538–47.

49. **Ducasse M-A, Williams P, Meudec E, Cheynier V, Doco T**. 2010. Isolation of Carignan and Merlot red wine oligosaccharides and their characterization by ESI-MS. Carbohydr. Polym. **79**:747–754.

50. **Ducasse M-A, Williams P, Canal-Llauberes R-M, Mazerolles G, Cheynier V, Doco T**. 2011. Effect of macerating enzymes on the oligosaccharide profiles of Merlot red wines. J. Agric. Food Chem. **59**:6558–67.

51. **Doco T, Williams P, Cheynier V**. 2007. Effect of flash release and pectinolytic enzyme treatments on wine polysaccharide composition. J. Agric. Food Chem. **55**:6643–9.

52. **Wightman JD, Price SF, Watson BT, Wrolstad R.** 1997. Some effects of processing enzymes on anthocyanins and phenolics in Pinot noir and Cabernet Sauvignon wines. Am. J. Enol. Vitic. **48**:39–48.

53. **Wightman JD, Wrolstad RE**. 1996. Beta-glucosidase activity in juice-processing enzymes based on anthocyanin analysis. J. Food Sci. **61**:544–548.

54. **Rocha SM, Coutinho P, Delgadillo I, Cardoso AD, Coimbra MA**. 2005. Effect of enzymatic aroma release on the volatile compounds of white wines presenting different aroma potentials. J. Sci. Food Agric. **85**:199–205.

55. **Tamborra P, Martino N, Esti M**. 2004. Laboratory tests on glycosidase preparations in wine. Anal. Chim. Acta **513**:299–303.

56. **Van Sluyter SC, Warnock NI, Schmidt S, Anderson P, van Kan JAL, Bacic A, Waters EJ**. 2013. Aspartic acid protease from *Botrytis cinerea* removes haze-forming proteins during white winemaking. J. Agric. Food Chem. **61**:9705–11.

57. **Swiegers JH, Pretorius IS**. 2005. Yeast modulation of wine flavor. Adv. Appl. Microbiol. **57**:131–75.

58. **Goussard PG**. 2008. Grape cultivars for wine production in South Africa. Cheviot Publishing, Cape Town.

59. **Ortega-Regules A, Ros-García JM, Bautista-Ortín AB, Lopez-Roca JM, Gomez-Plaza E**. 2008. Changes in skin cell wall composition during the maturation of four premium wine grape varieties. J. Sci. Food Agric. **88**:420–428.

60. **Moore JP, Fangel JU, Willats WGT, Vivier MA**. 2014. Pectic-β(1,4)-galactan, extensin and arabinogalactan-protein epitopes differentiate ripening stages in wine and table grape cell walls. Ann. Bot. **114**:1279–1294.

61. **Kammerer D, Claus A, Scieber A, Carle R**. 2005. A novel process for the recovery of polyphenols from grape (*Vitis vinifera L* .) pomace. Food Chem. Toxicol. **70**:157–163.

62. **Gnekow B, Ough CS**. 1976. Methanol in wines and musts: source and amounts. Am. J. Enol. Vitic. **27**:1–6.

63. **Revilla I, Gonzalez-SanJose ML**. 1998. Methanol release during fermentation of red grapes treated with pectolytic enzymes. Food Chem. **63**:307–312.

64. **Hou C-Y, Lin Y-S, Wang YT, Jiang C-M, Lin KT, Wu M-C**. 2008. Addition of phenolic acids on the reduction of methanol content in wine. J. Food Sci. **73**:C432–7.

65. **Nerantzis ET, Tataridis P**. 2006. Integrated enology-Utilization of winery by-products into high added value products. J. Food Sci. Technol. **3**:1–12.

66. **Arvanitoyannis IS, Ladas D, Mavromatis A**. 2006. Potential uses and applications of treated wine waste: a review. Int. J. Food Sci. Technol. **41**:475–487.

67. **Alipour D, Rouzbehan Y**. 2010. Effects of several levels of extracted tannin from grape pomace on intestinal digestibility of soybean meal. Livest. Sci. **128**:87–91.

68. **Green Cape**. 2013. Devoloping a business case for sustainable biofuels in south africa: A focus on waste-based bioethanol for fleet transport in the Western Cape.

69. **Mendes JAS, Xavier AMRB, Evtuguin D V., Lopes LPC**. 2013. Integrated utilization of grape skins from white grape pomaces. Ind. Crops Prod. **49**:286–291.

70. **Kammerer D, Claus A, Carle R, Schieber A**. 2004. Polyphenol screening of pomace from red and white grape varieties (*Vitis vinifera L.*) by HPLC-DAD-MS/MS. J. Agric. Food Chem. **52**:4360–7.

71. **Makris DP, Boskou G, Andrikopoulos NK**. 2007. Polyphenolic content and in vitro antioxidant characteristics of wine industry and other agri-food solid waste extracts. J. Food Compos. Anal. **20**:125–132.

72. **De la Cerda-Carrasco A, López-Solís R, Nuñez-Kalasic H, Peña-Neira A, Obreque-Slier E**. 2014. Phenolic composition and antioxidant capacity of pomaces from four grape varieties (*Vitis vinifera L.*). J. Sci. Food Agric.

73. **Pinelo M, Arnous A, Meyer AS**. 2006. Upgrading of grape skins: Significance of plant cell-wall structural components and extraction techniques for phenol release. Trends Food Sci. Technol. **17**:579–590.

74. **Brazinha C, Cadima M, Crespo JG**. 2014. Optimization of extraction of bioactive compounds from different types of grape pomace produced at wineries and distilleries. J. Food Sci. **79**:E1142–9.

75. **Chamorro S, Viveros A, Alvarez I, Vega E, Brenes A**. 2012. Changes in polyphenol and polysaccharide content of grape seed extract and grape pomace after enzymatic treatment. Food Chem. **133**:308–314.

76. **Zheng H, Hwang I-W, Chung S-K**. 2009. Enhancing polyphenol extraction from unripe apples by carbohydrate-hydrolyzing enzymes. J. Zhejiang Univ. Sci. B **10**:912–9.

77. **Rodríguez LA, Toro ME, Vazquez F, Correa-Daneri ML, Gouiric SC, Vallejo MD**. 2010. Bioethanol production from grape and sugar beet pomaces by solid-state fermentation. Int. J. Hydrogen Energy **35**:5914–5917.

78. **Zheng Y, Lee C, Yu C, Cheng Y-S, Simmons CW, Zhang R, Jenkins BM, VanderGheynst JS**. 2012. Ensilage and bioconversion of grape pomace into fuel ethanol. J. Agric. Food Chem. **60**:11128–34.

79. **Prozil SO, Evtuguin D V., Lopes LPC**. 2012. Chemical composition of grape stalks of *Vitis vinifera L.* from red grape pomaces. Ind. Crops Prod. **35**:178–184.

80. **Manara P, Zabaniotou A, Vanderghem C, Richel A**. 2014. Lignin extraction from Mediterranean agro-wastes: Impact of pretreatment conditions on lignin chemical structure and thermal degradation behavior. Catal. Today **223**:25–34.

81. **Mendes JAS, Prozil SO, Evtuguin D V., Lopes LPC**. 2013. Towards comprehensive utilization of winemaking residues: Characterization of grape skins from red grape pomaces of variety Touriga Nacional. Ind. Crops Prod. **43**:25–32.

82. **Maier T, Göppert A, Kammerer DR, Schieber A, Carle R**. 2007. Optimization of a process for enzyme-assisted pigment extraction from grape (*Vitis vinifera L*.) pomace. Eur. Food Res. Technol. **227**:267–275.

83. **Hanlin RL, Hrmova M, Harbertson JF, Downey MO**. 2010. Review: Condensed tannin and grape cell wall interactions and their impact on tannin extractability into wine. Aust. J. Grape Wine Res. **16**:173–188.

84. **Jarvis MC**. 2011. Plant cell walls: Supramolecular assemblies. Food Hydrocoll. **25**:257–262.

85. **Fleischer A, O'Neill M, Ehwald R**. 1999. The pore size of non-graminaceous plant cell walls is rapidly decreased by Borate ester cross-linking of the pectic polysaccharide rhamnogalacturonan II. Plant Physiol. **121**:829–838.

86. **Xu C, Yagiz Y, Borejsza-Wysocki W, Lu J, Gu L, Ramírez-Rodrigues MM, Marshall MR**. 2014. Enzyme release of phenolics from muscadine grape (*Vitis rotundifolia Michx.*) skins and seeds. Food Chem. **157**:20–9.

87. **Paës G**. 2014. Fluorescent probes for exploring plant cell wall deconstruction: a review. Molecules **19**:9380–402.

88. **Albersheim P, Darvill A, Roberts K, Sederoff R, Staehelin A**. 2010. Plant cell walls (From chemistry to biology). Garland Science, New York.

89. **Wolf S, Hématy K, Höfte H**. 2012. Growth control and cell wall signaling in plants. Annu. Rev. Plant Biol. **63**:381–407.

90. **Keegstra K**. 2010. Plant cell walls. Plant Physiol. **154**:483–6.

91. **Brett CT, Waldron KW**. 1996. Cell wall architecture and the skeletal role of the cell wall, p. 44–74. *In* Physiology and biochemistry of plant cell walls, 2nd ed. Chapman & Hall, London.

92. **Ding S-Y, Himmel ME**. 2006. The maize primary cell wall microfibril: a new model derived from direct visualization. J. Agric. Food Chem. **54**:597–606.

93. **Himmel M, Ding S, Johnson D, William S, Nimlos M, Brady J, Foust T**. 2007. Biomass recalcitrance: engineering plants and enzymes for biofuels production. Science (80-.). **315**:804–807.

94. **Somerville C, Bauer S, Brininstool G, Facette M, Hamann T, Milne J, Osborne E, Paredez A, Persson S, Raab T, Vorwerk S, Youngs H**. 2004. Toward a systems approach to understanding plant cell walls. Science **306**:2206–11.

95. **Knox JP, Benitez-Alfonso Y**. 2014. Roles and regulation of plant cell walls surrounding plasmodesmata. Curr. Opin. Plant Biol. **22C**:93–100.

96. **Scheller HV, Ulvskov P**. 2010. Hemicelluloses. Annu. Rev. Plant Biol. **61**:263–89.

97. **Franková L, Fry SC**. 2013. Biochemistry and physiological roles of enzymes that “cut and paste” plant cell-wall polysaccharides. J. Exp. Bot. **64**:3519–50.

98. **Park YB, Cosgrove DJ**. 2012. A revised architecture of primary cell walls based on biomechanical changes induced by substrate-specific endoglucanases. Plant Physiol. **158**:1933–43.

99. **Caffall KH, Mohnen D**. 2009. The structure, function, and biosynthesis of plant cell wall pectic polysaccharides. Carbohydr. Res. **344**:1879–900.

100. **O’Neill M., York W.** 2003. The composition and structure of plant primary cell walls, p. 1–44. *In* Rose, JK. (ed.), The plant cell wall. Annual plant reviews, volume 8. Blackwell Publishing Ltd, Oxford.

101. **Yoo S-H, Fishman ML, Savary BJ, Hotchkiss AT**. 2003. Monovalent salt-induced gelation of enzymatically deesterified pectin. J. Agric. Food Chem. **51**:7410–7.

102. **Harholt J, Suttangkakul A, Vibe Scheller H**. 2010. Biosynthesis of pectin. Plant Physiol. **153**:384–95.

103. **Pellerin P, O’Neill MA**. 1998. The interaction of the pectic polysaccharide Rhamnogalacturonan II with heavy metals and lanthanides in wines and fruit juices. Analusis **26**:32–36.

104. **Pérez S, Rodríguez-carvajal MA, Doco T**. 2003. A complex plant cell wall polysaccharide : rhamnogalacturonan II . A structure in quest of a function. Biochimie **85**:109–121.

105. **Pabst M, Fischl RM, Brecker L, Morelle W, Fauland A, Köfeler H, Altmann F, Léonard R**. 2013. Rhamnogalacturonan II structure shows variation in the side chains monosaccharide composition and methylation status within and across different plant species. Plant J. **76**:61–72.

106. **Buffetto F, Ropartz D, Zhang XJ, Gilbert HJ, Guillon F, Ralet M-C**. 2014. Recovery and fine structure variability of RGII sub-domains in wine (*Vitis vinifera* Merlot). Ann. Bot. **114**:1327–37.

107. **Dumont M, Lehner A, Bouton S, Kiefer-Meyer MC, Voxeur A, Pelloux J, Lerouge P, Mollet J-C**. 2014. The cell wall pectic polymer rhamnogalacturonan-II is required for proper pollen tube elongation: implications of a putative sialyltransferase-like protein. Ann. Bot. **114**:1177–88.

108. **Willats WG, McCartney L, Mackie W, Knox JP**. 2001. Pectin: cell biology and prospects for functional analysis. Plant Mol. Biol. **47**:9–27.

109. **Ferrari S, Galletti R, Denoux C, De Lorenzo G, Ausubel FM, Dewdney J**. 2007. Resistance to Botrytis cinerea induced in *Arabidopsis* by elicitors is independent of salicylic acid, ethylene, or jasmonate signaling but requires PHYTOALEXIN DEFICIENT3. Plant Physiol. **144**:367–79.

110. **Paniagua C, Posé S, Morris VJ, Kirby AR, Quesada MA, Mercado JA**. 2014. Fruit softening and pectin disassembly: an overview of nanostructural pectin modifications assessed by atomic force microscopy. Ann. Bot. **114**:1375–83.

111. **Lamport DTA, Kieliszewski MJ, Chen Y, Cannon MC**. 2011. Role of the extensin superfamily in primary cell wall architecture. Plant Physiol. **156**:11–9.

112. **Varner JE, Louis S**. 1989. Plant Cell Wall Architecture Review **56**:231–239.

113. **Johnson KL, Jones BJ, Schultz CJ, Bacic A**. 2003. Non-enzymatic cell wall (glyco)proteins, p. 111–154. *In* Rose, KC (ed.), The plant cell wall. Annual plant reviews, volume 8. Blackwell Publishing Ltd, Oxford.

114. **Ellis M, Egelund J, Schultz CJ, Bacic A**. 2010. Arabinogalactan-proteins: key regulators at the cell surface? Plant Physiol. **153**:403–19.

115. **Lamport DTA, Varnai P, Seal CE**. 2014. Back to the future with the AGP-Ca2+ flux capacitor. Ann. Bot. **114**:1069–85.

116. **Cosgrove DJ**. 2003. Expansion of the plant cell wall, p. 237–263. *In* Rose, JKC (ed.), The plant cell wall. Annual plant reviews, volume 8. Blackwell Publishing Ltd, Oxford.

117. **Bargel H, Koch K, Cerman Z, Neinhuis C**. 2006. Evans Review No. 3 : Structure–function relationships of the plant cuticle and cuticular waxes — a smart material? Funct. Plant Biol. **33**:893.

118. **Brummell DA**. 2006. Review : Cell wall disassembly in ripening fruit. Funct. plant Biol. **33**:103–119.

119. **Moreira N, Pina C, Mendes F, Couto JA, Hogg T, Vasconcelos I**. 2011. Volatile compounds contribution of *Hanseniaspora guilliermondii* and *Hanseniaspora uvarum* during red wine vinifications. Food Control **22**:662–667.

120. **Ali J, Abid H, Hussain A**. 2010. Study on some macronutrients composition in peels of different citrus fruits grown in NWFP. J. Chem. Soc. Pakistan **32**:83–86.

121. **Jamal P, Saheed, Olorunnisola K, Alam Z**. 2012. Bio-valorization potential of banana peels (*Musa sapientum)*: An overview. Asiaqn J. Biotechnol. **4**:1–14.

122. **Kirtane RD, Suryawanshi PC, Patil MR, Chaudhari AB, Kothari RM**. 2009. Optimization of organic loading rate for different fruit wastes during biomethanization. J. Sci. Ind. Res. **68**:252–255.

123. **Arnous A, Meyer AS**. 2009. Quantitative prediction of cell wall polysaccharide composition in grape (*Vitis vinifera L.*) and apple (*Malus domestica*) skins from acid hydrolysis monosaccharide profiles. J. Agric. Food Chem. **57**:3611–9.

124. **Apolinar-Valiente R, Romero-Cascales I, Gómez-Plaza E, López-Roca JM, Ros-García JM**. 2015. The composition of cell walls from grape marcs is affected by grape origin and enological technique. Food Chem. **167**:370–7.

125. **Bindon KA, Smith PA, Kennedy JA**. 2010. Interaction between grape-derived proanthocyanidins and cell wall material. 1. Effect on proanthocyanidin composition and molecular mass. J. Agric. Food Chem. **58**:2520–8.

126. **Keegstra K, Talmadge KW, Bauer WD, Albersheim P**. 1973. The Structure of Plant Cell Walls. Plant Physiol. **51**:188–196.

127. **Fry SC**. 1988. The growing plant cell wall: Chemical and metabolic analysis. Longman Scientific UK Limited, Essex.

128. **Hayashi T**. 1989. Xyloglucans in the primary cell wall. Annu. Rev. Plant Physiol. Plant Mol. Biol. **40**:139–168.

129. **Talbott LD, Ray PM**. 1992. Molecular size and separability features of pea cell wall polysaccharides : Implications for models of primary wall structure. Plant Physiol. **98**:357–368.

130. **Ha M-A, Apperley DC, Jarvis MC**. 1997. Molecular rigidity in dry and hydrated onion cell walls. Plant Physiol. **115**:593–598.

131. **Carpita NC, Gibeaut DM**. 1993. Structural models of primary cell walls in flowering plants: consistency of molecular structure with the physical properties of the walls during growth. Plant J. **3**:1–30.

132. **Vincken J, Schols HA, Oomen RJFJ, Mccann MC, Ulvskov P, Voragen AGJ, Visser RGF**. 2003. If Homogalacturonan were a side chain of Rhamnogalacturonan I . Implications for cell wall architecture. Plant Physiol. **132**:1781–1789.

133. **Coenen GJ, Bakx EJ, Verhoef RP, Schols HA, Voragen AGJ**. 2007. Identification of the connecting linkage between homo- or xylogalacturonan and rhamnogalacturonan type I. Carbohydr. Polym. **70**:224–235.

134. **Yi H, Puri VM**. 2014. Contributions of the mechanical properties of major structural polysaccharides to the stiffness of a cell wall network model. Am. J. Bot. **101**:244–54.

135. **Tan L, Eberhard S, Pattathil S, Warder C, Glushka J, Yuan C, Hao Z, Zhu X, Avci U, Miller JS, Baldwin D, Pham C, Orlando R, Darvill A, Hahn MG, Kieliszewski MJ, Mohnen D**. 2013. An *Arabidopsis* cell wall proteoglycan consists of pectin and arabinoxylan covalently linked to an arabinogalactan protein. Plant Cell **25**:270–87.

136. **Fry S**. 2004. Primary cell wall metabolism: tracking the careers of wall polymers in living plant cells. New Phytol. **16**:641–675.

137. **De Lima DU, Buckeridge MS**. 2001. Interaction between cellulose and storage xyloglucans : the influence of the degree of galactosylation. Carbohydr. Polym. **46**:157–163.

138. **Whitney SEC, WIlson E, Webster J, Bacic A, Reid GJS, Gidley MJ**. 2006. Effects of structural variation in xyloglucan polymers on interactions with bacterial cellulose. Am. J. Bot. **93**:1402–1414.

139. **Whitney SEC, Brigham JE, Darke AH, Reid JSG, Gidley MJ**. 1998. Structural aspects of the interaction of mannan-based polysaccharides with bacterial cellulose. Carbohydr. Res. **307**:299–309.

140. **Marcus SE, Blake AW, Benians TAS, Lee KJD, Poyser C, Donaldson L, Leroux O, Rogowski A, Petersen HL, Boraston A, Gilbert HJ, Willats WGT, Knox JP**. 2010. Restricted access of proteins to mannan polysaccharides in intact plant cell walls. Plant J. **64**:191–203.

141. **Cumming CM, Rizkallah HD, McKendrick KA, Abdel-Massih RM, Baydoun EA-H, Brett CT**. 2005. Biosynthesis and cell-wall deposition of a pectin-xyloglucan complex in pea. Planta **222**:546–55.

142. **Cornuault V, Manfield IW, Ralet M-C, Knox JP**. 2014. Epitope detection chromatography: a method to dissect the structural heterogeneity and inter-connections of plant cell-wall matrix glycans. Plant J. **78**:715–22.

143. **Popper ZA, Fry SC**. 2008. Xyloglucan-pectin linkages are formed intra-protoplasmically, contribute to wall-assembly, and remain stable in the cell wall. Planta **227**:781–94.

144. **Zykwinska A, Thibault J-F, Ralet M-C**. 2007. Organization of pectic arabinan and galactan side chains in association with cellulose microfibrils in primary cell walls and related models envisaged. J. Exp. Bot. **58**:1795–802.

145. **Hijazi M, Roujol D, Nguyen-Kim H, Del Rocio Cisneros Castillo L, Saland E, Jamet E, Albenne C**. 2014. Arabinogalactan protein 31 (AGP31), a putative network-forming protein in *Arabidopsis thaliana* cell walls? Ann. Bot. **114**:1087–97.

146. **Nunan KJ, Sims IM, Bacic A, Robinson SP, Fincher GB**. 1997. Isolation and characterization of cell walls from the mesocarp of mature grape berries (*Vitis vinifera*). Planta **203**:93–100.

147. **Ortega-Regules A, Ros-García JM, Bautista-Ortín AB, López-Roca JM, Gómez-Plaza E**. 2008. Differences in morphology and composition of skin and pulp cell walls from grapes (*Vitis vinifera L.*): technological implications. Eur. Food Res. Technol. **227**:223–231.

148. **Lecas M, Brillouet J**. 1994. Cell wall composition of grape berry skins. Phytochemistry **35**:1241–1243.

149. **Rosenquist JK, Morrison JC**. 1989. Some factors affecting cuticle and wax accumulation on grape berries. Am. J. Enol. Vitic. **40**:241–244.

150. **Kök D, Çelik S**. 2004. Determination of characteristics of grape berry skin in some table grape cultivars *(V. vinifera L.*). J. Agron **3**:141–146.

151. **Nunan K, Sims I, Bacic A**. 1998. Changes in cell wall composition during ripening of grape berries. Plant Physiol. **118**:783–792.

152. **Casado CG, Heredia A**. 1999. Structure and dynamics of reconstituted cuticular waxes of grape berry cuticle (*Vitis vinifera L.*). J. Exp. Bot. **50**:175–182.

153. **Commenil P, Brunet L, Audran J**. 1997. The development of the grape berry cuticle in relation to susceptibility to bunch rot disease. J. Exp. Bot. **48**:1599–1607.

154. **Szakiel A, Pączkowski C, Pensec F, Bertsch C**. 2012. Fruit cuticular waxes as a source of biologically active triterpenoids. Phytochem. Rev.

155. **Coombe B**. 1973. The regulation of set and development of the grape berry. Acta Hortic. **34**:261–273.

156. **Bapat V a, Trivedi PK, Ghosh A, Sane V a, Ganapathi TR, Nath P**. 2010. Ripening of fleshy fruit: molecular insight and the role of ethylene. Biotechnol. Adv. **28**:94–107.

157. **Minic Z, Jouanin L**. 2006. Plant glycoside hydrolases involved in cell wall polysaccharide degradation. Plant Physiol. Biochem. **44**:435–49.

158. **Nunan KJ, Davies C, Robinson SP, Fincher GB**. 2001. Expression patterns of cell wall-modifying enzymes during grape berry development. Planta **214**:257–264.

159. **Yakushiji H, Sakurai N, Morinaga K**. 2001. Changes in cell-wall polysaccharides from the mesocarp of grape berries during veraison. Physiol. Plant. **111**:188–195.

160. **Guillaumie S, Fouquet R, Kappel C, Camps C, Terrier N, Moncomble D, Dunlevy JD, Davies C, Boss PK, Delrot S**. 2011. Transcriptional analysis of late ripening stages of grapevine berry. BMC Plant Biol. **11**:165.

161. **Vicens A, Fournand D, Williams P, Sidhoum L, Moutounet M, Doco T**. 2009. Changes in polysaccharide and protein composition of cell walls in grape berry skin (Cv. Shiraz) during ripening and over-ripening. J. Agric. Food Chem. **57**:2955–60.

162. **Huang Q, Fu W-L**. 2005. Comparative analysis of the DNA staining efficiencies of different fluorescent dyes in preparative agarose gel electrophoresis. Clin. Chem. Lab. Med. **43**:841–2.

163. **Kennedy J**. 2008. Grape and wine phenolics: Observations and recent findings. Cienc. e Investig. Agrar. **35**:107–120.

164. **Fontes N, Geros H, Delrot S**. 2011. Grape Berry Vacuole: A Complex and Heterogeneous Membrane System Specialized in the Accumulation of Solutes. Am. J. Enol. Vitic. **62**:270–278.

165. **Joutei KA, Glories Y, Mercier M**. 1994. Localisation des tanins dans la pellicule de baie de raisin. Vitis **33**:133–138.

166. **Iiyama K, Lam TB-T, Stone BA**. 1994. Covalent cross-links in the cell wall. Plant Physiol. **104**:315–320.

167. **Le Bourvellec C, Guyot S, Renard CMGC**. 2004. Non-covalent interaction between procyanidins and apple cell wall material: Part I. Effect of some environmental parameters. Biochim. Biophys. Acta **1672**:192–202.

168. **Ruiz-Garcia Y, Smith PA, Bindon KA**. 2014. Selective extraction of polysaccharide affects the adsorption of proanthocyanidin by grape cell walls. Carbohydr. Polym. **114**:102–114.

169. **Le Bourvellec C, Watrelot AA, Ginies C, Imberty A, Renard CMGC**. 2012. Impact of processing on the noncovalent interactions between procyanidin and apple cell wall. J. Agric. Food Chem. **60**:9484–94.

170. **Adams DO**. 2006. Phenolics and ripening in grape berries. Am. J. Enol. Vitic. **57**:249–256.

171. **Fournand D, Vicens A, Sidhoum L, Souquet J-M, Moutounet M, Cheynier V**. 2006. Accumulation and extractability of grape skin tannins and anthocyanins at different advanced physiological stages. J. Agric. Food Chem. **54**:7331–8.

172. **Río Segade S, Soto Vázquez E, Díaz Losada E**. 2008. Influence of ripeness grade on accumulation and extractability of grape skin anthocyanins in different cultivars. J. Food Compos. Anal. **21**:599–607.

173. **González-Neves G, Gil G, Barreiro L**. 2008. Influence of grape variety on the extraction of anthocyanins during the fermentation on skins. Eur. Food Res. Technol. **226**:1349–1355.

174. **Canals R, Llaudy MC, Valls J, Canals JM, Zamora F**. 2005. Influence of ethanol concentration on the extraction of color and phenolic compounds from the skin and seeds of Tempranillo grapes at different stages of ripening. J. Agric. Food Chem. **53**:4019–25.

175. **Romero-Cascales I, Ortega-Regules A, López-Roca JM, Fernández-Fernández JI, Gómez-Plaza E**. 2005. Differences in anthocyanin extractability from grapes to wines according to variety. Am. J. Enol. Vitic. **3**:212–219.

176. **Ortega-Regules A, Romero-Cascales I, Ros-García JM, López-Roca JM, Gómez-Plaza E**. 2006. A first approach towards the relationship between grape skin cell-wall composition and anthocyanin extractability. Anal. Chim. Acta **563**:26–32.

177. **Serratosa MP, Marquez A, Moyano L, Zea L, Merida J**. 2014. Chemical and morphological characterization of Chardonnay and Gewürztraminer grapes and changes during chamber-drying under controlled conditions. Food Chem. **159**:128–36.

178. **Río Segade S, Giacosa S, Gerbi V, Rolle L**. 2011. Berry skin thickness as main texture parameter to predict anthocyanin extractability in winegrapes. LWT - Food Sci. Technol. **44**:392–398.

179. **Hernández-Hierro JM, Quijada-Morín N, Rivas-Gonzalo JC, Escribano-Bailón MT**. 2012. Influence of the physiological stage and the content of soluble solids on the anthocyanin extractability of *Vitis vinifera L*. cv. Tempranillo grapes. Anal. Chim. Acta **732**:26–32.

180. **Hernández-Hierro JM, Quijada-Morín N, Martínez-Lapuente L, Guadalupe Z, Ayestarán B, Rivas-Gonzalo JC, Escribano-Bailón MT**. 2014. Relationship between skin cell wall composition and anthocyanin extractability of *Vitis vinifera L*. cv. Tempranillo at different grape ripeness degree. Food Chem. **146**:41–7.

181. **Bindon KA, Madani SH, Pendleton P, Smith PA, Kennedy JA**. 2014. Factors affecting skin tannin extractability in ripening grapes. J. Agric. Food Chem. **62**:1130–41.

182. **Bindon KA, Bacic A, Kennedy JA**. 2012. Tissue-specific and developmental modifications of grape cell walls influence the adsorption of proanthocyanidins. J. Agric. Food Chem. **60**:9249–9260.

183. **Arnous A, Meyer AS**. 2010. Discriminated release of phenolic substances from red wine grape skins (*Vitis vinifera L*.) by multicomponent enzymes treatment. Biochem. Eng. J. **49**:68–77.

184. **DeMartini JD, Pattathil S, Avci U, Szekalski K, Mazumder K, Hahn MG, Wyman CE**. 2011. Application of monoclonal antibodies to investigate plant cell wall deconstruction for biofuels production. Energy Environ. Sci. **4**:4332.

185. **Busse-Valverde N, Gómez-Plaza E, López-Roca JM, Gil-Muñoz R, Fernández-Fernández JI, Bautista-Ortín AB**. 2010. Effect of different enological practices on skin and seed proanthocyanidins in three varietal wines. J. Agric. Food Chem. **58**:11333–9.

186. **May PF**. 2009. PINOTAGE: Behind the Legends of South Africa's Own Wine, 1st ed. Inform and Enlighten, St Albans.

187. **Rio-Segade S, Torchio F, Giacosa S, Aimonino DR, Gay P, Lambri M, Dordoni R, Gerbi V, Rolle L**. 2014. Impact of several pre-treatments on the extraction of phenolic compounds in winegrape varieties with different anthocyanin profiles and skin mechanical properties. J. Agric. Food Chem. **62**:8437–8451.

188. **Álvarez I, Aleixandre JL, García MJ, Lizama V**. 2006. Impact of prefermentative maceration on the phenolic and volatile compounds in Monastrell red wines. Anal. Chim. Acta **563**:109–115.

Chapter 3

Research results

Following the compositional changes of fresh grape skin cell walls during the fermentation process in the presence and absence of maceration enzymes

This manuscript has been accepted for publication in **Journal of Agricultural and Food Chemistry**

Following the compositional changes of fresh grape skin cell walls during the fermentation process in the presence and absence of maceration enzymes

Anscha J. J. Zietsman[1], John P. Moore[1], Jonatan U. Fangel[2], William G.T. Willats[2], Johan Trygg[3], and Melané A. Vivier[1*]

1. Institute for Wine Biotechnology, Department of Viticulture and Oenology, Faculty of AgriSciences, Stellenbosch University, Matieland 7602, South Africa
2. Department of Plant and Environmental Sciences, Faculty of Science, University of Copenhagen, DK-1001, Denmark
3. Computational Life Science Cluster (CLiC), Department of Chemistry, Umeå University, Sweden

ABSTRACT

Cell wall profiling technologies were used to follow compositional changes that occurred in the skins of grape berries (from two different ripeness levels) during fermentation and enzyme maceration. Multivariate data analysis showed that the fermentation process yielded cell walls enriched in hemicellulose components because pectin was solubilized (and removed) with a reduction as well as exposure of cell wall proteins usually embedded within the cell wall structure. The addition of enzymes caused even more depectination and the enzymes unravelled the cell walls enabling better access to, and extraction of, all cell wall polymers. Overripe grapes had cell walls that were extensively hydrolysed and depolymerized probably by natural grape tissue ripening enzymes and this enhanced the impact that the maceration enzymes had on the cell wall monosaccharide profile. The combination of the techniques that were used is an effective direct measurement of the hydrolysis actions of maceration enzymes on the cell walls of grape berry skin.

Keywords: Cell Wall, Grape Skin, Maceration Enzymes, Grape Maturity, Multivariate Data Analysis

Contact information for Corresponding Author

Melané A. Vivier, Institute for Wine Biotechnology, Department of Viticulture and Oenology, Faculty of AgriSciences, Stellenbosch University, Matieland 7602, South Africa, Tel. +27 21 808 3773, Fax +27 21 808 3771, mav@sun.ac.za

INTRODUCTION

The quality of a red wine is determined primarily by the presence and relative abundance of phenolic and varietal aroma compounds[1].Studies investigating the distribution of the aroma and phenolic compounds between the juice, pulp and skin of the grape berry show that the grape skin, specifically the skin cell vacuoles, are a primary source of these compounds[2–5]. During red wine maceration the cell walls of the grape berry are disrupted and become perforated, promoting the leaching of aroma and phenolic compounds into the fermenting must[6]. The maceration process can be enhanced with the addition of maceration enzymes including pectinolytic enzymes, hemicellulases and cellulases[7].

The efficacy of cell wall hydrolysis by maceration enzyme preparations is often tested by measuring the indirect consequences of cell wall breakdown. For example the release of total polyphenols, polysaccharides and specific anthocyanins can be quantified; or the color of the resulting wine; the free run juice collected at the press; or the free and bonded aroma compounds of the wine can be measured as an indirect indication of enzyme action[8–13]. Using the known plant cell wall polysaccharide molar ratios (e.g. XXXG which has a molar ratio of 3:4 for xylose to glucose) and then combining these reference data with the quantitative data (from monosaccharide analysis[14]) of samples selected before and after enzyme treatment it is possible to calculate and predict the composition of the original polymers of the sample and the changes due to enzyme treatment[15]. With this approach it was shown[15] that maceration enzymes caused a decrease in arabinose, galactose, uronic acid and total sugar concentration which suggested that pectin degradation took place, although these polymers were not directly monitored.

Similar changes (a decrease in galactose, an increase in the water-soluble fraction and de-esterification of uronic acids) were seen in the grape skin cell wall during grape ripening[16,17]. In fruit, cell wall loosening and pectin degradation lead to pore formation[18]. New studies[19,20] have shown that high cell wall porosity implies an increase in binding sites between cell wall polymers and polyphenols such as condensed tannins and anthocyanins. Due to the retention of these polyphenols by cell wall particles, a lower concentration might end up in the wine. Cell wall porosity can also influence the ability of the maceration enzymes to penetrate the cell wall and reach their targets [21–23]. Thus, both ripening and maceration enzymes might have positive and negative impacts on wine quality and therefore it is extremely important to understand how both these concepts influence the cell wall composition and deconstruction.

Our aim with this study was to perform an evaluation of the cell walls of fresh *Vitis vinifera cv* Pinotage grape skins, fermented skins and skins macerated with enzymes during fermentation,

by applying cell wall profiling methods that were optimised for grape berries[24]. Both ripe and overripe grapes were used in order to investigate the impact of cell wall degradation due to ripening on these processes. We have applied comprehensive microarray polymer profiling (CoMPP) to monitor the cell wall polysaccharides and proteins directly by virtue of the presence of epitopes. This is the first study, to our knowledge, that uses CoMPP to investigate the effect of maceration enzymes on the cell walls of grape berry skin during wine fermentation. CoMPP analysis is a semi-quantitative high throughput profiling technique and consists of the sequential extraction of the pectin (CDTA extract) and hemicellulose (NaOH extract) fractions from cell wall material[25]. These fractions are then printed onto nitrocellulose membranes and then probed with monoclonal antibodies (mAbs) as well as carbohydrate binding modules (CBMs). The data obtained provides an indication of the relative abundance of specific cell wall polysaccharides in a sample. The CoMPP data is supported by monosaccharide compositional analysis (GC-MS) and reflectance spectroscopy (FT-MIR) data. Multivariate data analysis tools were used to identify the components that characterized the differences in cell walls sourced from the different treatments. The combination of methods employed are complementary and produced valuable information on the variation in both the surface polymers as well as the profile of polymer building blocks present at different ripeness levels, winemaking stages or after different enzyme treatments.

MATERIALS AND METHODS

Vinification of wine. *Vitis vinifera* cv Pinotage grapes were sourced from vineyards in the Boland region of South Africa, during the 2012 and 2013 vintages. Fermentations were done in triplicate in 2012 and quadruplicate in 2013 in polypropylene buckets with 5 kg de-stemmed and crushed grapes per bucket (weighed, de-stemmed and crushed individually; one bucket is one biological repeat). After the grapes were crushed, sodium metabisulfite was added (30 ppm SO_2) and the total acid was adjusted to 6.5 g/L. The yeast strain, *Saccharomyces cerevisiae* VIN13 (Anchor Yeast, Johannesburg, South Africa) were rehydrated and inoculated according to the manufacturer's recommendations and yeast nutrition was supplemented with Fermaid K™ (Lallemand, Bellville, South Africa). Where applicable, Rapidase® Ex Color, -CB and -Expression (DSM Food Specialties, Heerlen, The Netherlands) were added to the crushed grapes at a dosage of 0.03 g/L. The manufacturer of these enzymes declares (Product data sheets, www.dsm-foodspecialities.com) that all the mixes have primarily pectinolytic activity but that Rapidase®CB has been formulated with enhanced polygalacturonase activity, Rapidase® Ex Color has additional hemicellulases for optimum grape skin extraction during maceration and Rapidase® Expression formulations contain arabinases and rhamnogalacturonases. Fermentations were conducted at 25°C and the grape skin caps were punched down twice

daily. At the end of alcoholic fermentation the wines were pressed and transferred to 4.5 L glass bottles fitted with fermentation caps. The pomace was stored at 4 °C until analysis (up to one week). Freeze dried *Oenococcus oeni*, Lalvin VP41 (Lallemand, South Africa), supplemented with OPTI-MALO-PLUS® (Lallemand), was inoculated in the wine to induce malolactic fermentation (MLF) and the fermentations were incubated at 20°C. At the end of MLF the wine was racked off the lees, sulfited (80 ppm SO_2), stabilised at 4°C and then filtered and bottled.

General oenological parameters. Three 50 mL samples of the juice were randomly selected from the buckets after the grapes were crushed, and analyzed for sugar and acid concentration using Fourier transform infrared (FT-IR) spectroscopy with a WineScan™ FT120 Basic (FOSS Analytical,Hillerød, Denmark). The same instrument was used to analyse the pH, volatile acidity, total acid, glucose + fructose and ethanol of two 50 mL wine samples from each biological repeat at the end of MLF. The FT-IR scans were done in duplicate per sample (two technical repeats). Wine samples for color analysis were collected three months after the wines have been bottled. The pH of all samples was adjusted to 3.5 and the color characteristics were determined according to Iland et al.[26] using a Specord 50 UV/VIS spectrophotometer (Analytik Jena, Jena, Germany). The analysis was done in triplicate.

Pinotage skin cell wall preparation. For the fresh grape skin samples the grapes were selected from different harvest crates, from different bunches and from the top, middle and bottom of a bunch to mimic the variability that is found in a commercial harvest batch. The berries were frozen and stored at -20°C before the skins were obtained by manually peeling the grapes with a scalpel and flash-freezing the skins in liquid nitrogen. Twenty-one samples of 10 g each (wet weight) were collected in 2012 and twelve in 2013, kept at -80 °C before freeze-drying. The fermented grape skin samples (with and without enzyme treatment) were collected at the end of alcoholic fermentation after pressing (at least two samples per biological repeat) and stored at 4°C before excess pulp was removed from the skins with a scalpel and the skins were freeze-dried. Samples of 10 g (wet weight) were milled and homogenized with a Retsch MM400 mixer mill (Retsch, Haan, Germany) at a frequency of 30Hz for 30 seconds and the resulting powder was used for the isolation of the cell walls using the method described by Ortega-Regules et al. [27] with the following changes. The first acetone step after the buffered phenol extraction was omitted. Furthermore, after the third acetone wash the alcohol insoluble residue (AIR) was air-dried and then mixed with a volume of MilliQ water, roughly equal to the pellet size of the AIR, frozen at -80°C and then freeze-dried.

Mid-infrared spectroscopy. AIR isolated from fresh and fermented Pinotage skins (with and without the addition of maceration enzymes) was analyzed by infrared spectroscopy. The samples were placed in direct contact with the diamond window and the spectra between 4000 and 600 cm^{-1} were acquired using a NEXUS 670 (Thermo Scientific, MA, USA) fitted with a Golden Gate Diamond ATR (attenuated total reflectance). A Geon-KBr beam splitter and DTGS/Csl detector were used and each sample was scanned 128 times. The FT-MIR spectra data were filtered with a MSC (multiplicative scatter correction) filter to compensate for light scattering and differences in the effective path length. The spectra for the fingerprint region (1400 – 800 cm^{-1}) where every polysaccharide has its own unique pattern, as well as wavelengths from 1400 up to 1800 cm^{-1} that conveys information about functional groups [28,29] were compared between treatments. The spectra shown in the results section represent the average absorbance from at least five AIR samples per treatment. Technical repeats were done once every tenth scan to control for technical reproducibility.

Monosaccharide analysis of cell wall samples. The monosaccharide composition of the AIR isolated from the grape skins were analyzed according to the method described in [30] and used on grape cell walls in [24] including a few modifications. Approximately 5 mg of AIR was hydrolyzed to monosaccharides using 2M TFA and incubated for 2 hours at 110°C[30]. This was followed by derivatization to methoxy sugars at 80 °C for 16 h. After silylation with HMDS + TMCS + Pyridine 3:1:9 (Sylon HTP) kit (Sigma-Aldrich, MO, USA) the derivatives were separated and analyzed in a gas chromatograph, Agilent 6890 N (Agilent Technologies, CA, USA) coupled to a Agilent 5975 MS mass spectrometer detector, using a polar (95% dimethylpolysiloxane) ZB-Semivolatiles Guardian (30 m, 0.25 mm ID, 0.25 µm film thickness) GC column. The oven temperature was maintained at 70 °C for 2 min, ramped at 1 °C/min to 76 °C, then at 8 °C/min to 300 °C and then held for 5 min. The monosaccharide composition was expressed as the mole percentage contribution of each monosaccharide in relation to the nine monosaccharides present. Error bars in the histograms or the standard deviation in the tables represents the mean of at least three biological samples.

Comprehensive microarray polymer profiling (CoMPP) analysis of cell wall fractions. The pectin- and hemicellulose-rich fractions of the cell wall samples were sequentially extracted from 10 mg AIR samples using the solvents CDTA (diamino-cyclo-hexane-tetra-acetic acid) and NaOH respectively according to the procedure described elsewhere[24]. Arrays printed with the different fractions were probed individually with 26 different monoclonal antibodies (mAbs) and carbohydrate binding modules (CBMs) as previously described[25]. A mean spot signal was

calculated where after it was normalized to the highest signal (set as 100) in the dataset and a cut-off value of five was used.

Multivariate and univariate statistics. Univariate statistical analysis were done (ANOVA, with P = 0.05) under the guidance of the Centre for Statistical Consultation at Stellenbosch University (Prof Martin Kidd) using Statistica 10 (StatSoft Southern Africa - Analytics, Sandton, South Africa). Multivariate analysis by means of principle component analysis (PCA)[31] and orthogonal projections to latent structures (OPLS) were performed using SIMCA 13 software package (Umetrics AB, Umeå, Sweden).

RESULTS AND DISCUSSION

In this study we used Pinotage grapes that were at different ripeness levels as reflected in the Glucose + Fructose (2012: 227 g/L and 2013: 265 g/L) and total acid (2012: 5.37 g/L and 2013: 4.85 g/L) concentrations of the juice samples (Table S1). According to traditional ripeness criteria discussed in the supplementary data (S 1.1), the grapes at 22.7 °B were considered to be at optimum ripeness while those at 26.5 °B are deemed overripe [32,33]. Each year we compared the cell wall composition of fresh (unfermented) skins with skins that went through an alcoholic fermentation. Additionally, we investigated the cell walls from fermentations supplemented with commercial maceration enzymes and compared them to their no-enzyme-added counterparts to determine the changes due to enzymatic hydrolysis. In order to evaluate the influence of ripeness levels, we compared the results from the samples over the two years with each other.

Effect of ripeness level in the fresh grape skin cell walls. The mol% ratio of the nine main monosaccharides found in grape skin cell walls of Pinotage is shown in Figure 1 and confirms the abundance (ca. 35 mol%) in galacturonic acid (GalA) as previously shown for grape skin[14]. The profile obtained (ca. 20 mol% arabinose [Ara], 15 mol% xylose [Xyl] and galactose [Gal], and lower than 10 mol% for the other sugars) compared well with other red wine cultivars such as Cabernet Sauvignon, Merlot and Shiraz [27,34]. However, direct comparisons of monosaccharides levels should be avoided due to different methods (TMS methyl glycosides or alditol acetates [30]) that were used to determine the uronic acids since this influences the relative molar ratios obtained.

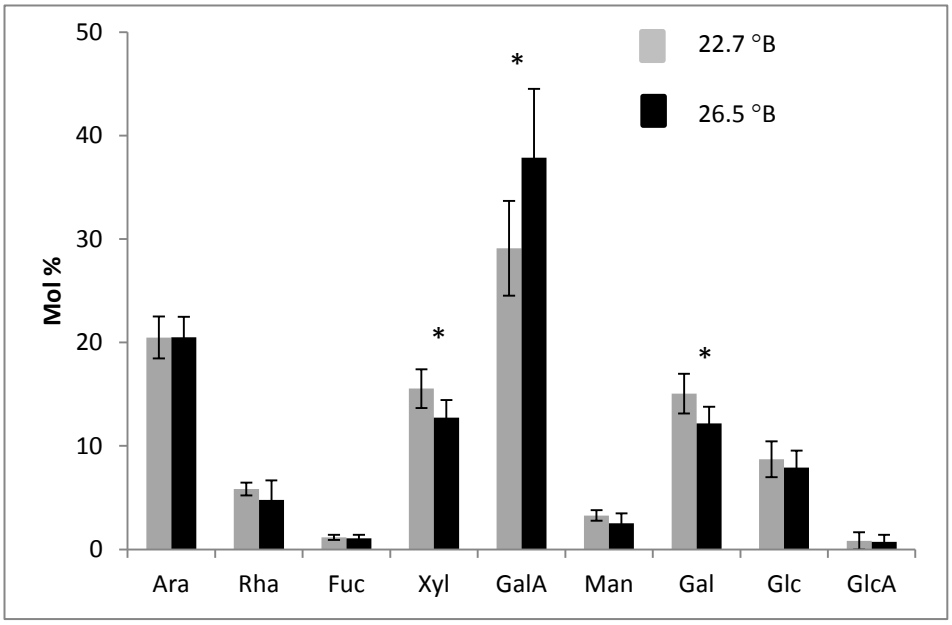

Figure 1. The monosaccharide composition of cell walls from ripe (22.7 ° B, 2012) and overripe (26.5° B, 2013) fresh Pinotage grape skin.The bars represent the average of at least 10 biological repeats. The stars indicate a statistical significant difference for of a specific monosaccharide (T-test, 95% confidence level) between the two ripeness levels. Ara, arabinose; Rha, rhamnose; Fuc, fucose; Xyl, xylose; GalA, galacturonic acid; Man, mannose; Gal, galactose; Glc, glucose; GlcA, glucoronic acid.

The abundance of homogalacturonan (HG) in the skin cell walls was confirmed with the CoMPP analysis, as indicated by the signal values in the heat map (Figure 2, CDTA fraction, fresh samples). The cell walls also contained high levels of xyloglucan (mAbs LM15 and LM25) and cellulose (mAb CBM3a), with the latter dissolving along with the hemicellulose fraction (Figure 2, NaOH fraction, fresh samples) which might be a reflection of the known association between the cellulose and hemicellulose network in plant cell walls[35]. Both the pectin and the hemicellulose fraction showed the presence of arabinogalactan proteins (AGPs) and extensins. α-1,5-L-Arabinan and β-1,4-D-galactan, probably linked to rhamnogalaturonan I (RG-I), were found in the hemicellulosic fraction. This corresponded with work done by Zykwinska et al.[36] on alkali extracts from potato and sugar beet cell walls where they observed strong interaction between arabinan or galactan side chains and the cellulose microfibrils surface and were also observe in grape tissue[24].

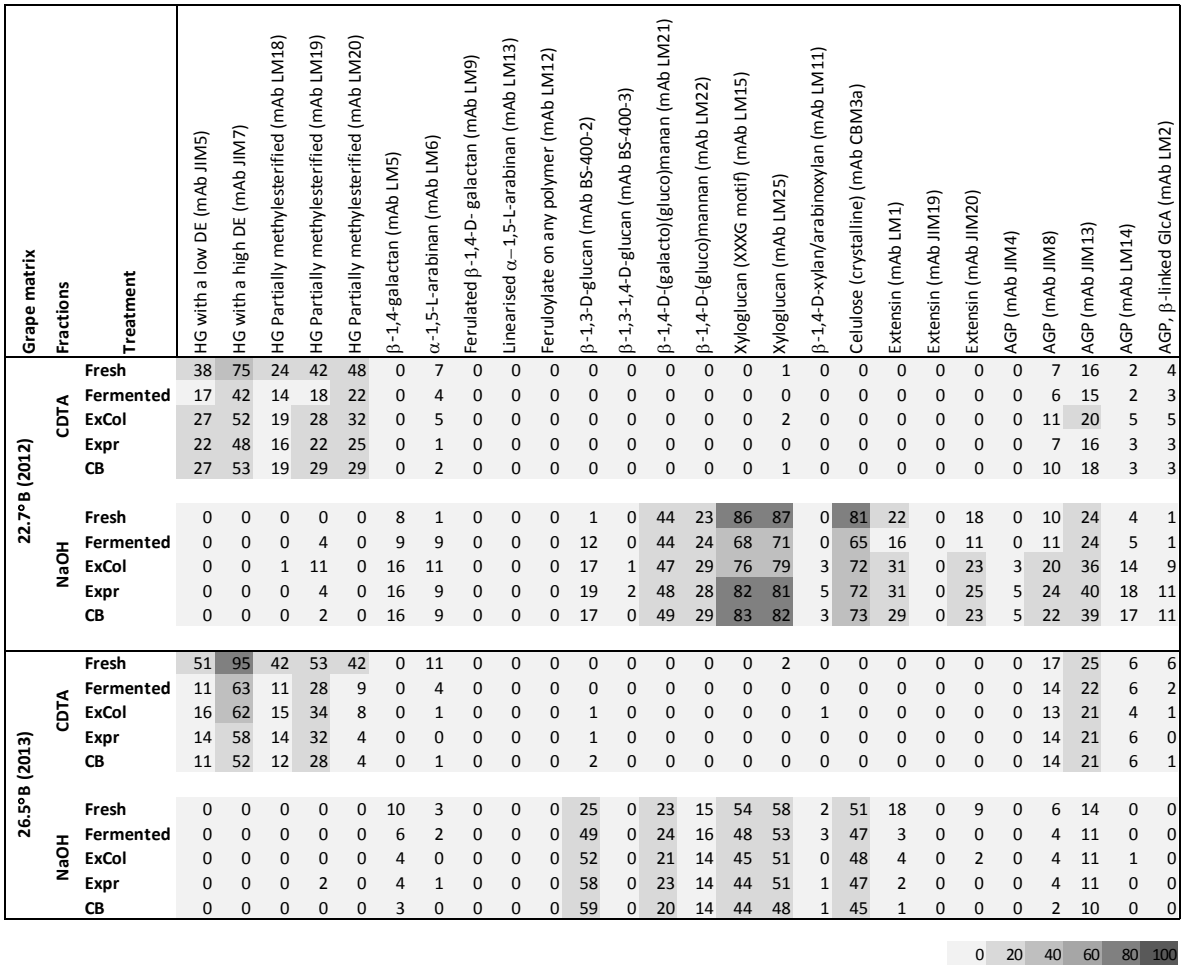

Grape matrix	Fractions	Treatment	HG with a low DE (mAb JIM5)	HG with a high DE (mAb JIM7)	HG Partially methylesterified (mAb LM18)	HG Partially methylesterified (mAb LM19)	HG Partially methylesterified (mAb LM20)	β-1,4-galactan (mAb LM5)	α-1,5-L-arabinan (mAb LM6)	Ferulated β-1,4-D- galactan (mAb LM9)	Linearised α−1,5-L-arabinan (mAb LM13)	Feruloylate on any polymer (mAb LM12)	β-1,3-D-glucan (mAb BS-400-2)	β-1,3-1,4-D-glucan (mAb BS-400-3)	β-1,4-D-(galacto)(gluco)manan (mAb LM21)	β-1,4-D-(gluco)mannan (mAb LM22)	Xyloglucan (XXXG motif) (mAb LM15)	Xyloglucan (mAb LM25)	β-1,4-D-xylan/arabinoxylan (mAb LM11)	Celulose (crystalline) (mAb CBM3a)	Extensin (mAb LM1)	Extensin (mAb JIM19)	Extensin (mAb JIM20)	AGP (mAb JIM4)	AGP (mAb JIM8)	AGP (mAb JIM13)	AGP (mAb LM14)	AGP, β-linked GlcA (mAb LM2)
22.7°B (2012)	CDTA	Fresh	38	75	24	42	48	0	7	0	0	0	0	0	0	0	0	1	0	0	0	0	0	0	7	16	2	4
		Fermented	17	42	14	18	22	0	4	0	0	0	0	0	0	0	0	0	0	0	0	0	0	0	6	15	2	3
		ExCol	27	52	19	28	32	0	5	0	0	0	0	0	0	0	0	2	0	0	0	0	0	0	11	20	5	5
		Expr	22	48	16	22	25	0	1	0	0	0	0	0	0	0	0	0	0	0	0	0	0	0	7	16	3	3
		CB	27	53	19	29	29	0	2	0	0	0	0	0	0	0	0	1	0	0	0	0	0	0	10	18	3	3
	NaOH	Fresh	0	0	0	0	0	8	1	0	0	0	1	0	44	23	86	87	0	81	22	0	18	0	10	24	4	1
		Fermented	0	0	0	4	0	9	9	0	0	0	12	0	44	24	68	71	0	65	16	0	11	0	11	24	5	1
		ExCol	0	0	1	11	0	16	11	0	0	0	17	1	47	29	76	79	3	72	31	0	23	3	20	36	14	9
		Expr	0	0	0	4	0	16	9	0	0	0	19	2	48	28	82	81	5	72	31	0	25	5	24	40	18	11
		CB	0	0	0	2	0	16	9	0	0	0	17	0	49	29	83	82	3	73	29	0	23	5	22	39	17	11
26.5°B (2013)	CDTA	Fresh	51	95	42	53	42	0	11	0	0	0	0	0	0	0	0	2	0	0	0	0	0	0	17	25	6	6
		Fermented	11	63	11	28	9	0	4	0	0	0	0	0	0	0	0	0	0	0	0	0	0	0	14	22	6	2
		ExCol	16	62	15	34	8	0	1	0	0	0	1	0	0	0	0	0	1	0	0	0	0	0	13	21	4	1
		Expr	14	58	14	32	4	0	0	0	0	0	1	0	0	0	0	0	0	0	0	0	0	0	14	21	6	0
		CB	11	52	12	28	4	0	1	0	0	0	2	0	0	0	0	0	0	0	0	0	0	0	14	21	6	1
	NaOH	Fresh	0	0	0	0	0	10	3	0	0	0	25	0	23	15	54	58	2	51	18	0	9	0	6	14	0	0
		Fermented	0	0	0	0	0	6	2	0	0	0	49	0	24	16	48	53	3	47	3	0	0	0	4	11	0	0
		ExCol	0	0	0	0	0	4	0	0	0	0	52	0	21	14	45	51	0	48	4	0	2	0	4	11	1	0
		Expr	0	0	0	2	0	4	1	0	0	0	58	0	23	14	44	51	1	47	2	0	0	0	4	11	0	0
		CB	0	0	0	0	0	3	0	0	0	0	59	0	20	14	44	48	1	45	1	0	0	0	2	10	0	0

Figure 2. Heat map (CoMPP results) showing the relative abundance of the cell wall polysaccharides found in the pectin (CDTA) and hemicellulose (NaOH) fractions extracted from the cell walls of fresh and fermented (with and w/o maceration enzyme treatment) grape skins. Fresh = extracts from fresh skin cell walls. Fermented = extracts prepared from the cell walls of skins sampled at the end of alcoholic fermentation (without enzyme addition). ExCol, Expr and CB = the same as Fermented but with the addition of Rapidase ®ExColor, Rapidase ®Expression and Rapidase ®CB enzymes. Values are the average of at least 3 biological repeats.

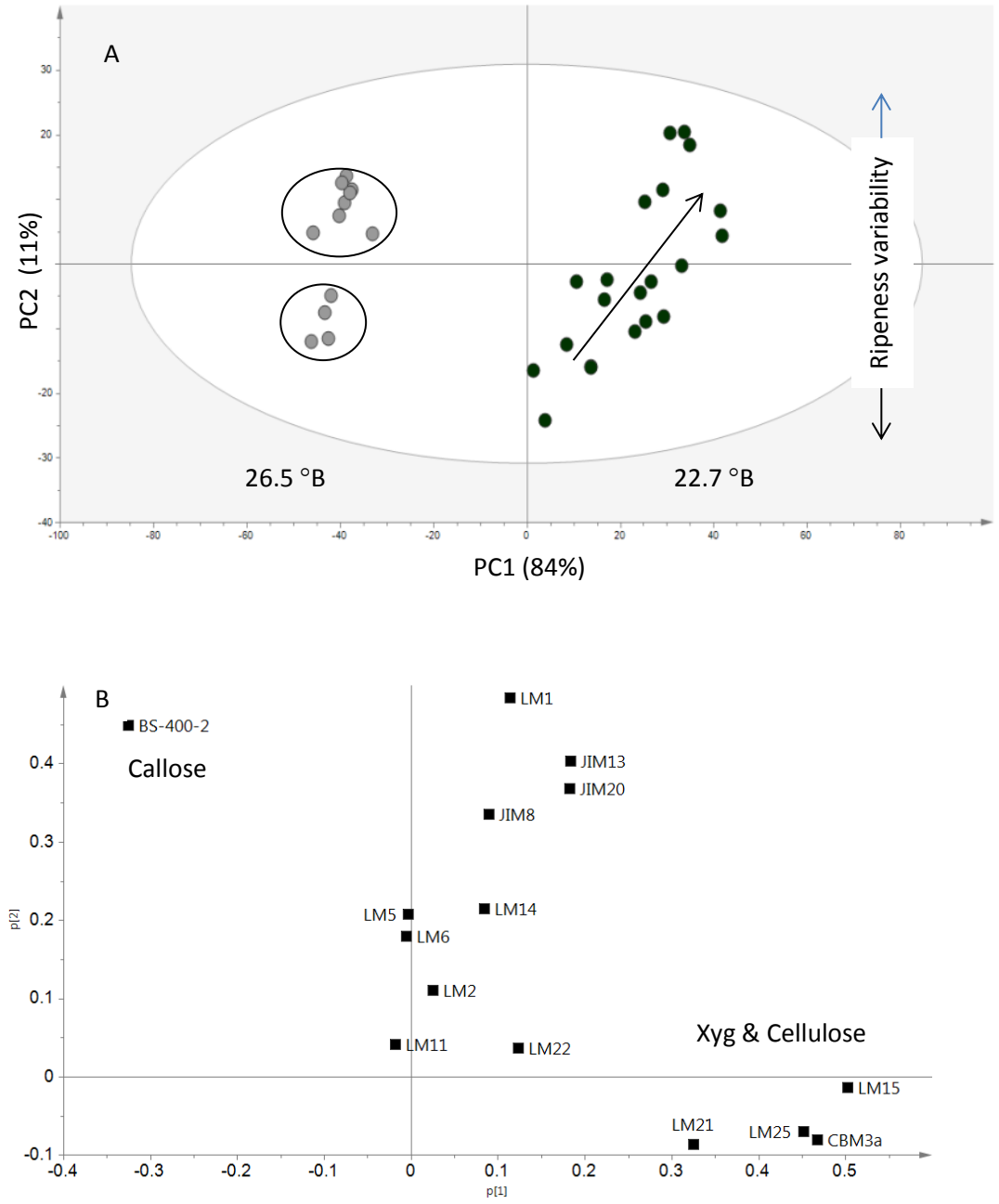

Figure 3. ComPP results showing a PCA score plot (A) and loading plot (B) of the hemicellulose fraction (NaOH) of cell walls from fresh skins for ripe (22.7 °B, 2012, • Black circle) and overripe (26.5 °B, 2013, • Grey circle) grapes. Subgroups are circled and the variance in the ripe (22.7 °B) skin data is highlighted with an arrow. Xyg, xyloglucan.

Comparing ripe (22.7 °B) with overripe (26.5 °B) Pinotage skin cell walls (Figure 1) the overripe samples had significantly (95% confidence level) less Gal (2.9 mol % decrease) and Xyl (2.8 mol % decrease) but more GalA (8.8 mol % increase). The lower percentage contribution of Gal in the overripe grapes corresponds with what other authors[17,24,34] described as typical changes during fruit and grape berry ripening and is believed to be related to arabinogalactan

degradation as fruit softens. The lower mol % of Xyl and Gal in the overripe grapes is corroborated by the CoMPP analysis (Figure 2, fresh samples and PCA plot of NaOH fraction, Figure 3 A-B) where a decrease in xyloglucan (mAbs LM15 and LM25) and β-1,4-D-(galacto)(gluco)mannan (mAb LM21) was observed in the skin cell walls of the riper grapes. This was accompanied by a decrease in cellulose (mAb CBM3a); similar results were seen by Yakushiji et al.,[37] and Vicens et al.[17] reported a decrease in Xyl with a concurrent decrease in xyloglucan during ripening, confirming that not only pectin polysaccharides depolymerize with fruit ripening, but also hemicelluloses.

There is no consensus yet on the fate of GalA in the grape skin during ripening. According to the data from Ortega-Regules et al.[34] the uronic acid concentration reaches a peak before grape maturity and then declines (Monastrel and Cabernet Sauvignon grapes), but this was not confirmed for all the cultivars that were tested (Syrah increased and Merlot decreased with ripening). The higher levels of GalA found in our overripe grape skins might be due to mesocarp material that peeled off along with the skin. The higher GalA levels were confirmed with the CoMPP data (Figure 2 and PCA plot, Figure 4 A-B, CDTA extract) where the overripe skins were more abundant in HG epitopes (mAbs LM18, LM19, JIM7, and JIM5) than the ripe skins. Additionally the overripe skins showed more arabinogalacturonan proteins (AGPs) (mAbs JIM8, JIM13) which corresponded well with the observed accumulation of structural cell wall proteins during fruit ripening[17,38]. The overripe samples were more abundant in β-1,3-D-glucan (callose) (NaOH fraction, Figure 3B, PC2 = 11 %) which is typically formed in response to pathogen-induced stress or wounding[39]. The overripe and softer grapes were probably more vulnerable to wounding during the harvest and the peeling of the skins. (The separation of the 22.7 from the 26.5°B samples is not dominated by the abundance of mAb BS400-2 (callose) as suggested by Figure 3, because the overall pattern of a PCA where we excluded this antibody [results not shown] were unchanged from the PCA in Figure 3).

The PCA plots of the CoMPP data for fresh cell walls sampled from grapes at the two different ripeness levels (Figure 3A and Figure 4A) showed significant heterogeneity between the samples within a harvest. This is indicated in the NaOH fraction (Figure 3) by the different subgroups formed by the 26.5 °B samples (circled) as well as a strong spread of the 22.7 °B samples along the second component axis, shown by an arrow. Closer examination of the CDTA fraction revealed that certain samples from both ripeness levels clustered together (Figure 4, indicated in a block) because they have an abundance of HG, AGPs and extensins. These samples thus contained a higher percentage of riper skins than the other samples from

their respective ripeness-level-groups, and demonstrated the heterogeneity found in the grapes harvested for a standard commercial wine fermentation.

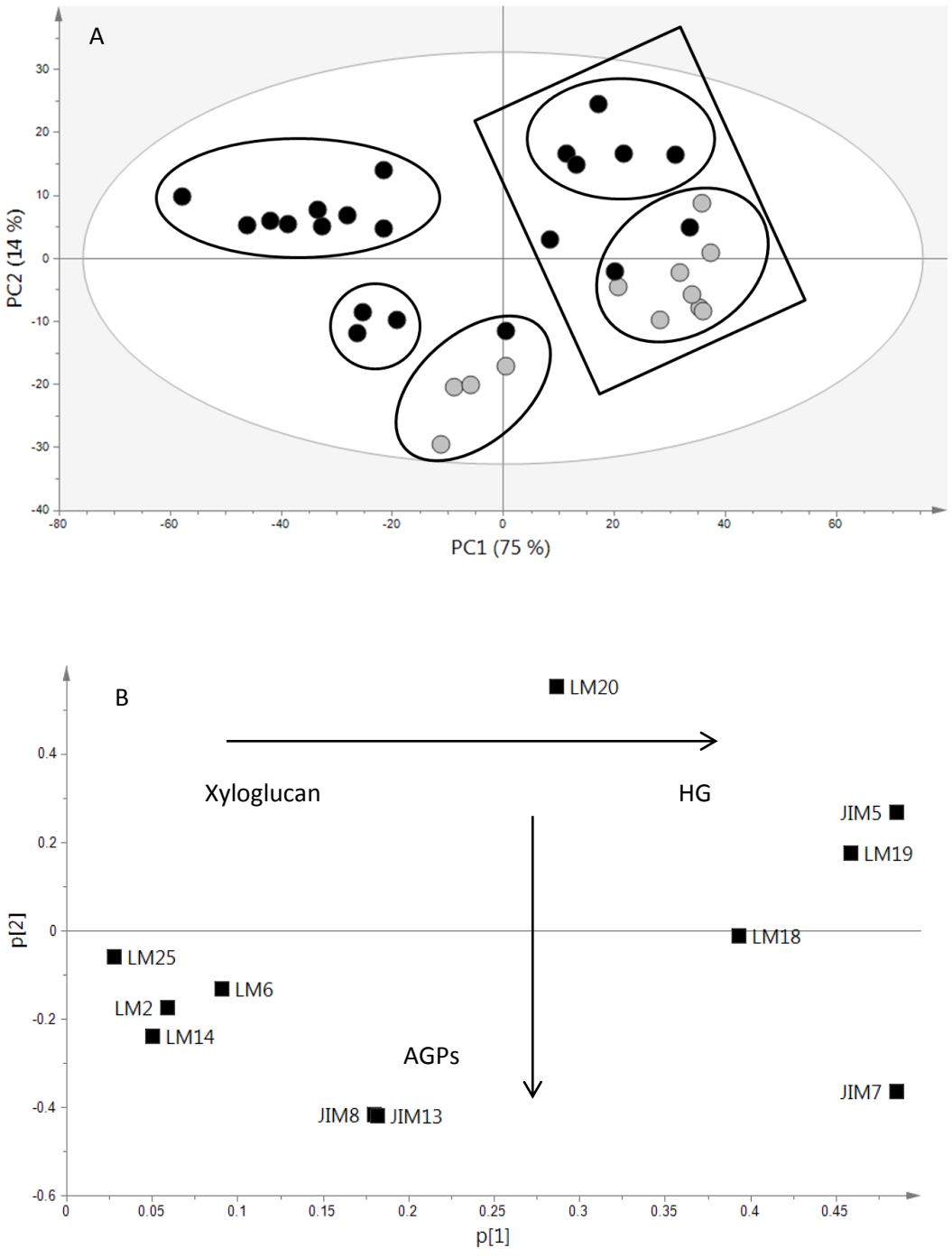

Figure 4. ComPP results showing a PCA score plot (A) and loading plot (B) of the pectin fraction (CDTA) of cell walls from fresh Pinotage skins at different ripeness levels (22.7 °B, 2012, • Black circle) and 26.5°B, 2013, • Grey circle). Subgroups are encircled and indicate that the separation of the groups is driven by an abundance in AGPs and HG.

Effect of the maceration enzymes on the fermented grape skin cell walls. During the maceration step of red wine fermentation the ethanol formed, penetrates the berry cell walls and permeabilize the plasma- and the vacuolar membranes of the cells and serves as an extraction solvent for a range of molecules including high molecular weight tannins[6]. Furthermore, pectin solubilization also occurs during fermentation because organic acids such as malate, citrate and phytic acids present in grape must, act as chelating agents, removing the calcium ions that form bridges between HG polymers[22]. Thus, even with no addition of maceration enzymes, cell wall modifications probably occur as a consequence of the fermentation process alone.

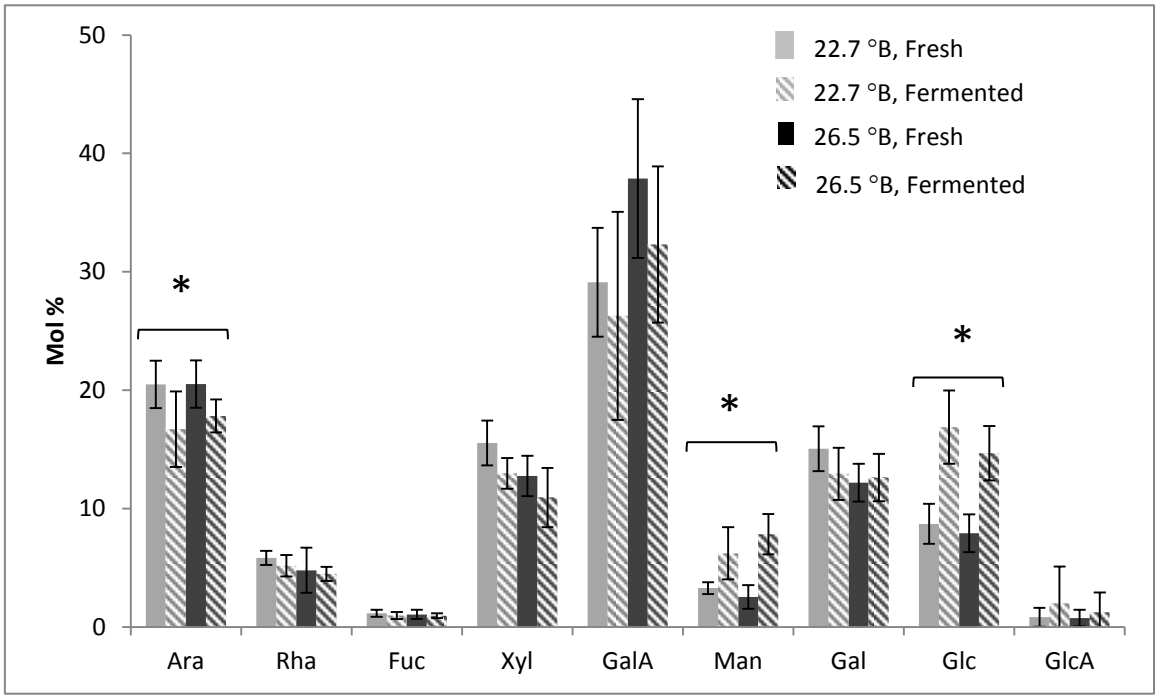

Figure 5. Mol % changes in the monosaccharide composition of the cell walls extracted from fresh and fermented Pinotage skins in 2012 and 2013. Significant changes (indicated by stars) brought about by the fermentation process is an increase in Man and Glc and a slight decrease in Ara (95 % confidence level, ANOVA). The bars represent the average of at least three biological repeats.

The most marked impact of the fermentation process (Figure 5) was an increase in mannose (Man) (2.9 mol% in 2012 and 5.3 in 2013) and glucose (Glc) (8.2 mol% in 2012 and 6.8 in 2013) and a slight decrease in Ara (3.8 mol% in 2012 and 2.7 in 2013). The increase in Glc and Man is probably due to a reduction in pectin polymers leading to a relative increase in polymers such as cellulose, mannan and xyloglucan. Although not statistically significant, GalA values showed a decreasing trend (2.8 mol% in 2012 and 5.6 in 2013, T-test, 90% significance) as a result of the fermentation. This decrease was also clearly visible in the CoMPP data of Figure S1 A-B.

This PCA plot shows the fermented (without enzymes) samples on the left separating from the fresh, unfermented samples on the right. The separation or variance was due to the abundance of HG polymers (labelled by mAbs JIM5, JIM7, LM18, LM19 and LM20) in the fresh samples. A similar analysis with the FT-MIR spectra (Figure 6) also indicated that the fresh skin cell walls had more pectin (high absorbance at 1095 and 1157 – 1147 cm^{-1}).

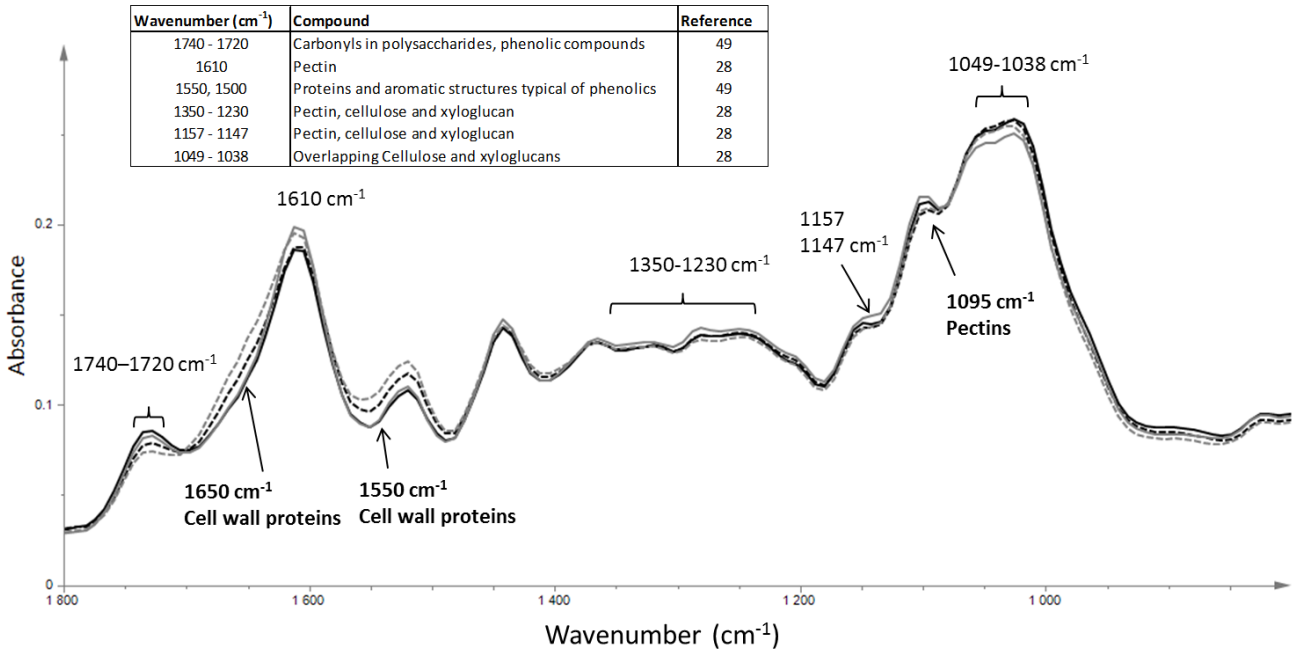

Figure 6. FT-MIR spectra of the fresh versus fermented (without enzymes) cell walls at two ripeness levels. _____ Fresh (22.7°B, 2012);_ _ _ _ _Fermented (22.7°B, 2012); . _____ Fresh (26.5°B, 2013);_ _ _ _ _ _Fermented (26.5°B, 2013). The areas and peaks that represent typical chemical groups found in plant cell walls are shown on the spectra and in the table. The biggest variations are at wavelengths 1650 and 1550 cm^{-1} where the cell walls isolated from the fresh skins have a lower absorbance than the fermented samples indicating that they have less cell wall proteins. Another interesting area is the peak at 1095 cm^{-1} that shows that the cell walls isolated from fresh skins have more pectin than the fermented samples. The spectra represent the average absorbance from at least five AIR samples per treatment.

Another explanation for the elevated Man concentration (Figure 5) of the fermented samples may be the presence of the wine yeast. Forty percent of the wine yeast cell wall (dry weight) consists of mannoproteins and 98 % of the sugar in this cell wall component is Man[40]. Yeast cell wall debris that sticks to grape skin fragments could possibly end up in the cell wall extracts and thus inflate the Man values. Similarly, yeast cell wall debris that contains β-1,3-D-glucan[41] might also have contributed to the elevation in Glc concentration seen, but a more likely source could be from callose (β-1,3-D-glucan) formation in the fermented grape skins. The formation of callose in grape berries that are crushed and punched down during the red wine production

process is plausible and CoMPP analysis confirmed the presence of β-1,3-D-glucan (mAb BS-400-2, specific to callose). It is not known whether this mAb will also label β-1,3-D-glucan in yeast cell walls, but from other results by our group (unpublished) we regularly see a signal for mAb BS-400-2 in grape tissue that did not undergo fermentation.

Finally, the decrease in Ara because of the fermentation process may be attributed to the release of AGPs and type II arabinogalactans into the fermenting must. These molecules constitute ca. 40% of the total polysaccharides found in red wine[42,43] and Guadalupe and Ayestarán[44] showed the Ara concentration increased to more than 150 mg/L at the end of alcoholic fermentation. However, the FT-MIR data (Figure 6) showed that the fermented skin cell walls had more protein (high absorbance at 1650 and 1550 cm^{-1}) than the fresh skins. This seems to be in contrast to the decrease in Ara and the assumed loss of AGPs, but it needs to be considered that the monosaccharide analysis measured the total amount of Ara in the samples, whereas the FT-MIR spectra only "evaluated" the surface or cell wall proteins exposed after depectination. In general, therefore, we see that the fermentation process caused similar compositional changes in the skin cell walls of grapes, irrespective of the ripeness level of the skins. However, the ripeness might have an influence on the magnitude of the changes observed. This can be seen in Figure 6 at wavelengths 1550 and 1650 cm^{-1}, where the grey dotted line that represents the fermented samples at 26.5 °B showed the largest deviation from the fresh samples.

Color analysis (results in supplementary section [S 1.2 and Table S1]) on the wine prepared in this study showed no significant improvement in the color density of the wines produced from enzyme treated fermentations. To supplement this indirect evaluation of the impact of enzymes, we were asking the question whether this implies that the maceration enzymes did not alter the cell walls of the skins. This led to the final investigation of this study where we aimed to determine how typical, commercial maceration enzymes change the cell walls of grape skins during fermentation. We therefore compared the samples from the enzyme-free fermentations with samples from the enzyme-assisted fermentations. The most dominant changes (Figure 7, 95 % confidence level, ANOVA) to the monosaccharide composition of the cell walls brought about by the enzymes were: (1) an increase in the Man (avg. of 3.7 mol% in 2012 and 4.8 in 2013) and Glc (no significant increase in 2012 and avg. of 4.7 mol% in 2013) and a (2) decrease in Ara (avg. of 2.3 mol% in 2012 and 2.9 in 2013), Rha (avg. of 0.9 mol% in 2012 and 1.1 in 2013) and GalA (no significant increase in 2012 and an avg. of 9.6 mol% in 2013) composition. As previously discussed, the relative increase of the cellulose, mannan and xyloglucan monosaccharides (Man and Glc) is a consequence of the degradation of pectin

polymers (HG and RG) but this time it was due to the hydrolysis and depectination of the cell wall polysaccharides by the maceration enzymes (enzyme treated values were compared to control fermentation values). Similarly, the decrease in Ara and Rha is an indication of RG-I, arabinan and AGP degradation. We thus see the same type of monosaccharide changes occurring in enzyme-free and enzyme-assisted fermentation, but the enzymes increased the magnitude of the changes. Maceration enzymes might also introduce additional changes to the cell wall, such as the proportional decrease in Rha (Figure 7), since a similar decrease was not observed under enzyme-free conditions (Figure 5).

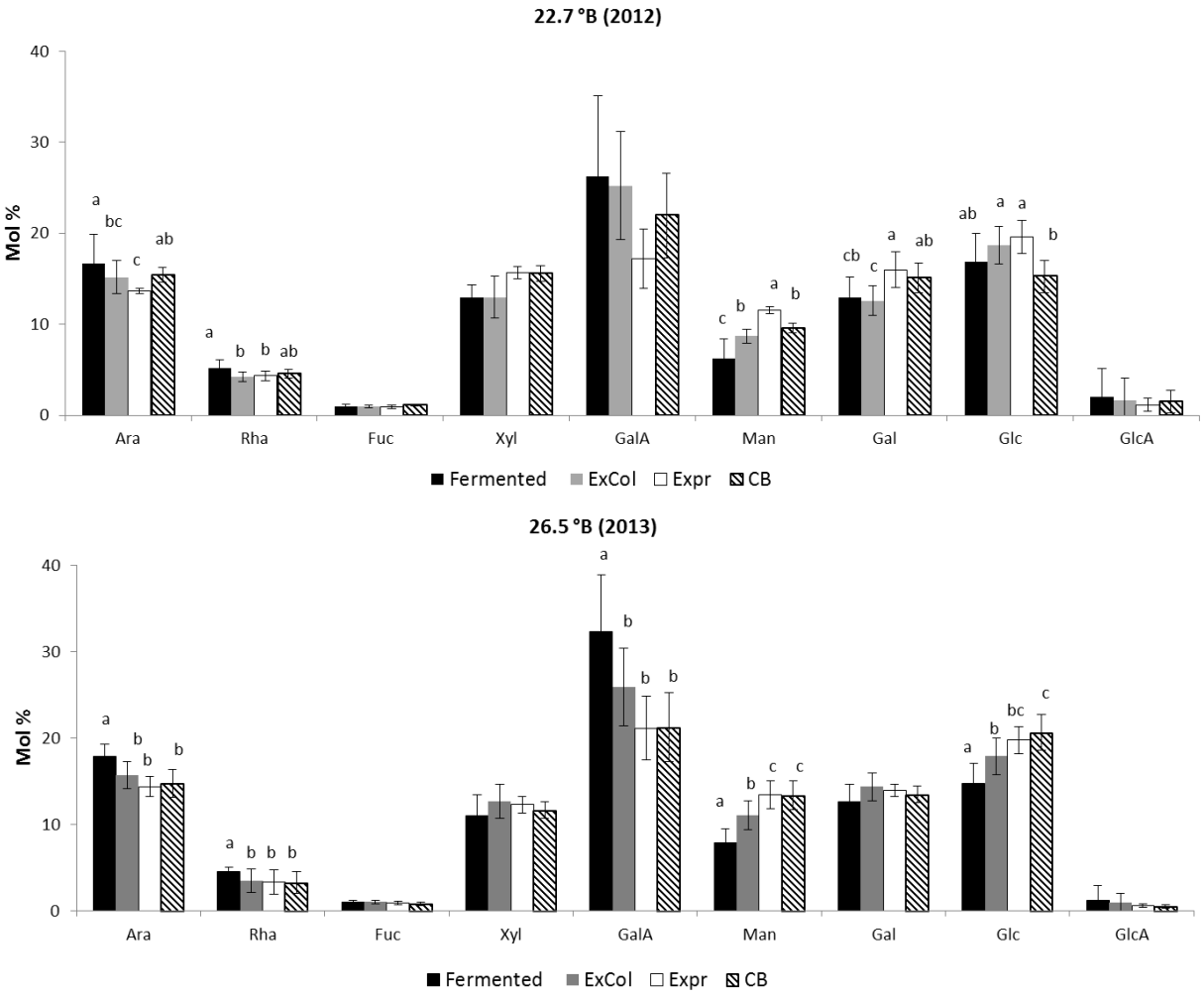

Figure 7. Mol % changes in the monosaccharide composition of the cell walls from Pinotage skins from fermented (no enzyme addition) and maceration enzyme treated fermentations at 22.7 and 26.5 °B. Different letters indicate a significant difference for a specific sugar, between the different treatments (95 % confidence level, ANOVA). Fermented stands for cell wall samples from fermentation without enzyme addition. ExCol, Expr and CB is cell wall samples from fermentation with the addition of Rapidase® Ex Color, Rapidase® Expression and Rapidase® CB respectively. The values represent the average of three biological repeats.

On the polymer level (CoMPP data) one would expect to see that maceration enzyme action lead to a consequential decrease in pectin polymers reflecting the decrease in GalA and Rha values. (We did in fact note a loss of pectin in the FT-MIR spectra [Figure S2] for the enzyme treated samples). One would expect depectination to be the most prominent change because pectinases are the major enzyme activity present in the maceration enzyme preparations that were used. However, the CoMPP heat map (Figure 2) showed an increase in HG labelling (CDTA fraction, all HG mAbs) of the enzyme treated skins of 2012 (22.7 °B) compared to the control fermentation skins. Considering that the polymers that were identified in the different fractions of the CoMPP analysis were those polymers extracted and dissolved in CDTA and NaOH respectively, we can speculate that the increase in HG was the result of enzyme hydrolysis that unravelled the cell wall structure. This process allowed more of the HG that is interspersed with the hemicellulose-cellulose scaffold to move out and dissolve in the CDTA leading to higher labelling signals. In the overripe grape skins (26.5 °B) however, the values only increased for mAbs JIM5 andLM19 and only for ExCol treated samples. In general, for the overripe grape skins there was only an initial marked decrease in HG and α-1,5-L-arabinan as a result of the depectination that took place during the standard red wine fermentation (no added enzymes).

In the hemicellulose fraction of the ripe grapes 2012 (Figure 2) there was an increase in the dissolved β-1,4-D-galactan, mannans (slight), xyloglucans (mAbs LM15 and LM25), cellulose mAb CBM3a), extensins (mAb JIM20) and AGPs (mAbs JIM4, JIM8, JIM13, LM14 and LM2) which can all be ascribed to the hydrolysis actions of the enzymes that enhanced the solubilization of these polymers in the NaOH extract. As with the CDTA fraction, these effects were not repeated in the NaOH fraction of the overripe grapes. This may indicate that the high degree of cell wall degradation that took place due to the natural grape ripening processes in the overripe grapes led to a near complete removal of all easily accessible cell wall polymers during the fermentation, even in the control fermentation. No significant additional change due to hydrolysis by the maceration enzymes could be detected in the overripe cell walls. Thus, quantitatively (monosaccharide data) the maceration enzyme actions have a similar effect than the natural grape tissue ripening enzymes (depectination) but their mode of action might be different. The former seems to contribute to an increase in cell wall porosity, which is not seen with the latter. This might indicate that the plant ripening enzymes act in a block wise fashion (as seen with plant pectin methyl esterases (pPME)[45,46] while the fungal enzymes from commercial maceration preparations act more randomly (as seen with some fungal pectin methyl esterases)[47]. However, the differences observed might just be a factor of the degree of degradation that has taken place. As hydrolysis time increase (as grapes ripen or longer incubation with maceration enzymes), the degradation might progress in alternating stages of

depolymerization and diffusion of the resulting oligomers into the surrounding matrix (fermenting must) and pore formation.

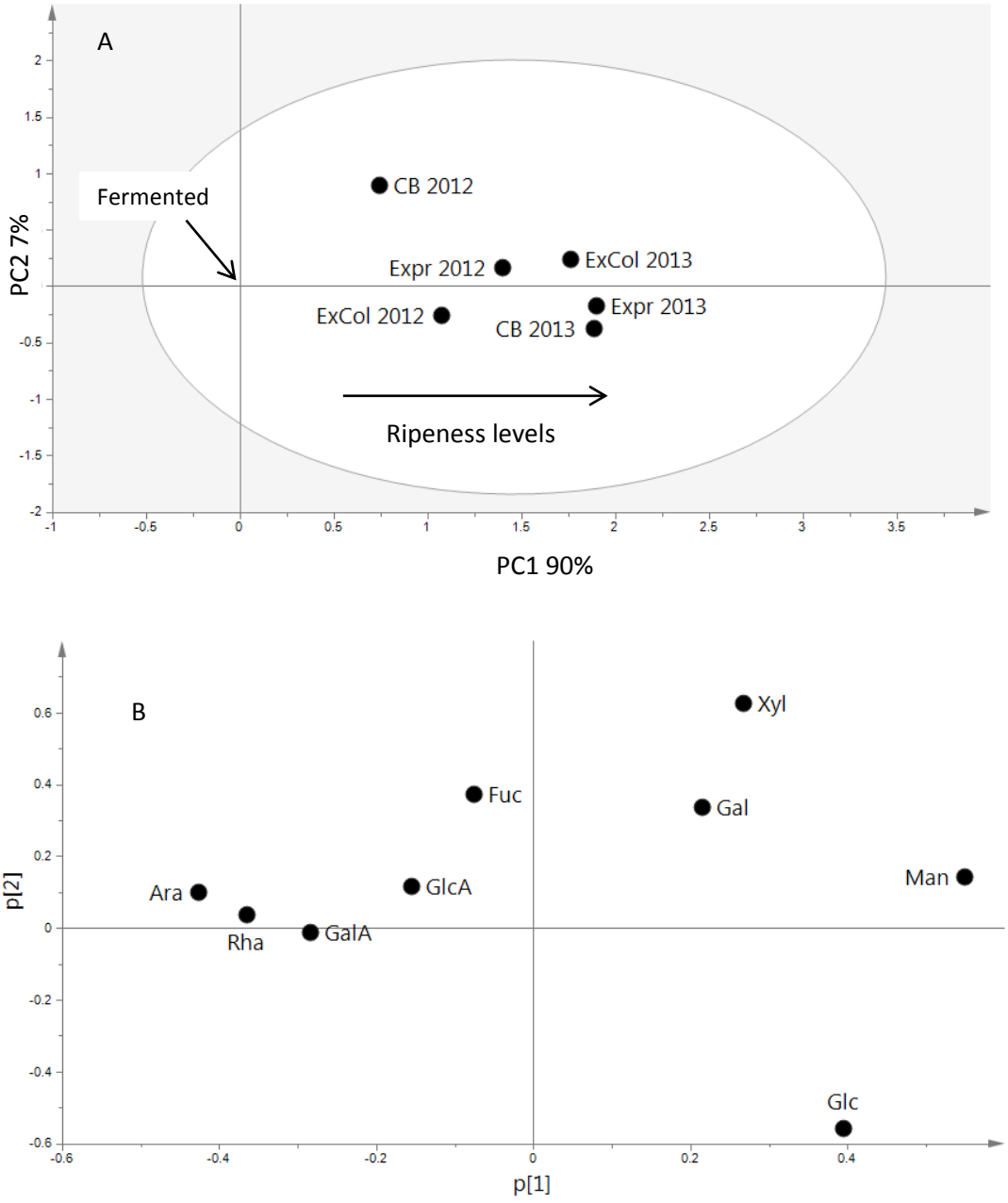

Figure 8. Score (A) and loading (B) plot of a correlation matrix analysis on the monosaccharide composition of enzyme treated grape skin cell walls compared to samples from the control fermentation (no enzyme addition, represented by the intersection of the axis) at two different ripeness levels.

Orthogonal projections to latent structures (OPLS) models[48] were used to focus more specifically on the difference between each enzyme treatment effect versus its control. The resulting six OPLS models (three treatments /vintage) can be summarized by its correlation

loadings. These correlation values of the models were portrayed in principle component analysis (PCA) plots (Figure 8 for monosaccharides and Figure 9 for CoMPP data). This showed (Figure 8) that in terms of monosaccharide composition all the enzymes had a similar effect on the cell wall (all are in the same direction, a distance away from the control samples represented by the intersection of the axis). However, the 2013 enzyme treated samples were further removed along the first component axis (PC1 = 90%) than the 2012 samples indicating a greater impact on monosaccharide composition. This impact is partly due to the hydrolysis by the commercial maceration enzymes but it is also the result endogenous cell wall enzymes. The loading plot confirms that the enzyme treated cell walls have a higher proportion of Man and Glc and lower percentage of Ara, Rha and GalA than the control group. The cell walls treated with Rapidase® CB during 2012 are the main contributors to the variance along the second component of the model and this variance is driven by a relative abundance of Xyl in the samples. According to the manufacturer, Rapidase® CB has primarily pectinase activity with enhanced polygalacturonases thus, this unique behaviour could not be connected to a specific enzyme activity present in Rapidase® CB.

On a polymer level (CoMPP data), the correlation values obtained from OPLS models on individual enzyme treatments versus the enzyme-free fermentation are shown in the PCA plots of Figure 9. In the analysis of the CDTA fraction (Figure 9A and B) ExCol 2012 and CB 2012 were positively correlated with an abundance in HG (mAbs JIM7 and LM20) in the first component (PC1 = 68%), and xyloglucan (mAb LM25), α-1,5-L-arabinan (mAb LM6) and AGPs (mAb JIM13, LM14 and LM2) in the second component (PC2 = 26%). Expr 2012 had a positive correlation with HG labelled by mAbs LM18 and LM19 and JIM5. In 2013, Expr and ExCol showed a positive correlation with an abundance in HG (mAbs LM19, LM18 and JIM5) (also seen in heat map, Figure 2), but CB 2013 was not showing the same effect. In the NaOH fraction (Figure 9C and D) all the enzyme treatments in 2012 correlated positively (PC1 = 82 %), with the abundance in β-1,4-galactan (mAb LM5), mannan (mAb LM21 and LM22), xyloglucan, cellulose and AGP. The opposite was true for all the enzymes in 2013. Thus, the enzyme action of ExCol 2012, CB 2012, Expr 2013 and ExCol 2013 enhanced extraction of HG in the CDTA fraction although the effect was much stronger in 2012. In the hemicellulose fraction, all the enzymes during 2012 enhanced the extraction of hemicelluloses, cellulose and AGPs while none of the enzyme treatments in 2013 caused any changes.

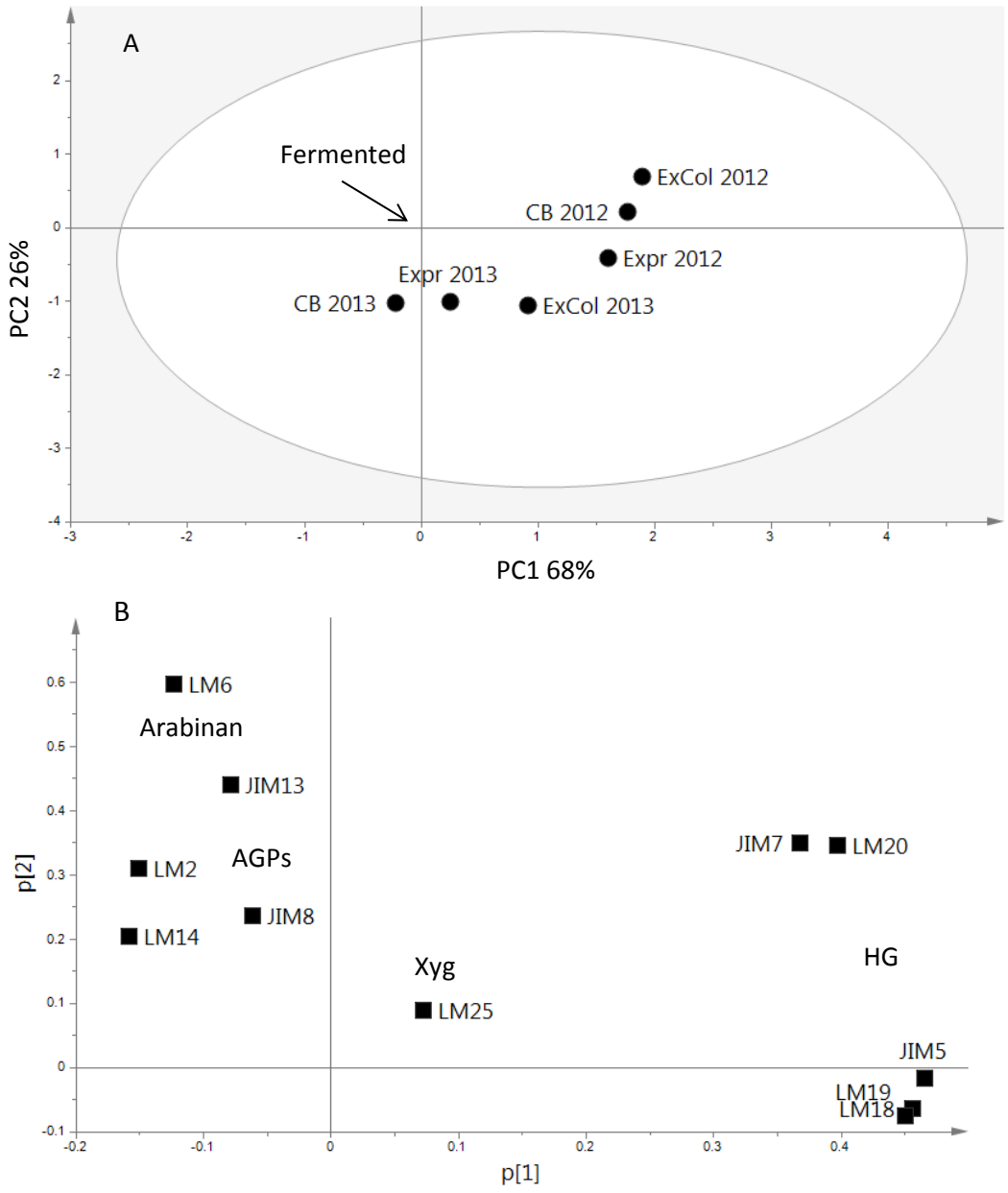

Figure 9. Score (A) and loading (B) plot of a correlation matrix analysis on the CDTA fraction (CoMPP data) of enzyme treated grape skin cell walls compared to samples from the control fermentation (no enzyme addition). Score (C) and loading (D) plot of a correlation matrix analysis on the NaOH fraction (CoMPP data) of enzyme treated grape skin cell walls compared to samples from the control fermentation (no enzyme addition). The codes for the epitopes are described in Figure 2. Xyg, xyloglucan.

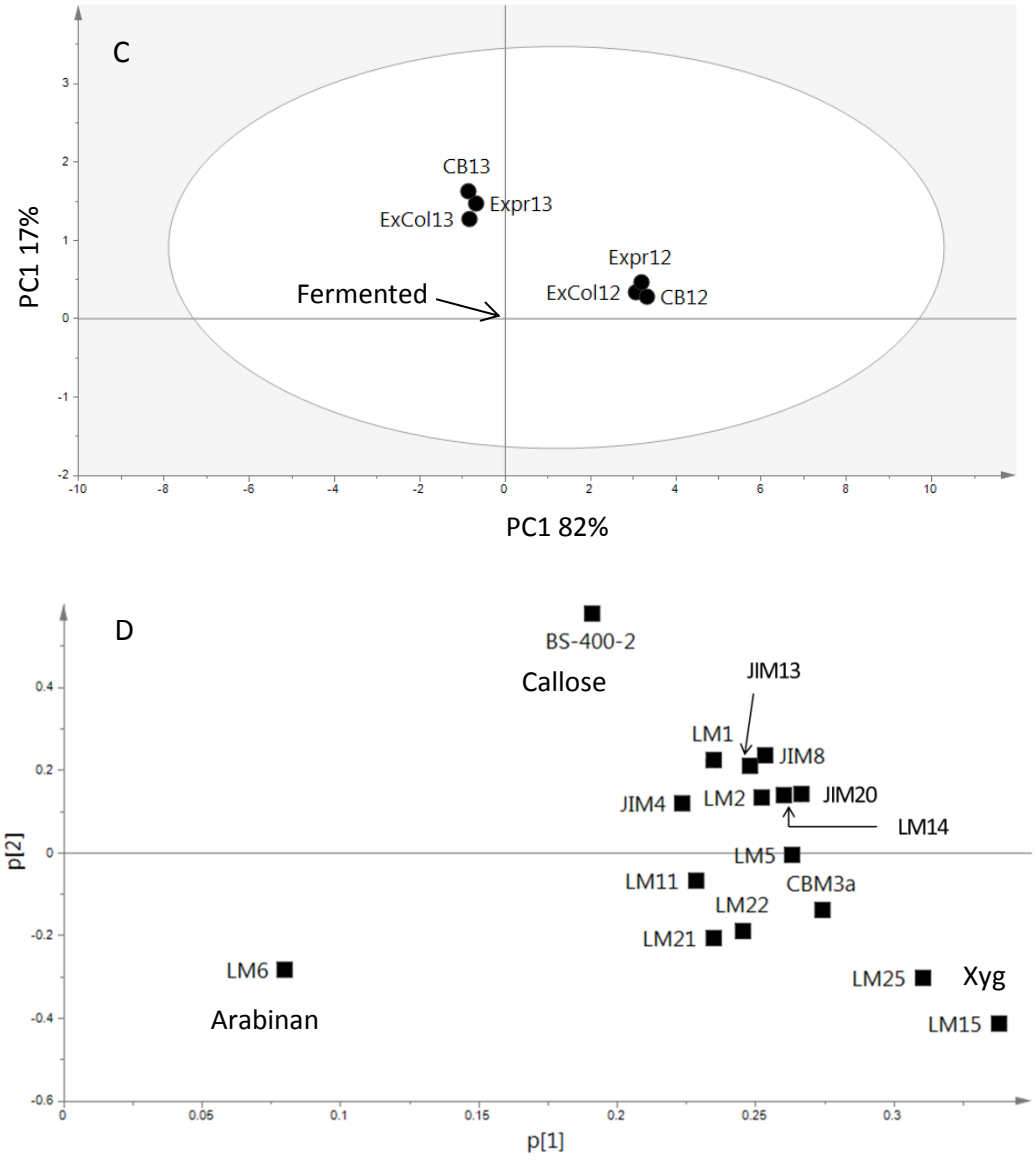

Figure 9 C-D

Taken together, we saw that all enzyme treatments group together in the same direction for grapes from a specific year, which indicated that they affected the cell walls in a similar fashion. The ripeness level of grapes had a significant effect on the cell walls of the grape tissue as a result of the action of the endogenous enzymes. The maceration enzymes appear to have similar activity profiles than these enzymes, which makes it difficult to distinguishing between the action of the ripening enzymes and the maceration enzymes. However, this could also be due to the limitations of the CoMPP technique.

In conclusion, this study shows that depectination and consequential exposure of the hemicellulose-cellulose framework and proteins of the cell walls in the skin occurs as a

consequence of the fermentation (no enzymes) process. With the addition of maceration enzymes, further depectination takes place and depending on the ripeness level of the grapes it was possible to infer an unravelling of the cell wall. We were unable to distinguish between the different maceration enzyme preparations in terms of their specific effects on the cell walls. Future work could use samples from the same vineyard at different harvest dates (levels of ripeness) and different concentrations of maceration enzymes to refine the observations made here. Together with wine colour analysis, it is necessary to look at the concentration of polyphenols retained in the grape skin tissue after fermentation and maceration enzyme treatment.

Supporting Information Available: A detailed discussion on the ripeness levels of the grapes, the FT-IR analysis of the wine as well as the results obtained with the wine color analysis are provided in the supplementary data. A PCA plot that shows the patterns in the data when comparing fresh and fermented samples as well as the FT-MIR spectra for the enzyme treated cell walls are also shown. This material is available free of charge via the Internet at http://pubs.acs.org.

REFERENCES

(1) Garrido, J.; Borges, F. Wine and grape polyphenols — A chemical perspective. *Food Res. Int.* **2013**, *54*, 1844–1858.

(2) Pinelo, M.; Arnous, A.; Meyer, A. S. Upgrading of grape skins: Significance of plant cell-wall structural components and extraction techniques for phenol release. *Trends Food Sci. Technol.* **2006**, *17*, 579–590.

(3) Gomez, E.; Martinez, A.; Laencina, J. Localization of free and bound aromatic compounds among skin , juice and pulp fractions of some grape varieties. *Vitis* **1994**, *4*, 1–4.

(4) Darriet, P.; Thibon, C.; Dubourdieu, D. Aroma and Aroma Precursors in Grape Berry. In *The biochemistry of the grape berry*; Geros, H.; Chaves, M. M.; Delrot, S., Eds.; Bentham e Books, 2012; pp. 111–136.

(5) Fontes, N.; Corte-Real, M.; Geros, H. New observations on the integrity, structure, and physiology of flesh cells from fully ripened grape berry. *Am. J. Enol. Vitic.* **2011**, *62*, 279–284.

(6) González-Neves, G.; Gil, G.; Ferrer, M.; Charamelo, D.; Balado, J.; Bochicchio, R.; Gatto, G.; Tessore, A. Prediction of the colour and polyphenolic composition of the young red wines from the phenolic potential of the grapes. *Int. J. Food Sci. Technol.* **2010**, *45*, 1843–1851.

(7) Jackson, R. S. Wine science: Principles and applications. *Wine science: Principles and applications*; 3rd ed.; Academic Press, Inc.: San Diego, 2008.

(8) Ducasse, M.-A.; Canal-Llauberes, R.-M.; de Lumley, M.; Williams, P.; Souquet, J.-M.; Fulcrand, H.; Doco, T.; Cheynier, V. Effect of macerating enzyme treatment on the polyphenol and polysaccharide composition of red wines. *Food Chem.* **2010**, *118*, 369–376.

(9) Wightman, J. D.; Price, S. F.; Watson, B. T.; Wrolstad, R. . Some effects of processing enzymes on anthocyanins and phenolics in Pinot noir and Cabernet Sauvignon wines. *Am. J. Enol. Vitic.* **1997**, *48*, 39–48.

(10) Haight, K.; Gump, B. The use of macerating enzymes in grape juice processing. *Am. J. Enol. Vitic.* **1994**, *45*, 113–116.

(11) Busse-Valverde, N.; Gómez-Plaza, E.; López-Roca, J. M.; Gil-Muñoz, R.; Bautista-Ortín, A. B. The extraction of anthocyanins and proanthocyanidins from grapes to wine during fermentative maceration is affected by the enological technique. *J. Agric. Food Chem.* **2011**, *59*, 5450–5455.

(12) González-Pombo, P.; Fariña, L.; Carrau, F.; Batista-Viera, F.; Brena, B. M. Aroma enhancement in wines using co-immobilized *Aspergillus niger* glycosidases. *Food Chem.* **2014**, *143*, 185–191.

(13) Arnous, A.; Meyer, A. S. Discriminated release of phenolic substances from red wine grape skins (*Vitis vinifera L.*) by multicomponent enzymes treatment. *Biochem. Eng. J.* **2010**, *49*, 68–77.

(14) Arnous, A.; Meyer, A. S. Quantitative prediction of cell wall polysaccharide composition in grape (*Vitis vinifera L.*) and apple (*Malus domestica*) skins from acid hydrolysis monosaccharide profiles. *J. Agric. Food Chem.* **2009**, *57*, 3611–3619.

(15) Romero-Cascales, I.; Ros-García, J. M.; López-Roca, J. M.; Gómez-Plaza, E. The effect of a commercial pectolytic enzyme on grape skin cell wall degradation and colour evolution during the maceration process. *Food Chem.* **2012**, *130*, 626–631.

(16) Hernández-Hierro, J. M.; Quijada-Morín, N.; Martínez-Lapuente, L.; Guadalupe, Z.; Ayestarán, B.; Rivas-Gonzalo, J. C.; Escribano-Bailón, M. T. Relationship between skin cell wall composition and anthocyanin extractability of *Vitis vinifera L*. cv. Tempranillo at different grape ripeness degree. *Food Chem.* **2014**, *146*, 41–47.

(17) Vicens, A.; Fournand, D.; Williams, P.; Sidhoum, L.; Moutounet, M.; Doco, T. Changes in polysaccharide and protein composition of cell walls in grape berry skin (Cv. Shiraz) during ripening and over-ripening. *J. Agric. Food Chem.* **2009**, *57*, 2955–2960.

(18) Brummell, D. A. Review : Cell wall disassembly in ripening fruit. *Funct. plant Biol.* **2006**, *33*, 103–119.

(19) Bindon, K. A.; Madani, S. H.; Pendleton, P.; Smith, P. A.; Kennedy, J. A. Factors affecting skin tannin extractability in ripening grapes. *J. Agric. Food Chem.* **2014**, *62*, 1130–1141.

(20) Ruiz-Garcia, Y.; Smith, P. A.; Bindon, K. A. Selective extraction of polysaccharide affects the adsorption of proanthocyanidin by grape cell walls. *Carbohydr. Polym.* **2014**, *114*, 102–114.

(21) Hanlin, R. L.; Hrmova, M.; Harbertson, J. F.; Downey, M. O. Review: Condensed tannin and grape cell wall interactions and their impact on tannin extractability into wine. *Aust. J. Grape Wine Res.* **2010**, *16*, 173–188.

(22) Jarvis, M. C. Plant cell walls: Supramolecular assemblies. *Food Hydrocoll.* **2011**, *25*, 257–262.

(23) Fleischer, A.; O'Neill, M.; Ehwald, R. The pore size of non-graminaceous plant cell walls is rapidly decreased by Borate ester cross-linking of the pectic polysaccharide rhamnogalacturonan II. *Plant Physiol.* **1999**, *121*, 829–838.

(24) Moore, J. P.; Fangel, J. U.; Willats, W. G. T.; Vivier, M. A. Pectic-β(1,4)-galactan, extensin and arabinogalactan-protein epitopes differentiate ripening stages in wine and table grape cell walls. *Ann. Bot.* **2014**, *114*, 1279–1294.

(25) Moller, I.; Sørensen, I.; Bernal, A. J.; Blaukopf, C.; Lee, K.; Øbro, J.; Pettolino, F.; Roberts, A.; Mikkelsen, J. D.; Knox, J. P.; Bacic, A.; Willats, W. G. T. High-throughput mapping of cell-wall polymers within and between plants using novel microarrays. *Plant J.* **2007**, *50*, 1118–1128.

(26) Iland, P. .; Ewart, A.; Sitters, J.; Markides, A.; Bruer, N. Techniques for chemical analysis and quality monitoring during winemaking. *Techniques for chemical analysis and quality monitoring during winemaking*; Patrick Iland Wine Promotions: Campbelltown, Australia, 2000.

(27) Ortega-Regules, A.; Ros-García, J. M.; Bautista-Ortín, A. B.; López-Roca, J. M.; Gómez-Plaza, E. Differences in morphology and composition of skin and pulp cell walls from grapes (*Vitis vinifera L.*): technological implications. *Eur. Food Res. Technol.* **2008**, *227*, 223–231.

(28) Szymanska-Chargot, M.; Zdunek, A. Use of FT-IR spectra and PCA to the bulk characterization of cell wall residues of fruits and vegetables along a fraction process. *Food Biophys.* **2013**, *8*, 29–42.

(29) Kacurakova, M.; Capek, P.; Sasinkova, V.; Wellner, N.; Ebringerova, A.; Kac, M. FT-IR study of plant cell wall model compounds : pectic polysaccharides and hemicelluloses. *Carbohydr. Polym.* **2000**, *43*, 195–203.

(30) York, W. S.; Darvill, A. G.; L, M. M.; Stevenson, T. T.; Albersheim, P. Isolation and characterization of plant cell walls and cell wall components. *Methods Enzymol.* **1985**, *2*, 3–40.

(31) Jackson, J. E. A User's Guide to Principal Components. *A User's Guide to Principal Components*; Wiley Series in Probability and Statistics; John Wiley & Sons, Inc.: Hoboken, NJ, USA, 1991.

(32) Coombe, B. G.; Dundon, R. J.; Short, A. W. S. Indices of sugar-acidity as ripeness criteria for winegrapes. *J. Sci. Food Agric.* **1980**, *31*, 495–502.

(33) Du Plessis, C. . Optimum maturity and quality parameters in grapes: A review. *South African J. Enol. Vitic.* **1984**, *5*.

(34) Ortega-Regules, A.; Ros-García, J. M.; Bautista-Ortín, A. B.; Lopez-Roca, J. M.; Gomez-Plaza, E. Changes in skin cell wall composition during the maturation of four premium wine grape varieties. *J. Sci. Food Agric.* **2008**, *88*, 420–428.

(35) Hayashi, T. Xyloglucans in the primary cell wall. *Annu. Rev. Plant Physiol. Plant Mol. Biol.* **1989**, *40*, 139–168.

(36) Zykwinska, A. Organization of pectic arabinan and galactan side chains in association with cellulose microfibrils in primary cell walls and related models envisaged. **2007**, *58*, 1795–1802.

(37) Yakushiji, H.; Sakurai, N.; Morinaga, K. Changes in cell-wall polysaccharides from the mesocarp of grape berries during veraison. *Physiol. Plant.* **2001**, *111*, 188–195.

(38) Huang, X.-M.; Huang, H.-B.; Wang, H.-C. Cell walls of loosening skin in post-veraison grape berries lose structural polysaccharides and calcium while accumulate structural proteins. *Sci. Hortic. (Amsterdam).* **2005**, *104*, 249–263.

(39) Albersheim, P.; Darvill, A.; Roberts, K.; Sederoff, R.; Staehelin, A. Plant cell walls (From chemistry to biology). Garland Science: New York, 2010.

(40) Quirós, M.; Morales, P.; Pérez-Través, L.; Barcenilla, J. M.; Gonzalez, R. A new methodology to determine cell wall mannoprotein content and release in wine yeasts. *Food Chem.* **2011**, *125*, 760–766.

(41) Dallies, N.; François, J.; Paquet, V. A new method for quantitative determination of polysaccharides in the yeast cell wall. Application to the cell wall defective mutants of *Saccharomyces cerevisiae*. *Yeast* **1998**, *14*, 1297–1306.

(42) Pellerin, P.; Vidal, S.; Williams, P.; Brillouet, J. M. Characterization of five type II arabinogalactan-protein fractions from red wine of increasing uronic acid content. *Carbohydr. Res.* **1995**, *277*, 135–143.

(43) Vidal, S.; Williams, P.; Doco, T.; Moutounet, M.; Pellerin, P. The polysaccharides of red wine: total fractionation and characterization. *Carbohydr. Polym.* **2003**, *54*, 439–447.

(44) Guadalupe, Z.; Ayestarán, B. Polysaccharide profile and content during the vinification and aging of Tempranillo red wines. *J. Agric. Food Chem.* **2007**, *55*, 10720–10728.

(45) Willats, W. G. T.; Gilmartin, P. M.; Mikkelsen, J. D.; Knox, J. P. Cell wall antibodies without immunization : generation and use of de-esterified homogalacturonan block-specific antibodies from a naive phage display library. *plant J.* **1999**, *18*, 57–65.

(46) Micheli, F. Pectin methylesterases: cell wall enzymes with important roles in plant physiology. *Trends Plant Sci.* **2001**, *6*, 414–419.

(47) Benen, J. A. E.; Van Alebeek, G. J.; Voragen, A. G. J.; De Vries, R. P.; Visser, J. Pectic esterases. In *Handbook of Food enzymology*; Whitaker, J. R.; Voragen, A. G. J.; Wong, D. W. S., Eds.; Marcel Dekker: New York, 2003; pp. 849–856.

(48) Trygg, J.; Wold, S. Orthogonal projections to latent structures (O-PLS). *J. Chemom.* **2002**, *16*, 119–128.

(49) Lu, P.; Hsieh, Y.-L. Cellulose isolation and core–shell nanostructures of cellulose nanocrystals from Chardonnay grape skins. *Carbohydr. Polym.* **2012**, *87*, 2546–2553.

AUTHOR INFORMATION

A. Zietsman collected the data, interpreted the results and drafted the manuscript. J. Moore and M. Vivier designed the study, helped with data interpretation and preparation of the final document. J. Fangel and W. Willats did the CoMPP analysis. J. Trygg advised on multivariate data analysis.

Funding

Funding for this study was provided by the Wine industry network of expertise and technology (Winetech), Technology and Human Resources for Industry Programme (THRIP), Institute for Wine Biotechnology (IWBT), Stellenbosch University, and the National Research Fund (NRF).

SUPPLEMENTARY DATA

S 1.1 Wine fermentation. Table S1 shows the chemical and color characteristics of the juice and the wine as determined during the harvest seasons of 2012 and 2013. The ripeness of the grapes from the two vintages showed a large difference as reflected in the Glc + Fruc (2012: 227 g/L and 2013: 265 g/L) and total acid (2012: 5.37 g/L and 2013: 4.85 g/L) values of the juice. During the 1980s various publications advised different equations for determining the optimum ripeness of wine grapes. Using the Coombe et al.[1] equation (sugar concentration [B°] x pH^2) the viticulturist should aim for a value between 200 and 270 while Du Plessis[2] proposed a sugar:acid ratio (B°: Total Acid in g/L) of four.

Table S1. Chemical properties of Pinotage juice (before yeast inoculation) and the resulting wine at the end of alcoholic fermentation for 2012 and 2013. Colour density (420 + 520 nm) was determined after three months of bottle aging. The values are the average of three biological repeats. Only the volatile acidity of 2012 showed a statistical significant difference between the values and they were marked with letters to indicate the differences (unpaired T-test, 95% confidence interval) between them. Fermented = wine without enzyme addition. ExCol, Expr and CB is wine fermented with the addition of Rapidase® Ex Color, Rapidase® Expression and Rapidase® CB respectively.

		pH		Volatile acidity		Total Acid (g/L)		Gluc + Fruc (g/L)		Ethanol %		Colour density	
2012	Juice	3.28	±0.02			5.37	±0.11	227	±1.42				
	Fermented	3.39	±0.01	0.43[a]	±0.03	6.59	±0.09	1.30	±0.14	14.32	±0.12	11.76	±1.09
	ExCol	3.35	±0.04	0.45[a]	±0.04	6.87	±0.29	1.29	±0.02	14.07	±0.38	12.39	±0.65
	Expr	3.40	±0.02	0.50[b]	±0.01	6.60	±0.14	1.30	±0.11	14.15	±0.10	12.34	±0.68
	CB	3.40	±0.01	0.47[a]	±0.03	6.62	±0.12	1.28	±0.06	14.38	±0.19	12.33	±0.97
2013	Juice	3.71	±0.07			4.85	±0.20	265	±0.96				
	Fermented	3.71	±0.04	0.24	±0.04	4.47	±0.19	3.51	±0.60	14.55	±0.49	9.66	±1.74
	ExCol	3.63	±0.07	0.25	±0.02	4.64	±0.15	3.12	±0.54	13.36	±1.60	8.78	±1.71
	Expr	3.75	±0.04	0.32	±0.04	4.47	±0.16	3.71	±0.38	14.21	±0.48	9.61	±0.71
	CB	3.74	±0.04	0.32	±0.03	4.44	±0.10	3.03	±0.68	13.93	±0.90	9.57	±0.72

Thus, the Pinotage harvested in 2012 meet the criteria with values of 246 and 4.2 respectively while the 2013 Pinotage would be qualified as overripe. However the current opinion of the Pinotage association (www.pinotage.co.za; April 2014) of South Africa recommends a minimum sugar level of 23 B° and that the optimum ripeness for the production of a “fuller style” Pinotage is at sugar levels between 24 and 26 B° with the total acid > 5.5 g/L and pH < 3.7. Both fermentations were fermented dry (< 5 g/L Glc + Fruc) after five and six days respectively with acceptable (0.3 – 0.6 g/L) volatile acidity levels. Furthermore, it is clear that the enzyme treatments did not significantly alter the chemical characteristics (pH, volatile acidity, total acidity, residual sugar and ethanol %) of the wine compared to the control wine of each vintage.

S 1.2 Wine color results. The wine color characteristics were measured to give an indication of the amount of anthocyanins that leached from the grape skin cells during the maceration period. This is an indirect method, in contrast to the other methods used in this article, with which to determine the extent of the permeabilization that occurred in the grape skin cell wall as a result of the action of the maceration enzymes. For the analysis the wine pH was adjusted to pH 3.5 and an excess of acetaldehyde were added to eliminate the bleaching effect of SO_2 after which the absorbance of samples was measured at OD_{420} and $OD_{520.}$ The sum of the measurements is the value for the colour density of the wine.

In a study[3] where the grape phenolics of Pinotage were compared with four other red cultivars (Merlot, Shiraz, Cabernet franc and Cabernet Sauvignon), Pinotage had the highest anthocyanin (mg/g berry) and total phenolics (mg/g berry) content of all five cultivars. When comparing the modified color densities of the wines from the different cultivars, Pinotage had the second highest value (11.65) after Shiraz (12.3), placing it in the “deep red” wine color category. The modified color density of the control wine of 2012 from this study compares well with the results from Du Toit[3] having a modified color density of 11.8, but in 2013 the value for the control wine was only 9.7. According to Fournand and others[4] some cultivars exhibit a decline in anthocyanin content near or after maturity and this can be ascribed to β-glycosidase and peroxidase activity.

For both the 2012 and 2013 vintages, treatment with maceration enzymes did not improve the color density of the resulting wines, with color densities only slightly higher, equal to, or even lower than the control fermentation. This emphasizes the value of the CoMPP method that shows the direct impact of the enzymes on the cell wall composition.

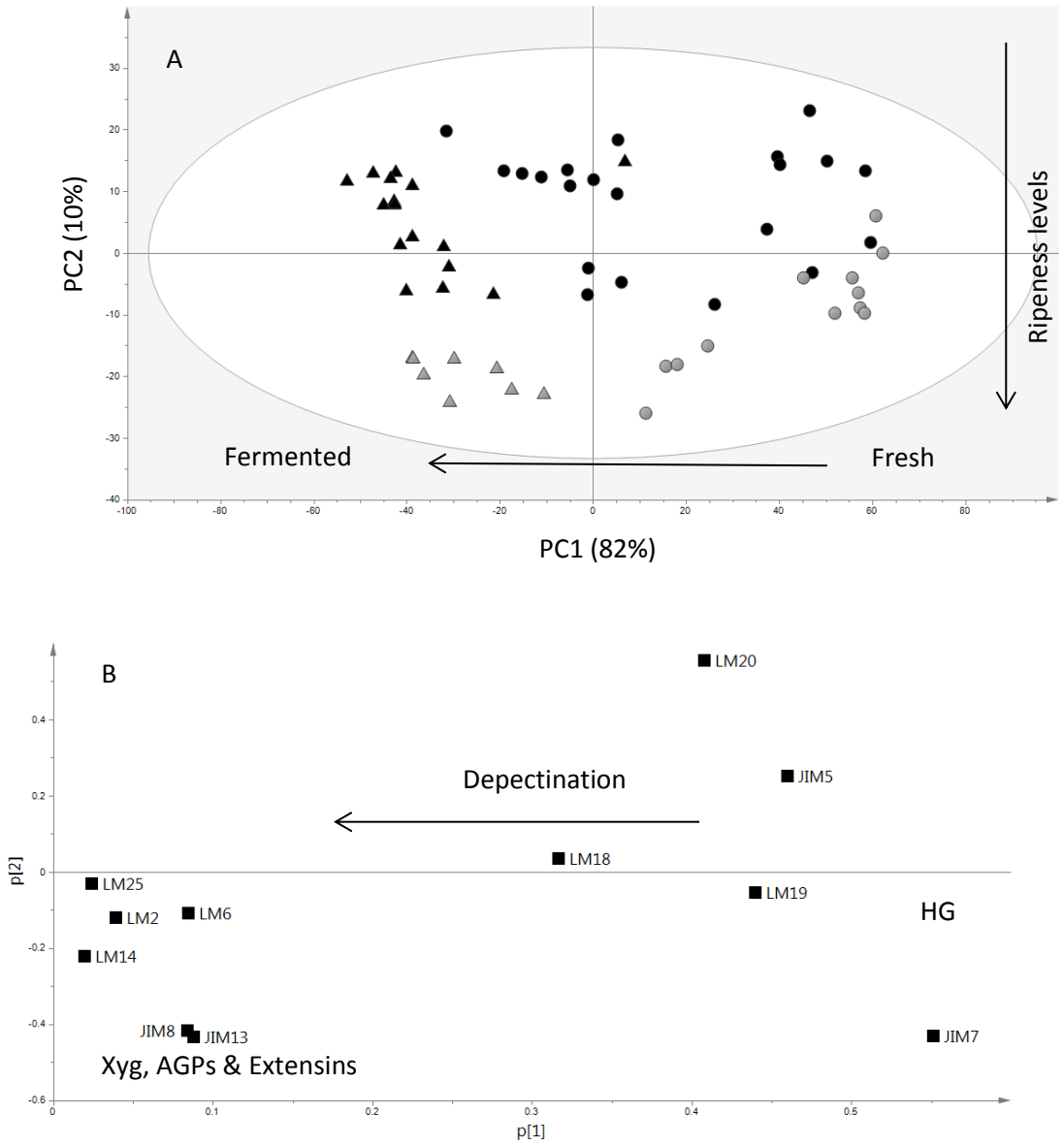

Figure S1. CoMPP results showing the effect that the fermentation has on the cell wall composition in the CDTA fraction;(A) score plot and (B) loading plot. Fresh grape skin cell walls (22.7 °B, 2012, • black circle and 26.5°B, 2013, • grey circle) are compared to fermented (without enzymes) (22.7 °B, 2012, ▲ black triangle and 26.5°B, 2013, ▲ grey triangle) cell walls. Xyg, xyloglucan.

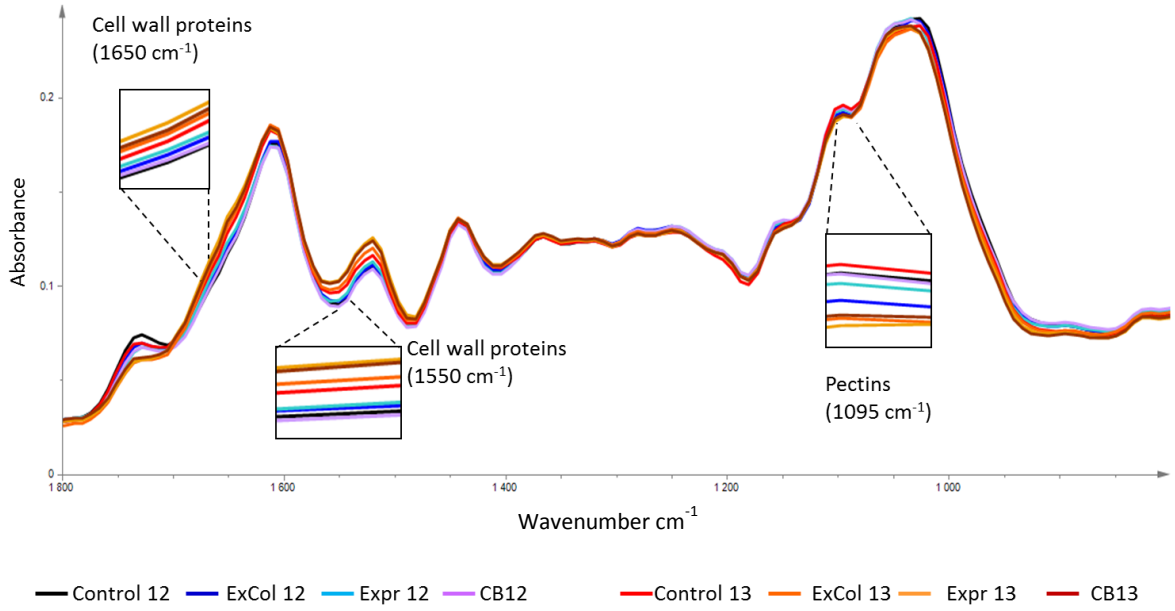

Figure S2. The effect of maceration enzymes on the FT-MIR spectra of the skin cell walls. Similarly to Figure 7 there is an increase in cell wall proteins (exposure on surface of AIR particles) and a decrease in pectins for enzyme treated skins compared to fermented (without enzyme addition) skins. The spectra represent the average absorbance from at least five AIR samples per treatment. Control = Fermented cell wall samples without enzyme addition, ExCol, Expr and CB = Fermented cell wall samples with the addition of Rapidase®ExColor, -Expression and –CB respectively, 12 = 2012 and 13 = 2013.

REFERENCES

(1) Coombe, B. G.; Dundon, R. J.; Short, A. W. S. Indices of sugar-acidity as ripeness criteria for winegrapes. *J. Sci. Food Agric.* **1980**, *31*, 495–502.

(2) Du Plessis, C. . Optimum maturity and quality parameters in grapes: A review. *South African J. Enol. Vitic.* **1984**, *5*.

(3) Du Toit, W. Colour and phenolic characteristics of different clones of Pinot noir, Pinotage, Merlot, Shiraz, Cabernet franc and Cabernet Sauvignon. *Wynboer* **2008**, *September*.

(4) Fournand, D.; Vicens, A.; Sidhoum, L.; Souquet, J.-M.; Moutounet, M.; Cheynier, V. Accumulation and extractability of grape skin tannins and anthocyanins at different advanced physiological stages. *J. Agric. Food Chem.* **2006**, *54*, 7331–7338.

Chapter 4

Research results

Unravelling grape skin and pomace cell walls with enzymes and heat pretreatment

This manuscript will be submitted for publication in the journal
Carbohydrate Polymers

Unravelling grape skin and pomace cell walls with enzymes and heat pretreatment

Anscha J. J. Zietsman[1], John P. Moore[1], Jonatan U. Fangel[2], William G.T. Willats[2], Melané A. Vivier[1*]

[1]Institute for Wine Biotechnology, Department of Viticulture and Oenology, Faculty of AgriSciences, Stellenbosch University, Matieland 7602, South Africa

[2]Department of Plant and Environmental Sciences, Faculty of Science, University of Copenhagen, DK-1001, Denmark

Abstract

Enzymes are used as processing aids to facilitate extraction of compounds from grapes and need to effectively act on the cell walls of berry skin and pulp. Cell walls from fresh, ripe, red berry skins, as well as crushed berry pomace were hydrolysed with different pure and commercial enzymes in buffered conditions. Cell wall profiling techniques were used to monitor the compositional changes in the grape cell wall polymers during enzyme hydrolysis and heat-pretreatment. Extensive enzymatic hydrolysis, achieved with a mixture of pectinases, cellulase and hemicellulase enzymes, completely removed or reduced levels of pectin polymers but less extensive hydrolysis only opened up the cell wall structure and allowed extraction of polymers from within the cell wall layers. Heat pretreatment had a similar depectination effect but it also uncovered xylan polymers. The sequence in which cell wall polymers could be extracted and the role that specific enzymes played in facilitating the extraction enabled us to form a picture of the accessibility of specific cell wall polymers and demonstrated enzyme synergism.

Keywords: Cell wall polymer, Grape berry, Grape pomace, Enzyme, Pretreatment

Contact information for Corresponding Author

Melané A. Vivier, Institute for Wine Biotechnology, Department of Viticulture and Oenology, Faculty of AgriSciences, Stellenbosch University, Matieland 7602, South Africa, Tel. +27 21 808 3773, Fax +27 21 808 3771, mav@sun.ac.za

1. Introduction

Enzymes are important processing tools when utilizing plant material in the feed and food, paper and pulp, biofuel or biopharmaceutical industries (Mabee et al., 2010; Sieiro et al., 2010; Singh et al., 2014). The plant resources either need to be made accessible to extract desired compounds and/or processed directly to form a product (Alvira et al., 2010; Hendriks et al., 2009). Typically, the role of the enzymes is to disrupt the cellular structures of the plant material, specifically acting on the plant cell walls. These are highly complex structurally and chemically, but also dynamic and under control of both developmental and environmental signals (Keegstra, 2010). This may explain the frequent observation that enzymes used in industries reliant on plant material, do not always deliver the desired effect, due to inherent batch and/or seasonal variability of the starting material (Himmel et al., 2007; Ortega-Heras, Pérez-Magariño, & González-Sanjosé, 2012).

In the wine industry hydrolytic enzymes are used to degrade the grape berry cell walls to release aromatic and phenolic compounds that are important contributors towards wine quality, as well as reduce cell wall components such as pectins to aid processing of the wines (Romero-Cascales, Ros-García, López-Roca, & Gómez-Plaza, 2012). A by-product of the wine-making process is the pomace, essentially made up of skins with some pulp, seeds and stalks (Yu et al., 2013). This by-product has several uses and enzymes have the potential to support the harvesting of revenue-generating compounds (e.g. nutraceuticals, antioxidants) from grape pomace, or using pomace as biomass (Nerantzis et al., 2006; Rodríguez et al., 2010) in the production of bioethanol. All these processes could still be significantly improved with more comprehensive knowledge and understanding of the structure and composition of grape berry cell walls to select the most appropriate (mixture of) enzymes and the industrial conditions to favour the desired reaction.

The aim of this study was to evaluate the impact of enzymes on the berry cell wall matrix by focusing on enzymes as fermentation supplements for quality wine production, as well as processing aids in pomace “deconstruction”. Factors that can affect the extent of enzyme hydrolysis of grape tissue, such as the type of enzyme, the enzyme-substrate ratio, the time and temperature of the reaction, inhibition by the substrate and the incorporation of a pre-treatment step when processing pomace, are some of the factors that were previously investigated (Chamorro et al., 2012; Kammerer et al., 2005; Maier et al., 2007; Meyer et al., 1998; Xu et al., 2014). It was found that commercial wine enzyme preparations (Fia et al., 2014; Romero-Cascales et al., 2008) that are marketed for specific applications do not always have the optimal enzymatic profile. Furthermore, grape berry cell walls of certain cultivars (Ortega-Regules et al., 2008; Xu et al., 2014) are quite recalcitrant to enzyme hydrolysis. Better extraction of

polyphenols are observed if a pretreatment step is included and/or a combination of enzymes is used (Alvira et al., 2010; Kammerer et al., 2005; Maier et al., 2007). It was previously speculated that the natural pore size (between 4 and 10 kDa) of the grape cell wall (Hanlin et al., 2010) excluded most hydrolytic enzymes from entering (Fleischer et al., 1999; Jarvis, 2011) the cell wall and reaching their targets.

Most studies that investigate the success of enzymes in wine preparation or pomace processing, focus on measuring the release of the desired compounds (Arnous et al., 2010; Xu et al., 2014). This is then used to infer information regarding the grape berry cell wall matrix and its deconstruction, without studying the cell wall residues, or the changes to the composition of the cell wall. Our study had as focus the grape berry cell wall deconstruction process as influenced by enzymes and studied the cell wall directly. We investigated the effect of hydrolytic enzymes (different types and combinations) on isolated cell walls from Pinotage grape skins and on Chardonnay pomace. Pinotage is a thick-skinned, red wine cultivar with relatively high levels of polyphenolics (Goussard, 2008; May, 2009) and used for quality wine production. Cell walls from this cultivar were used to evaluate how enzymes deconstruct berry cell walls under ideal (temperature and pH) conditions, with potential impacts on quality and wine processing. The Chardonnay pomace was used to study how the enzymes degrade this matrix and how autoclaving, as a pretreatment, change the matrix encountered by the enzymes. Chardonnay has thin berry skins (Goussard, 2008; Serratosa et al., 2014) and the Chardonnay pomace was derived from just-pressed grapes, as is typical for most white wine fermentations. With this analysis we aimed to shed light on how enzymes change the cell wall composition on a polymer level by using established cell wall profiling tools viz. Comprehensive Microarray Polymer Profiling (CoMPP) coupled with monosaccharide compositional analysis. (Fangel, 2013; Moore et al., 2014; Nguema-Ona et al., 2012; Pedersen et al., 2012). From our results we could see a clear distinction between extensive and moderate enzymatic hydrolysis and specific synergistic relationships between enzymes were detected. We could also document for the first time, to our knowledge, the cell wall changes that occur in grape tissue due to heat pretreatment, a common practice in pomace valorisation used to reduce the grape tissue recalcitrance.

2. Materials and methods

2.1 Pinotage skin cell wall preparation.

Vitis vinifera cv Pinotage grapes were harvested in 2012 in the Boland wine producing area of South Africa. The sugar concentration of the grapes were established to be 22.7 °B by using Fourier transform infrared (FT-IR) spectroscopy with a WineScan™ FT120 Basic (FOSS

Analytical,Hillerød, Denmark). Three random juice samples (50 ml each) were generated from the harvested grapes and the FT-IR scans were done in duplicate per sample. Berries were sampled from bunches randomly selected from different harvest crates and the berries were picked from the top, middle and bottom of a bunch. The grapes were frozen at -20°C before the skins were manually peeled with a scalpel and flash frozen with liquid nitrogen in twenty 10 g (wet weight) batches. The frozen skins were kept at -80°C and then freeze-dried. The freeze-dried skins were dry milled and homogenized with a Retsch MM400 mixer mill (Retsch, Germany) at 30 Hz for 30 seconds and from the resulting powder, the cell wall or alcohol insoluble residue (AIR) was extracted. The AIR extraction method described by Ortega-Regules et al. (2008) was followed except that the first acetone step after the buffered phenol extraction was omitted and after the third acetone wash, the AIR was air-dried, mixed with an equal volume of MilliQ water, frozen at -80°C and then freeze-dried and stored until further analysis.

2.2 Enzymatic hydrolysis of Pinotage AIR using purified enzymes.

A representative sample of AIR was obtained by mixing together 200 mg from each of the twenty AIR samples. From this pooled sample, 50 mg were used per reaction or biological repeat. The AIR was suspended in citrate phosphate buffer, pH 5 to form a 7.5 % (w/v) suspension and sodium azide was added at a final concentration of 0.02 % (w/v). The enzymes used in the experiment (Pect, EPG, EG, EA and XG) are described in Table 1. A Thermo Scientific™ Pierce™ BCA™ Protein Assay (Thermo Fisher Scientific Inc., USA) kit was used to determine the protein concentration of each enzyme. A dosage of 180 U/g dry matter of pectinase containing enzymes (Pect and EPG) and 40 U/g of all other enzymes (EG, EA and XG) were added individually or in combinations (EPG-EG; EPG-EG-EA; Pect-XG; Pect-EG). The reactions, performed in triplicate, were incubated at 40 °C for 48 h, where after the residual solids were washed with sterile distilled water, and finally freeze-dried.

2.3 Chardonnay pomace preparation

Vitis vinifera cv Chardonnay grapes were harvested in the Boland region of South Africa and the pomace was obtained after the grapes were pressed with a hydraulic press (pressure not exceeding 1.5 bar). The moisture content of the Chardonnay pomace samples were 97.4 %, using the method described in (Özcan, 2006). The pomace was thoroughly mixed and randomly divided into three batches and kept at -20 °C until processed for sample preparation.

For analyses, sample preparation entailed manual seed removal and blending of the pomace with a stick blender. To evaluate the impact of a processing step such as heat pretreatment on the cell wall profile of pomace, five 10 g (wet weight) samples were freeze-dried and another five were autoclaved (121°C, 15 min, 100 kPa) before freeze-drying. These samples were stored until AIR isolation. For enzyme analysis the deseeded, and blended pomace pulp was mixed with a 0.12 M citrate phosphate buffer (pH 5 for purified enzyme analyses and pH 3 for commercial enzymes) to form a 15 % (wet weight/v) suspension and autoclaved (121°C, 15 min, 100 kPa) to inactivate the native grape and microbial enzymes. These suspensions were then used for the various enzyme treatments described below.

Table 1: Purified and commercial enzymes used in this study**.**

	Name	Supplier	Catalogue name	Description	Declared activity
Purified enzymes	Pect	Sigma-Aldrich	Pectinase	**Pectolytic** enzyme preparation: contains mainly pectintranseliminase, polygalacturonase, pectin esterase and small amounts of hemicellulases and cellulases.	19 U/mg
	EPG	Megazyme	E-PGALS	**Endo-polygalacturonase** from *A. niger* , contains minor levels of endo-galactanase, endo-arabinase, pectin transeliminase, arabinofuranosidase and b-galactosidase activity.	280 U/mg protein, polygalacturonic acid as substrate
	EG	Megazyme	E-CELTR	**Endo-1,4-β-glucanase** with minor levels of endo-1,4-β-xylanase, endo-1,4-β-mannanase, α-glucosidase, β-glucosidase, β-xylosidase, α- and β-galactosidase, β-mannosidase and α-L-arabinofuranosidase activities.	19 - 71[a] U/mg, assumed 40 U/mg for this study
	XG	Megazyme	E-XEGP	Xyloglucan-specific **endo-1,4-β-glucanase**, recombinant enzyme.	104 U/mg
	EA	Megazyme	E-EARAB	**Endo-arabinase** with α-L-arabinofuranosidase < 0.01% (on beet arabinan); endo-galactanase < 0.01%.	15 U/mg
Commercial enzymes	Cellc	Novozymes	Celluclast ® 1.5L	**Cellulase**, hydrolysing β-1,4-D-glucosidic linkages.	700 EGU/g (endoglucanase units)
	ExCol	DSM	Rapidase® ExColor	**Pectolytic** enzyme with additional hemicellulases, negligible levels of anthocyanases and cinnamyl esterases.	No information available
	Expr	DSM	Rapidase® Expression	**Pectolytic** activities with arabinase and rhamnogalacturonase, negligible levels of cinnamyl esterase.	No information available

[a] Depending on substrate

2.4 Enzymatic hydrolysis of Chardonnay pomace with commercial enzymes

The autoclaved pomace suspension in 0.12 M citrate phosphate buffer pH 3 was used. The commercial enzymes used in the experiment were Celluclast® 1.5L, Rapidase®ExColor and R

apidase®Expression (Table 1). Factorial experimental design (MODDE software, Umetrics, Sweden) was used to design a preliminary experiment to optimize the pH (pH 3, pH 4.5 or pH 6), temperature (15 °C, 32.5 °C or 50 °C), enzyme loading (25 000 ppm or 50 000 ppm) and enzyme combinations that gave the best results (measured as level of methanol produced, results not shown). Other methods to determine the degree of cellulosic biomass degradation, such as the fluorescent cellulose decay assay by Wischmann et al. (Wischmann et al., 2012) and the Congo red/polysaccharide complex method by Woods et al. (Wood et al., 1988), were tried, but gave unreliable/unreproducible results under our conditions. The six conditions that produced the highest levels of methanol were chosen for the subsequent experiment and the experimental layout (enzyme combinations and incubation conditions) are shown in Table 2. Enzymes were filter sterilised (0.25-micron pore size) and added to the suspension and the different hydrolysis reactions were done in triplicate at 15 or 50 °C for 72 h. After enzyme hydrolysis the supernatant and the residual pellet were separated with centrifugation and frozen at -20 °C until further analyses of supernatants or AIR extraction from the solid residue.

Table 2: Experimental layout of Chardonnay pomace incubated with commercial enzymes. The enzymes are described in Table 1.

	ppm				
Sample	**Cellc**	**ExCol**	**Expr**	**°C**	**pH**
Control15	0	0	0	15	3
ExCol15	0	50000	0	15	3
Expr15	0	0	50000	15	3
Cellc, ExCol, Expr15	50000	50000	50000	15	3
Control50	0	0	0	50	3
Cellc, ExCol50	50000	50000	0	50	3
Cellc, Expr50	50000	0	50000	50	3
ExCol, Expr50	0	50000	50000	50	3

2.5 Characterizing the supernatant of the Chardonnay pomace incubated with commercial enzymes.

The methanol concentrations and the levels of reducing sugars that were released in the supernatant of the Chardonnay samples that were incubated with commercial enzymes were determined according to the GC-FID method described in Louw et al. (2010) and the method

published by Miller (1959), respectively. The assays were performed in duplicate for each biological repeat.

2.6 Enzymatic hydrolysis of Chardonnay pomace with purified enzymes

The prepared and autoclaved pomace, suspended in 0.12 M citrate phosphate buffer pH 5 was used to evaluate the impact of purified enzymes on the cell walls of this matrix. Filter sterilized purified enzymes (Pect, EPG, EG, EA and XG, Table 1) were added to the suspension individually or in combinations (EPG-EG; EPG-EG-EA; Pect-XG; Pect-EG). For the pectinase containing enzymes (Pect and EPG) 180 U/g dry matter was added and 40 U/g of all other enzymes (EG, EA and XG) were added. The enzyme hydrolysis treatments as well as a control sample (pomace suspension with no enzyme added) were done in triplicate. After incubation at 40 °C for 48 h, the supernatants and residual pellets were separated with centrifugation and the pellets were freeze-dried and stored at room temperature until further analyses.

2.7 Cell wall isolation from hydrolysed Chardonnay pomace

The freeze-dried pellets containing the solid residues from the enzyme hydrolysis treatments (both the purified and the commercial enzyme treatments) were milled and homogenized with a Retsch MM400 mixer mill (Retsch, Germany) at 30 Hz for 30 seconds. The cell walls (AIR) were isolated from the resulting powder as described in Ortega-Regules et al. (2008) with a few exceptions: The first acetone step after the buffered phenol extraction was omitted and after the third acetone wash, the AIR was air-dried, mixed with an equal volume of MilliQ water, frozen at -80°C and then freeze-dried and stored until further analysis.

2.8 Cell wall profiling of AIR samples.

The monosaccharide composition of the AIR isolated, after enzyme hydrolysis, was analysed following the method of Nguema-Ona et al. (2012) with a few modifications. Briefly, 5 mg of AIR was hydrolysed to monosaccharides using trifluoroacetic acid (TFA), followed by derivatization to methoxy sugars at 80 °C for 16 h. After silylation with HMDS + TMCS + Pyridine 3:1:9 (Sylon HTP) kit (Sigma-Aldrich, MO, USA) the derivatives were analysed in a gas chromatograph, Agilent 6890 N (Agilent Technologies, CA, USA) coupled to a Agilent 5975 MS mass spectrometer detector, using a polar (95% dimethylpolysiloxane) ZB-Semivolatiles Guardian (30 m, 0.25 mm ID, 0.25 µm film thickness) GC column. The oven temperature was maintained at 70 °C for 2 min, ramped at 1 °C/min to 76 °C, then at 8 °C/min to 300 °C and then held for 5 min. The monosaccharide composition was expressed as pM/mg AIR. Each biological repeat

was analysed twice and standard deviations in the tables represent the average of three biological samples.

One sample for each biological repeat (enzyme hydrolysis reaction) was analysed with the CoMPP technique. CoMPP analysis entails the sequential extracted of the pectin- and hemicellulose-rich fractions from 10 mg AIR per sample, using the solvents CDTA (diamino-cyclo-hexane-tetra-acetic acid) and NaOH respectively according to the procedure described in Moore et al. (2014). Arrays printed with the different fractions were probed individually with 26 different monoclonal antibodies (mAbs) and carbohydrate binding modules (CBMs) as previously described (Moller et al., 2007). The probes that were used are listed in Table A1 in the appendix. A mean spot signal was calculated where after it was normalized to the highest signal (set as 100) in the dataset and a cut-off value of five was used.

2.9 Univariate and multivariate data analysis.

Statistical significant differences in the results were determined by using the unpaired T-Test (95% confidence level). The patterns within the data were investigated with principle component analysis (PCA) (Jackson, 1991) and partial least squares projections to latent structures (PLS) (Eriksson et al., 2013) using SIMCA 13 software (Umetrics, Sweden).

3. RESULTS

3.1 The evaluation and profiling of the hydrolysis of fresh berry cell walls with purified enzymes by using CoMPP and monosaccharide compositional analyses

The cell walls or AIR isolated from fresh Pinotage grape berry skins sampled at the ripe stage were incubated with a collection of purified enzymes (Table 1) under buffered conditions favouring the enzymes (pH 5, 40 °C) to evaluate the (maximum) potential and impact of hydrolysis on this matrix. By using isolated cell walls as substrate, we aimed to eliminate any potential interfering substances (e.g. high sugar concentrations, phenolics, tannins and organic acids present in grape juice) and improve the accessibility of enzymes to the target polysaccharides. The enzymes were chosen to degrade different polysaccharide targets, namely pectins, celluloses and hemicelluloses and the purified enzyme preparations exhibited these main activities, although most (except the xyloglucanase) also contained some lesser side activities (Table 1).

The enzymatically hydrolysed AIR was analysed using CoMPP analysis and the results in the heat map (Fig. 1) shows the relative abundance of a specific cell wall polysaccharide, depicted as a percentage of the whole dataset. Overall, the analysis showed that the CDTA fraction of

the control samples (no enzyme added) contained mostly pectin type polymers (Fig. 1), but there was also xyloglucan (mAb LM25), arabinogalactan proteins (AGPs) and extensins present, as expected. The second extraction with NaOH dissolved mainly hemicelluloses but also contained cellulose (mAb CBM3a) and some unbranched RG-I. In all the reactions where the Pect enzyme was involved (CDTA fraction) there was a drastic decrease in the values for homogalacturonan (HG) epitopes (mAbs JIM5 and JIM7, LM19 and to a lesser degree LM18) compared to the control samples. This indicated that the HG polymers were probably degraded into smaller oligosaccharides, which could diffuse out from within the AIR particles, into the incubation buffer and were subsequently removed at the end of the enzyme incubation period. The HG with very low methylesterification, recognized by mAb PAM1, was an exception with the values staying more or less stable with or without enzyme addition. There was also a complete removal of rhamnogalacturonan-I (RG-I) (mAbs INRA-RU1 and INRA-RU2) and xyloglucan (mAb LM25). The presence of xyloglucan (mAb LM25) in the pectin fraction and the concomitant removal of the xyloglucan and pectin polymers in the Pect treated samples may be a confirmation of the xyloglucan-pectin association found in grape (Vidal et al., 2003) and other plant cell walls (Popper et al., 2008).

All the other enzymes (EPG, EG, EA, XG and combination of these) nearly doubled the levels of HG (specifically mAbs JIM5 and JIM7) that could be extracted with CDTA from the AIR (Fig. 1). The XG treatment delivered the highest values in HG (mAbs JIM5, JIM7, LM18, and LM19) compared to the control samples, possibly indicating that the hydrolysis of the xyloglucan that cross-links the cellulose microfibrils has an influence on the release of polymers from within the cell wall. The levels of unbranched RG-I (mAbs INRA-RU1 and INRA-RU1), xyloglucan (mAb LM25) and AGPs (mAb JIM13) were not altered by these enzymes (in contrast with Pect).

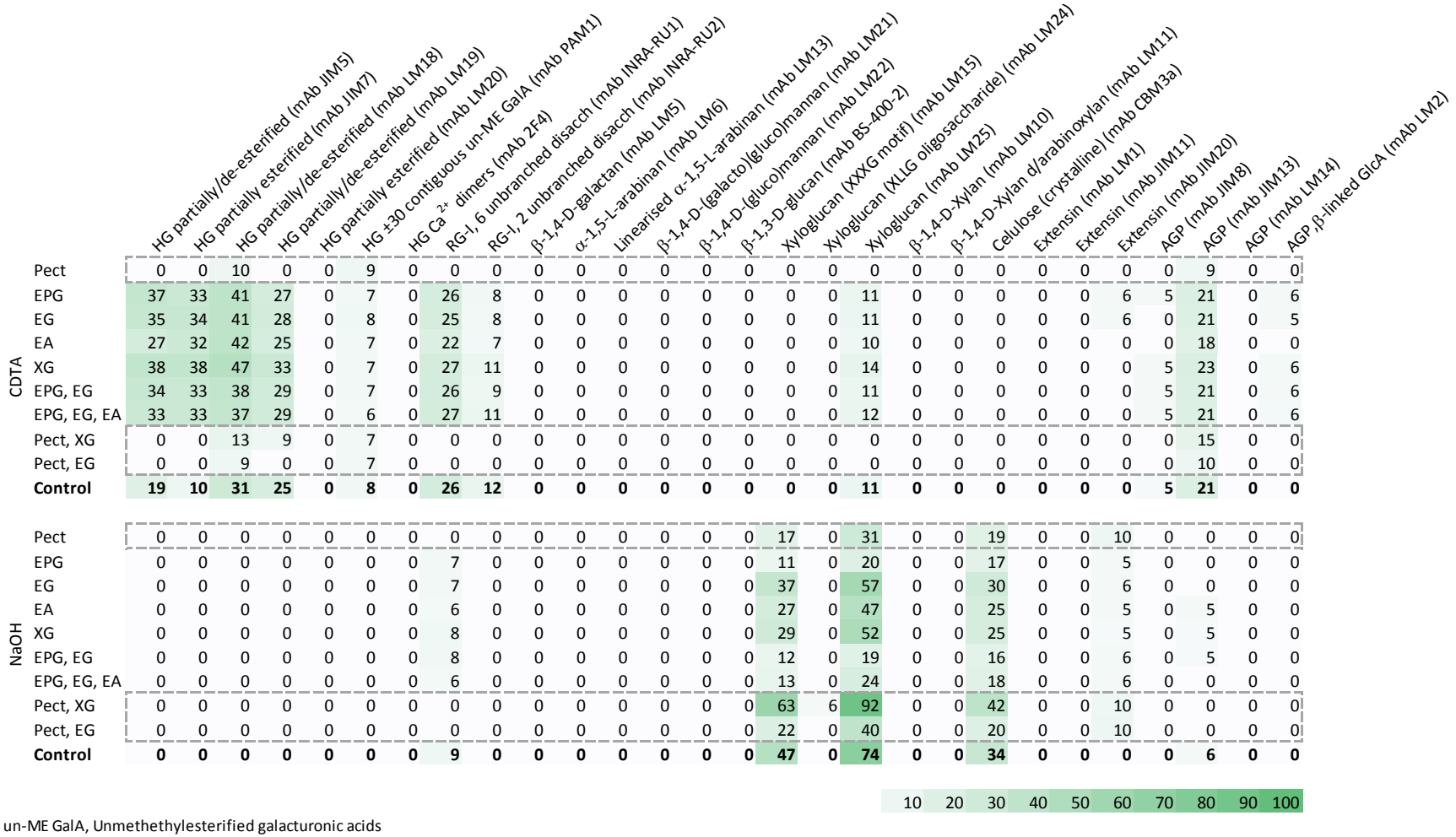

un-ME GalA, Unmethethylesterified galacturonic acids

Figure 1. CDTA and NaOH fractions extracted from Pinotage skin AIR hydrolysed with pure enzymes, showing the relative abundance of the different epitopes. The boxed sections indicate enzymes that caused extensive enzymatic hydrolysis. Values are the average of three biological samples. The enzymes that were used are described in Table 1 and the monoclonal antibodies are listed in the appendix (Table A1).

Although all of the mAb INRA-RU2 labelled RG-I were removed, either by enzyme hydrolysis or during CDTA extraction, low quantities of mAb INRA-RU1 labelled RG-I could be extracted with NaOH (Fig. 1). This is seen in the control as well as the EPG, EG, EA and XG treated .The major epitopes recognized in the NaOH fraction were xyloglucan (mAbs LM15 and mAbs LM25), cellulose (mAb CBM3a) and extensins (mAb JIM20). A synergistic relationship was seen with the Pect-XG combination where the XG enzyme could cause an increase in the extraction of xyloglucan only when combined with the depectination action of Pect. The other enzymes all decreased the xyloglucan signals presumably by removing some surface exposed, pectin-associated xyloglucan due to pectin hydrolysis (EPG, Pect and Pect-EG) or by direct xyloglucan hydrolysis (XG). All enzyme treatments increased the signal for extensins (mAb JIM20) compared to the control.

The monosaccharide compositional analysis of the AIR samples after enzyme hydrolysis revealed some interesting results (Table 3). Compared to the control samples, Pect-XG hydrolysis led to a decrease (statistically significant, 95 % confidence interval) in Ara while Pect-XG and Pect-EG decreased the Rha values. This corresponds well with the decrease in unbranched RG-I and AGPs (CoMPP analysis, Fig. 1) of the Pect enzyme treated samples. In addition, the Pect and Pect combination treatments caused a decrease in GalA which can be attributed to depectination and this is confirmed by the decrease in the signal for all the HG polymers (except mAb PAM1). In contrast, all the other enzymes caused an increase in GalA monosaccharides. An increase (compared to the control samples) in the monosaccharide concentration is only possible if we consider that incomplete TFA hydrolysis took place during the preparation steps prior to GC-MS monosaccharide analysis.

Table 3: Monosaccharide composition of Pinotage AIR treated with different enzymes and enzyme combinations. The values are the averages of three samples. Samples that are statistically different (95 % confidence level) from the control are shaded in grey. Ara, arabinose; Rha, rhamnose; Fuc, fucose; Xyl, xylose; GalA, galacturonic acid; Man, mannose; Gal, galactose; Glc, glucose; GlcA, glucuronic acid.

	pM/mg AIR																	
	Pect		EPG		EG		EA		XG		Pect		EPG+EG+EA		Pect+XG		Pect+EG		Control	
Ara	52	± 9	78	± 28	103	± 10	71	± 17	102	± 7	89	± 25	56	± 25	36	± 10	48	± 6	**73**	± 5
Rha	25	± 3	37	± 4	42	± 3	40	± 6	42	± 3	38	± 6	35	± 6	21	± 3	23	± 2	**35**	± 3
Fuc	31	± 3	28	± 3	32	± 2	30	± 5	31	± 3	29	± 5	28	± 5	26	± 6	29	± 3	**32**	± 2
Xyl	77	± 17	64	± 8	80	± 5	66	± 7	79	± 5	65	± 20	51	± 20	52	± 20	74	± 15	**74**	± 6
GalA	123	± 22	381	± 44	440	± 43	366	±35	452	± 33	435	± 62	294	± 9	72	± 22	100	± 29	**226**	± 10
Man	36	± 5	28	± 2	34	± 2	29	± 2	33	± 2	29	± 6	25	± 6	28	± 8	34	± 5	**34**	± 1
Gal	39	± 6	39	± 5	48	± 3	40	± 7	46	± 2	40	± 8	33	± 8	30	± 11	34	± 11	**45**	± 2
Glc	39	± 6	32	± 2	40	± 2	33	± 3	38	± 0	33	± 7	27	± 7	31	± 9	37	± 4	**39**	± 2
GlcA	41	± 5	88	± 20	80	± 7	64	± 9	91	± 14	74	± 41	54	± 41	30	± 7	36	± 3	**53**	± 11

This incomplete acid hydrolysis took place in the control samples but in contrast, the AIR treated with EPG, EG, EA and XG were already partially hydrolysed or unravelled. This led to a more complete acid hydrolysis by allowing better access for the TFA, delivering higher quantities of monosaccharides than the control samples. This unravelling and rendering of access to the inner cell wall spaces by the action of the EPG, EG, EA and XG enzymes were also demonstrated with the CoMPP results (Fig. 1). In the case of the Pect treated samples, the enzymatic hydrolysis already removed a large fraction of the pectin cell wall polymers (HG and RG-I) and the remaining residue thus contained less GalA. For this to be true we have to presume that complete acid hydrolysis could take place in the Pect samples by virtue of the extensive enzymatic degradation/unravelling.

Multivariate data analysis of monosaccharide composition of the samples reveals (PCA plot, Fig. 2) the Pect treated samples clustering together at the bottom of the plot. The control samples formed a second group in the middle and the rest of the samples were spread out along the top half of the plot. The spread of all the samples along the first component axis (PC1 69 %) illustrates the variation in the efficiency of the TFA hydrolysis which led to differences in the monosaccharide values (pM/mg AIR) recorded. Further analysis (shown in Appendix, Fig. A1 and A2) using a Partial Least Squared (PLS) (Eriksson et al., 2013) plot (Fig. A1) and Variable Importance for the Projection (VIP) plot (Fig. A2) showed that Pect treated samples separated from the other samples due to a scarcity in GalA and Rha.

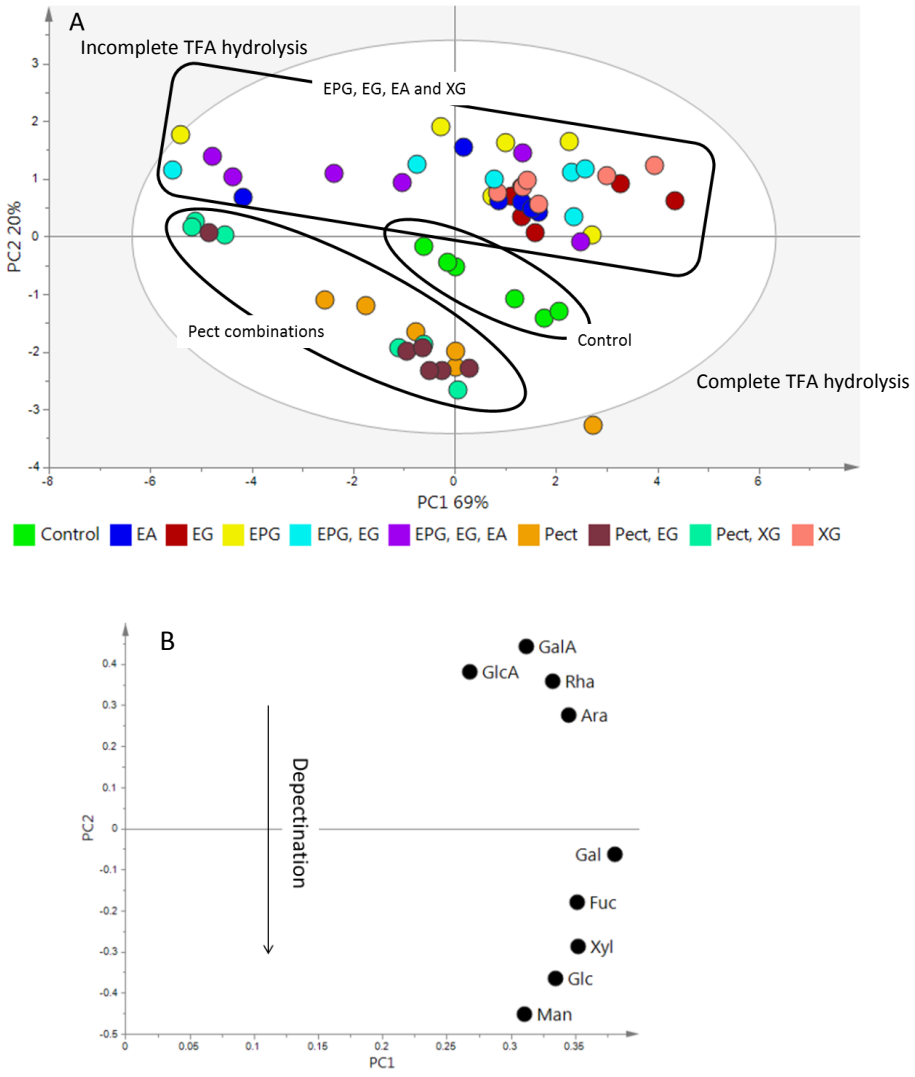

Figure 2. PCA score (A) and loading (B) plot of monosaccharide analysis on Pinotage AIR treated with pure enzymes. The enzymes are described in Table 1.

3.2 The evaluation and profiling of the hydrolysis of Chardonnay pomace cell walls with purified and commercial enzymes by using CoMPP and monosaccharide compositional analyses.

3.2.1 Autoclaving as a pre-processing step removes pectin and exposes xylan in the cell walls of Chardonnay pomace

The preparation of the Chardonnay pomace involved an autoclaving step in order to destroy the endogenous grape tissue enzymes as well as any microbial enzymatic activity present on the pomace. It also gave us the opportunity to investigate how the autoclaving step, which is to a certain extent similar to the industrial hot water/steam pre-treatment of lignocellulosic biomass (Alvira et al., 2010), changes the cell wall polymers. The autoclaving step had a considerable impact (Fig. 3) on the composition of the cell walls as it removed HG (mAbs JIM5, JIM7, LM18,

LM19, LM20) and uncovered RG-I side chains (mAb LM6) and AGPs (mAbs JIM8 and JIM13) in the CDTA fraction. In the NaOH fraction it enhanced the extraction of HG (mAbs LM18 and LM19), RG-I side chains (mAbs LM5 and LM6), mannan (mAb LM21 and LM22) and AGPs (mAbs JIM8 and JIM13). The most interesting result however, is the high level of xylan polymers (mAbs LM10 and LM11) extracted from the autoclaved samples (Fig 3, NaOH fraction).

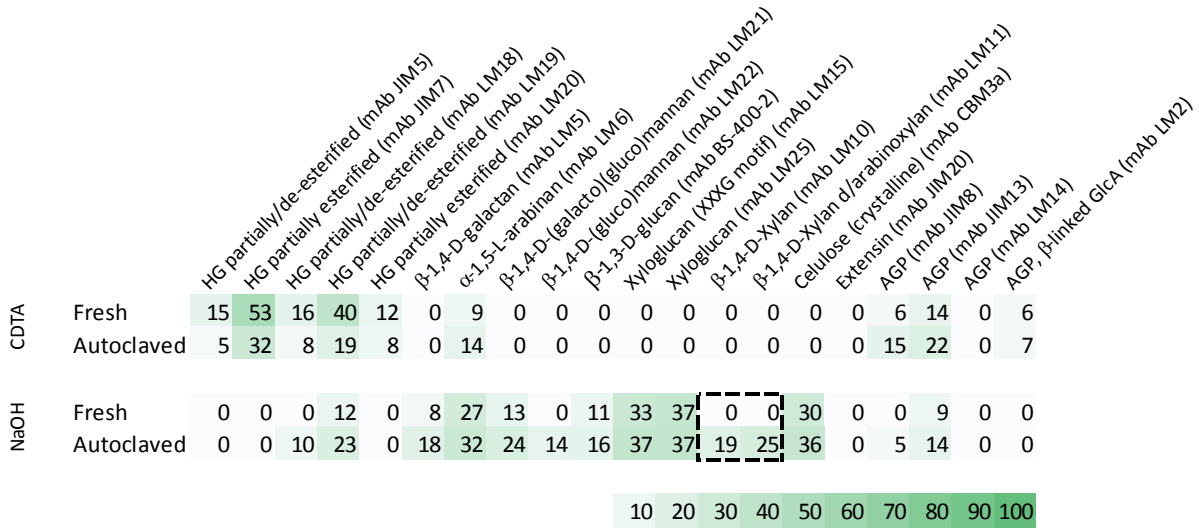

Figure 3. The relative abundance of the cell wall polymers of fresh and autoclaved Chardonnay pomace, demonstrated with CoMPP analysis. The boxed section indicates the exposure of xylan. The values are the averages of five biological repeats.

3.2.2 Investigating the cell wall polymers of Chardonnay pomace, using commercial maceration enzymes

In this investigation, we incubated autoclaved Chardonnay pomace with commercial enzymes in order to form a general picture on how these enzymes would change the cell wall polymer composition. The enzymes used in this experiment are listed in Table 1 and the best enzyme combinations and loadings as well as the incubation conditions (Table 2) were determined in an initial multi-factorial designed experiment (Modde software, Umetrics, Sweden) (results not shown). The Rapidase® ExColor (ExCol) and -Expression (Expr) enzymes contained mostly pectinases and the Celluclast® 1.5L (Cellc) degrades β-1,4-D-glucosidic links as found in cellulose and xyloglucan. After enzymatic hydrolysis the turbidity, pH, methanol concentration and reducing sugars were measured in the supernatant of the samples and the results are shown in the appendix (Table A2).

The cell walls were isolated from the residue collected after enzymatic hydrolysis and analysed with CoMPP (Fig. 4). In the absence of commercial enzymes (control samples) we detected some HG (mAb JIM7, LM18 and LM19) and unbranched RG-I (mAb INRA-RU1 and INRA-RU2), β-1,4-D-galactan (mAb LM5), xyloglucan (mAb LM25 only), extensins (mAb JIM20) and

AGPs (mAb JIM13, LM14 and LM2) in the CDTA fraction. At 50 °C there was slightly less HG (mAb JIM7), RG-I (mAb INRA-RU1), β-1,4-D-galactan (mAb LM5) and AGPs (mAb JIM13) than at 15°C. This decrease might be due to acidic hydrolysis that took place in the low pH buffer (pH3) at the higher temperature and corresponds with the decrease in pH seen for these samples (Table A2). The enzyme action in all samples supplemented with commercial enzymes and at both temperatures (Fig. 4), reduced all exposed and CDTA-dissolvable pectin or other polymers that might be associated with pectin, such as xyloglucan. At 50°C, all the enzyme combinations removed virtually all extensins and AGPs too, except those recognized by mAb JIM13, which were only reduced by half. This was also true for the three-enzyme combination (Cellc, ExCol, Expr) at 15° C, but Expr at 15° C had no effect while ExCol caused a reduction in AGPs (mAb JIM8, JIM13 and LM2) and extensins (mAbJIM20).

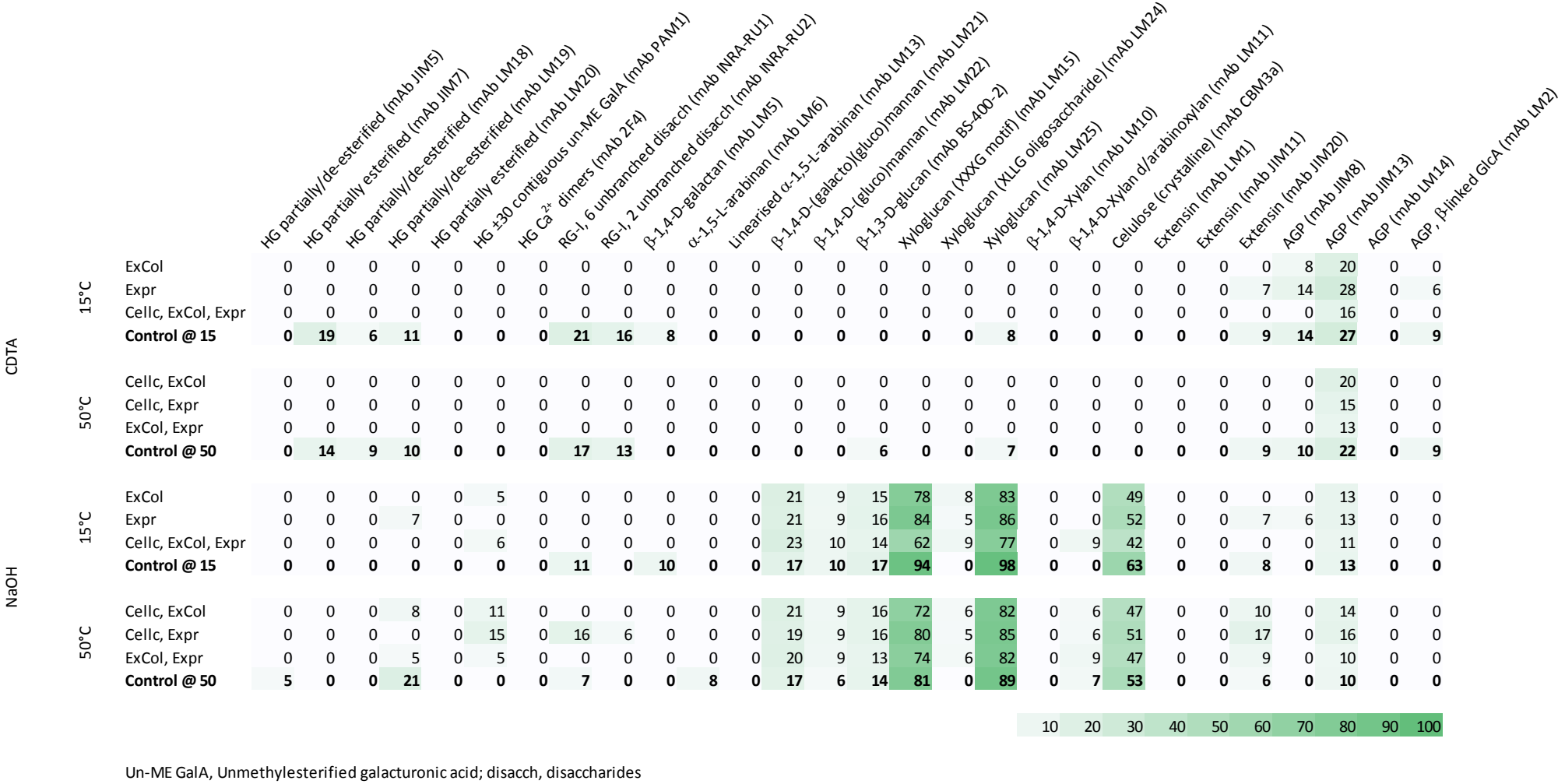

			HG partially/de-esterified (mAb JIM5)	HG partially esterified (mAb JIM7)	HG partially/de-esterified (mAb LM18)	HG partially/de-esterified (mAb LM19)	HG partially esterified (mAb LM20)	HG ±30 contiguous un-ME GalA (mAb PAM1)	HG Ca^{2+} dimers (mAb 2F4)	RG-I, 6 unbranched disacch (mAb INRA-RU1)	RG-I, 2 unbranched disacch (mAb INRA-RU2)	β-1,4-D-galactan (mAb LM5)	α-1,5-L-arabinan (mAb LM6)	Linearised α-1,5-L-arabinan (mAb LM13)	β-1,4-D-(galacto)(gluco)mannan (mAb LM21)	β-1,4-D-(gluco)mannan (mAb LM22)	β-1,3-D-glucan (mAb BS-400-2)	Xyloglucan (XXXG motif) (mAb LM15)	Xyloglucan (XLLG oligosaccharide) (mAb LM24)	Xyloglucan (mAb LM25)	β-1,4-D-Xylan (mAb LM10)	β-1,4-D-Xylan d/arabinoxylan (mAb LM11)	Cellulose (crystalline) (mAb CBM3a)	Extensin (mAb LM1)	Extensin (mAb JIM11)	Extensin (mAb JIM20)	AGP (mAb JIM8)	AGP (mAb JIM13)	AGP (mAb LM14)	AGP, β-linked GlcA (mAb LM2)
CDTA	15°C	ExCol	0	0	0	0	0	0	0	0	0	0	0	0	0	0	0	0	0	0	0	0	0	0	0	8	20	0	0
		Expr	0	0	0	0	0	0	0	0	0	0	0	0	0	0	0	0	0	0	0	0	0	0	0	7	14	28	0	6
		CellC, ExCol, Expr	0	0	0	0	0	0	0	0	0	0	0	0	0	0	0	0	0	0	0	0	0	0	0	0	0	16	0	0
		Control @ 15	**0**	**19**	**6**	**11**	**0**	**0**	**0**	**21**	**16**	**8**	**0**	**0**	**0**	**0**	**0**	**0**	**0**	**8**	**0**	**0**	**0**	**0**	**0**	**9**	**14**	**27**	**0**	**9**
	50°C	CellC, ExCol	0	0	0	0	0	0	0	0	0	0	0	0	0	0	0	0	0	0	0	0	0	0	0	0	0	20	0	0
		CellC, Expr	0	0	0	0	0	0	0	0	0	0	0	0	0	0	0	0	0	0	0	0	0	0	0	0	0	15	0	0
		ExCol, Expr	0	0	0	0	0	0	0	0	0	0	0	0	0	0	0	0	0	0	0	0	0	0	0	0	0	13	0	0
		Control @ 50	**0**	**14**	**9**	**10**	**0**	**0**	**0**	**17**	**13**	**0**	**0**	**0**	**0**	**0**	**6**	**0**	**0**	**7**	**0**	**0**	**0**	**0**	**0**	**9**	**10**	**22**	**0**	**9**
NaOH	15°C	ExCol	0	0	0	0	0	5	0	0	0	0	0	0	21	9	15	78	8	83	0	0	49	0	0	0	0	13	0	0
		Expr	0	0	0	7	0	0	0	0	0	0	0	0	21	9	16	84	5	86	0	0	52	0	0	7	6	13	0	0
		CellC, ExCol, Expr	0	0	0	0	0	6	0	0	0	0	0	0	23	10	14	62	9	77	0	9	42	0	0	0	0	11	0	0
		Control @ 15	**0**	**0**	**0**	**0**	**0**	**0**	**0**	**11**	**0**	**10**	**0**	**0**	**17**	**10**	**17**	**94**	**0**	**98**	**0**	**0**	**63**	**0**	**0**	**8**	**0**	**13**	**0**	**0**
	50°C	CellC, ExCol	0	0	0	8	0	11	0	0	0	0	0	0	21	9	16	72	6	82	0	6	47	0	0	10	0	14	0	0
		CellC, Expr	0	0	0	0	0	15	0	16	6	0	0	0	19	9	16	80	5	85	0	6	51	0	0	17	0	16	0	0
		ExCol, Expr	0	0	0	5	0	5	0	0	0	0	0	0	20	9	13	74	6	82	0	9	47	0	0	9	0	10	0	0
		Control @ 50	**5**	**0**	**0**	**21**	**0**	**0**	**0**	**7**	**0**	**0**	**8**	**0**	**17**	**6**	**14**	**81**	**0**	**89**	**0**	**7**	**53**	**0**	**0**	**6**	**0**	**10**	**0**	**0**

10	20	30	40	50	60	70	80	90	100

Un-ME GalA, Unmethylesterified galacturonic acid; disacch, disaccharides

Figure. 4. CoMPP results of Chardonnay pomace incubated with commercial maceration enzymes. The values are the average of three samples. ExCol, Rapidase® ExColor; Expr, Rapidase® Expression; CellC, Celluclast

In the NaOH fraction that were extracted from the control samples there were some traces of β-1,4-D-galactan, α-1, 5-L-arabinan, HG (mAbs JIM5 and LM19) and RG-I (mAb INRA-RU1). With enzyme treatment (Cellc combinations with ExCol and Expr at 50°C), a signal for mAb PAM1 appeared for the first time. In general the enzyme treatment removed HG (mAbs LM19) and the neutral RG-I side chains (mAb LM5 and LM6) and led to a decrease in the xyloglucan (mAb LM15 and LM25) and cellulose (mAb CBM3a) (except for Cellc, Expr at 50 °C). In contrast, a weak signal for xyloglucan, labelled by mAb LM24, became visible only after pectin removal by enzymatic hydrolysis.

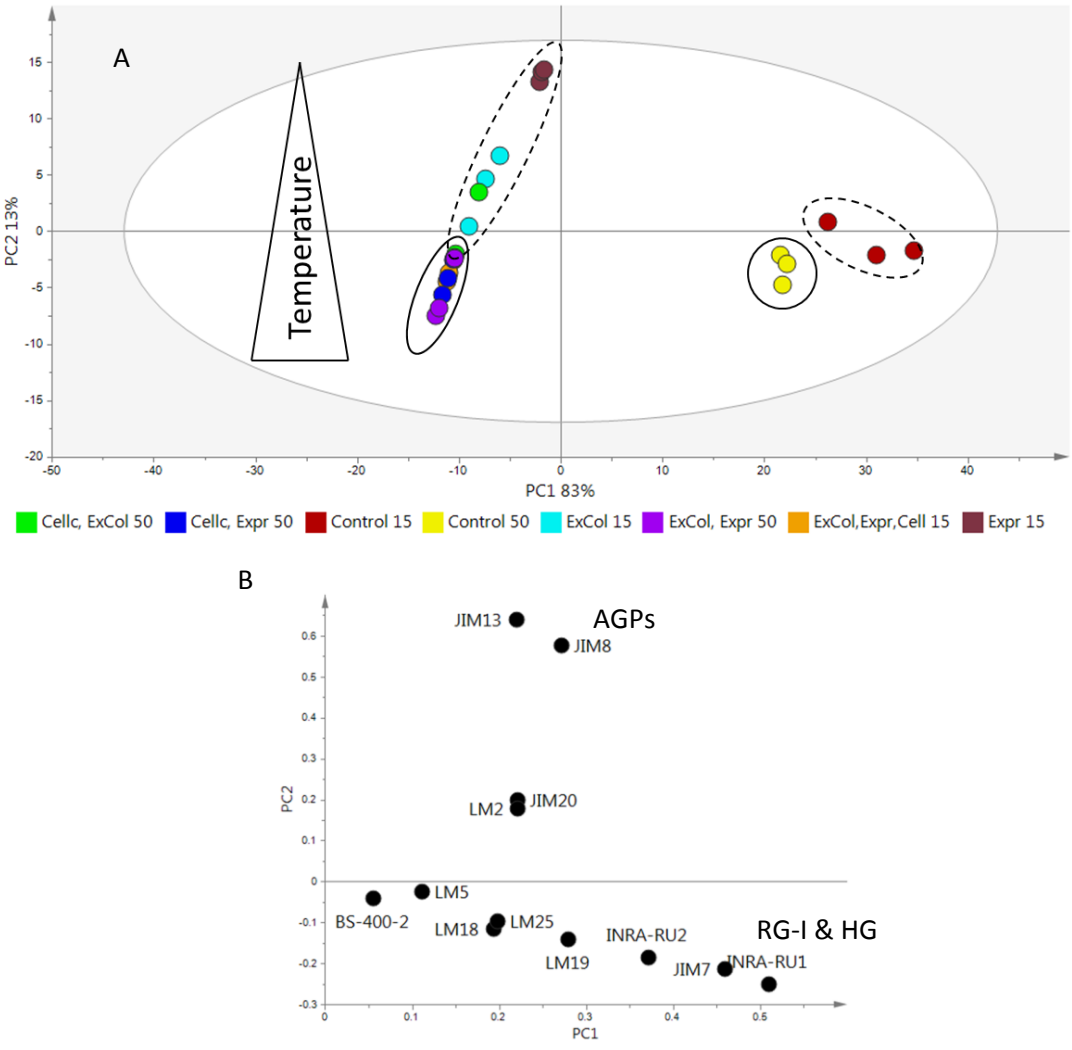

Figure 5. PCA score (A) and loading (B) plots of CDTA fraction of Chardonnay pomace treated with commercial enzymes at 15 and 50°C.

In a PCA model (Fig. 5) of the CDTA fraction, the enzyme treated samples all displayed a lower abundance in RG-I (mAbs INRA-RU1 and INRA-RU2) and HG (mAb JIM7) compared to the control samples (PC1 83%). Expr and ExCol treated samples at 15 °C (encircled with a dashed

line) have an abundance in residual AGPs (mAb JIM13 and JIM8) and this drive their separation (PC2 13 %) from the other enzyme treated samples (encircled with a solid line).

Monosaccharide analysis of the AIR isolated after enzyme treatment of pomace showed that there were two statistically significant (95% confidence interval) changes: Glc decreased from 51 to 35 pM/mg for the ExCol15 treatment, whereas GalA decreased from 57 to 34 pM/mg for the ExCol-Expr50 treatment (Table A3). In general the enzyme treated samples had lower monosaccharide levels than the controls which correspond with their lower levels of polymers as seen in the CoMPP data (Fig. 4 and Fig. 5).

3.2.3 Investigating the cell wall polymers of Chardonnay pomace, using purified enzymes

Finally, purified enzymes, which have one dominant activity, were incubated with the autoclaved Chardonnay pomace in an effort to link specific enzyme activities with specific cell wall modifications. The enzymes were used individually or in combinations, identical to the Pinotage AIR enzymatic hydrolysis. AIR was isolated from the pomace residues that remained, and the relative signal strengths obtained for the mAb set are shown in Fig. 6. The extreme depectination (CoMPP results, CDTA fraction) that took place during the autoclaving step is demonstrated by the absence of any HG polymers and the low levels of RG-I and RG-I side chains (mAbs INRA-RU1, INRA-RU2 and LM5) in the control samples. The Pect enzyme as well as the Pect-XG and -EG combinations removed all unbranched RG-I (both mAbs INRA-RU1 and INRA-RU2) and RG-I side branches (β-1,4-D-galactan), extensins (mAbs JIM11 and 20) , AGP mAb JIM8 and reduced the signal for mAb JIM13. The EG on its own and the EPG-EG combination only caused a reduction of the signals for mAbs INRA-RU1 and -2 (in contrast with complete removal seen with Pect enzymes), the extensins (mAb JIM20) and AGPs (mAb JIM13). Curiously, when a third enzyme (EA) was added to the EPG-EG combination there was no further reduction. In fact, the samples, now, had in most cases the same values as the control.

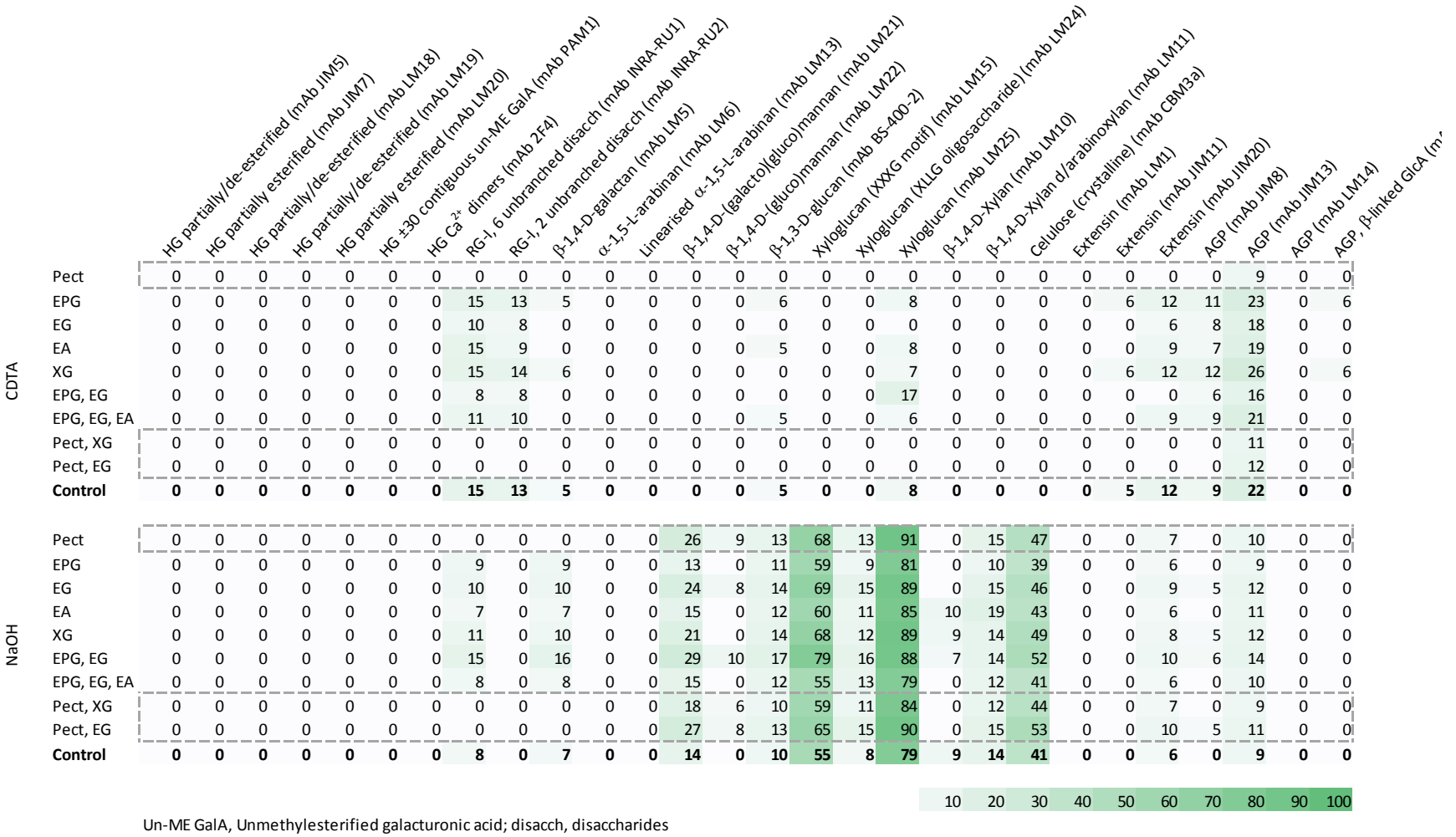

Un-ME GalA, Unmethylesterified galacturonic acid; disacch, disaccharides

Figure 6. CoMPP analysis performed on the solid residue after Chardonnay pomace was incubated with purified enzymes. The CDTA and NaOH fraction are shown in the heat map and values are the average of three samples. The boxed sections indicate enzymes that caused extensive hydrolysis. The enzymes that were used are described in Table 1.

In the NaOH fraction (Fig. 6) the Pect enzymes removed all RG-I (mAb INRA-RU1) and β-1,4-D-galactan (mAb LM5) while the other enzymes had no effect. The only exception is a slight increase in the mAb INRA-RU1 and LM5 signals for the EPG-EG treated samples. Most of the enzymes enhanced the levels of xyloglucan (mAbs LM15, LM24 and LM25) and cellulose (mAb CMB3a) extraction from Chardonnay pomace (except EPG and EPG-EG-EA). Mannan extraction (mAb LM21 and LM22) is also increased by Pect, Pect-EG, EG, EPG-EG and XG treatment.

Table 4: Monosaccharide analysis of the Chardonnay pomace treated with pure enzymes. Shaded values indicate the monosaccharides that is significantly lower (95 % confidence level) than the control sample. Values are the average of three samples. Ara, arabinose; Rha, rhamnose; Fuc, fucose; Xyl, xylose; GalA, galacturonic acid; Man, mannose; Gal, galactose; Glc, glucose; GlcA, glucuronic acid.

	pM/mg AIR																					
	Pect		EPG		EG		EA		X		EPG + EG		EPG + EG + EA		Pect + X		Pect + EG		Control	
Ara	39	± 12	43	± 22	53	± 2	45	± 10	51	± 11	53	± 5	38	± 7	46	± 2	38	± 7	**51**	± 6
Rha	16	± 1	18	± 5	21	± 0	21	± 2	20	± 2	20	± 1	18	± 2	18	± 0	16	± 1	**21**	± 1
Fuc	23	± 5	22	± 9	26	± 0	25	± 2	24	± 4	25	± 0	21	± 3	26	± 1	22	± 3	**25**	± 1
Xyl	83	± 11	118	± 22	115	± 10	103	± 32	105	± 28	108	± 20	84	± 19	110	± 6	89	± 27	**111**	± 11
GalA	22	± 1	27	± 11	36	± 1	32	± 4	33	± 5	31	± 3	30	± 3	24	± 5	28	± 8	**35**	± 3
Man	24	± 4	29	± 12	30	± 2	29	± 3	31	± 5	33	± 4	26	± 5	30	± 4	27	± 5	**31**	± 1
Gal	30	± 6	36	± 20	42	± 2	40	± 7	40	± 9	43	± 3	35	± 8	36	± 0	30	± 6	**42**	± 2
Glc	39	± 7	50	± 22	52	± 4	61	± 5	56	± 13	65	± 13	44	± 8	51	± 15	45	± 12	**59**	± 4
GlcA	21	± 2	22	± 5	25	± 3	24	± 1	23	± 2	23	±	22	± 3	22	± 2	22	± 2	**26**	± 1

In Table 4 the monosaccharide composition of the Chardonnay pomace cell walls only changed significantly for the Pect treated samples. There was a decrease in Rha (compared to the control) for all these samples which is similar to the Pinotage AIR results and probably due to the loss in RG-I seen in the CoMPP results (Fig. 6). There is also a reduction in Xyl (xyloglucan degradation seen in the CDTA fraction) and GalA (RG-I degradation) for the Pect treated samples and Gal decreased (mAb LM5 and JIM8 and JIM13 labelling decreased [Fig. 6]) in the presence of the Pect-XG combination. Overall, we see very high values for Xyl, (111 pM/mg AIR for the Chardonnay control samples) which corresponds to the presence of signals for mAbs LM10 and LM11 (Fig. 6, NaOH fraction).

4. Discussion

4.1 Pinotage skin cell wall enzymatic hydrolysis

Wine must and fermentation conditions can be a challenging environment for maceration enzymes because of the low pH and temperatures, the high sugar concentration as well as the presence of tannins which can bind and inhibit enzymes (Kennedy, 2008; Sieiro et al., 2010; Van Rensburg et al., 2000). Previous results from our group (Chapter 3) showed how the grape skin cell wall was modified during a red wine fermentation with the aid of maceration enzymes. Results suggested that depectination took place but the major effect of the maceration enzymes

was described as a loosening of the cell wall structure. Another important factor that made a large contribution towards the cell wall changes were the ripeness level of the grapes. Here we aimed to create the ideal enzyme hydrolysis conditions by using isolated cell walls from grape skins incubated with single purified enzymes (and combinations of these enzymes), in buffered conditions close to the optimum temperature and pH of the enzymes. The CoMPP results in combination with the monosaccharide analysis enabled us to form a picture of the cell walls (AIR) of Pinotage grape skins in which there were some HG, unbranched RG-I, xyloglucan (mAb LM25-binding motifs only), AGPs and extensins exposed on the surface of the AIR particles (no enzyme treatment). During the CDTA extraction, the pectins and associated compounds are removed from the surface area of the AIR particles. When the extraction was preceded by enzymatic hydrolysis, the composition of the extracted fraction depended on the extent of the hydrolysis that took place. Extensive hydrolysis (as seen with Pect treated samples), removed some AGPs and more or less all pectin polymers except some HG (labelled by mAbs PAM1, LM18 and LM19) which correlates with the low levels of GalA and Rha measured in these samples. With less extensive enzyme hydrolysis (EPG, EG, EA, XG and combinations of these enzymes) some of the bonds between the cell wall polysaccharides were broken but not enough to allow the complete removal of polymers into the hydrolysis buffer, as was seen with the Pect enzymes. Instead, it is better described as an “opening up” action, or unravelling and partial degradation of the AIR structure to allow better access for the CDTA in the subsequent extraction step to dissolve the pectins (HG extraction is enhanced) from the surface and sub-surface layers of the particle. This is in contrast with the control samples where only the outer pectin rich layers were dissolved. This unravelling action is similar to our previous results (Chapter 3) in the cell walls from Pinotage skins retrieved from fermentations done with commercial maceration enzymes. The results indicate (Table 3, Fig. 1 and 2) that depectination by both extreme and mild enzymatic hydrolysis unmasked the core hemicellulose-cellulose framework and this presumably enabled cellulases and hemicellulases to remove some of the xyloglucan and cellulose (lower values than the control samples in the NaOH fraction, Fig.1). This demonstration of the different levels of enzymatic hydrolysis on grape skin cell walls has not been shown previously and CoMPP is thus an effective method to determine which enzyme combinations and enzyme types are the most successful for grape tissue degradation.

The Pect-XG combination was the only treatment that increased both mAbs LM15 and LM25 labelling in the NaOH fraction compared to the control (Fig.1). Neither the XG nor the Pect enzymes on their own could show the same effect, confirming a synergism between the two enzymes under these conditions and on this substrate. Depectination by Pect probably facilitated better access for the XG enzyme to its target, leading to xyloglucan hydrolysis and an increased extraction (with NaOH) of partially degraded xyloglucan from within the hemicellulose-cellulose structure. We know plant cell wall xyloglucan is shielded by pectin

(Marcus et al., 2008) but this synergistic effect between pectinases and xylanases has not been shown previously (to our knowledge) in grape tissues and it is the first time that the CoMPP was used to demonstrate synergism. According to Hu et al. (Hu et al., 2013) synergistic effects are highly substrate specific which also depend on the substrate preparation, thus this synergism seen on AIR would not necessarily be observed in fresh grape tissue.

4.2 Chardonnay as a matrix for enzyme hydrolysis

The fresh Chardonnay pomace used in this study consisted of deseeded, pressed berries (skin and pulp) and the CoMPP data showed (Fig. 3, Fresh) a high abundance of HG as well as some α-1,5-L-arabinan, and AGPs extracted with CDTA. In the NaOH fraction xyloglucan, cellulose, mannan and AGPs were extracted as well as HG and RG-I side chains, presumably associated with the xyloglucan and cellulose. This is comparable to the overall polymer profile of Pinotage skin (Chapter 3) and whole berries of Crimson Seedless and Cabernet Sauvignon (Moore et al., 2014).

We included a pre-treatment step (autoclaving) in the analysis of the cell walls of the pomace. In general, information on the cell wall polymer changes occurring during the pre-treatment of lignocellulosic biomass is scarce. Previous studies investigated the effect of steam treatment on wheat straw (Hendriks et al., 2009) and showed that it caused partial hemicellulose hydrolysis which resulted in acid formation. The acids catalysed further hemicellulose hydrolysis, which led to the formation of pores, thus enhancing the access of enzymes to the cellulose. Hydrothermal pretreatment of *Populus* biomass was shown to initially disrupt the lignin-polysaccharide interactions, leading to pectins and arabinogalactans being removed, and subsequently also xylans and xyloglucans (DeMartini et al., 2011) (shown with immunolabeling). The pressurised heating treatment of the pomace in this study removed a large fraction of the HG (Fig. 3), presumably from the middle lamella, but also enhanced the extraction of mannan, cellulose and pectin molecules associated with the hemicellulose-cellulose structure. Additionally, there were strong signals for xylan labelling mAbs (LM11 and LM10) in the NaOH fraction after the treatment, also corresponding to the high levels of Xyl found in all the autoclaved Chardonnay pomace samples (111 -125 pM/mg AIR). The level of xylan polymers in grape tissue (probably originating from the vascular strands of the berry) have been calculated to be between 3 and 7 mol% of total cell wall polysaccharides (Nunan et al., 1998) and CoMPP data usually displays no to very low abundance of xylan and arabinoxylan in the NaOH fraction of ripe fresh grapes (Moore et al., 2014; Chapter 3). The data suggest that this exposure of xylan is an effect strongly associated with the pre-treatment and not due to enzyme hydrolysis. This base-line information of the processed pomace is important in the evaluation of the influence of the commercial and purified enzymes on this matrix.

The commercial enzymes, especially the Cellc-ExCol-Expr (15 °C), Cellc-ExCol and ExCol-Expr (50 °C) enzyme combinations made large modifications to the polymers extracted with CDTA, while there was only slight changes (compared to the control sample) in the NaOH fraction (Fig. 4). Although we would classify this as a strong hydrolysis effect (compared to the other data sets in this study), there are however, no other published data available (to our knowledge) on pomace cell wall polymer changes due to commercial enzyme degradation, with which we can compare our results. The reducing sugar concentration measured in the supernatants of these enzyme reactions did not increase significantly (Fig. A2) thus, these conditions (enzyme type, - combination, - loading and incubation conditions) tested here might be suitable for the extraction of polyphenols from the grape tissue, but would not be sufficient for biomass saccharification.

These pomace results also provide some interesting data to contribute to the development of an hypothesis regarding the spatial locations of polymers in grape cells. The CoMPP analyses showed the processed and enzyme hydrolysed pomace samples to be cleared of HG and RG-I and most of the AGPs were also removed (Fig. 4). Labelling for HG (mAb PAM1) showed up in the NaOH fraction and the levels were enhanced after enzyme treatment at 50°C. This antibody bind specifically to blocks of de-esterified HG, which is the result of block wise action of plant pectin methylesterases (pPME) (Willats et al., 1999). Fungal pectin methylesterases have a more random action. In *Arabidopsis thaliana* (Willats et al., 1999) and in carrot parenchyma cells (Christiaens et al., 2011) these blocks of unesterified HG occur in the cell wall lining the intercellular spaces. However, from the carrot study, it became clear that when the carrot tissue was subjected to a blanching treatment (60 °C for 48 h), the endogenous pPMEs were stimulated, leading to blocks of unesterified HG appearing throughout the whole inner face of the cell wall adjacent to the plasma membrane (Christiaens et al., 2011). This distribution of unesterified HG seems to be species specific because in broccoli, pPME stimulation only led to the enhancement of the labelling in the intercellular spaces. This might indicate that in grape the unesterified HG polymers are also found in the intercellular space between cells because it was easily extracted (no enzyme action needed) in the CDTA fraction of the Pinotage cell walls (although only low levels were found). In the Chardonnay pomace this polymer could only be extracted after enzyme hydrolysis and removal of the CDTA fraction. Our preliminary interpretation of this result is that during the first few minutes of the pre-processing step, the pPME was able to de-esterify some of the HG that lines the inner face of the cell wall adjacent to the plasma membrane. At the end of the autoclaving step, most of the pectin from the intercellular regions was probably removed, but enzyme hydrolysis exposed this newly unesterified HG and some of this could be dissolved in the NaOH. It would be interesting to add

immunofluorescence microscopy analysis to the polymer profiling studies to investigate the validity of our speculations.

With the use of purified enzymes on Chardonnay pomace, different levels of enzyme hydrolysis were seen. The Pect and Pect enzyme combinations caused the highest level of modifications which entailed strong depectination coupled with the enhancement of extraction of cellulose and hemicellulose polymers. EG and the EPG-EG combination caused milder depectination, but also enhanced the extraction of polymers in the NaOH fraction. The EPG-EG combination was synergistic: EPG on its own gave similar results than the control samples, but when combined with EG, more modifications were evident. Interestingly, when a third enzyme (EA) was added, similar values than the control samples were obtained in this matrix. This was not seen in the Pinotage AIR hydrolysis and would require further investigation. Synergistic effects between pectinases and cellulases are well known and has been shown previously in grape tissue (Kammerer et al., 2005) to deliver the best results for the isolation of polyphenols from grapes. Successful wine maceration enzyme preparations also usually contain a combination of pectinase and cellulase activities (Fia et al., 2014).

4.3 General observations of enzyme action on grape cell walls

4.3.1 Influence of the matrix on enzyme hydrolysis

When comparing the extent of the enzymatic hydrolysis by the purified enzymes on the Pinotage AIR and the Chardonnay pomace it was clear that the latter was more resistant towards degradation. The matrices were clearly different, both in inherent composition and preparation: the pomace contained both pulp and skin tissue, whereas the Pinotage analysis was only on skins; the pomace was not exposed to organic solvents or was not freeze-dried prior to enzymatic hydrolysis, whereas the Pinotage skin samples were subjected to both. In apple cell walls, freeze-drying caused the collapse and compaction of the material (Le Bourvellec et al., 2012). Compared to the Pinotage AIR from skins, the pomace contains interfering substances (e.g. sugars, organic acids, phenolic compounds) which could have decreased the activity of the enzymes, or prevented access to the cell wall polymers. Moreover, the pomace might have contained more cuticular matter than the Pinotage skins. Cuticular matter can decrease the accessibility of the polysaccharides to enzymes (Mendes, Prozil, et al., 2013; Mendes, Xavier, et al., 2013). In our study the chloroform wash that is part of the AIR preparation protocol, could have eliminated some of this cuticular matter from the Pinotage AIR, favouring enzyme action on this matrix compared to the pomace. In addition, Fangel (Fangel, 2013) reported that the organic solvents used in AIR preparation opens up the cell wall structure which could have contributed to the Pinotage AIR being an “easier” substrate to hydrolyse than the Chardonnay pomace.

4.3.2 Enzymatic hydrolysis- and extraction patterns as well as associations between cell wall polymers, as shown by the CoMPP technique

Despite these differences in the matrix and processing of it (section 4.3.1), some shared features were observed for both matrices. The labelling patterns observed for xyloglucans were very interesting. We always (in both the Chardonnay and the Pinotage samples) found low levels of mAb LM25 in the CDTA fraction, strong signals for LM25 and LM15 in the NaOH fraction and a weak signal for mAb LM24 in the NaOH fraction that was enhanced by enzyme treatment. Pedersen et al. (2012) observed with immunofluorescence imaging in tobacco stem parenchyma cells, that LM15 were predominantly located in the corners of intercellular spaces, LM24 was found in adhered cell walls between intercellular spaces and LM25 was localized in the cell walls lining intercellular spaces. Although CoMPP analysis does not show the cellular location of epitopes we are still tempted to speculate that according to the patterns we observed and the spatial distribution information from Pedersen (Pedersen et al., 2012) , it is likely that degradation in our samples initiated in the intercellular triangle (low levels of mAb LM25 in the CDTA fraction). Once a portion of the pectin polymers has been removed (enzyme action and/or removal with CDTA), the signal for mAb LM25 increased while a signal for LM15 appeared in the NaOH fraction (depectination spreads to the corners) for the first time, in combination with a weaker signal for LM24. The appearance of mAb LM24 labelling might indicate that the individual cells were detaching from each other which has been shown to occur when vegetables are cooked (Jarvis, 2011). For future work it would be interesting to confirm our hypothesis by treating grape tissue sections with enzymes and visualise the sequence and extent of degradation using immunofluorescence microscopy.

The enzyme hydrolysis in combination with the sequential extraction steps, as used in CoMPP analysis, provide the ability to identify possible associations between the cell wall polymers of grape berry. For example, AGPs recognized by mAb JIM13 were reduced by Pect action (Fig. 1) and the labelling pattern was similar to mAb INRA-RU1. This can indicate that these AGPs are bound to pectin polymers [as previously reported in other plants (Hijazi et al., 2014; Keegstra et al., 1973; Tan et al., 2013)], and subsequently removed during pectin hydrolysis. It might also just confirm the RG-I hydrolysis because it should be noted that mAb JIM13 showed cross reactivity with RG-I of sycamore maple (Pattathil et al., 2010). Another example is the association between the RG-I (specifically mAb INRA-RU1) and xyloglucan (Popper et al., 2008). In both grape matrices a signal for mAb INRA-RU1 was detectable in the NaOH fraction (even after enzyme hydrolysis and extraction with CDTA) which was probably due to the interaction between this RG-I and xyloglucan. Interestingly, the RG-I labelled by mAb INRA-RU2 I (that has more galactosyl side chains than INRA-RU1 labelled RG-I) were more easily removed. Furthermore, in the Pinotage AIR the relative abundance of xyloglucan (mAb LM25) and RG-I (mAbs INRA-RU1 and INRA-RU2) was similarly influenced by the different enzyme

treatments but there was no resemblance between mAb LM25 and HG which is an additional indication of a xyloglucan-RG-I specific association in grape berry tissue.

It is necessary to mention that the actual values between CoMPP data sets (Fig. 3, 4 and 6) should not be directly compared since the collection of antibodies used for each data set were not identical and CoMPP results are not directly comparable across datasets obtained on different occasions (personal experience).

The CoMPP analyses proved to be a valuable, sensitive and high-throughput method to trace modifications in the polymers of grape berries cell walls. It highlighted synergism between different enzymes and gave indications of polymer associations. Furthermore, we could distinguish between the different levels of enzymatic hydrolysis. Mild degradation was typified by pore formation, presumably by the partial hydrolysis of pectin polymers, and seen with CoMPP analysis as an enhancement in the CDTA extraction. As the degradation advanced, these smaller degradation products were removed during the enzyme hydrolysis step resulting in a decrease in polymers that could be extracted with CDTA. With moderate degradation the pores became large enough for the enzymes to penetrate into the cell wall and break up hemicellulose polymers (xyloglucan and mannan). At first those partially degraded polymers could only be removed from within the cell wall framework by extraction with NaOH. If however, the degradation proceeded far enough (pores are large enough or polymer size reduction went far enough) those partially degraded polymers will diffuse out unassisted during the enzymatic hydrolysis step. For future work it might be informative to use different enzyme-to-AIR/pomace ratios to study the effect of enzyme loading and improve the observation of subtle differences.

This study provided us with a completely new method for evaluating different enzymes or enzyme combinations. This method can also be used to test the effect of enzymes on different substrates or different incubation conditions and it can be a valuable tool to use not only in the development of enzyme preparations for the wine and pomace valorisation industries but should be applicable in any industry where enzymes are used for the degradation of plant tissues.

References

lvira, P., Tomás-Pejó, E., Ballesteros, M., and Negro, M. J. (2010). Pretreatment technologies for an efficient bioethanol production process based on enzymatic hydrolysis: A review. *Bioresour. Technol.*, **101**, 4851–61.

Arnous, A., and Meyer, A. S. (2010). Discriminated release of phenolic substances from red wine grape skins (*Vitis vinifera L.*) by multicomponent enzymes treatment. *Biochem. Eng. J.*, **49**, 68–77.

Chamorro, S., Viveros, A., Alvarez, I., Vega, E., and Brenes, A. (2012). Changes in polyphenol and polysaccharide content of grape seed extract and grape pomace after enzymatic treatment. *Food Chem.*, **133**, 308–314.

Christiaens, S., Van Buggenhout, S., Ngouémazong, E. D., Vandevenne, E., Fraeye, I., Duvetter, T., Van Loey, A. M., and Hendrickx, M. E. (2011). Anti-homogalacturonan antibodies: A way to explore the effect of processing on pectin in fruits and vegetables?. *Food Res. Int.*, **44**, 225–234.

DeMartini, J. D., Pattathil, S., Avci, U., Szekalski, K., Mazumder, K., Hahn, M. G., and Wyman, C. E. (2011). Application of monoclonal antibodies to investigate plant cell wall deconstruction for biofuels production. *Energy Environ. Sci.*, **4**, 4332.

Eriksson, L., Byrne, T., Johansson, E., Trygg, J., and Vikström, C. (2013). *Multi- and megavariate data analysis. Basic principles and applications* (3rd ed.). Malmo: MKS Umetrics AB.

Fangel, J. U. (2013). Ph.D. thesis. *Advanced technologies for plant cell wall evolution and diversity*. University of Copenhagen, Copenhagen, Denmark.

Fia, G., Canuti, V., and Rosi, I. (2014). Evaluation of potential side activities of commercial enzyme preparations used in winemaking. *Int. J. Food Sci. Technol.*, **49**, 1902–1911.

Fleischer, A., O'Neill, M., and Ehwald, R. (1999). The pore size of non-graminaceous plant cell walls is rapidly decreased by Borate ester cross-linking of the pectic polysaccharide rhamnogalacturonan II. *Plant Physiol.*, **121**, 829–838.

Goussard, P. G. (2008). *Grape cultivars for wine production in South Africa*. Cape Town: Cheviot Publishing.

Hanlin, R. L., Hrmova, M., Harbertson, J. F., and Downey, M. O. (2010). Review: Condensed tannin and grape cell wall interactions and their impact on tannin extractability into wine. *Aust. J. Grape Wine Res.*, **16**, 173–188.

Hendriks, A. T. W. M., and Zeeman, G. (2009). Pretreatments to enhance the digestibility of lignocellulosic biomass. *Bioresour. Technol.*, **100**, 10–8.

Hijazi, M., Roujol, D., Nguyen-Kim, H., Del Rocio Cisneros Castillo, L., Saland, E., Jamet, E., and Albenne, C. (2014). Arabinogalactan protein 31 (AGP31), a putative network-forming protein in *Arabidopsis thaliana* cell walls?. *Ann. Bot.*, **114**, 1087–97.

Himmel, M., Ding, S., Johnson, D., William, S., Nimlos, M., Brady, J., and Foust, T. (2007). Biomass recalcitrance: engineering plants and enzymes for biofuels production. *Science*, **315**, 804–807.

Hu, J., Arantes, V., Pribowo, A., and Saddler, J. N. (2013). The synergistic action of accessory enzymes enhances the hydrolytic potential of a "cellulase mixture" but is highly substrate specific. *Biotechnol. Biofuels*, **6**, 112.

Jackson, J. E. (1991). *A User's Guide to Principal Components*. Hoboken, NJ, USA: John Wiley & Sons, Inc.

Jarvis, M. C. (2011). Plant cell walls: Supramolecular assemblies. *Food Hydrocoll.*, **25**, 257–262.

Kammerer, D., Claus, A., Scieber, A., and Carle, R. (2005). A novel process for the recovery of polyphenols from grape (*Vitis vinifera L* .) pomace. *Food Chem. Toxicol.*, **70**, 157–163.

Keegstra, K. (2010). Plant cell walls. *Plant Physiol.*, **154**, 483–6.

Keegstra, K., Talmadge, K. W., Bauer, W. D., and Albersheim, P. (1973). The Structure of Plant Cell Walls. *Plant Physiol.*, **51**, 188–196.

Kennedy, J. (2008). Grape and wine phenolics: Observations and recent findings. *Cienc. e Investig. Agrar.*, **35**, 107–120.

Le Bourvellec, C., Watrelot, A. A., Ginies, C., Imberty, A., and Renard, C. M. G. C. (2012). Impact of processing on the noncovalent interactions between procyanidin and apple cell wall. *J. Agric. Food Chem.*, **60**, 9484–94.

Louw, L., Tredoux, A. G. J., Rensburg, P. Van, Kidd, M., Naes, T., and Nieuwoudt, H. H. (2010). Fermentation-derived aroma compounds in varietal young wines from South Africa, **31**, 213–225.

Mabee, W. E., and Saddler, J. N. (2010). Bioethanol from lignocellulosics: Status and perspectives in Canada. *Bioresour. Technol.*, **101**, 4806–13.

Maier, T., Göppert, A., Kammerer, D. R., Schieber, A., and Carle, R. (2007). Optimization of a process for enzyme-assisted pigment extraction from grape (*Vitis vinifera L.*) pomace. *Eur. Food Res. Technol.*, **227**, 267–275.

Marcus, S. E., Verhertbruggen, Y., Hervé, C., Ordaz-Ortiz, J. J., Farkas, V., Pedersen, H. L., Willats, W. G. T., and Knox, J. P. (2008). Pectic homogalacturonan masks abundant sets of xyloglucan epitopes in plant cell walls. *BMC Plant Biol.*, **8**, 60.

May, P. F. (2009). *PINOTAGE: Behind the Legends of South Africa's Own Wine* (1st ed.). St Albans: Inform and Enlighten.

Mendes, J. A. S., Prozil, S. O., Evtuguin, D. V., and Lopes, L. P. C. (2013). Towards comprehensive utilization of winemaking residues: Characterization of grape skins from red grape pomaces of variety Touriga Nacional. *Ind. Crops Prod.*, **43**, 25–32.

Mendes, J. A. S., Xavier, A. M. R. B., Evtuguin, D. V., and Lopes, L. P. C. (2013). Integrated utilization of grape skins from white grape pomaces. *Ind. Crops Prod.*, **49**, 286–291.

Meyer, A. S., Jepsen, S. M., and Sørensen, N. S. (1998). Enzymatic release of antioxidants for human low-density lipoprotein from grape pomace. *J. Agric. Food Chem.*, **46**, 2439–2446.

Miller, G. (1959). Use of dinitrosalicylic acid reagent for determination of reducing sugar. *Anal. Chem.*, **31**, 426–428.

Moller, I., Sørensen, I., Bernal, A. J., Blaukopf, C., Lee, K., Øbro, J., Pettolino, F., Roberts, A., Mikkelsen, J. D., Knox, J. P., Bacic, A., and Willats, W. G. T. (2007). High-throughput mapping of cell-wall polymers within and between plants using novel microarrays. *Plant J.*, **50**, 1118–28.

Moore, J. P., Fangel, J. U., Willats, W. G. T., and Vivier, M. A. (2014). Pectic-β(1,4)-galactan, extensin and arabinogalactan-protein epitopes differentiate ripening stages in wine and table grape cell walls. *Ann. Bot.*, **114**, 1279–1294.

Nerantzis, E. T., and Tataridis, P. (2006). Integrated enology-Utilization of winery by-products into high added value products. *J. Food Sci. Technol.*, **3**, 1–12.

Nguema-Ona, E., Moore, J. P., Fagerström, A., Fangel, J. U., Willats, W. G. T., Hugo, A., and Vivier, M. a. (2012). Profiling the main cell wall polysaccharides of tobacco leaves using high-throughput and fractionation techniques. *Carbohydr. Polym.*, **88**, 939–949.

Nunan, K., Sims, I., and Bacic, A. (1998). Changes in cell wall composition during ripening of grape berries. *Plant Physiol.*, **118**, 783–792.

Ortega-Heras, M., Pérez-Magariño, S., and González-Sanjosé, M. L. (2012). Comparative study of the use of maceration enzymes and cold pre-fermentative maceration on phenolic and anthocyanic composition and colour of a Mencía red wine. *LWT - Food Sci. Technol.*, **48**, 1–8.

Ortega-Regules, A., Ros-García, J. M., Bautista-Ortín, A. B., López-Roca, J. M., and Gómez-Plaza, E. (2008). Differences in morphology and composition of skin and pulp cell walls from grapes (*Vitis vinifera L.*): technological implications. *Eur. Food Res. Technol.*, **227**, 223–231.

Özcan, E. (2006). *Ultrasound assisted extraction of phenolics from grape pomace*. M.Sc. thesis: Middle east technical university, Ankara, Turkey.

Pattathil, S., Avci, U., Baldwin, D., Swennes, A. G., McGill, J. a, Popper, Z., Bootten, T., Albert, A., Davis, R. H., Chennareddy, C., Dong, R., O'Shea, B., Rossi, R., Leoff, C., Freshour, G., Narra, R., O'Neil, M., York, W. S., and Hahn, M. G. (2010). A comprehensive toolkit of plant cell wall glycan-directed monoclonal antibodies. *Plant Physiol.*, **153**, 514–25.

Pedersen, H. L., Fangel, J. U., McCleary, B., Ruzanski, C., Rydahl, M. G., Ralet, M.-C., Farkas, V., von Schantz, L., Marcus, S. E., Andersen, M. C. F., Field, R., Ohlin, M., Knox, J. P., Clausen, M. H., and Willats, W. G. T. (2012). Versatile high resolution oligosaccharide microarrays for plant glycobiology and cell wall research. *J. Biol. Chem.*, **287**, 39429–38.

Popper, Z. A., and Fry, S. C. (2008). Xyloglucan-pectin linkages are formed intra-protoplasmically, contribute to wall-assembly, and remain stable in the cell wall. *Planta*, **227**, 781–94.

Rodríguez, L. A., Toro, M. E., Vazquez, F., Correa-Daneri, M. L., Gouiric, S. C., and Vallejo, M. D. (2010). Bioethanol production from grape and sugar beet pomaces by solid-state fermentation. *Int. J. Hydrogen Energy*, **35**, 5914–5917.

Romero-Cascales, I., Fernández-Fernández, J. I., Ros-García, J. M., López-Roca, J. M., and Gómez-Plaza, E. (2008). Characterisation of the main enzymatic activities present in six commercial macerating enzymes and their effects on extracting colour during winemaking of Monastrell grapes. *Int. J. Food Sci. Technol.*, **43**, 1295–1305.

Romero-Cascales, I., Ros-García, J. M., López-Roca, J. M., and Gómez-Plaza, E. (2012). The effect of a commercial pectolytic enzyme on grape skin cell wall degradation and colour evolution during the maceration process. *Food Chem.*, **130**, 626–631.

Serratosa, M. P., Marquez, A., Moyano, L., Zea, L., and Merida, J. (2014). Chemical and morphological characterization of Chardonnay and Gewürztraminer grapes and changes during chamber-drying under controlled conditions. *Food Chem.*, **159**, 128–36.

Sieiro, C., García-Fraga, B., López-Seijas, J., Da Silva, A. F., and Villa, T. G. (2010). Microbial pectic enzymes in the food and wine industry. *Food Ind. Process. - Methods Equip.* (pp. 201–218). Rijeka: InTech.

Singh, A. P., and Singh, T. (2014). Biotechnological applications of wood-rotting fungi: A review. *Biomass and Bioenergy*, **62**, 198–206.

Tan, L., Eberhard, S., Pattathil, S., Warder, C., Glushka, J., Yuan, C., Hao, Z., Zhu, X., Avci, U., Miller, J. S., Baldwin, D., Pham, C., Orlando, R., Darvill, A., Hahn, M. G., Kieliszewski, M. J., and Mohnen, D. (2013). An *Arabidopsis* cell wall proteoglycan consists of pectin and arabinoxylan covalently linked to an arabinogalactan protein. *Plant Cell*, **25**, 270–87.

Van Rensburg, P., and Pretorius, I. S. (2000). Enzymes in Winemaking : Harnessing Natural Catalysts for Efficient Biotransformations - A Review. *South African J. Enol. Vitic.*, **21**, 52–73.

Vidal, S., Williams, P., Doco, T., Moutounet, M., and Pellerin, P. (2003). The polysaccharides of red wine: total fractionation and characterization. *Carbohydr. Polym.*, **54**, 439–447.

Wischmann, B., Toft, M., Malten, M., and McFarland, K. C. (2012). Biomass conversion determined via fluorescent cellulose decay assay. *Methods Enzymol.*, **510**, 19–36.

Wood, P. J., Erfle, J. D., and Teather, R. M. (1988). Use of complex formation between Congo Red and polysaccharides in detection and assay of polysaccharide hydrolases. *Methods Enzymol.*, **160**, 59–74.

Xu, C., Yagiz, Y., Borejsza-Wysocki, W., Lu, J., Gu, L., Ramírez-Rodrigues, M. M., and Marshall, M. R. (2014). Enzyme release of phenolics from muscadine grape (*Vitis rotundifolia Michx*.) skins and seeds. *Food Chem.*, **157**, 20–9.

Yu, J., and Ahmedna, M. (2013). Functional components of grape pomace: their composition, biological properties and potential applications. *Int. J. Food Sci. Technol.*, **48**, 221–237.

Appendix

Table A1

Monoclonal antibodies and carbohydrate binding module used in this study.

Monoclonal antibody	Reference
HG partially/de-esterified (mAb JIM5)	(Verhertbruggen et al., 2009)
HG partially esterified (mAb JIM7)	(Verhertbruggen et al., 2009)
HG partially/de-esterified (mAb LM18)	(Verhertbruggen et al., 2009)
HG partially/de-esterified (mAb LM19)	(Verhertbruggen et al., 2009)
HG partially esterified (mAb LM20)	(Verhertbruggen et al., 2009)
HG ±30 contiguous unmethylesterified GalA[a] units (mAb PAM1)	(Willats et al., 1999)
HG Ca^{2+} dimers (mAb 2F4)	(Liners et al., 1989)
RG-I, 6 unbranched disaccharide (mAb INRA-RU1)	(Ralet et al., 2010)
RG-I, 2 unbranched disaccharide (mAb INRA-RU2)	(Ralet et al., 2010)
β-1,4-D-galactan (mAb LM5)	(Jones et al., 1997)
α-1,5-L-arabinan (mAb LM6)	(Willats et al., 1998)
Linearised α-1,5-L-arabinan (mAb LM13)	(Moller et al., 2008)
β-1,4-D-(galacto)(gluco)mannan (mAb LM21)	(Marcus et al., 2010)
β-1,4-D-(gluco)mannan (mAb LM22)	(Marcus et al., 2010)
β-1,3-D-glucan (mAb BS-400-2)	(Moller et al., 2008)
Xyloglucan (XXXG motif) (mAb LM15)	(Marcus et al., 2010)
Xyloglucan (XLLG oligosaccharide) (mAb LM24)	(Pedersen et al., 2012)
Xyloglucan (mAb LM25)	(Pedersen et al., 2012)
β-1,4-D-Xylan (mAb LM10)	(McCartney et al., 2005)
β-1,4-D-Xylan d/arabinoxylan (mAb LM11)	(McCartney et al., 2005)
Celulose (crystalline) (mAb CBM3a)	(Blake et al., 2006)
Extensin (mAb LM1)	(Smallwood et al., 1995)[c]
Extensin (mAb JIM11)	(Smallwood et al., 1994)
Extensin (mAb JIM20)	(Smallwood et al., 1994)
AGP (mAb JIM8)	(Pennell et al., 1991)
AGP (mAb JIM13)	(Yates et al., 1996)
AGP (mAb LM14)	(Moller et al., 2008)
AGP,β-linked GlcA[b] (mAb LM2)	(Yates et al., 1996)

[a]galacturonic acid; [b]GlcA, glucuronic acid; [c]Cited in (Neumetzler et al., 2012)

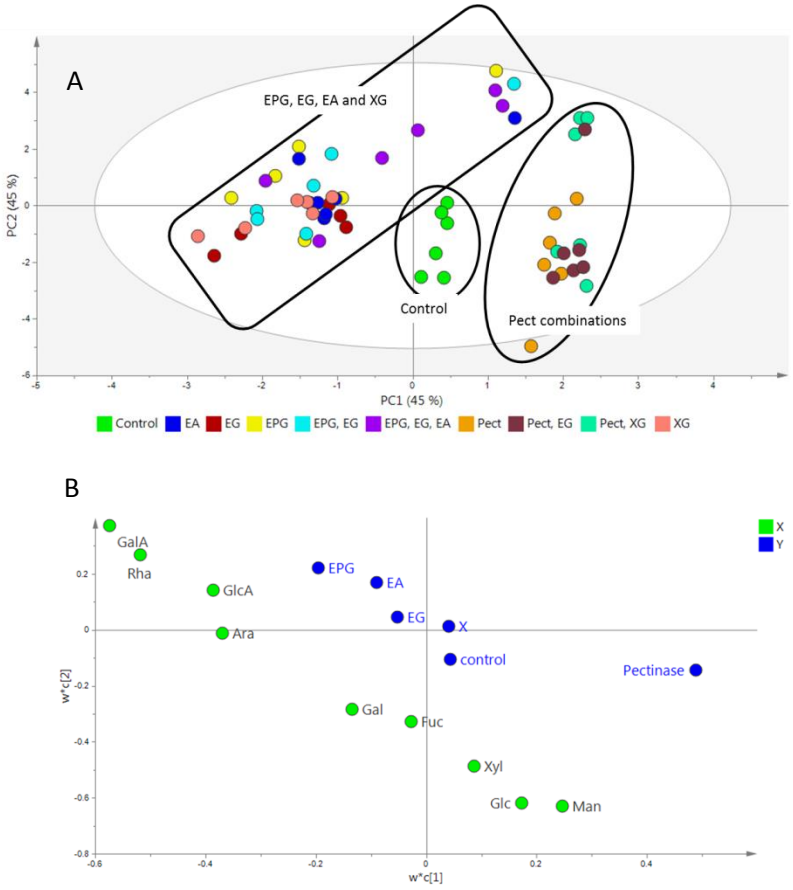

Figure. A1. PLS score (A) and loading plot (B) of the monosaccharide analysis of Pinotage AIR treated with pure enzymes show the Pect treated samples separating from the other samples due to an abundance of Man, Glc and Xyl and a scarcity of GlcA, Rha and GalA. PLS is a regression technique for modelling the association between two sets of variables and has the ability to analyse noisy, collinear and incomplete sets of variables (Eriksson et al., 2013).

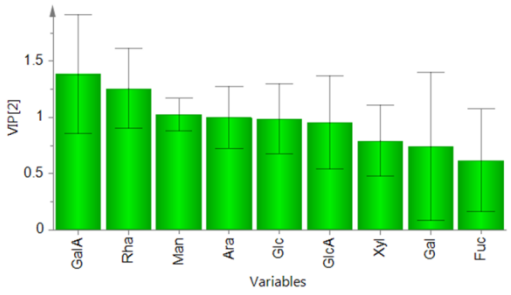

Figure. A2. VIP plot (Variable Importance for the Projection) is an interpretation tool that summarizes the importance of variables in a PLS model and a VIP value larger than one indicates that a variable has an above average influence on the model. The VIP plot indicated that GalA, followed by Rha and Man were the most important contributors towards the configuration of the samples in the PLS plot.

Properties of the supernatants of Chardonnay pomace suspensions incubated with commercial enzymes.

After the autoclaving step, the supernatants of the samples had a turbid appearance indicating that a high percentage of pectin polymers were released into the buffer. These pectins form soluble, viscous, colloidal structures that stay in suspension and keep other grape solids in suspension by electrostatic repulsion between particles (Pinelo et al., 2010). After the incubation with enzymes, the samples that were incubated at 50 °C had absolute clear supernatants (Table A2).

Table A2

The turbidity, pH, methanol and reducing sugar values of the supernatant of Chardonnay pomace after incubation with commercial enzymes at 15 and 50 °C. The values are the average of three biological repeats. Different letters per column indicate statistical significant differences (95 % confidence interval). A plus sign for turbidity means the supernatant had a turbid appearance and a negative sign means the supernatant was clear. ExCol, Rapidase®ExColor; Expr, Rapidase®Expression; Cellc, Celluclast®1.5L

		Turbidity	pH		Methanol (mg/mL)		Reducing sugar (mg/mL)	
15 °C	Control @ 15	+ + +	3.29^{a}	±0.03	$< 45^{a}$	±0	25.26^{a}	±0.85
	ExCol	+ +	3.22^{b}	±0.02	85.71^{b}	±2.4	25.97^{a}	±1.17
	Expr	+ + +	3.22^{b}	±0.03	84.51^{b}	±2.1	26.14^{a}	±1.17
	Cellc, ExCol, Expr	+ + +	3.22^{a}	±0.04	82.17^{b}	±3.9	27.29^{a}	±0.41
50 °C	Control @ 50	+ + +	3.03^{c}	±0.04	$< 45^{a}$	±0	26.12^{a}	±0.49
	Cellc, ExCol	–	2.98^{c}	±0.01	80.22^{b}	±4.5	26.02^{a}	±2.62
	Cellc, Expr	–	3.00^{c}	±0.04	81.75^{b}	±5.7	25.81^{a}	±1.23
	ExCol, Expr	–	2.97^{c}	±0.03	81.08^{b}	±5.1	25.51^{a}	±1.41

In contrast, all the enzyme treated samples at 15 °C were still turbid after incubation, with the exception of ExCol at 15 °C that were slightly less turbid than the rest. This indicates a higher level of activity for the enzymes at 50 °C than at 15 °C and that ExCol might have a higher activity than Expr and Cellc at this low temperature. Table A2 also shows the pH, the methanol and the reducing sugar levels of the supernatants after enzyme hydrolysis. The pH of the pomace-in-citrate phosphate buffer suspension was 3.25 after autoclaving. The pH of all the reactions (including the control) at 50 °C decreased to three during the incubation period while

the pH for the reactions at 15 °C were more or less stable. The decrease in pH for the control (no enzyme added) sample at 50 °C can be due to acid hydrolysis at this elevated temperature. The pH values of the enzyme treated samples at 50 °C probably also decreased due to the release of galacturonic acid during enzyme hydrolysis. The methanol levels increased from below 45 mg/mL for the control samples (no enzymes), [45 mg/mL is the detection threshold of the GC-FID method (Louw et al., 2010)] to values between 80 and 82 mg/l for the enzyme hydrolysed samples incubated at 50 °C. For the samples incubated at 15 °C, slightly higher methanol values (82 to 86 mg/l) were produced. Methanol production is the result of the de-esterification of pectin by pectinmethylesterases present in the commercial enzyme preparations. In acidic solutions and at low temperature, de-esterification of pectin is the dominant activity while at high temperature, depolymerization occurs more rapidly (Thakur et al., 1997). This might explain why the seemingly higher enzyme action at 50 °C (clear supernatant, decrease in pH) does not correspond to the highest methanol concentrations. The reducing sugar concentration in the supernatants did not increase significantly indicating that the enzyme hydrolysis did not produce a high number of monosaccharides but rather resulted in a lower number of large oligosaccharides (i.e. partial degradation of polysaccharides) rendering fewer reducing sugar ends.

Table A3

Monosaccharide analysis cell walls isolated from Chardonnay pomace that were treated with commercial enzymes. The values are the average of three samples. All light grey shaded values indicate a decrease compared to the control sample at that specific temperature with 90 % confidence interval. The dark grey shaded values are the same but the confidence interval is 95 %.

	pM/mg AIR											
	15°C						50°C					
	ExCol		Expr		Cellc + ExCol + Exp		15°C control		Cellc + ExCol		Cellc + Expr		ExCol + Expr		50°C control	
Ara	32	± 2	36	± 7	32	± 3	**44**	± 7	43	± 7	36	± 11	36	± 3	**44**	± 5
Rha	16	± 0	17	± 3	17	± 0	**22**	± 8	19	± 1	17	± 3	17	± 0	**21**	± 1
Fuc	20	± 2	24	± 4	18	± 1	**31**	± 13	23	± 2	22	± 4	23	± 1	**25**	± 2
Xyl	90	± 9	103	± 5	63	± 16	**125**	± 14	113	± 14	85	± 31	109	± 23	**116**	± 11
GalA	33	± 2	41	± 12	41	± 3	**66**	± 14	40	± 3	34	± 9	34	± 3	**57**	± 7
Man	25	± 1	30	± 10	25	± 2	**41**	± 10	32	± 4	27	± 7	28	± 2	**31**	± 2
Gal	30	± 3	40	± 12	28	± 5	**50**	± 9	41	± 7	34	± 12	37	± 4	**41**	± 4
Glc	35	± 0	40	± 16	35	± 3	**51**	± 6	44	± 12	38	± 8	40	± 4	**40**	± 4
GlcA	22	± 1	27	± 6	25	± 3	**31**	± 7	27	± 4	25	± 3	25	± 3	**28**	± 4

References

Blake, A. W., McCartney, L., Flint, J. E., Bolam, D. N., Boraston, A. B., Gilbert, H. J., and Knox, J. P. (2006). Understanding the biological rationale for the diversity of cellulose-directed carbohydrate-binding modules in prokaryotic enzymes. *J. Biol. Chem.*, **281**, 29321–9.

Eriksson, L., Byrne, T., Johansson, E., Trygg, J., and Vikström, C. (2013). *Multi- and megavariate data analysis. Basic principles and applications* (3rd ed.). Malmo: MKS Umetrics AB.

Jones, L., Seymour, B., and Knox, J. P. (1997). Localization of pectic galactan in tomato cell walls using a monoclonal antibody specific to 1,4-β-D-Galactan. *Plant Physiol.*, **113**, 1405–1412.

Liners, F., Letesson, J.-J., Didembourg, C., and Van Cutsem, P. (1989). Monoclonal antibodies against pectin: Recognition of a conformation induced by calcium. *Plant Physiol.*, **91**, 1419–1424.

Louw, L., Tredoux, A. G. J., Rensburg, P. Van, Kidd, M., Naes, T., and Nieuwoudt, H. H. (2010). Fermentation-derived aroma compounds in varietal young wines from South Africa, **31**, 213–225.

Marcus, S. E., Blake, A. W., Benians, T. A. S., Lee, K. J. D., Poyser, C., Donaldson, L., Leroux, O., Rogowski, A., Petersen, H. L., Boraston, A., Gilbert, H. J., Willats, W. G. T., and Knox, J. P. (2010). Restricted access of proteins to mannan polysaccharides in intact plant cell walls. *Plant J.*, **64**, 191–203.

McCartney, L., Marcus, S. E., and Knox, J. P. (2005). Monoclonal antibodies to plant cell wall xylans and arabinoxylans. *J. Histochem. Cytochem.*, **53**, 543–6.

Moller, I., Marcus, S. E., Haeger, A., Verhertbruggen, Y., Verhoef, R., Schols, H., Ulvskov, P., Mikkelsen, J. D., Knox, J. P., and Willats, W. (2008). High-throughput screening of monoclonal antibodies against plant cell wall glycans by hierarchical clustering of their carbohydrate microarray binding profiles. *Glycoconj. J.*, **25**, 37–48.

Neumetzler, L., Humphrey, T., Lumba, S., Snyder, S., Yeats, T. H., Usadel, B., Vasilevski, A., Patel, J., Rose, J. K. C., Persson, S., and Bonetta, D. (2012). The *FRIABLE1* gene product affects cell adhesion in Arabidopsis. *PLoS One*, **7**, e42914.

Pedersen, H. L., Fangel, J. U., McCleary, B., Ruzanski, C., Rydahl, M. G., Ralet, M.-C., Farkas, V., von Schantz, L., Marcus, S. E., Andersen, M. C. F., Field, R., Ohlin, M., Knox, J. P., Clausen, M. H., and Willats, W. G. T. (2012). Versatile high resolution oligosaccharide microarrays for plant glycobiology and cell wall research. *J. Biol. Chem.*, **287**, 39429–38.

Pennell, R., Janniche, L., Kjellbom, P., Scofield, G. N., and Peart, J. M. (1991). Developmental regulation of a plasma membrane arabinogalactan protein epitope in oilseed rape. *Plant Cell*, **3**, 1317–1326.

Pinelo, M., Zeuner, B., and Meyer, A. S. (2010). Juice clarification by protease and pectinase treatments indicates new roles of pectin and protein in cherry juice turbidity. *Food Bioprod. Process.*, **88**, 259–265.

Ralet, M.-C., Tranquet, O., Poulain, D., Moïse, a, and Guillon, F. (2010). Monoclonal antibodies to rhamnogalacturonan I backbone. *Planta*, **231**, 1373–83.

Smallwood, M., Beven, A., Donovan, N., Neill, S. J., Peart, J., Roberts, K., and Knox, J. P. (1994). Localization of cell wall proteins in relation to the developmental anatomy of the carrot root apex. *Plant J.*, **5**, 237–246.

Smallwood, M., Martin, H., and Knox, J. P. (1995). An epitope of rice threonine- and hydroxylproline-rich glycoprotein is common to cell wall hydrophobic plasma-membrane glycoproteins. *Planta*, **196**, 510–522.

Thakur, B. R., Singh, R. K., and Handa, a K. (1997). Chemistry and uses of pectin--a review. *Crit. Rev. Food Sci. Nutr.*, **37**, 47–73.

Verhertbruggen, Y., Marcus, S. E., Haeger, A., Ordaz-Ortiz, J. J., and Knox, J. P. (2009). An extended set of monoclonal antibodies to pectic homogalacturonan. *Carbohydr. Res.*, **344**, 1858–62.

Willats, W. G. T., Gilmartin, P. M., Mikkelsen, J. D., and Knox, J. P. (1999). Cell wall antibodies without immunization : generation and use of de-esterified homogalacturonan block-specific antibodies from a naive phage display library. *plant J.*, **18**, 57–65.

Willats, W. G. T., Marcus, S. E., and Knox, J. P. (1998). Generation of a monoclonal antibody specific to 1,5-a-L-arabinan. *Carbohydr. Res.*, **308**, 149–152.

Yates, E. A., Valdor, J. F., Haslam, S. M., Morris, H. R., Dell, A., Mackie, W., and Knox, J. P. (1996). Characterization of carbohydrate structural features recognized by anti-arabinogalactan-protein monoclonal antibodies. *Glycobiology*, **6**, 131–9.

Chapter 5

Research results

Commercial wine yeast strains expressing a polygalacturonase and glucanase unravel the cell walls of Chardonnay grape pomace

This manuscript was written in the style of the journal Applied and Environmental Mircobiology

Commercial wine yeast strains expressing a polygalacturonase and glucanase unravel the cell walls of Chardonnay grape pomace

Anscha J. J. Zietsman[1], John P. Moore[1], Jonatan U. Fangel[2], William G.T. Willats[2], Melané A. Vivier[1*]

[1]Institute for Wine Biotechnology, Department of Viticulture and Oenology, Faculty of AgriSciences, Stellenbosch University, Matieland 7602, South Africa

[2]Department of Plant and Environmental Sciences, Faculty of Science, University of Copenhagen, DK-1001, Denmark

Industrial wine yeast strains expressing hydrolytic enzymes were fermented on Chardonnay pomace in buffered conditions. The enzymes produced were a native endo-polygalacturonase (EPG) and/or a recombinant endo-glucanase (EG). Analysis of the cell walls of the grape berry tissue by Comprehensive Microarray Polymer profiling (CoMPP) analysis at the end of fermentation revealed that the EG alone did not modify the cell walls but the EPG removed some homogalacturonan. A recombinant yeast strain expressing both the EPG and the EG during the fermentation displayed an even more pronounced effect with signs that the cell wall was unravelled, enabling more polymers such as rhamnogalacturonan-I (RG-I), RG-I side chains and cell wall proteins to be extracted in a pectin solvent (CDTA). Moreover, a NaOH extract (for glucan extraction) showed that the yeast expressing both enzymes could liberate more RG-I and side branches of RG-I during the fermentation. This provides the first information on the specific polymer changes brought about by a hydrolytic enzyme producing yeast strain during a fermentation on grape pomace. The cell wall profiling techniques used in this study is a valuable tool to evaluate the potential of enzyme producing microorganisms and/or enzymes added to degrade grape berry (and other plant) cell walls.

Grape processing regularly involves the use of enzymes, whether it is during the production of wine or with the valorisation of pomace, a waste product of the wine industry. These enzymes are either commercially produced and added during the production step or they can originate from the microorganisms (wild or inoculated yeast and bacteria) present in the fermenting must (1, 2). Microorganisms producing wine processing enzymes during the normal fermentation process would be highly advantageous as discussed in (3, 4). Many studies isolate and investigate the natural yeast populations found in the grape and wine environment (5) in the hope of finding new strains that will be able to conduct the wine

fermentation while contributing towards the production of beneficial enzymes. Similarly, microorganisms that can hydrolyse polysaccharides of the grape cell walls and promote the extraction of revenue-generating molecules such as polyphenols from pomace, would reduce the cost of pomace conversion (6, 7) by eliminating the need for the addition of external enzymes.

The yeast PR7 is a hybrid between *Saccharomyces paradoxus* R088 (8), a malic acid degrading strain with good oenological characteristics, and VIN13 (Anchor yeast, South Africa), a *Saccharomyces cerevisiae* commercial wine strain. This interspecies hybrid has been created at the Institute for Wine Biotechnology (IWBT) at Stellenbosch University (9) and has been commercialized by Anchor yeast (South Africa) under the trade name Exotics SPH. *S. paradoxus* R088 produces an endo-polygalacturonase (*PGU1*) (9) and PR7 inherited this gene during the hybridization process and displays similar polygalacturonase (EPG) activity than *S. paradoxus* R088, on a plate assay (10). The *S. paradoxus* RO88 Pgu1 enzyme has an optimal temperature of 45°C with only 25% residual activity at 25°C and the optimal pH is 5.5 with 43% residual activity at pH3.5 (10).

In previous studies we saw that an EPG enzyme on its own did not change the cell wall composition of grape pomace (Chapter 4), but when this was combined with an EG a synergistic (larger than EG alone) cell wall degradation effect was seen. Endo-β-1,4-glucanases randomly hydrolyzes internal β-1,4-D-glycosidic bonds in cellulose and xyloglucan, producing oligosaccharides and reducing the polymer length. An endo-glucanase gene (*end1*, EC 3.2.1.4) used in this study was obtained (11) from the bacteria *Butyrivibrio fibrisolvens* H17c. This bacterium is an important rumen bacterium and was isolated from the rumen of sheep (12), reindeer and semi-starved Zebu cattle in Kenya (13). The *end1* gene codes for a protein (*END1*) with 547 amino acids residues (11) with the catalytic domain at the N-terminus and five perfect repeats (PDPTPVD) from amino acid 412 to 447. Proline rich repeats are characteristic of bacterial cellulases (14) and often constitute the linker between the cellulose-binding domain and the rest of the protein. Proline rich regions are also common in cell wall proteins (15) and facilitate binding to other proteins and polyphenols molecules.

In an article by Van Rensburg et al. (16) the *end1* gene was expressed by *S. cerevisiae* ISP53, a haploid laboratory strain, together with the pectate lyase and polygalacturonase of *Erwinia chrysanthemi*. They found that the *END1* secretion was delayed by 24 hours compared to the two pectinases and ascribed this to the PDPTPVD repeats. The enzyme activity of *END1* was tested on a range of substrates and it was highly active against carboxymethylcellulose and lichenan which has β1-4 and β1-4; β1-3 linkages respectively. It

showed no activity against laminarin which has only β1-3 linkages, indicating activity specific for β1-4 linkages. Low activity was also found with the substrates xylan (β1-4) and p-nitrophenyl-β-D-cellobioside (β1-4), but no glucosidase and xylosidase activity could be detected. According to (17) this enzyme is irreversibly inactivated when the pH decreases below 4.5, thus this enzyme would not be active in a grape must matrix where the pH is usually below 4 (18).

With this study, we asked if the EPG produced by PR7 can degrade or change the composition of grape berry cell walls under optimal pH conditions. Additionally we wanted to investigate if the presence of an endo-glucanase would augment the cell wall degrading effect of the EPG. To this end, we produced a recombinant PR7 strain that expressed a β-1,4-D-glucanase from a genome-integrated cassette. The VIN13 strain was used as a negative control (no EPG or EG activity) and a VIN13 engineered to express the *end1* of *B. fibrisolvens* H17c gene (VIN13 END1) was used to demonstrate the effect of the endo-glucanase activity on its own. The yeast strains were fermented on autoclaved Chardonnay pomace (deseeded pulp and skins) suspended in a buffer at pH6 to ensure that both the EPG and EG expressed by the yeast strains would be active and close to their optimum pH. After the fermentation the cell walls of the Chardonnay pomace were studied with Comprehensive Microarray Polymer Profiling analysis (19) where monoclonal antibodies and carbohydrate binding modules that are specific for epitopes on the plant cell wall are used to indicate the presence and relative abundance of certain cell wall polymers. This technique was supported by the monosaccharide compositional analysis of the Chardonnay pomace cell walls, reporting the variation in the single sugar composition of the cell wall due to the different conditions/treatments in the study. Multivariate data analysis was used to detect and confirm the major patterns and trends in the data.

MATERIALS AND METHODS

Microbial strains and culture conditions. The sources and relevant genotypes of bacterial and yeast strains, as well as plasmids used in this study, are listed in Table 1. *Escherichia coli* transformants were grown in Luria-Bertani (LB) broth (Biolab) containing 12 g/l tryptone, 12 g/l NaCl and 6 g/l yeast extract supplemented with 100 μg/ml ampicillin (Roche) for plasmid selection. Yeast peptone dextrose (YPD) broth (Biolab) containing 1% yeast extract, 2% peptone and 2% glucose was used for the general culturing of yeast cells. *S. cerevisiae* transformants were cultured on yeast extract (YE) plates containing 0.5% yeast extract, 2% glucose and 3% Pastagar B (Bio-Rad Laboratories) supplemented with 150 μg/ml phleomycin (Sigma-Aldrich) or 200 μg/ml G418 (geneticin) (Sigma-Aldrich).

DNA manipulations and plasmid construction. Standard methods were used for plasmid DNA isolation, restriction enzyme digestion, ligation reactions and transformation of *E. coli* DH5α (20). All gel isolations of DNA fragments were performed with the Zymoclean DNA recovery kit (Zymo Research Corp.). TaKaRa ExTaq™ DNA polymerase (TAKARA BIO INC) was used in polymerase chain reactions (PCR) required for the manipulation of DNA while GoTaq® DNA Polymerase (Promega corporation) was used for screening and confirmation PCR reactions.

The primers and the PCR programs used in this study are listed in Table 2. PCR amplification were performed with a thermo cycler (Hybaid PCR express) and the PCR product fragments were isolated from an agarose gel, ligated into pGEM®-T Easy and transformed into *E. coli* DH5α. The integrity of the PCR products and the different clones were verified by restriction analysis and sequencing (Central Analytical Facility, Stellenbosch University).

TABLE 1 Strains and plasmids used and created in this study

STRAIN OR PLASMID	DESCRIPTION	SOURCE OR REFERENCE
Bacterial strain		
E. coli DH5a	F'ø 80ΔlacZΔM15Δ(lacZYA-*arg*F)U169 *deoR reA1 hsdR17* (r_k^- m_k^+) *supE44*l^- *thi1 gyr A96 relA1/F'proABlacI*^{q}*ZΔM15,zzf::Tn5*[*Km*^{r}]	[a]GIBCO-BRL/ Life Technologies
Plasmids		
pGEM®-T Easy	*Ap*^{R} Δ*lacZ*	[b]Promega Corporation
pUT332	*Ap*^{R} *Tn5 ble*	(21)
pUG6	*Ap*^{R} *loxP TEF2*$_P$ *kan*^{r} *TEF2*$_T$ *loxP*	(22)
pDRIVE	*Ap*^{R} *kan*^{r}Δ*lacZ*	[c]Qiagen GmbH
pAR5	*Ap*^{R}*Gt*^{R}*LEU2 ADC1*$_P$ *MF*a1$_S$ *end1 TRP5*$_T$ *ADC1*$_P$ *MF*a1$_S$ *pelE TRP5*$_T$ *ADC1*$_P$ *MF*a1$_S$ *peh1 TRP5*$_T$	(16)
pPOF1	PCR product POF1 cloned into pGEM®-T Easy	This study
pPOF1b	pPOF1 with the *Sal*I site in the [d]MCS destroyed and a new *Sal*I site introduced within the POF1 ORF	This study
pPOF1b KMX	[e]KanMX^R cloned in the *Bam*HI and *Sal*I sitesof pPOF1b	This study
pMPOF1	PCR product MPOF1 cloned into pGEM®-T Easy	This study
pMPOF1b	pMPOF1 with the *Sal*I site in the MCS destroyed and a new *Sal*I site introduced within the MPOF1 ORF	This study
pMPOF1bEND1	pGEM®-T Easy with *ADC1*$_P$ *MF*a1$_S$ *end1 TRP5*$_T$ cloned between MPOF1 homologous flanks	This study
Yeast strains		
VIN13	*Saccharomyces cerevisiae,* Commercial diploid strain	[f]Anchor yeast.
V13 KMX	VIN13 pof1::KanMX^R	This study
V13 END1	VIN13 pof1:: *ADC1*$_P$ *MFa1*$_S$ *end1 TRP5*$_T$	This study
PR7	VIN13 x *Saccharomyces paradoxus* RO88 hybrid	(9)
PR7 KMX	PR7 pof1::KanMX^R	This study
PR7 END1	PR7 pof1:: *ADC1*$_P$ *MF*a1$_S$ *end1 TRP5*$_T$	This study

[a]GIBCO/Bethesda Research Laboratories, Life Technologies Ltd.; [b]Promega corporation; [c]QIAGEN; [d]MSC, Multiple cloning site; [e]KanMX^R, geneticin resistance expression cassette; [f]Anchor yeast

Construction of integration cassette POF1-*TEF2*$_P$-*kan*^{r}-*TEF2*$_T$-POF1 (POF1-KMX). Primers POF1-L and POF1-R (Table 2) were designed to amplify the region from 112 bp on the 5' side of the start codon of the *POF1* gene, up to 466 bp on the 3' side of the stop codon. Program 1 (Table 2) were used to obtain the 1302 bp fragment (POF1) which were cloned into pGEM®-T Easy yielding pPOF1. The *Sal*I site in the multiple cloning site of this plasmid was destroyed by first cutting with this restriction enzyme and then filling up the 5' protruding ends with the DNA Polymerase I (Klenow) Large fragment (Promega Corporation) and then ligating the blunt ends. The resulting plasmid was named pPOF1a and was further modified by introducing a new *Sal*I site within the coding sequence of the *POF1* gene on the plasmid. This was achieved by using primers POF1-L and POF1-R and plasmid pMPOF1b (described in the next section) as template and PCR program 1. The 1270 bp PCR fragment was cloned into pDRIVE forming plasmid pDRIVE POF1b, whereafter the POF1b fragment (with the *Sal*I site) from pDRIVE POF1b was isolated by digestion with *Stu*I; this fragment replaced the POF1 fragment (without the *Sal*I site) in pPOF1a to yield pPOF1b. Finally, the *TEF2*$_P$ *kan*^{r} *TEF2*$_T$ cassette was isolated from pUG6 by digesting with *Xho*I and *Bgl*II and this was cloned into the *Bam*HI and *Sal*I sites of pPOF1b to yield pPOF1b KMX.

TABLE 2 Primers and PCR programs used in this study

Primer name	Sequence 5'- 3	Restriction sites included
POF1-L	AGGCCTGCCCGGGCACCCATTTTTAAGATTGGTG	*Stu* I, *Srf* I
POF1-R	AGGCCTGCCCGGGCTTGGTGATGTAATAATGTCAAG	*Stu* I, *Srf* I
POF1-M	GTACGGATCCACGTGTCGACTCGTTGGGAAGGAATAAA	*Bam* HI, *Sal* I
MaxiPOF1-L	TCGCGAGCCCGGGCCCATGGATGTTCTATGAATG	*Nru* I, *Srf* I
MaxiPOF1-R	TCGCGAGCCCGGGCCTTACACTCCAGCAAATAATC	*Nru* I, *Srf* I
exPOF1-L	AATAGCCCGACTCCGTAG	
ENDSEQ	GCCTTCAGCTTCTGTAGACT	

PCR program number	Amplification cycle*
1	94 °C, 30 s; 53 °C, 30 s; 72 °C, 90 s
2	45 °C, 30 s; 55 °C, 30 s; 72 °C, 140 s
3	94 °C, 30 s; 55 °C, 30 s; 72 °C, 34 s
4	94 °C, 30 s; 52 °C, 30 s; 72 °C, 240 s
5	94 °C, 30 s; 53 °C, 30 s; 72 °C, 150 s

* All PCR programs had an initial denaturation step at 94 °C for 5 min and a final elongation step at 72 °C for 7 min

Construction of integration cassette $_M$POF1-ADC1$_P$-MFα1s-END1-TRP5$_T$-$_M$POF1 (MPOF END1). Primers MaxiPOF1-L and -R (Table 2) were used to amplify the region from 815 bp on the 5' side of the start codon of the *POF1* coding sequence up to 784 bp 3' from the stop codon. Genomic DNA from VIN13 was used as template with PCR program 2 (Table 2). The PCR

product (MPOF1) was cloned into pGEM®-T Easy resulting in pMPOF1. The *Sal*I site of this plasmid was destroyed in the same way as with pPOF1. This plasmid was called pMPOF1a.
The next step was to introduce a new *Sal*I site within the open reading frame of the *POF1* gene that can serve as a position to introduce the END1 expression cassette. An 846 bp PCR fragment were produced using pPOF1 as template, primer pair POF1-M and POF1-R and PCR program 3. This PCR product was cut with restriction enzymes *BamH*I and *Sna*BI and ligated into the corresponding restriction enzyme sites of pMPOF1a, yielding pMPOF1b. The final step was to isolate the 2820 bp *ADC1*$_P$-*MFα1s-END1-TRP5*$_T$ fragment from pAR5 (*Sal*I) and clone this into the newly created *Sal*I site of pMPOF1b to yield pMPOF1bEND1 (Fig.1B).

Yeast transformation. Plasmids pPOF1b KMX and pMPOF1bEND1 were digested with *Stu*I and *Sma*I respectively to liberate the integration cassettes from the rest of the plasmids. VIN13 and PR7 were transformed, first with the POF KMX integration cassette (from pPOF1b KMX), according to the electrophoresis protocol described in (23). However, a few changes were made: the yeast culture was grown until exponential phase (OD_{600} = 0.8), the DNA integration cassette concentration was increased to 4 µg and the regeneration after the electroporation pulse was done overnight. The integration events were targeted to the *POF1* locus by exploiting the natural yeast homologous recombination system. Putative (V13 KMX and PR7 KMX) transformants were selected from YE-G418 plates. After confirming the integration event with PCR (see next section), two transformed yeasts were selected for the next round of transformations. During this round, the POF-KMX cassette was replaced by the MPOF END1 expression cassette. This was a co-transformation where 100 ng of pUT332 plasmid was added to the 4 µg MPOF END1 expression cassette DNA. The pUT332 plasmid was used as a screening tool in order to limit background colonies. Putative transformants were selected from YE-phleomycin plates and transferred with sterile toothpicks to YE-G418 plates (negative screen) in order to select colonies whose POF KMX cassette was putatively replaced by the MPOF END1 cassette.

Verifying the yeast transformants and the position of integration. The integration of the POF1 KMX cassette into the POF1 locus of the VIN13 and PR7 genome was confirmed by using primers POF1-L and KanMX-Rp (PCR program 2) on genomic DNA isolated (according to the protocol by (24)) from colonies growing on YE-G418 plates. After replacing the POF KMX with MPOF END1 expression cassette, primers END1SEQ and MaxiPOF1-L were used with PCR program 4, to screen the putative VIN13 END1 and PR7 END1 strains. The presence of a PCR product of 1971 bp indicated that the *POF1* locus was successfully interrupted by the *END1* expression cassette.

The position of the integration event was further investigated by designing a primer, exPOF1-L that aligns on the yeast genome, 167 bp 5' from the target for homologous recombination. This

primer was used together with primer ENDSEQ (PCR program 5) to yield a band size of 2138 bp that indicated a successful integration.

By using primers POF1-L and POF1-R and genomic DNA of V13 END1 transformant # 1.8 and PR7 END1 transformant # 4.7 we could establish whether the integration event happened only at the one POF1 locus or at both loci of these two diploid yeast strains. A PCR product of 1274 bp would indicate the presence of an undisrupted POF1 locus while a band at 3944 bp would indicate that the locus was disrupted with the MPOF END1 integration cassette.

Enzyme activity. To confirm that the integrated expression cassettes lead to the production of an active recombinant β-1,4-glucanase, cells from VIN13 END1 and PR7 END1 colonies were transferred to carboxymethyl cellulose (CMC) plates (0.5% yeast extract, 2% glucose, 2% agar, 1% CMC) and grown for 3 days at 30°C, whereafter the colonies were washed off with sterile distilled water. The plates were then flooded with 0.1% Congo red for two hours followed by a de-staining step with 1 M $NaCl_2$. A clear/light yellow zone indicated β-1,4-glucanase activity. The activity of the native polygalacturonase enzyme of PR7 and PR7 END1 strains was confirmed with a plate assay previously described in (25).

Curing of the pUT332 plasmid and stability of yeast transformants. The yeast strains were cultivated in YPD media at 30°C for 100 generations. Each day some cells were transferred to fresh media and the absorbance at OD_{600} were determined at the end and start of each subculture in order to calculate the number of generations. At the end of 100 generations the GMY culture were plated on YPD medium. One hundred randomly selected colonies were analysed for the presence of the *end1* gene. Two different methods were used. Initially, yeast colonies were dissolved in 5 µL of sterile distilled water and the suspension were transferred to QIAcard FTA cards (QIAGEN). The cards were prepared as specified by the manufacturer and used as template in a PCR reaction to detect the presence of the *end1* gene using primers END1SEQ and exPOF1-L as previously described. Additionally the colonies were transferred to CMC plates and tested for the activity of the β-1,4-glucanase activity as previously described. Finally, the colonies were tested for sensitivity towards phleomycin by transferring them with sterile toothpicks to YE-pheomycin plates. If colonies were unable to grow on these plates, it is an indication that the yeast cells discarded the pUT332 plasmid during the 100 generations that they were grown under non-selective conditions.

Fermentation on pomace. *Vitis vinifera* cv Chardonnay grapes were harvested in the Boland region of South Africa and the pomace was obtained after the grapes were pressed. The pomace was kept at -20°C until processed, which entailed seed removal and blending with a

food processor. The chopped/blended pomace was then suspended as a 15% (w/v, wet weight) suspension in a 0.12 M citrate phosphate buffer at pH 6 and autoclaved (121°C, 15 min, 100 kPa) to sterilize as well as destroy the native grape and microbial enzymes. The yeast strains (VIN13, V13 END1, PR7 and PR7 END1) were grown in YPD and inoculated at a cell density of ca. 2.2 x 10^7 cells/ml into the pomace suspension (determined with plate counts just after inoculation). The pomace cultures were fitted with fermentation caps and incubated with shaking at 30°C for 144 h. All fermentations were done in quadruplicate and after incubation, the supernatant and solids were separated by centrifugation and frozen at -20°C until further analysed.

Analysis of the pomace fermentation supernatants. Two samples per biological repeat were taken one hour after inoculation, at 48 h, 120 h and at 144 h (end of fermentation) in order to determine the reducing sugars using the method described by Ghose (26). The pH of all the supernatants (the average of two technical repeats), as well as the viable yeast cell count, was determined on the final day.

Isolation of cell walls or alcohol insoluble residue (AIR) from pomace solids. The frozen pomace pellets (representing all the solid material from one biological repeat), collected at the end of the fermentation, were freeze-dried and then dry milled and homogenized with a Retsch MM400 mixer mill (Retsch, Germany) at a frequency of 30 Hz for 30 seconds. The resulting powder was used for the isolation of the cell walls using the method described by Ortega-Regules et al. (27) with some changes. The first acetone step after the buffered phenol extraction was omitted. Furthermore, after the third acetone wash the excess acetone was removed under a slight vacuum and the remaining cell walls or alcohol insoluble residue (AIR) was then mixed with an equal volume of sterile distilled water, frozen at -80°C and then freeze-dried.

Monosaccharide analysis of cell wall samples. The monosaccharide composition of the AIR isolated from the pomace was analyzed according to the method described in (28, 29), with some modifications. Approximately 5 mg of AIR was hydrolyzed (two technical repeats per biological repeat) to monosaccharides followed by derivatization to methoxy sugars at 80°C for 16 h. After silylation with HMDS + TMCS + Pyridine 3:1:9 (Sylon HTP) kit (Supelco, USA) the derivatives were separated and analyzed in a gas chromatograph, Agilent 6890 N (Agilent, Palo Alto, CA) coupled to a Agilent 5975 MS mass spectrometer detector, using a polar (95% dimethylpolysiloxane) ZB-Semivolatiles Guardian (30 m, 0.25 mm ID, 0.25 µm film thickness) GC column. The oven temperature was maintained at 70°C for 2 min, ramped at 1°C/min to 76°C, then at 8°C/min to 300°C and then held for 5 min. We expressed the monosaccharide composition as the mole percentage contribution of each monosaccharide in relation to the nine

common plant cell wall monosaccharides present. Error bars in the histogram represent the mean of four biological samples.

Comprehensive microarray polymer profiling (CoMPP) analysis of cell wall fractions. One AIR sample (10 mg) from each biological repeat was weighed off and used for CoMPP analysis. Sequential extractions, according to the procedure described in Moore et al. (30), were performed on these 10 mg AIR samples, using the solvents CDTA (diamino-cyclo-hexane-tetra-acetic acid) and NaOH respectively. CDTA extracts mainly pectin-rich polymers from the cell wall particles and the second extraction with NaOH extracts all the hemicellulose-rich polymers. A selection of monoclonal antibodies (mAbs) and carbohydrate binding modules (CBMs) were chosen to cover the variety of epitopes expected in the grape cell wall. A full list is provided in the Appendix (Table A1). Arrays printed with the different fractions were probed individually with the mAbs and CBMs as described in Moller et al. (2007). Each sample was represented by five microarray spots and a mean spot signal was calculated whereafter it was normalized to the highest signal (set as 100) in the dataset. A cut-off value of five was imposed on the data.

Multivariate and univariate statistics. Univariate statistical analysis (unpaired T-test, 95% confidence level) was performed on monosaccharide data. Multivariate analysis by means of principle component analysis (PCA) (31) was performed using SIMCA 13 software package (Umetrics AB, Sweden).

RESULTS

Construction of genetically modified yeast. Two integration cassettes were developed for this study. The one (Fig. 1A) contained the expression cassette that conveys resistance towards geneticin/G418 (*TEF_P kan^r TEF_T*) with flanking regions that are homologous to the *POF1* locus on the genome of *S. cerevisiae*. The second integration cassette (Fig. 1B) contained the expression cassette for the EG gene (*end*1) from *B. fibrisolvens* under control of the *S. cerevisiae ADC*1 promoter and MFα1 secretion signal. This expression cassette is also flanked with the *POF1* homologous regions of the first integration cassette but the homologous regions were larger (extended outwards towards the 5'and 3' ends of the *POF1* locus). The larger homologous region in the MPOF END1 integration cassette was designed to ensure that the MPOF END1 integration cassette would be able to replace the first integration cassette (POF KMX) on the yeast genome in two consecutive integration events. With the second integration, the pUT332 plasmid was co-transformed with the linear MPOF END1 integration cassette and the putative transformants were plated on YE-phleomycin plates. This ensured that only colonies that took up foreign DNA (pUT332 and MPOF END1 expression cassette or just pUT332) would need further screening for EG activity. After curing the yeast of the pUT332

plasmid, this strategy (32) ensured that the final recombinant yeast would have no bacterial resistance markers or other foreign DNA, except the *end1* gene, in its genome.

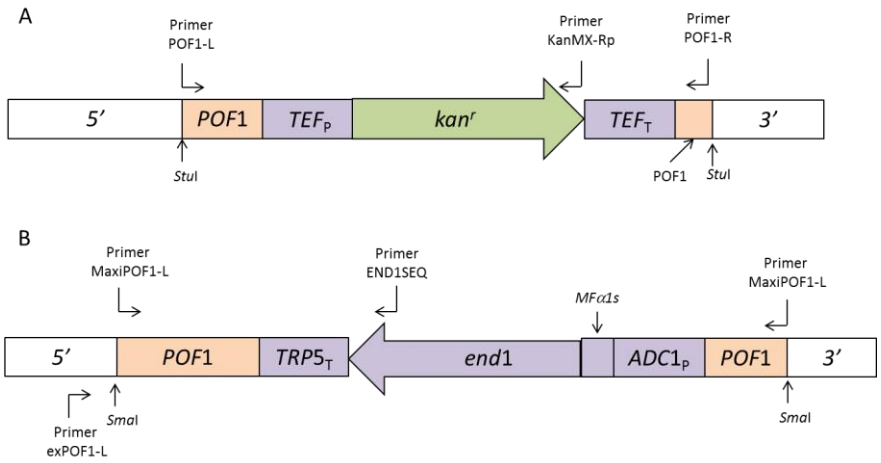

FIG 1A & B. Schematic presentation of the integration cassettes prepared for the disruption of the *POF1* gene on the genome of VIN13 and PR7. The primer alignment positions of POF1-L and –R as well as MaxiPOF1-L and –R, that were used to amplify the *POF1* homologous regions are indicated on the diagram. Primers that were used to confirm the integration event at the intended position on the genome (exPOF1-L, MaxiPOF1-L and END1SEQ) are indicated.

VIN13 transformed with the *kan*^{r} integration cassette delivered more than 200 putative transformants showing resistance to G418. Genomic DNA of ten of these putative transformants (randomly chosen) were tested for the presence of the *kan*^{r} integration cassette with primers POF1-L and KanMX-Rp, and 9 of the transformants gave the correct PCR product of 2130bp (Fig. 2A). The first transformant was selected for the subsequent co-transformation with MPOF END1 and pUT332 and this resulted in 1700 putative transformants. These putative transformants were screened for restored sensitivity towards G418, which would indicate that the *kan*^{r} integration cassette was replaced by the MPOF END1 integration cassette. Eighteen putative V13 END1 transformants were isolated from the master plates and transferred to CMC plates to test for *end1* enzyme activity. Nine of the eighteen putative V13 END1 transformants showed EG activity on the CMC plates (data not shown) and from those genomic DNA were isolated. Primer pair END1SEQ and MPOF-1 was used to test for positive integration events (Fig. 2B) and a PCR product at 1971bp (indicating the presence of the END1 expression cassette at the intended position on the yeast genome) was achieved for all of the nine transformants.

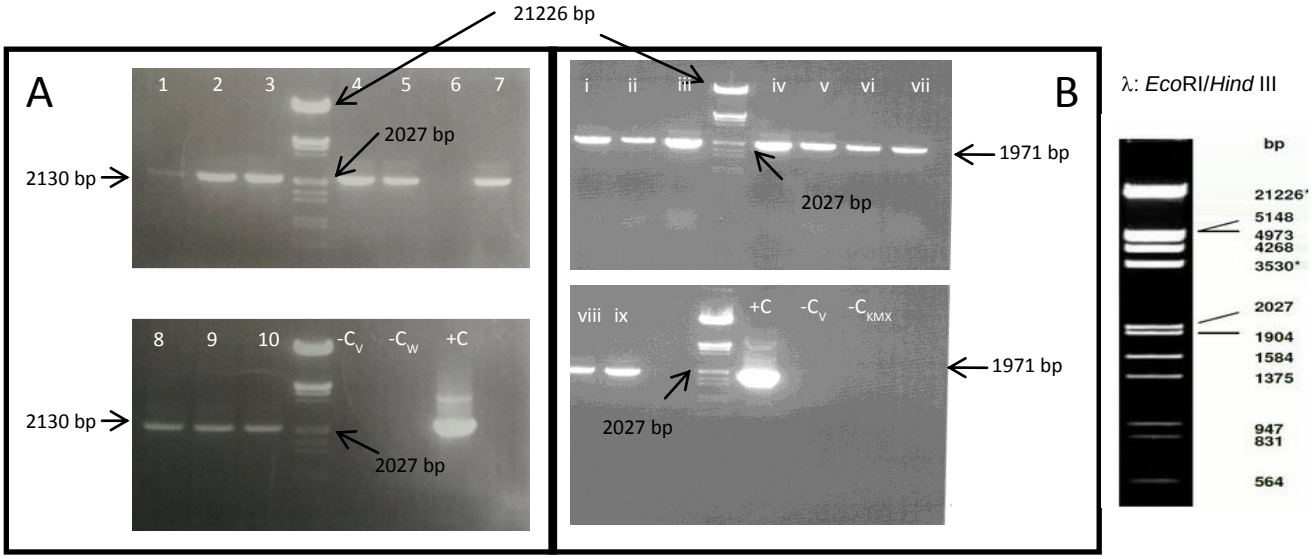

Fig 2 (A) Proof of integration of the *kan*^{r} integration cassette into the VIN13 genome with ten putative transformants of V13 KMX. A PCR product of 2130bp with primer pair POF1-L and KanMX-Rp were obtained for nine of the ten transformants. Genomic DNA of VIN13 (-C_V) and MilliQ water (-C_W) were used as a negative control while pPOF1bKMX DNA were used as positive control (+C) for the PCR reaction. **(B)** A PCR product of 1971 bp indicated that the correct integration of the END1 integration cassette took place at the *POF1* locus of VIN13. On the gel the V13 END1 yeast transformants were in lane i, transformant # 1.8; lane ii, 1.26; iii, 29.30; iv, 36.31; v, 45.18; vi, 46.29; vii, 47.1; viii, 52.14; ix, 34.3. Plasmid pMPOF1bEND1 was used a positive control (+C), and negative controls were VIN13 (-C_V) and V13 KMX (-C_{KMX}). The DNA molecular weight marker was Lambda DNA cut with restriction enzymes *Eco*RI and *Hind*III.

The same procedure for the integration of the END1 integration cassette was followed for the PR7 yeast strain. Eleven PR7 KMX transformants were obtained and verified with primers exPOF1-L and KanMX-Rp (PCR product 2297bp) (data not shown). The first positive transformant (named PR7 KMX # 1) were used in the follow up transformation, which rendered 1800 putative transformants. After screening 520 of these transformants for G418 sensitivity, eleven did not grow on YE-G418 plates and eight of the eleven gave a PCR product (1971bp) using the exPOF1-L and ENDSEQ primer pair (Fig. 3). Two transformants (PR7 END1 # 10.10 and 4.17) were tested on CMC plates for endo-glucanase activity and both were positive (Fig. 4). The integration strategy was therefore successful in both the VIN13 and PR7 yeast strains.

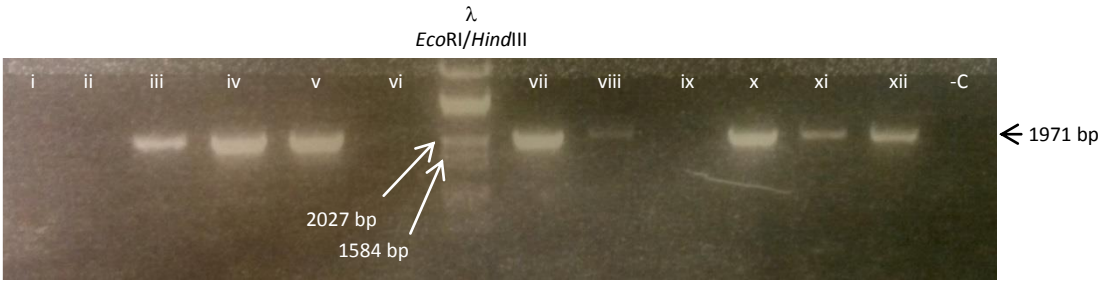

FIG 3 PR7 END1 recombinant transformants identified with PCR using primer pair exPOF1-L and ENDSEQ. A product of 1971 bp indicates that the END1 integration cassette was integrated at the correct position on the PR7 genome. Lane i, transformant # 2.31; ii, 3.1; iii, **3.28**; iv, **4.17**, v, **4.31**; vi, 4.40; DNA molecular weight marker (λ: *Eco*RI/*Hind*III), vii, **4.51;** viii, 6.44; ix, 7.17; x, **10.10**; xi, **10.19**; xii, **10.41.** The transformants that gave the correct PCR product are shown in bold letters. Genomic DNA of PR7 was used as negative control (-C).

VIN13 and PR7 are both diploid yeast strains (9) which would allow the integration of two copies of the MPOF END1 integration cassette into the genome of these yeast strains. A PCR reaction on the genomic DNA of V13 END1 # 1.8 and PR7 END1 # 4.17 with primers POF1-L and POF1-R yielded PCR products of 3944 bp (data not shown) indicating that both copies of the *POF1* gene were disrupted. The undisrupted POF1 gene would have given a PCR product of 1274 bp.

Activity of the recombinant and native yeast enzymes. After confirmation of the integration of the MPOF END1 expression cassette into the genomes of VIN13 and PR7 the activity of the recombinant EG enzyme in the V13 END1 and PR7 END1 strains as well as the native polygalacturonase strains was tested. Positive (light yellow to clear zones on CMC plates) zones could be seen (Fig. 4A) for all the VIN13 END1 and PR7 END1 GMY's (indicating EG activity) while the untransformed VIN13 and PR7 strains showed no zone. All the PR7 strains showed clear zones inside a white ring (Fig. 4B) indicating an active native polygalacturonase, while VIN13 strains gave no clearing zones.

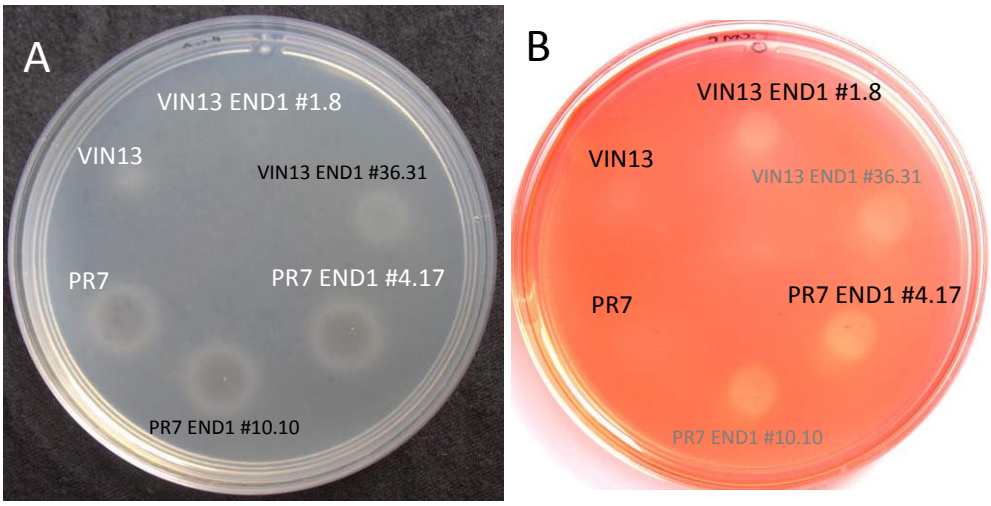

FIG 4A & B. (A) Polygalacturonase activity (clear zones inside white rings) on a polygalacturonic agar plate and (B) endo-β-1,4-glucanase activity (light yellow zones) on a CMC agar plate with the yeast strains used in this study (VIN13, VIN13 END1 # 1.8, PR7, PR7 END1 # 4.7). Other strains that were also successfully integrated with the MPOF END1cassette (VIN13 END1 # 36.31 and PR7 END1 # 10.10) are also shown here, but they were not used in the pomace fermentations.

Curing of pUT332 and stability and of the integrated expression cassette. Yeast colonies harboring the β-1,4-glucanase expression cassette were tested for the stability of the integration event. The GMY were cultivated for 100 generations whereafter 100 colonies of each strain were tested by PCR and on activity plates for the presence of the recombinant gene. All strains showed 100% stability of the integration (data not shown) and the loss of pUT332 were proven by their inability to grow on agar plates containing phleomycin.

Fermetation on Chardonnay pomace. Transformed yeast strains VIN13 END1 # 1.8 and PR7 END1 # 4.17 (henceforth called VIN13 END1 and PR7 END1) were chosen to use in all subsequent fermentations on pomace, together with untransfromed VIN13 and PR7. The reducing sugar in the supernatant of the pomace suspension increased from 22 mg/ml to 25.9 mg/ml during the autoclaving process. The progress of the fermentation was followed by recording the weight loss (data not shown) and the decrease in reducing sugars on the first day (an hour after inoculation), after 48 h, 120 h and 144 h (last day) (Fig. 5). All the yeast fermentations reduced the sugar within 48 h to less than 3 mg/ml and at the end of the fermentation period (144 h) the reducing sugar concentrations were 1.93 (VIN13), 1.87 (V13 END1), 2.04 (PR7) and (PR7 END1) 2.04 mg/ml repectively.

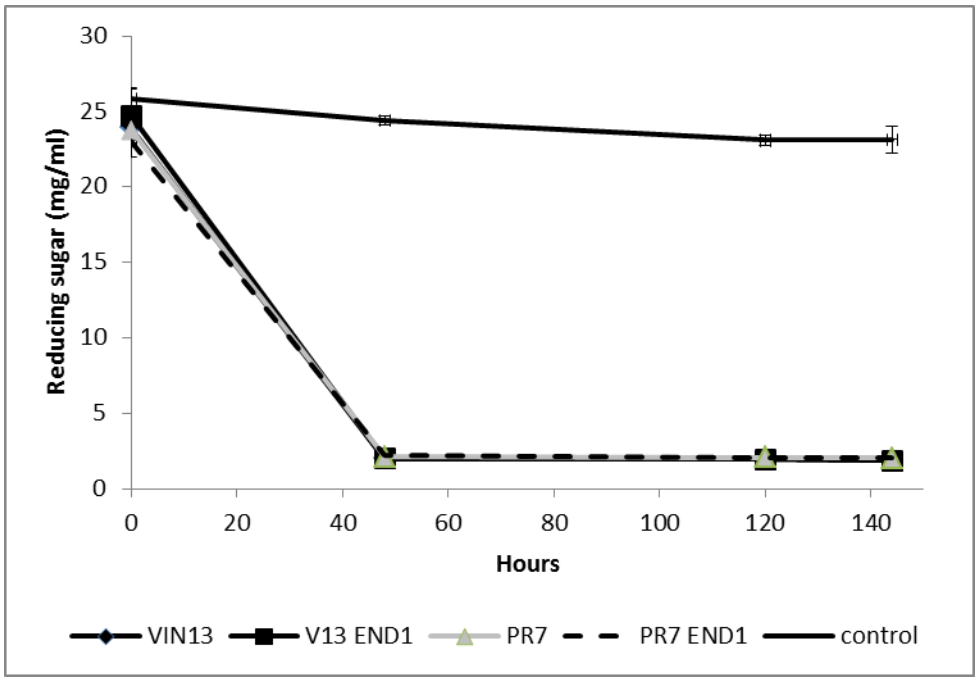

FIG 5. Reducing sugars in the supernatant of the fermentations with the yeast strains VIN13, VIN13 END1, PR7 and PR7 END1, with Chardonnay pomace suspension as substrate. The values are the average of four biological repeats.

The pH of the pomace suspension after autoclaving was 5.7 and this changed to 5.9 in the control reaction while the pH of the yeast fermentations was stable at 5.7. Thus, the recombinant EG protein that is irreversibly inactivated at pH values below 4.5 (17) would not have been negatively affected by pH during the fermentation. The same applies for the native EPG of PR7 [optimum pH of 5.5 (10)] if we assume that it has the same properties as the EPG expressed by the parent strain, *S. paradoxus* RO88.

Analysis of the pomace fermentation residue. In order to determine if the hydrolytic enzymes (EG and EPG) produced by the yeast strains (V13 END1, PR7 and PR7 END1) changed the cell wall composition of the pomace, we analysed the AIR isolated from pomace residue at the end of the fermentations. The results from V13 END1, PR7 and PR7 END1 were compared with the control fermentation (no yeast present) and the VIN13 fermentation (no EG or EPG activity).

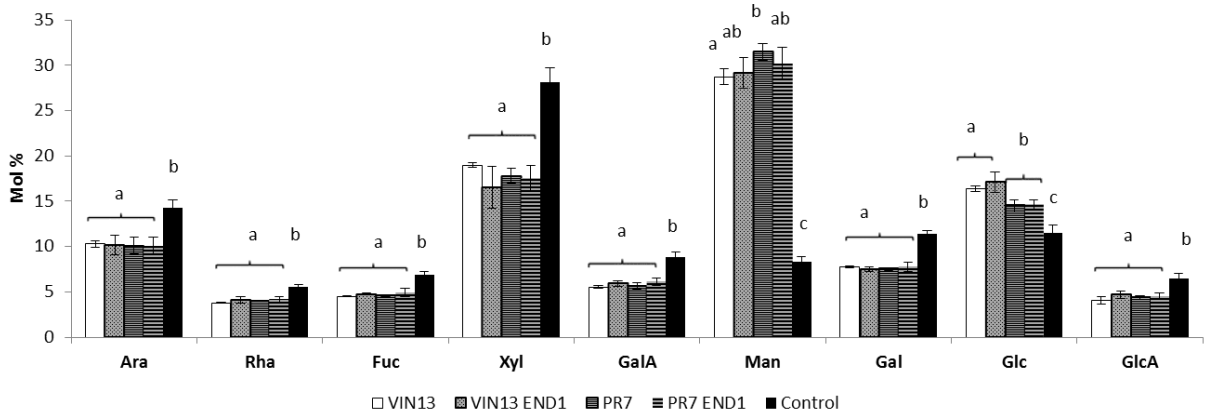

FIG 6 Monosaccharide composition of the cell walls isolated from Chardonnay pomace fermented with different yeast strains. The bars represent the average of four biological and two technical repeats. Different letters indicate a statistical significant difference (95% confidence interval) between the different treatments for a specific monosaccharide. Ara, arabinose; Rha, rhamnose; Fuc, fucose; Xyl, xylose; GalA, galacturonic acid; Man, mannose; Gal, galactose; Glc, glucose, GlcA, glucuonic acid.

There is a significant (95% confidence interval) difference in the monosaccharide levels between the unfermented (control) samples and all the other treatments (VIN13, PR7, VIN13 END1 and PR7 END1). The fermentation process decreases the mol% of all the monosaccharides except Man (mannose) and Glc (glucose). These two monosaccharides were higher in the fermented samples probably due to the high levels of Man and Glc present in the cell walls of the yeast inoculated to perform the fermentations. At the end of the fermentation, the pomace solids were separated from the supernatant by centrifugation and the yeast cells were thus collected and freeze-dried together with the pomace residue. The *S. cerevisiae* cell wall composition varies depending on the growing conditions but on average it contains 35 – 40 % mannoproteins, 5-10% β-1,6-glucan, 50-55% β-1,3-glucan and 1-2% chitin (wall dry weight [%]) (33). The slight differences between VIN13 and PR7 Glc (16.4% and 14.5% respectively) levels are probably due to differences in their glucan cell wall content (Moore et al, unpublished). It is not clear why all the other monosaccharides were lower in the fermented pomace cell walls than in the control samples. From previous results, we know that the levels of Ara (arabinose) in cell walls of Pinotage skins decrease during alcoholic fermentation (Chapter 3) which is probably due to the mobilisation of arabinan and arabinogalacturonan proteins (AGPs) to the fermenting must. However, none of the other decreases was previously seen and because the monosaccharide levels are given as a mol% relative to each other, the decrease might only be in response to the increase in Man and Glc (due to the presence of yeast cell walls).

The CoMPP data (Fig. 7) analyzing the CDTA (pectin rich) fraction shows that only low levels of homogalacturonan (HG) (mAbs LM18 and LM19) were still present in the pomace cell walls after the autoclaving step (control sample). Relative high levels of unbranched rhamnogalacturonan-I (RG-I) (mAbs INRA-RU1 and INRA-RU2) could be extracted as well as some RG-I side chains (mAbs LM5 and LM6). The CDTA fraction extracted from the control samples also contained β-1,3- D-glucan (mAb BS-400-2), xyloglucan (mAb LM25), extensins (mAbs JIM11 and JIM20) and AGPs (mAbs JIM8, JIM13 and LM2). A clear fermentation response is a high signal for β-1,3-D-glucan (mAb BS-400-2) in all the fermented samples. The BS-400-2 mAb recognize β-1,3- D-glucan, also known as callose (a polymer formed in plant tissue as a response to wounding or pathogen attack), but it also probably recognizes the β-1,3-D-glucan that is part of the yeast cell wall. This corresponds with the high levels of Man and Glc found with the monosaccharide analysis of the fermented samples.

	HG, low DE (mAb JIM5)	HG, high DE (mAb JIM7)	HG, Partially ME (mAb LM18)	HG, Partially ME (mAb LM19)	HG, Partially ME (mAb LM20)	HG (±30 contiguous non-ME GalA)(mAb PAM1)	HG (Ca2+ dimers)(mAb 2F4)	Xylogalacturonan (mAb LM8)	RG-I (unbranched, 6 disacch) (mAb INRA-RU1)	RG-I (unbranched, 2 disacch) (mAb INRA-RU2)	(1→4)-β-D-galactan (mAb LM5)	(1→5)-α-L-arabinan (mAb LM6)	Linearised (1→5)-α-L-arabinan (mAb LM13)	(1→4)-β-D-(galacto)(gluco)mannan (mAb LM21)	(1→4)-β-D-(gluco)mannan (mAb LM22)	(1→3)-β-D-glucan (mAb BS-400-2)	Xyloglucan (XXXG motif) (mAb LM15)	Xyloglucan (XLLG oligosaccharide) (mAb LM24)	Xyloglucan (mAb LM25)	(1→4)-β-D-xylan (mAb LM10)	(1→4)-β-D-xylan/arabinoxylan (mAb LM11)	Cellulose (crystalline) (mAb CBM3a)	Extensin (mAb LM1)	Extensin (mAb JIM11)	Extensin (mAb JIM20)	AGP (mAb JIM8)	AGP (mAb JIM13)	AGP (mAb LM14)	AGP, β-linked GlcA (mAb LM2)
VIN13	5	0	9	10	0	0	0	0	47	38	20	14	0	0	0	75	0	0	11	0	0	0	0	21	30	22	46	0	12
VIN13 END1	0	0	9	10	0	0	0	0	43	35	17	11	0	0	0	75	0	0	9	0	0	0	0	17	26	17	39	0	9
PR7	0	0	0	0	0	0	0	0	41	33	19	12	0	0	0	58	0	0	10	0	0	0	0	17	25	19	39	0	9
PR7 END1	0	0	0	0	0	0	0	0	51	43	22	16	0	0	0	74	0	0	14	0	0	0	6	27	37	26	51	0	15
Control	**0**	**0**	**11**	**13**	**0**	**0**	**0**	**0**	**46**	**36**	**16**	**11**	**0**	**0**	**0**	**8**	**0**	**0**	**13**	**0**	**0**	**0**	**0**	**17**	**27**	**22**	**47**	**0**	**12**

0	10	20	30	40	50	60	70	80	90	100

FIG 7. CoMPP data showing the relative abundance of cell wall polymers that were extracted with CDTA from AIR. The AIR was isolated from Chardonnay pomace fermented with yeast producing hydrolytic enzymes (V13 END1, PR7 and PR7 END1, as well as VIN13 as a no-enzyme control). The values are the average of four biological samples.

The recombinant PR7 END1 yeast strain that produces both a native EPG and a recombinant EG seems to have an influence on the pomace cell wall composition in the following ways: (1) There was a decrease in HG (mAbs LM18 and LM19) and this can also be seen for the untransformed PR7 that only produces an EPG. (2) The PR7 END1 strain caused an increase in the labelling for unbranched RG-I polymers (mAbs INRA-RU1 and INRA-RU2) (3) and a slight

increase in the RG-I side chains (mAbs LM5 and LM6). (4) Finally, we also saw an increase in the cell wall proteins for the samples fermented with PR7 END1 (mAbs JIM11, JIM20 and JIM13). All these changes suggest that cell wall depolymerization took place and the structure of the cell wall was unravelled which enabled depectination of the HG polymers and enhanced the solubilization of the other polymers mentioned, into the CDTA extract. The degradation and disappearance of partially methylesterified HG labelling (mAbs LM18 and LM19) for both PR7 strains might be an indication that this yeast strain has pectinmethylesterase activity in addition to the EPG activity although there is no evidence for this in literature. The study by Eschstruth and Divol (10) did not report an increase in methanol concentration for wine fermented by the PR7 or *S. paradoxus* R088 strains. Furthermore, it seems that the hydrolysis by the recombinant EG is making a significant contribution towards the unravelling effect since the PR7 strain without the EG does not show an increase in the labelling for any of the other polymers besides the HGs. In general, the strong signal for extensins labelled by mAbs JIM11 and JIM20 in all the samples indicates that the pomace is pulp rich and skin cell walls are not dominating the results (Moore et al., unpublished). Finally, it is also interesting to see the low value (compared to the other yeast fermented samples) for mAb MS-400-2 in the PR7 samples (Fig. 7), however this was only seen in the CDTA fraction and it is highly unlikely that this is due to hydrolytic action by PR7.

Multivariate data analysis (SIMCA 13, Umetrics AB, Sweden) (Fig. 8) show that the PR7 END1 samples cluster together and separate from the control samples along the first component axis (PC1 47%). The separation is driven by an abundance of RG-I side chains, unbranched RG-I and cell wall proteins in the PR7 END1 samples. PR7 and PR7 END1 separated from the VIN13 and control samples along the second component axis (PC2 13%) because of the abundance in mAbs LM18 and LM19 in the latter samples. In Fig. 8 the variable mAb BS-400-2 were excluded in the analysis to see the differences between the samples without the contribution of (presumably) the yeast cell wall. The exclusion of this variable had very little effect (PC1 changed from 46% to 47% and PC2 were unchanged), and furthermore, the samples and variables had nearly identical distribution patterns than on the original score and loading plot.

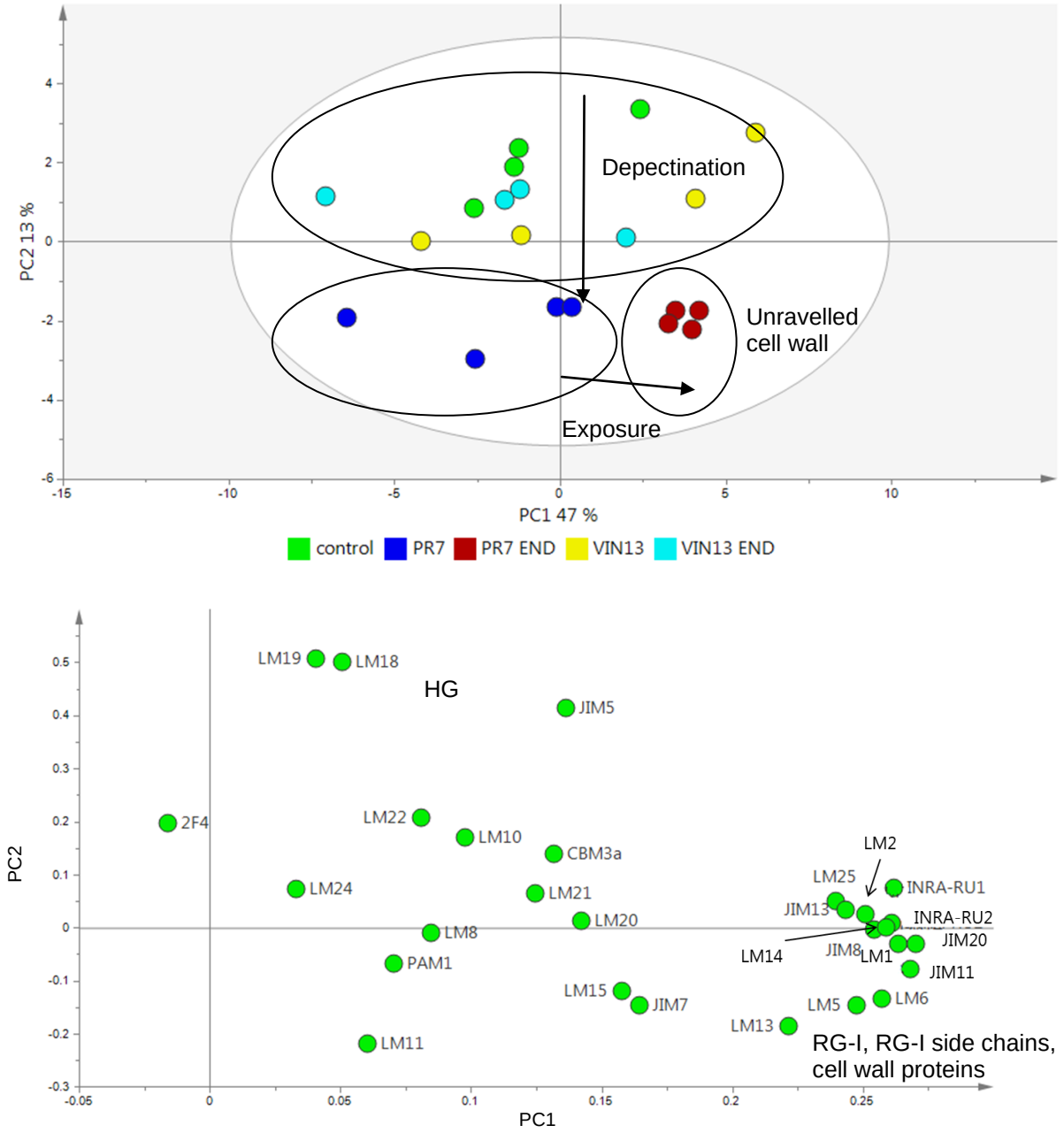

Fig 8. CDTA fraction of the CoMPP data showing the effect of the yeast fermentations on the pomace cell wall composition. The variable BS-400-2 were excluded from the analysis. The PCA score plot at the top shows the PR7 END1 samples clustering together on the opposite side of the control (unfermented) samples.

In the NaOH fraction (Fig. 9, heat map) all the fermented samples show a high abundance in β-1,3-glucan (mAb BS-400-2) similar to the CDTA fraction, but they also showed an increase in the labelling for HG (mAbs PAM1 and LM19), RG-I (mAbs INRA-RU1 and INRA-RU2) and β-1,4-D-galactan and α-1,5-L-arabinan (mAbs LM 5 and LM6 respectively). The combination of EPG and EG activity in PR7 END1 showed the largest increase (compared to the other fermented samples) in RG-I and RG-I side chains but in contrast to the CDTA fraction they caused no increase in the cell wall proteins in the NaOH fraction. Thus, although it was possible

to see a difference between PR7 END1 and all the other fermented samples, the effect was less clear as in the CDTA fraction.

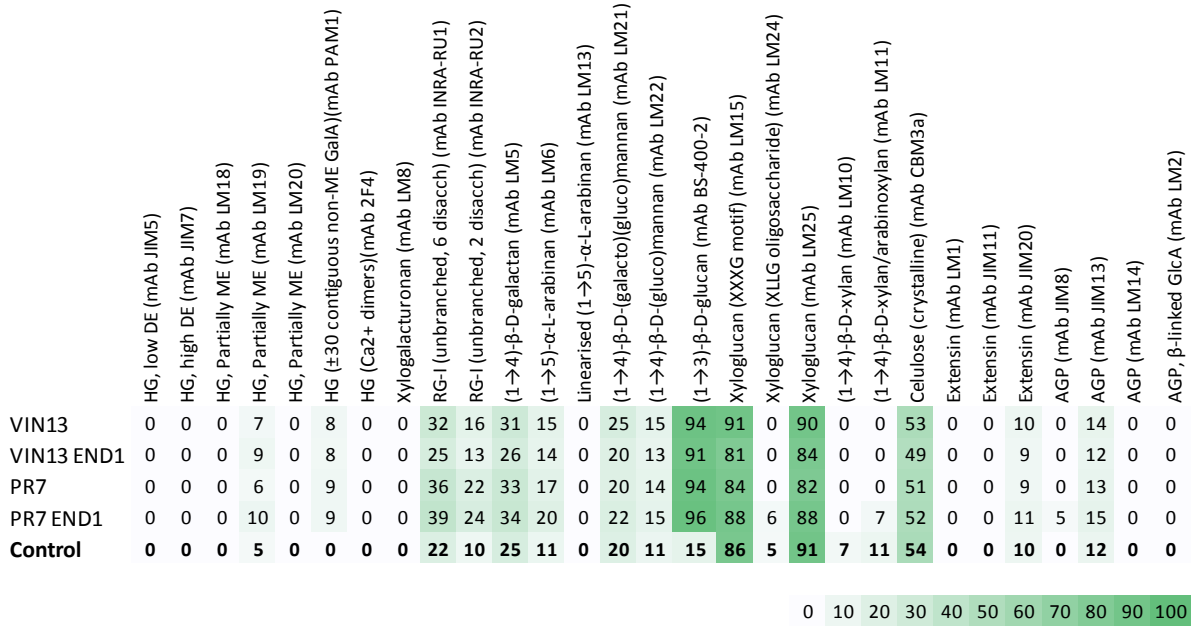

	HG, low DE (mAb JIM5)	HG, high DE (mAb JIM7)	HG, Partially ME (mAb LM18)	HG, Partially ME (mAb LM19)	HG, Partially ME (mAb LM20)	HG (±30 contiguous non-ME GalA)(mAb PAM1)	HG (Ca2+ dimers)(mAb 2F4)	Xylogalacturonan (mAb LM8)	RG-I (unbranched, 6 disacch) (mAb INRA-RU1)	RG-I (unbranched, 2 disacch) (mAb INRA-RU2)	(1→4)-β-D-galactan (mAb LM5)	(1→5)-α-L-arabinan (mAb LM6)	Linearised (1→5)-α-L-arabinan (mAb LM13)	(1→4)-β-D-(galacto)(gluco)mannan (mAb LM21)	(1→4)-β-D-(gluco)mannan (mAb LM22)	(1→3)-β-D-glucan (mAb BS-400-2)	Xyloglucan (XXXG motif) (mAb LM15)	Xyloglucan (XLLG oligosaccharide) (mAb LM24)	Xyloglucan (mAb LM25)	(1→4)-β-D-xylan (mAb LM10)	(1→4)-β-D-xylan/arabinoxylan (mAb LM11)	Celulose (crystalline) (mAb CBM3a)	Extensin (mAb LM1)	Extensin (mAb JIM11)	Extensin (mAb JIM20)	AGP (mAb JIM8)	AGP (mAb JIM13)	AGP (mAb LM14)	AGP, β-linked GlcA (mAb LM2)
VIN13	0	0	0	7	0	8	0	0	32	16	31	15	0	25	15	94	91	0	90	0	0	53	0	0	10	0	14	0	0
VIN13 END1	0	0	0	9	0	8	0	0	25	13	26	14	0	20	13	91	81	0	84	0	0	49	0	0	9	0	12	0	0
PR7	0	0	0	6	0	9	0	0	36	22	33	17	0	20	14	94	84	0	82	0	0	51	0	0	9	0	13	0	0
PR7 END1	0	0	0	10	0	9	0	0	39	24	34	20	0	22	15	96	88	6	88	0	7	52	0	0	11	5	15	0	0
Control	**0**	**0**	**0**	**5**	**0**	**0**	**0**	**0**	**22**	**10**	**25**	**11**	**0**	**20**	**11**	**15**	**86**	**5**	**91**	**7**	**11**	**54**	**0**	**0**	**10**	**0**	**12**	**0**	**0**

0 10 20 30 40 50 60 70 80 90 100

FIG 9. CoMPP data showing the relative abundance of cell wall polymers extracted with NaOH from AIR. The AIR was isolated from Chardonnay pomace fermented with yeast that produces hydrolytic enzymes (EPG and/or EG). The values are the average of four biological samples.

A PCA plot (that excludes mAb BS-400-2) confirmed the differences seen in Figure 9 and showed the PR7 strains located on the opposite side of the plot from the control samples. The separation was driven by an abundance in RG-I and RG-I side chains. The fermented samples were separated from the controls because of an abundance in HG (mAb PAM1). Again, the exclusion of mAb BS-400-2 did not influence the PCA analysis with the general distribution pattern staying the same and PC1 only changing from 34 to 35% and PC2 from 20 to 18%.

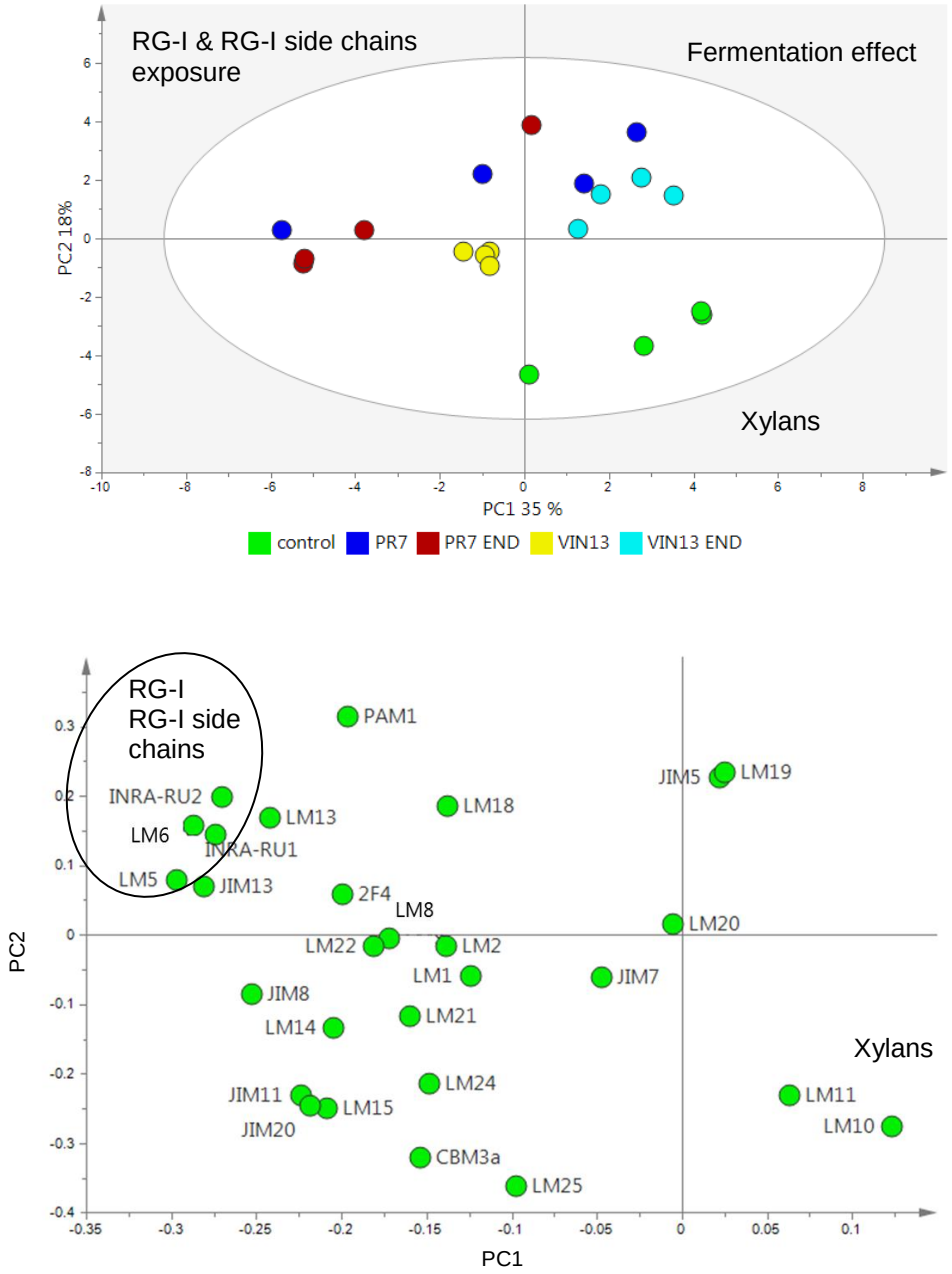

FIG 10. NaOH fraction of the CoMPP data showing the impact of the hydrolytic enzymes (secreted by the yeast strains during the fermentation) on the pomace cell wall composition. Variable BS-400-2 was excluded from the analysis.

DISCUSSION

In this study, we demonstrated the successful and stable integration of two copies of an expression cassette into the genome of two industrial wine yeast strains, VIN13 and PR7 (Exotics SPH). The MPOF END1 expression cassette enabled these yeast strains (V13 END1 and PR7 END1) to produce an active EG originating from a rumen bacteria (11). After the integration and removal of the pUT332 plasmid, the only foreign DNA still present in the yeast

was the *end1* gene. The POF1 genome locus (also known as PAD1) was targeted for integration at position 663 of the open reading frame that has 728 bp.

The recombinant yeast strains showed that an active EG as well an EPG, in the case of PR7 strains, were produced when the yeast were grown on agar plates containing the respective substrates for the enzymes. These yeast strains were all capable fermenters in a grape pomace suspension and decreased the reducing sugars within 48 h from 26 mg/ml to 2 mg/ml. No difference could be observed between the untransformed and the recombinant strains in terms of fermentation ability.

The VIN13 strain was chosen as a fermentation control that does not secrete any of the enzymes evaluated in this study. *S. cerevisiae* produce several extracellular, intracellular and cell wall bound glucanases (*EXG1, BGL1, EXG2, SSG1/SPR1* and *BGL2*) but they all are β-1,3-specific glucanases and thus inactive towards the β-1,4- linked cellulose and xyloglucan of the grape berry cell wall (34). The VIN13 and VIN13 END1 strains did not alter the cell wall composition (CoMPP results) apart from the "fermentation" modifications seen for all the fermented samples. It thus seems that the EG enzyme on its own is not capable of degrading noticeable amounts of cell wall polymers. Furthermore, the VIN13 strains did not decrease the mAb BS-400-2 labelling which indicate that none of the enzymes secreted by VIN13 can degrade this specific polymer or that this polymer were not within reach (shielded by other cell wall polymers, presumably pectin) of the VIN13 glucanases.

Previous attempts at our Institute (IWBT) to demonstrate the effect of the PR7 EPG activity on wine characteristics showed an increase in aroma compounds for Shiraz wine produced with PR7, but a decrease in polyphenol levels (with the exception of quercetin) (10). The authors speculated that the polyphenols were caught in the thick sediment visible in the PR7 wines. In other unpublished wine-making trials with PR7 at the IWBT, filter sterilized wine, sampled at the end of the fermentation gave a positive zone on polygalacturonase activity plate (data not shown) but no significant increase in colour density or total phenolics, (compared to wine fermented by the parent strain VIN13) was visible for PR7 (data not shown). It is interesting to see that despite these previous results, it is still possible to detect the effect of the EPG hydrolysis on the cell walls of grape berries using CoMPP analysis. However, we have to consider that the buffered conditions of these fermentations (pH 5.7) in contrast with wine pH (± 3.5) might have been crucial to obtain these results.

With the addition of the *end1* gene, the resulting PR7 END1 strain shows an enhanced effect suggesting a synergistic action between the two enzymes. In the samples fermented with PR7 END1, cell wall polymers were unravelled due to presumed partial degradation. This possibly

facilitated better access for the extraction solutions to extract more cell wall polymers that rendered an enhanced signal for those mAbs. This mild enzyme hydrolysis was thus only breaking up the cell wall polysaccharides into oligosaccharides that were not small enough to exit the cell wall environment unless aided by an extraction solvent.

Mild enzyme hydrolysis can in fact cause the development of a more porous cell wall and a consequential increase in cell wall surface. These are conditions conducive for the increased binding of proanthocyanidins to the cell wall polymers (35, 36). Thus, when PR7 and PR7 END1 were previously used in wine fermentations the enzymes that were produced might have done some minor damage to the cell walls of the grape berries. This might have been just enough to form numerous new pores in the cell wall and proanthocyanidins that were released during the crushing and fermentation of the grapes would bind to these newly created surface area (36). This can lead to lower proanthocyanidin concentration in the wine and thus less stabilizing factors for anthocyanins to bind with and thus a wine with lower colour stability and perhaps also a lower colour density. Furthermore, in studies done on apple pomace (37) it was found that if proanthocyanidins absorb to cell walls during mechanical disruption of fruit, limited pectin depolymerization takes place and low levels of polysaccharide polymers can be extracted from the tissue. They speculated that the presence of the proanthocyanidins restricted the access of polysaccharide degrading enzymes to the cell wall polymers. These authors also saw an increase in pectins that were extracted in the NaOH fraction of apple pomace and they associated this with the proanthocyanidins bound to the cell wall polymers (37). This corresponded with our results where the composition of the NaOH extracts was dominated by pectin polymers (RG-I and RG-I side chains). PR7 END1 samples showed the largest increase in these polymers and extracted HG (mAb LM19) which can substantiate the pore forming activity of this yeast.

It would be interesting to determine the extent of the role that the buffered conditions played in the results that were obtained. Furthermore, if polyphenols are retained in porous grape cell walls, it is crucial to determine if there is a critical level of enzyme hydrolysis which will ensure the release of these compounds instead of forming new bonds with cell wall polymers. However, since there is resistance against the use of genetically engineered microorganisms in wine preparation, these or similarly adapted yeast strains might rather found an application in the pomace valorisation industry where the pH can easily be adjusted if needed. Alternatively, another endo-glucanase with a suitable optimum pH can be integrated into the yeast genome.

The cell wall profiling methods (CoMPP and monosaccharide analysis) used in this study enabled us to show for the first time, how hydrolytic enzymes produced by fermenting yeast strains modify the cell walls of grape berries and will be a very valuable tool for the evaluation of

the capacity of any microorganism, isolated or engineered, to change the plant cell wall composition.

References

1. **Ciani M, Comitini F**. 2010. Non-*Saccharomyces* wine yeasts have a promising role in biotechnological approaches to winemaking. Ann. Microbiol. **61**:25–32.

2. **Sumby KM, Grbin PR, Jiranek V**. 2010. Microbial modulation of aromatic esters in wine: Current knowledge and future prospects. Food Chem. **121**:1–16.

3. **Sieiro C, García-Fraga B, López-Seijas J, Da Silva AF, Villa TG**. 2010. Microbial pectic enzymes in the food and wine industry, p. 201–218. *In* Valdez, B (ed.), Food industrial processes - Methods and Equipment. InTech, Rijeka.

4. **Cordente AG, Curtin CD, Varela C, Pretorius IS**. 2012. Flavour-active wine yeasts. Appl. Microbiol. Biotechnol. **96**:601–18.

5. **Barata a, Malfeito-Ferreira M, Loureiro V**. 2012. The microbial ecology of wine grape berries. Int. J. Food Microbiol. **153**:243–59.

6. **Karpe A V., Beale DJ, Harding IH, Palombo EA**. 2014. Optimization of degradation of winery-derived biomass waste by Ascomycetes. J. Chem. Technol. Biotechnol. DOI 10.1002/jctb.4486

7. **Jin B, Kelly JM**. 2009. Wine Industry Residues, p. 293–311. *In* Biotechnology for agro-industrial residues utilisation. Springer Netherlands.

8. **Redzepovic S, Orlic S, Majdak a., Kozina B, Volschenk H, Viljoen-Bloom M**. 2003. Differential malic acid degradation by selected strains of *Saccharomyces* during alcoholic fermentation. Int. J. Food Microbiol. **83**:49–61.

9. **Mocke B**. 2005. M.Sc. thesis The breeding of yeast strains for novel oenological outcomes. Stellenbosch University, Stellenbosch, South Africa.

10. **Eschstruth A, Divol B**. 2011. Comparative characterization of endo-polygalacturonase (*Pgu1*) from *Saccharomyces cerevisiae* and *Saccharomyces paradoxus* under winemaking conditions. Appl. Microbiol. Biotechnol. **91**:623–34.

11. **Berger E, Jones W, Jones D, Woods D**. 1989. Cloning and sequencing of an endoglucanase (*end1*) gene from *Butyrivibrio fibrisolvens* H17c. Mol. Gen. Genet. **219**:193–198.

12. **Hespell RB, Wolf R, Bothast RJ**. 1987. Fermentation of xylans by *Butyrivibrio fibrisolvens* and other ruminal bacteria. Appl. Environ. Microbiol. **53**:2849–53.

13. **Orpin CG, Mathiesen SD, Greenwood Y, Blix AS**. 1985. Seasonal changes in the ruminal microflora of the high-arctic Svalbard reindeer (*Rangifer tarandus platyrhynchus*). Appl. Environ. Microbiol. **50**:144–51.

14. **Gilkes NR, Henrissat B, Kilburn DG, Miller RC, Warren R a**. 1991. Domains in microbial β-1, 4-glycanases: sequence conservation, function, and enzyme families. Microbiol. Rev. **55**:303–15.

15. **Williamson MP**. 1994. The structure and function of proline-rich regions in proteins **260**:249–260.

16. **Van Rensburg, P., Van Zyl., W.H. Pretorius IS**. 1994. Expression of the *Butyrivibrio fibrisolvens* endo-β-1,4-glucanase gene together with the *Erwinia pectate* lyase and polygalacturonase genes in *Saccharomyces cerevisiae*. Curr. Genet. **27**:17–22.

17. **Scheirlinck T, Meutter J De, Arnaut G, Joos H, Claeyssens M, Michiels F**. 1990. Cloning and expression of cellulase and xylanase genes in *Lactobacillus plantarum*. Appl. Microbiol. Biotechnol. **33**:534–541.

18. **Jackson RS**. 2008. Wine science: Principles and applications, 3rd ed. Academic Press, Inc., San Diego.

19. **Moller I, Sørensen I, Bernal AJ, Blaukopf C, Lee K, Øbro J, Pettolino F, Roberts A, Mikkelsen JD, Knox JP, Bacic A, Willats WGT**. 2007. High-throughput mapping of cell-wall polymers within and between plants using novel microarrays. Plant J. **50**:1118–28.

20. **Sambrook J, Fritsch E., Maniatis T**. 1989. Molecular cloning: a laboratory manual, 2nd ed. Cold Spring harbour laboratories, New York.

21. **Gatignol A, Dassain M, Tiraby G**. 1990. Cloning of *Saccharomyces cerevisiae* promoters using a probe vector based on phleomycin resistance. Gene **91**:35–41.

22. **Güldener U, Heck S, Fielder T, Beinhauer J, Hegemann JH**. 1996. A new efficient gene disruption cassette for repeated use in budding yeast. Nucleic Acids Res. **24**:2519–24.

23. **Volschenk H, Viljoen-Bloom M, Van Staden J, Husnik J, Van Vuuren HJJ**. 2004. Genetic engineering of an industrial strain of *Saccharomyces cerevisiae* for L-malic acid degradation via an efficient malo-ethanolic pathway. South African J. Enol. Vitic. **25**:63–73.

24. **Hoffman CS, Winston F**. 1987. A ten-minute DNA preparation from yeast efficiently releases autonomous plasmids for trausformation of *Escherichia coli*. Gene **51**:267–272.

25. **Louw C, Young PR, van Rensburg P, Divol B**. 2010. Epigenetic regulation of *PGU1* transcription in *Saccharomyces cerevisiae*. FEMS Yeast Res. **10**:158–67.

26. **Ghose TK**. 1987. Measurement of cellulase activities. Pure Appl. Chem. **59**:257–268.

27. **Ortega-Regules A, Ros-García JM, Bautista-Ortín AB, López-Roca JM, Gómez-Plaza E**. 2008. Differences in morphology and composition of skin and pulp cell walls from grapes (*Vitis vinifera L.*): technological implications. Eur. Food Res. Technol. **227**:223–231.

28. **York WS, Darvill AG, L MM, Stevenson TT, Albersheim P**. 1985. Isolation and characterization of plant cell walls and cell wall components. Methods Enzymol. **2**:3–40.

29. **Nguema-Ona E, Moore JP, Fagerström A, Fangel JU, Willats WGT, Hugo A, Vivier MA**. 2012. Profiling the main cell wall polysaccharides of tobacco leaves using high-throughput and fractionation techniques. Carbohydr. Polym. **88**:939–949.

30. **Moore JP, Fangel JU, Willats WGT, Vivier MA**. 2014. Pectic-β(1,4)-galactan, extensin and arabinogalactan-protein epitopes differentiate ripening stages in wine and table grape cell walls. Ann. Bot. **114**:1279–1294.

31. **Jackson JE**. 1991. A User's Guide to Principal Components. John Wiley & Sons, Inc., Hoboken, NJ, USA.

32. **Puig S, Ramon D, Perez-Ortin, José E**. 1998. Optimized method to obtain stable food-safe recombinant wine yeast strains. J. Agric. Food Chem. **8561**:1689–1693.

33. **Klis FM, Mol P, Hellingwerf K, Brul S**. 2002. Dynamics of cell wall structure in *Saccharomyces cerevisiae*. FEMS Microbiol. Rev. **26**:239–256.

34. **Van Rensburg P, Van Zyl WH, Pretorius IS**. 1998. Engineering yeast for efficient cellulose degradation. Yeast **14**:67–76.

35. **Le Bourvellec C, Guyot S, Renard CMGC**. 2004. Non-covalent interaction between procyanidins and apple cell wall material: Part I. Effect of some environmental parameters. Biochim. Biophys. Acta **1672**:192–202.

36. **Ruiz-Garcia Y, Smith PA, Bindon KA**. 2014. Selective extraction of polysaccharide affects the adsorption of proanthocyanidin by grape cell walls. Carbohydr. Polym. **114**:102–114.

37. **Le Bourvellec C, Guyot S, Renard CMGC**. 2009. Interactions between apple (*Malus x domestica Borkh.*) polyphenols and cell walls modulate the extractability of polysaccharides. Carbohydr. Polym. **75**:251–261.

Supplementary data

TABLE S1: Monoclonal antibodies (mAbs) and carbohydrate binding modules (CBMs) used in this study.

Monoclonal antibody	Reference
HG partially/de-esterified (mAb JIM5)	(1)
HG partially esterified (mAb JIM7)	(1)
HG partially/de-esterified (mAb LM18)	(1)
HG partially/de-esterified (mAb LM19)	(1)
HG partially esterified (mAb LM20)	(1)
HG ±30 contiguous unmethylesterified GalA[a] units (mAb PAM1)	(2)
HG Ca^{2+} dimers (mAb 2F4)	(3)
RG-I, 6 unbranched disaccharide (mAb INRA-RU1)	(4)
RG-I, 2 unbranched disaccharide (mAb INRA-RU2)	(4)
β-1,4-D-galactan (mAb LM5)	(5)
α-1,5-L-arabinan (mAb LM6)	(6)
Linearised α-1,5-L-arabinan (mAb LM13)	(7)
β-1,4-D-(galacto)(gluco)mannan (mAb LM21)	(8)
β-1,4-D-(gluco)mannan (mAb LM22)	(8)
β-1,3-D-glucan (mAb BS-400-2)	(7)
Xyloglucan (XXXG motif) (mAb LM15)	(8)
Xyloglucan (XLLG oligosaccharide) (mAb LM24)	(9)
Xyloglucan (mAb LM25)	(9)
β-1,4-D-Xylan (mAb LM10)	(10)
β-1,4-D-Xylan d/arabinoxylan (mAb LM11)	(10)
Celulose (crystalline) (mAb CBM3a)	(11)
Extensin (mAb LM1)	(12)[c]
Extensin (mAb JIM11)	(13)
Extensin (mAb JIM20)	(13)
AGP (mAb JIM8)	(14)
AGP (mAb JIM13)	(15)
AGP (mAb LM14)	(7)
AGP,β-linked GlcA[b] (mAb LM2)	(15)

[a]galacturonic acid; [b]GlcA, glucuronic acid; [c]Cited in (16)

References

1. **Verhertbruggen Y, Marcus SE, Haeger A, Ordaz-Ortiz JJ, Knox JP**. 2009. An extended set of monoclonal antibodies to pectic homogalacturonan. Carbohydr. Res. **344**:1858–62.

2. **Willats WGT, Gilmartin PM, Mikkelsen JD, Knox JP**. 1999. Cell wall antibodies without immunization : generation and use of de-esterified homogalacturonan block-specific antibodies from a naive phage display library. plant J. **18**:57–65.

3. **Liners F, Letesson J-J, Didembourg C, Van Cutsem P**. 1989. Monoclonal antibodies against pectin: Recognition of a conformation induced by Calcium. Plant Physiol. **91**:1419–1424.

4. **Ralet M-C, Tranquet O, Poulain D, Moïse a, Guillon F**. 2010. Monoclonal antibodies to rhamnogalacturonan I backbone. Planta **231**:1373–83.

5. **Jones L, Seymour B, Knox JP**. 1997. Localization of pectic galactan in tomato cell walls using a monoclonal antibody specific to 1,4-β-D-Galactan. Plant Physiol. **113**:1405–1412.

6. **Willats WGT, Marcus SE, Knox JP**. 1998. Generation of a monoclonal antibody specific to 1,5-a-L-arabinan. Carbohydr. Res. **308**:149–152.

7. **Moller I, Marcus SE, Haeger A, Verhertbruggen Y, Verhoef R, Schols H, Ulvskov P, Mikkelsen JD, Knox JP, Willats W**. 2008. High-throughput screening of monoclonal antibodies against plant cell wall glycans by hierarchical clustering of their carbohydrate microarray binding profiles. Glycoconj. J. **25**:37–48.

8. **Marcus SE, Blake AW, Benians TAS, Lee KJD, Poyser C, Donaldson L, Leroux O, Rogowski A, Petersen HL, Boraston A, Gilbert HJ, Willats WGT, Knox JP**. 2010. Restricted access of proteins to mannan polysaccharides in intact plant cell walls. Plant J. **64**:191–203.

9. **Pedersen HL, Fangel JU, McCleary B, Ruzanski C, Rydahl MG, Ralet M-C, Farkas V, von Schantz L, Marcus SE, Andersen MCF, Field R, Ohlin M, Knox JP, Clausen MH, Willats WGT**. 2012. Versatile high resolution oligosaccharide microarrays for plant glycobiology and cell wall research. J. Biol. Chem. **287**:39429–38.

10. **McCartney L, Marcus SE, Knox JP**. 2005. Monoclonal antibodies to plant cell wall xylans and arabinoxylans. J. Histochem. Cytochem. **53**:543–6.

11. **Blake AW, McCartney L, Flint JE, Bolam DN, Boraston AB, Gilbert HJ, Knox JP**. 2006. Understanding the biological rationale for the diversity of cellulose-directed carbohydrate-binding modules in prokaryotic enzymes. J. Biol. Chem. **281**:29321–9.

12. **Smallwood M, Martin H, Knox JP**. 1995. An epitope of rice threonine- and hydroxylproline-rich glycoprotein is common to cell wall hydrophobic plasma-membrane glycoproteins. Planta **196**:510–522.

13. **Smallwood M, Beven A, Donovan N, Neill SJ, Peart J, Roberts K, Knox JP**. 1994. Localization of cell wall proteins in relation to the developmental anatomy of the carrot root apex. Plant J. **5**:237–246.

14. **Pennell R, Janniche L, Kjellbom P, Scofield GN, Peart JM**. 1991. Developmental regulation of a plasma membrane arabinogalactan protein epitope in oilseed rape. Plant Cell **3**:1317–1326.

15. **Yates EA, Valdor JF, Haslam SM, Morris HR, Dell A, Mackie W, Knox JP**. 1996. Characterization of carbohydrate structural features recognized by anti-arabinogalactan-protein monoclonal antibodies. Glycobiology **6**:131–9.

16. **Neumetzler L, Humphrey T, Lumba S, Snyder S, Yeats TH, Usadel B, Vasilevski A, Patel J, Rose JKC, Persson S, Bonetta D**. 2012. The *FRIABLE1* gene product affects cell adhesion in *Arabidopsis*. PLoS One **7**:e42914.

Chapter 6

General discussion and conclusions

6. General discussion and conclusion

This study contributed many new insights on the grape berry cell wall of two different grape cultivars. The cell wall profiling techniques that were used revealed, on a polymer level, how the grape berry cell wall changes during different grape processing procedures and highlighted the variance between grape skins at two different ripeness levels. This study laid the groundwork for new applications for the cell wall profiling techniques in the grape and enzyme industries.

6.1 Grape berry cell wall changes during a maceration enzyme assisted red wine fermentation

We investigated for the first time the cell wall composition of *Vitis vinifera* cv Pinotage, a cultivar which is known for its thick and tough skin. The monosaccharide profile of the Pinotage skin cell wall was similar to other cultivars with a high abundance of galacturonic acid followed by arabinose, xylose and galactose (1). Also, on the polymer level there were strong signals with cell wall probes that recognize homogalactoronan (HG), xyloglucan and cellulose. Thus we could not identify, with the methods that we used, any major difference or unique feature of the thick Pinotage skin. It would be interesting to compare the morphology of the Pinotage skin with other cultivars by means of optical microscopy as was done for Monastrell grapes (1). Furthermore, we should determine and compare the cell wall material per gram of skin of Pinotage with other cultivars to determine if the thick skin is linked to the amount of cell wall material. When the cell wall composition for the different ripeness levels was compared, some of the major changes that have previously been reported in grapes and other fruit during ripening such as the decrease in xylose and galactose and in xyloglucan, mannan and cellulose and an increase in arabinogalactan proteins were confirmed (2–6) in Pinotage skins. With multivariate statistical techniques we showed the high variability in ripeness levels found in the berries of a standard harvest batch and it seems that the heterogeneity decreased as the ripeness level increased. The riper berries also had elevated levels of callose which indicated that they were more susceptible to physical damage during the harvest and wine making procedures.

With this study we were also able to document for the first time the cell wall changes that happen in the skin cells of grapes during a standard red wine fermentation (in the absence of maceration enzymes). We saw that the fermentation process removes the HG from the cell wall samples and that cell wall proteins were exposed and some were also released into the must. These changes were presumably fermentation related and are mediated by the ethanol, organic acids and other metabolites in the must that acts on the permeabilization, solubilization and extraction of the cell membrane, cell wall macromolecules and calcium ions respectively (7,

8). When maceration enzymes were added to the fermentation we saw that even more pectin polymers were removed (decrease in galacturonic acid and HG labelling) but this was accompanied by an enhancement in the extraction of both pectin, hemicellulose and cellulose polymers which can indicate that pores were formed in the cell wall and that partially hydrolysed polymers were extracted from within the cell wall structure. An additional reduction in rhamnose (Rha) levels in the cell walls, indicated degradation by the maceration enzymes of presumably, rhamnogalacturonan I (RG-I). Unfortunately the mAbs for RG-I (INRA-RU1 and INRA-RU2) were not part of the antibody set that was used in this experiment, thus we could not confirm this on a polymer level. We were unable to differentiate between the three commercial maceration enzyme preparations that were used in the Pinotage fermentations in terms of their effect on the composition of the cell wall polymers but some preparations does seem to cause more extensive degradation than others. When the experiment was repeated with overripe grapes the effects of the maceration enzymes were insignificant (no additional loss of polymers or increase in pore formation /enhancement of extraction due to enzyme action). It seems that the endogenous grape enzymes involved in metabolic changes during ripening facilitated the removal of a large fraction of the cell wall polymers presumably by degradation. These degraded polymers were then easily removed during the fermentation, even in the control fermentation where no maceration enzymes were added. This information can be valuable for wine makers to prevent the unnecessary addition of enzymes to grapes of a certain ripeness level.

This first examination of enzyme hydrolysis on grape tissue generated new questions such as: (i) to what extent are the grape must environment (low pH and temperature and tannins) inhibiting the enzymes, and (ii) can the cell wall profiling methods be used to link specific enzymatic activities with specific cell wall changes? Thus, purified enzymes and different combinations of these purified enzymes were incubated with isolated Pinotage skin cell walls in close to optimal conditions for the enzymes, with regards to their temperature and pH optima. The results showed distinct differences in terms of the extent of enzymatic hydrolysis that took place depending on the enzyme(s) that were added. When an enzyme called “Pectinase” (Pect in Chapter 4) which is a combination of pectolytic activities (pectintranseliminase, polygalacturonase and pectin esterase) was used separately or in combination with an endo-glucanase extensive hydrolysis was seen with drastic depectination as well as a reduction in the hemicellulose and cellulose polymers. Less extensive hydrolysis was seen when an endo-polygalacturonase, endo-glucanase, endo-arabinase, xyloglucanase or a combination of these enzymes were used. This moderate response was typified by the partial degradation of HG polymers which enhanced their extraction into the CDTA fraction accompanied by a decrease in the xyloglucan and cellulose polymers that could be extracted in the NaOH fraction. This corresponds to what we classify as pore formation. Furthermore, the combination of the strong

pectolytic activities along with a xyloglucanase (Pect-XG) led to a very clear increase in the xyloglucan and cellulose that could be extracted which was not seen when either of these enzymes acted solo. This illustrates that a certain level of depectination is first needed before the xyloglucanase can reach its target and commence with hydrolysis. According to the manufacturer the XG is a endo-1,4-β-glucanase with specificity towards xyloglucan. This specific type of enzyme or the combination with pectinases has not been reported to be present in wine maceration enzyme preparations (9, 10). This enhanced extraction was perhaps only possible under the ideal experimental conditions that were used but it is still an interesting enzyme combination for further investigation.

6.2 Cell wall changes in grape pomace during heat treatment and enzymatic hydrolysis

Besides their application in the maceration step of wine making, enzymes are also used in processing pomace (pressed grape skin and pulp), a waste product of the wine making industry, for the isolation of revenue generating molecules that can be reemployed in the biopharmaceutical and food industries (11). Pomace also have the potential to be used for the production of second generation biofuel (12). To manage the recalcitrance of pomace towards enzymatic degradation it is common practice to include a pretreatment step before enzymatic hydrolysis (13). In our study we investigated how the polymers in the cell wall of grape tissue change during a pressurized heating (autoclave) step and this generated the first grape cell wall data, to our knowledge, on the influence of this pretreatment. With autoclaving the cell wall structure was opened up and a fraction of the HG was removed, while the extraction of all other pectin, hemicellulose, cellulose and cell wall protein polymers were enhanced. Additionally the autoclaving process exposed xylan polymers which led to the enhanced extraction of this polymer in the NaOH fraction.

The autoclaved pomace was incubated with a selection of commercial enzyme preparations in buffered conditions. The enzyme combinations, pH and temperature conditions were optimized in a preliminary experiment. We saw that extensive hydrolysis took place when a combination of enzyme activities (pectinases, cellulases and hemicellulases) were present and a higher temperature enhanced the hydrolysis. However, this degradation did not increase the levels of reducing sugars that were liberated into the buffer indicating that the cell wall polymers were only partially degraded. Thus, this enzymatic hydrolysis would perhaps be sufficient to liberate polyphenols from the grape tissue, but it would probably not generate single fermentable sugars if the aim was to saccharify the pomace in preparation for the fermentation to biofuel. However, the optimization of a saccharification process is complex and depends on many aspect related to the substrate composition but is also dependent on the type of pretreatment used, the enzyme dosage and efficiency of the enzyme (14). This study demonstrated that the methods

that we used to study the cell wall can be valuable tools to evaluate the efficiency of different enzyme preparations but also to determine the efficiency of pretreatments steps.

The pomace hydrolysis with commercial enzymes showed the combined effect of a mixture of enzymes. To learn more about the action of specific enzymes on the pomace cell wall the pomace was hydrolyzed with individual purified enzymes and combinations of these enzymes. Similarly to what we saw with the isolated Pinotage skin cell walls, different levels of enzymatic hydrolysis were visible and the Pect enzyme and combinations with this enzyme showed the highest degree of hydrolysis. A clear synergistic effect was seen between an endo-polygalacturonase (EPG) and an endo-glucanase (EG), with this combination of enzymes causing more extensive cell wall polymer modifications than when either of the enzymes was used on their own. In literature the combined hydrolysis effect of pectinases and cellulases does not always result in an increase in polyphenol release from grape tissue (15) but other factors such as high temperature during extraction can degrade the polyphenolics (16). If the only measure of the extent of enzymatic plant cell wall degradation is linked to polyphenolic yield, this will not give a true reflection of the efficacy of the enzymes that was used. The synergistic effect observed in our study corresponds with work by Kammerer et al. and Maier et al. (17, 18) but our method could pin point the effect of the enzymes on the cell wall polymer level.

The overall extraction patterns that we observed for the mAbs that recognize the xyloglucan epitopes and how this pattern was influenced by different enzymes in the CoMPP results gave us clues to speculate about the sequence in which the enzymatic degradation took place. Our speculation was also based on previous work done by Pedersen et al. (19) that showed differential labelling for xyloglucan in tobacco stem cells. We think that the hydrolysis initiates or occurs more regularly in the intercellular triangle and then moves into the corners of this area and finally spreads to the area between two adjacent cells. We also saw similarity in the extraction and degradation patterns of RG-I and xyloglucan (recognized by mAb LM25), while there were no resemblance between RG-I and HG hydrolysis- or extraction patterns which might indicate a specific association between this xyloglucan epitope and RG-I polymers.

6.3 Hydrolytic enzymes produced by yeast strains modify the cell wall composition of Chardonnay pomace

With the information gained on grape pomace cell wall polymers and their modifications during autoclaving and enzymatic hydrolysis, and with the demonstration of the synergism between the EPG and EG, we embarked on our final experiment. A wine yeast strain, PR7 (known as Exotics SPH Anchor yeast, South Africa), which is a hybrid between *Saccharomyces paradoxus* RO88 and VIN13 (*Saccharomyces cerevisiae* commercial wine yeast strain) that produced an EPG (native) were transformed with an genome integrating cassette that expresses an EG. This

yeast, called PR7 END1, produced the enzymes while using grape pomace as fermentation substrate and the changes in the pomace cell wall polymers were monitored. This experiment was set up to simulate to a certain degree what would happen if such a yeast strain are to be used in a wine fermentation or in a pomace valorisation effort. Different yeast strains were used and developed: PR7 that has the native EPG, PR7 END1 that expresses both the EPG and a recombinant EG, VIN13, which was used as a control strain that produced none of these enzymes and finally VIN13 END1 that produced the recombinant EG. The yeast strains were all able to reduce the reducing sugar concentrations to approximately 2 mg/ml within 48 h and with the CoMPP results we saw that the PR7 strain removed some HG from the grape cell walls. When both enzymes were present (PR7 END1) there was a decrease in HG but also an increase in the extraction of other pectin polymers (RG-I and RG-I side branches) and cell wall proteins (AGPs). This is a strong indication that the synergistic effect of the two enzymes expressed by the yeast (PR7 END1) has an unravelling effect on the cell wall of grape berries. This effect is quite mild in comparison to what was seen in the other experiments where we used commercial or purified enzymes probably due to low levels of enzyme produced by the strains. However, this proofs that recombinant strains have the potential to be used in wine making and valorisation processes, at least under ideal conditions. The cell wall profiling techniques enabled us to determine the extent of hydrolysis or modifications that did happen and it is thus a useful method for future optimizations of engineered microorganisms.

6.4 The cell wall profiling techniques

The Comprehensive Microarray Polymer Profiling (CoMPP) method that was extensively used in this study (Chapters 3 – 5), has many advantages: It uses monoclonal antibodies and carbohydrate binding modules that are specific for cell wall polymers and CoMPP is thus very specific and sensitive (20). It is an *in situ* method, but has the high-throughput advantage of microarrays and providing a profile. Isolated cell walls are first extracted with diamino-cyclo-hexane-tetra-acetic acid (CDTA) which solubilize pectins and any polymer that are strongly bonded or associated with pectins. After the first extraction, the residue is treated with 4 M NaOH that destroys hydrogen bonds and thus releases hemicelluloses. This fraction also contains other polymers that have a strong association with hemicelluloses. Thus, CoMPP give information about the actual carbohydrate structure, but furthermore, CoMPP can tell us about possible associations between different polymers when materials are co-extracted during the analysis procedures.

CoMPP results are however not fully quantitative because different probes bind with different avidities to their respective epitopes, but it is still extremely useful in comparing plant cell walls from different plant organs, from tissues differentially treated, or from tissues at different time

points (2, 20, 21). There are however, a few things to take into consideration when using this technique. Firstly, CoMPP results are influenced by the preparation method used during cell wall extraction and this should be considered carefully before commencing with an experiment (22). In general better results or more epitopes are detected when including a methanol/chloroform and acetone washing step after the ethanol wash. The methanol/chloroform solvent seems to loosen up the cell wall structure which gives better access to enzymes and/or solvents used in subsequent steps. One should also remember that there is a possibility that epitopes can be modified during the extraction or they may be masked by structural features (20). We saw that it is not possible to directly compare CoMPP results if the sets of antibodies that were used are not identical or if the analysis was not done as a single batch. We were also not able to distinguish clearly between the changes made by the different maceration enzyme preparations or distinguish between the action of the endogenous grape ripening enzymes and maceration enzymes added. This may be due to CoMPP that is not quantitative and high standard deviations for the signal strength of a mAb are sometimes visible between biological repeats. It is therefore important to have sufficient biological repeats (preferably five). Finally, there is the possibility of cross-reactivity of mAb JIM13 with RG-I and CBM3a carbohydrate binding module binds to crystalline cellulose (23), but were detected in the NaOH fraction (also previously seen by (21)). It is possible that mAb CBM3a might show some cross-reactivity with xyloglucan (personal communication with Dr J. Fangel) and this would correspond with the similar patterns observed for mAbs CBM3a, LM15 and LM25 for all treatments and matrices in this study. These matters as well as the possible recognition of yeast cell wall β-1,3-D-glucan by mAb BS-400-2 needs to be clarified specifically in the grape tissue matrix.

The data generated with CoMPP were supported by monosaccharide analysis and FT-IR absorption spectra of the isolated AIR particles. With monosaccharide analysis the AIR was degraded by trifluoroacetic acid (TFA), then derivatized to methoxy sugars followed by silylation (24). The derivatives were separated and analyzed in a gas chromatograph, enabling us to measure the quantities of the nine major single sugars that form the building blocks of the plant cell wall polysaccharides. We did detect evidence of incomplete TFA hydrolysis which showed that sample preparation methods could still be optimized further; on the positive side the incomplete TFA hydrolysis contributed towards the evidence for pore formation due to enzyme hydrolysis. The monosaccharide profiles provided a rough overview of polymers present while FT-IR provided the adsorption profile of all the chemical components present in the sample, thus not only carbohydrates but also proteins, lipids and polyphenolics. This provides a very complex picture and it is often difficult to interpret because of overlapping peaks and shifts in the spectral frequency due to interaction between different molecules present in the sample (25). However, the method was helpful in our study to detect the major differences between

treatments with regards to cell wall proteins and pectin concentration. Another advantage of FT-IR is that no additional sample preparation is needed, thus any treatment that can introduced undesired structural changes can be avoided (26). Multivariate data analysis was successfully used to detect patterns in the data sets.

6.5. Investigations for the future

In general these cell wall profiling methods has provided us with novel insights into the cell wall of the grape berry rendering indirect polymer visualization which is an advantage over all the other methods that was used to study the grape berry cell wall until now. With the knowledge gained on the restrictions of these methods we would be able to tweak future experimental layouts and the potential is there to learn much more. Furthermore, if more mAbs and cell wall binding modules with known specificities could be added to the collection that can be used in CoMPP analysis, it would open up new sections or show new dynamics of the cell wall.

It would be interesting to investigate the grape ripening changes and the influence that it has on the cell wall and the enzymes used for grape processing. We could optimize this experiment by selecting grapes from the same vineyard at few different time points, spanning the period from before harvest up to the overripe stage. The different parameters that can be monitored are the different ripeness stages and the effect of the fermentation process (with and w/o enzymes) on the grape berry cell wall. This method will enable us to rule out other factors that could have had an influence on the cell wall such as different vineyard practices and growing conditions. It would also be interesting to test different maceration enzyme concentrations in a fermentation in order to establish if the pore forming effect is coupled to low enzyme concentrations. Ideally the concentrations of polyphenols that are released at all stages should be monitored in order to determine how pore formation influences the possible absorption of these compounds onto the grape tissues.

Furthermore, in order to advance the process of elucidating the connection between specific enzyme activities and specific cell wall changes we should continue to use isolated cell walls (AIR) as substrate for this type of experiment (ruling out interfering substances), but by using different enzyme to substrate ratios we might be able to also observe the subtle cell wall modifications caused by the enzymes. The set of enzymes and combinations of enzymes tested can also be expanded and optimized. Finally, it would be interesting to test our hypothesis regarding the spatial distribution and hydrolysis sequence of the unmethylesteified HG

recognized by mAbs PAM1 and xyloglucan recognized by mAbs LM15 and LM24 with immunofluorescence microscopy.

6.6 References

1. **Ortega-Regules A, Ros-García JM, Bautista-Ortín AB, López-Roca JM, Gómez-Plaza E**. 2008. Differences in morphology and composition of skin and pulp cell walls from grapes (*Vitis vinifera L.*): technological implications. Eur. Food Res. Technol. **227**:223–231.

2. **Moore JP, Fangel JU, Willats WGT, Vivier MA**. 2014. Pectic-β(1,4)-galactan, extensin and arabinogalactan-protein epitopes differentiate ripening stages in wine and table grape cell walls. Ann. Bot. **114**:1279–1294.

3. **Ortega-Regules A, Ros-García JM, Bautista-Ortín AB, Lopez-Roca JM, Gomez-Plaza E**. 2008. Changes in skin cell wall composition during the maturation of four premium wine grape varieties. J. Sci. Food Agric. **88**:420–428.

4. **Vicens A, Fournand D, Williams P, Sidhoum L, Moutounet M, Doco T**. 2009. Changes in polysaccharide and protein composition of cell walls in grape berry skin (Cv. Shiraz) during ripening and over-ripening. J. Agric. Food Chem. **57**:2955–60.

5. **Yakushiji H, Sakurai N, Morinaga K**. 2001. Changes in cell-wall polysaccharides from the mesocarp of grape berries during veraison. Physiol. Plant. **111**:188–195.

6. **Huang X-M, Huang H-B, Wang H-C**. 2005. Cell walls of loosening skin in post-veraison grape berries lose structural polysaccharides and calcium while accumulate structural proteins. Sci. Hortic. (Amsterdam). **104**:249–263.

7. **González-Neves G, Gil G, Ferrer M, Charamelo D, Balado J, Bochicchio R, Gatto G, Tessore A**. 2010. Prediction of the colour and polyphenolic composition of the young red wines from the phenolic potential of the grapes. Int. J. Food Sci. Technol. **45**:1843–1851.

8. **Jarvis MC**. 2011. Plant cell walls: Supramolecular assemblies. Food Hydrocoll. **25**:257–262.

9. **Fia G, Canuti V, Rosi I**. 2014. Evaluation of potential side activities of commercial enzyme preparations used in winemaking. Int. J. Food Sci. Technol. **49**:1902–1911.

10. **Romero-Cascales I, Fernández-Fernández JI, Ros-García JM, López-Roca JM, Gómez-Plaza E**. 2008. Characterisation of the main enzymatic activities present in six commercial macerating enzymes and their effects on extracting colour during winemaking of Monastrell grapes. Int. J. Food Sci. Technol. **43**:1295–1305.

11. **Arvanitoyannis IS, Ladas D, Mavromatis A**. 2006. Potential uses and applications of treated wine waste: a review. Int. J. Food Sci. Technol. **41**:475–487.

12. **Rodríguez LA, Toro ME, Vazquez F, Correa-Daneri ML, Gouiric SC, Vallejo MD**. 2010. Bioethanol production from grape and sugar beet pomaces by solid-state fermentation. Int. J. Hydrogen Energy **35**:5914–5917.

13. **Hendriks ATWM, Zeeman G**. 2009. Pretreatments to enhance the digestibility of lignocellulosic biomass. Bioresour. Technol. **100**:10–8.

14. **Alvira P, Tomás-Pejó E, Ballesteros M, Negro MJ**. 2010. Pretreatment technologies for an efficient bioethanol production process based on enzymatic hydrolysis: A review. Bioresour. Technol. **101**:4851–61.

15. **Chamorro S, Viveros A, Alvarez I, Vega E, Brenes A**. 2012. Changes in polyphenol and polysaccharide content of grape seed extract and grape pomace after enzymatic treatment. Food Chem. **133**:308–314.

16. **Xu C, Yagiz Y, Borejsza-Wysocki W, Lu J, Gu L, Ramírez-Rodrigues MM, Marshall MR**. 2014. Enzyme release of phenolics from muscadine grape (*Vitis rotundifolia Michx.*) skins and seeds. Food Chem. **157**:20–9.

17. **Maier T, Göppert A, Kammerer DR, Schieber A, Carle R**. 2007. Optimization of a process for enzyme-assisted pigment extraction from grape (*Vitis vinifera L.*) pomace. Eur. Food Res. Technol. **227**:267–275.

18. **Kammerer D, Claus A, Scieber A, Carle R**. 2005. A novel process for the recovery of polyphenols from grape (*Vitis vinifera L* .) pomace. Food Chem. Toxicol. **70**:157–163.

19. **Pedersen HL, Fangel JU, McCleary B, Ruzanski C, Rydahl MG, Ralet M-C, Farkas V, von Schantz L, Marcus SE, Andersen MCF, Field R, Ohlin M, Knox JP, Clausen MH, Willats WGT**. 2012. Versatile high resolution oligosaccharide microarrays for plant glycobiology and cell wall research. J. Biol. Chem. **287**:39429–38.

20. **Moller I, Sørensen I, Bernal AJ, Blaukopf C, Lee K, Øbro J, Pettolino F, Roberts A, Mikkelsen JD, Knox JP, Bacic A, Willats WGT**. 2007. High-throughput mapping of cell-wall polymers within and between plants using novel microarrays. Plant J. **50**:1118–28.

21. **Alonso-Simón A, Kristensen JB, Obro J, Felby C, Willats WGT, Jørgensen H**. 2010. High-throughput microarray profiling of cell wall polymers during hydrothermal pre-treatment of wheat straw. Biotechnol. Bioeng. **105**:509–14.

22. **Fangel JU**. 2013. P.hD. thesis. Advanced technologies for plant cell wall evolution and diversity. University of Copenhagen.Copenhagen, Denmark.

23. **Blake AW, McCartney L, Flint JE, Bolam DN, Boraston AB, Gilbert HJ, Knox JP**. 2006. Understanding the biological rationale for the diversity of cellulose-directed carbohydrate-binding modules in prokaryotic enzymes. J. Biol. Chem. **281**:29321–9.

24. **York WS, Darvill AG, L MM, Stevenson TT, Albersheim P**. 1985. Isolation and characterization of plant cell walls and cell wall components. Methods Enzymol. **2**:3–40.

25. **Mouille G, Robin S, Lecomte M, Pagant S, Höfte H**. 2003. Classification and identification of *Arabidopsis* cell wall mutants using Fourier-Transform InfraRed (FT-IR) microspectroscopy. Plant J. **35**:393–404.

26. **Kačuráková M, Capek P, Sasinková V, Wellner N, Ebringerová A**. 2000. FT-IR study of plant cell wall model compounds : pectic polysaccharides and hemicelluloses. Carbohydr. Polym. **43**:195–203.